Fall 1980

NORMAL MODE SPECTRA OF SOUND WAVES IN VISCOUS SOLID AND FLUID MEDIA WITH PARTICULAR APPLICATIONS TO SHALLOW WATER ACOUSTICS

PETER GEOFFREY HARVEY

INFORMATION TO USERS

This was produced from a copy of a document sent to us for microfilming. While the most advanced technological means to photograph and reproduce this document have been used, the quality is heavily dependent upon the quality of the material submitted.

The following explanation of techniques is provided to help you understand markings or notations which may appear on this reproduction.

1. The sign or "target" for pages apparently lacking from the document photographed is "Missing Page(s)". If it was possible to obtain the missing page(s) or section, they are spliced into the film along with adjacent pages. This may have necessitated cutting through an image and duplicating adjacent pages to assure you of complete continuity.

2. When an image on the film is obliterated with a round black mark it is an indication that the film inspector noticed either blurred copy because of movement during exposure, or duplicate copy. Unless we meant to delete copyrighted materials that should not have been filmed, you will find a good image of the page in the adjacent frame.

3. When a map, drawing or chart, etc., is part of the material being photographed the photographer has followed a definite method in "sectioning" the material. It is customary to begin filming at the upper left hand corner of a large sheet and to continue from left to right in equal sections with small overlaps. If necessary, sectioning is continued again—beginning below the first row and continuing on until complete.

4. For any illustrations that cannot be reproduced satisfactorily by xerography, photographic prints can be purchased at additional cost and tipped into your xerographic copy. Requests can be made to our Dissertations Customer Services Department.

5. Some pages in any document may have indistinct print. In all cases we have filmed the best available copy.

University
Microfilms
International

300 N. ZEEB ROAD, ANN ARBOR, MI 48106
18 BEDFORD ROW, LONDON WC1R 4EJ, ENGLAND

HARVEY, PETER GEOFFREY

NORMAL MODE SPECTRA OF SOUND WAVES IN VISCOUS SOLID AND FLUID MEDIA WITH PARTICULAR APPLICATIONS TO SHALLOW WATER ACOUSTICS

University of New Hampshire PH.D. 1980

D. Library Copy

NORMAL MODE SPECTRA OF SOUND WAVES IN VISCOUS SOLID AND FLUID MEDIA WITH PARTICULAR APPLICATIONS TO SHALLOW WATER ACOUSTICS

BY

Peter Geoffrey Harvey
B.S., Purdue University, 1977

DISSERTATION

Submitted to the University of New Hampshire
in Partial Fulfillment of
the Requirements for the Degree of

Doctor of Philosophy

in

Engineering

(Theoretical and Applied Mechanics)

September, 1980

This dissertation has been examined and approved.

M. Yildiz

Dissertation director, Musa Yildiz,
Senior Research Fellow

John Dale

John Dale, Manager, Ocean Systems Division,
Sanders Associates, Nashua, New Hampshire

William Mosberg

William Mosberg, Associate Professor of
Mechanical Engineering

K. Sivaprasad

Kondagunta Sivaprasad, Associate Professor of
Electrical and Computer Engineering

M. Robinson Swift

M. Robinson Swift, Assistant Professor of
Mechanical Engineering

Asim Yildiz

Asim Yildiz, Professor of Mechanics

8/19/80

Date

ACKNOWLEDGEMENTS

The author extends his appreciation to Asim Yildiz whose leadership and enthusiasm instigated the desire to study in the Theoretical and Applied Mechanics Program and benefit from his extensive scientific and engineering background. The author expresses his deepest gratitude to Musa Yildiz for his countless hours of instruction, advice, and encouragement. His lectures and suggestions have been essential in making the past years productive and enjoyable. The author also thanks the following Professors for providing technical background: K. Sivaprasad, W. Mosberg, M.R. Swift, J. Wilson, R. Smith, and F. Glanz.

The author thanks John Dale and William Rusch of Sanders Associates for their suggestion to compare a shallow water acoustic model with experimental data they would provide and the subsequent financial support of this project. The time and effort of Paul Cox is gratefully acknowledged for this aid in the computer programming involved with this project. The author also appreciates A. Yildiz for coordinating the summer of 1978 spent at Harvard University where the author had the pleasure to work under Professors R.V. Pound and W. Vetterling on nuclear magnetic resonance. Thanks are slso extended to Haci Murat Hubey and Wayne Lundblad for their support and discussions and Jean Gahan for her patience in the typing of this dissertation.

These years of study have been made possible by a University of New Hampshire Fellowship.

TABLE OF CONTENTS

LIST OF TABLES

LIST OF FIGURES

NOMENCLATURE

C	Speed of sound
C.I.P.	Contribution of the imaginary-part of the complex-valued eigenvalue χ
C.R.P.	Contribution of the real-part of the complex-valued eigenvalue
G	Three-dimensional Green's function (3-space)
g	One-dimensional Green's function (1-space)
H	Depth of liquid layer
$H_\nu^{(1,2)}$	Hankel function of the first and second kind, respectively, of νth-order
$h_\nu^{(1,2)}$	Spherical Hankel functions
h_α	Eigenvalue of the separated-equation for the α-spatial direction
I	Specific acoustic impedance
I_ν	Modified Bessel function of νth-order
i	Imaginary unit($i^2 = -1$)
J_ν	Bessel function of νth-order
j_ν	Spherical Bessel function
K	Spatial propagation parameter in the $(\vec{R};\omega)$ domain, that is, the real part of χ, and eigenvalue ($h_\rho = K^2$) for ρ-direction
$\vec{k}$	Wavenumber vector
k	Magnitude of wavenumber vector
L	Differential operator
ℓ	Redefinition of eigenvalue $n^2 = \ell(\ell + 1)$

m	Mode type and number
n	Mode type and number, and eigenvalue ($h_\theta = n^2$) for θ-direction
P	Pressure
P_ℓ^ν	Associated Legendre polynomial
p	Mode type and number, and function in Sturm-Liouville equation
q	Function in Sturm-Liouville equation
$\vec{R}$	Distance vector
R	Magnitude of distance vector
$\vec{r}'$	Source position
$\vec{r}$	Field or receiver position
T	Time difference
t'	Time of initiation of source
t	Time coordinate
$\vec{u}$	Displacement vector
$\vec{v}$	Velocity vector
$\vec{w}$	Weighting function in Sturm-Liouville equation
X,Y,Z	Functions of separated equation in rectangular coordinate system
x,y,z	Cartesian or rectangular coordinates

Tensors

G_{jm}	Three-dimensional Greeen's function
P_{jm}	Polarization tensor in the $(\vec{k};\omega)$ domain

Q_{jm}	Polarization tensor in the $(\vec{R};\omega)$ domain
δ_{jm}	Kronnecker delta
∂_i	Spatial gradient operator
∂_t	Temporal gradient operator
f_i, u_i, v_i	Forcing, displacement, and velocity vectors

Greek Symbols

α, β, γ	Spatial coordinates in an arbitrary coordinate system
β	Phase velocity
Γ	Gamma function, eigenvalue ($h_r = \Gamma^2$) for the r-direction
γ	Spatial attenuation parameter
Δ	Wronskian
δ	Dirac delta function
η	Shear viscosity of fluid
ζ	Bulk viscosity of fluid
Λ	Temporal attenuation parameter
λ	Lame parameter, eigenvalue ($h_y = \lambda^2$) for the y-direction, and wavelength
λ', λ''	Elastic and Voigt damping components of λ
μ	Lame parameter, eigenvalue ($h_x = \mu^2$) for the x-direction
μ', μ''	Elastic and Voigt damping components of μ
ν	Eigenvalue ($h_\phi = \nu^2$) for the ϕ-direction
ρ	Mass density
Ψ	Scalar potential

ξ	Damping ratio and $\int\Omega(\bar{z},\Gamma)d\bar{z}$
Ω	Eigenvalue ($h_z = \Omega^2$) for the z-direction
ω	Angular frequency
ω_n	Natural oscillation frequency
ω_d	Temporal progapation parameter or damped natural frequency
χ	Complex-valued eigenvalue in the frequency domain
∂	Partial differentiation
∇	Vector notation for spatial gradient operator
$\cdot$	Scalar product of two vectors
$\times$	Vector product of two vectors

Subscripts

α,β,γ	Spatial directions in an arbitrary coordinate system
i,j,m	Tensorial indices
T,L	Transverse and longitudinal terms (also used as superscripts on polarization tensors)
q	Dummy variable to denote either T or L for the transverse or longitudinal polarization, respectively
ν,ℓ	Order of the Bessel functions
o,1	Index to denote fluid or solid properties, respectively, across an interface

ABSTRACT

NORMAL MODE SPECTRA OF SOUND WAVES IN VISCOUS SOLID AND FLUID MEDIA WITH PARTICULAR APPLICATIONS TO SHALLOW WATER ACOUSTICS

by

PETER GEOFFREY HARVEY
University of New Hampshire, September 1980

Sound propagation in shallow water is modelled using the Green's function formalism and normal mode techniques. The water layer is bounded above by a pressure-release condition and below by a halfspace of viscoelastic solid media. Nine different marine sediments are investigated by incorporating their published measured parameters into the bottom boundary condition utilizing the definition of specific acoustic impedance. A depth-dependent sound speed is treated in the ideal liquid layer.

In order to determine the most convenient mathematical representation for this shallow water model an investigation of the normal mode spectra of sound waves in viscous fluids and viscoelastic solids is first undertaken. Due to the non-self-adjoint property of the differential operator describing viscous media, complex-valued propagation constants (eigenvalues) were encountered and had to be dealt with in an appropriate manner.

A tensor Green's function is necessary to completely define vector fields. The velocity vector describes the fluid medium and the displacement vector the solid medium. It is found that both fields are composed of transverse and longitudinal polarizations due to shear and compressional effects, respectively. The ω- and k-poles of the inverse of the governing differential equation in the Fourier wavenumber-frequency domain prescribe the character of the sound waves in the wavenumber-time and space-frequency domains, respectively. It is shown that in each case the real- and imaginary-components of these complexed-value poles contribute independently to the propagation and attenuation of the acoustic energy, respectively. The longitudinal polarization of the viscous fluid and both polarizations of the viscoelastic solid are the transport modes of sound waves, while on the other hand the transverse polarization of the viscous fluid diffuses acoustic energy in both space and time.

The normal mode representations are constructed by a two-dimensional transform of a one-dimensional characteristic Green's function. The transforms are determined by the integral expressions of the Dirac delta function for the particular coordinate direction of the appropriate coordinate system. The delta function may be written as a summation of normal modes and hence is a convenient method for the treatment of boundary-value problems.

Using the appropriate normal mode representation numerically generated plots of transmission loss are produced from the shallow water model developed. The input parameters to the model are the conditions of an actual data-collection site in the Baltic Sea (1974). The computer simulation agrees qualitatively with the measured results at the test site and demonstrates the fundamental importance of the viscoelastic boundary on the attenuation of sound waves in shallow water.

CHAPTER I

PROBLEM STATEMENT AND SOLUTION METHOD

Problem Statement and Purpose

Interest in underwater surveillance has been on the increase for the last forty years. Beginning its modern era during the second World War with the desire to track submersible vessels, the application of underwater sound propagation are now moving into more commercial areas as well. For example, the ability to classify bottom sediment remotely using sound is desirable for mining and drilling operations since acoustic probing is more economical in both time and money for locating likely deposit sites.

The intent of this investigation, however, is long range detection of noise-producing objects. This passive detection problem invokes propagation theory (transmission), whereas active sonar systems invoke back-scatter theory (reflection).

In previous investigations, idealized models of varying complexity have been used in an attempt to understand observed sound propagation phenomena and sediment classification in shallow water regions. The simplest of these corresponds to a perfect homogeneous waveguide of the type discussed by Ide, Post, and Fry [39], who were the first to use waveguide theory

in interpreting their observations in the Potomac River. Later, Pekeris [11] made use of a partial or imperfect waveguide consisting of a homogeneous layer of water of constant sound speed overlying a fluid halfspace of greater sound speed. In this model the surface layer acted as a perfect waveguide only for waves incident at an angle greater than a critical value. Pekeris' detailed analysis of this problem met with considerable success and explained the chief properties of explosion-generated sound in coastal waters observed by Worzel and Ewing [22]. More recently, the interpretation of continuous-wave (c-w) sound-field experiments by Tolstoy [46] and Clay [36] has required the use of waveguide models consisting of several layers.

Few theoretical studies have been made of a fluid layer overlying a homogeneous, elastic solid half-space. The traditional approach to the theory of shallow-water sound propagation is to consider a number of homogeneous layers of different sound speeds, densities, and thicknesses, overlying a half-space (or a very thick layer) of greater sound speed. Such models will exhibit both the effects of partially reflected and totally reflected (guided) waves. In other words, one must distinguish between modes having continuous and discrete spectra, corresponding to important differences in behavior of the sound field at short and long ranges from the source. Thus, for source and receiver both situated in a low-velocity surface layer, the contribution of partial reflections (continuous spectrum) may be important or even dominant at short

range whereas at great distances guided waves (discrete spectrum) alone contribute significantly to the field.

In the present state of the art, the theory of layered waveguides constitutes the principal body of acoustics relevant to shallow-water propagation. Although the theory is built around extremely idealized models, it predicts a surprising number of observed characteristics of sound. It makes apparent the great importance of the sound speed profile in the liquid column and the parameters used to define the bottom sediment. Most existing models treat the bottom as another fluid layer or halfspace with a different sound profile (usually a constant sound speed greater than that in the fluid layer above it). Although computational advantages may be obtained from the treatment of the ocean bottom as another fluid layer, this method is far from being sufficient to describe the actual situation.

A more realistic model of the real ocean floor places emphasis on measured and extrapolated data for those parameters important in underwater acoustics. Such a geoacoustic model of the ocean floor has been developed at the Mechanics Research Laboratory (MRL) of the University of New Hampshire starting with the work of A. Yildiz [49] in 1970. The resulting visco-elastic soil model utilizes the elastic and damping parameters measured by Hamilton [29] for nine actual marine sediment compositions. The MRL-model incorporates these viscoelastic parameters into a boundary condition for the bottom interface

of the fluid layer by implementing the definition of acoustic impedance. There is no way the fluid model of the bottom can incorporate these measured bottom parameters into their theory of transmission loss.

This present investigation was motivated by talks with Sanders Associates of Nashua, New Hampshire who provided the Mechanics Research Laboratory with relevant experimental data for transmission loss in a shallow water region of the Baltic Sea (1974) collected by the Naval Underwater Systems Center (NUSC) of New London, Connecticut. MRL undertook a project to model sound propagation in an attempt to more closely simulate this transmission loss data than the existing model in their possession. The MRL-model utilizes the normal mode technique, a piece-wise linear depth-dependent sound speed in the ideal water column, and the viscoelastic soil boundary condition previously mentioned. The existing program (that Sanders possessed) utilized ray optic methods which are more convenient for short range and wide bandwidths. Normal modes are convenient for long range (only the discrete spectrum is significant) and finite bandwidths (which all instrumentation is limited to).

A more complete introduction to the underwater sound propagation problem is given at the beginning of Chapter III. The rest of Chapter III is the lead-up to and presentation of the MRL-model and its results. Plots of transmission loss are generated numerically by a computer program. A comparison of the MRL-model with the NUSC-data shows good qualitative

agreement.

In order to develop the MRL-model of sound propagation in shallow water an appropriate normal mode representation of the pressure field was required. So the first stage of this dissertation was the development of a systematic technique for evaluating the normal mode spectra of viscous media in the steady-state (space-frequency, $\vec{r};\omega$) domain. It was found that there are three different representations in both the rectangular and spherical coordinate systems and four representations in the cylindrical system (only these three coordinate systems were considered). The viscous media treated in this section (Chapter II) are viscous fluids and viscoelastic solids, while in Chapter III an ideal fluid overlying a viscoelastic solid bottom is considered. From this part of the investigation the most convenient normal mode representation was chosen for use in what became the MRL-model of transmission loss.

The Green's function formalism was selected to be used in conjunction with the normal mode technique. This formalism is a field theoretical approach which is more general and sensitive to the physical situation than the ray theoretical method. The latter method may be obtained from the field theoretical approach by applying appropriate approximation techniques [1]. The Green's function formalism is independent of the coordinate system, the mode of energy transport, and in principle the sophistication of the engineering model.

The Green's function itself is the response of a system to an impulsive point-source excitation. All the information about the system incorporated in the governing differential equation is also contained in the Green's function solution. This solution is a function of the system and independent of the forcing. The response of the system to arbitrary forcing is then a convolution of the Green's function with the forcing term in the space-time $(\vec{r};t)$ domain.

Prior to developing the normal mode spectra of viscous media the tensor Green's function of the viscous fluid and viscoelastic solid are evaluated in three Fourier domains for the rectangular coordinate system. A second-order tensor Green's function is required to describe the vector fields completely. It is found as expected that the field is polarized into transverse (shear effects) and longitudinal (compressional effects) components. Sound waves propagate with viscous attenuation in the longitudinal mode of the viscous fluid and both modes of the viscoelastic solid, while sound completely diffuses in the transverse mode of the viscous fluid.

It should be noted that the solutions and consequently temporal damping have been thoroughly investigated in association with the diffusion $(\partial^2-\partial_t/D)F_1 = 0$, Klein-Gordon $(\partial^2-\partial_t^2/C^2-a^2)F_2 = 0$, and dissipative wave $(\partial^2-2a\partial_t-\partial_t^2/C^2)F_3 = 0$ equations. The normal mode spectra of the solutions to these equations exist in literature ([7], [32], and [33],

respectively). There are no mathematical complications regarding temporal damping in these cases since the self-adjoint property of the above differential operators can be preserved. On the other hand, an operator with a term that exhibits space and time coupling of the form $(\partial^2\partial_t)$ is non-self-adjoint and complications arise when attempting to write its normal mode spectrum. In the course of investigating the normal mode spectrum of sound waves in viscous media, this type of non-self-adjoint operator was encountered and had to be dealt with in an appropriate manner.

Most problems in viscous fluids, viscoelastic solids, and aeroelasticity can be formulated as boundary-value problems in differential equations which are connected with the integral equations by proper Green's functions. It is well-known that the Green's functions are symmetric if the boundary-value problem defined by a differential equation is "self-adjoint" [35]. The nonsymmetry of the above mentioned operators is associated with the non-self-adjointness of the boundary-value problem. One can treat fluid, solid, and aeroelastic problems as eigenvalue problems. Under certain conditions, among which the Hermitian self-adjointness or the Hermitian symmetry of the kernel is the most important, it can be shown that eigenvalues always exist and are real-valued, that the eigenfunctions form a "complete" set of functions, that the itteration procedure for the calculation of the eigenvalues and eigenfunctions is valid, and that the bounds to the eigenvalues can be estimated.

The same is not always true with regard to non-self-adjoint problems, as in the case treated here. The eigenvalues of viscous systems are found to be complex-valued. This complication is not insurmountable as one finds that the real-part of the complex-eigenvalue is self-adjoint and prescribes the propagation of sound waves while the imaginary-part is non-self-adjoint and prescribes the attenuation of the field and modifies its natural oscillation frequency and amplitude.

Complex-valued eigenvalues are not discussed at great length in literature. The first to investigate this situation was M. Yildiz [51] in 1976 with his work in thermo-viscoelastic solids. This dissertation is an extension of his work to other representations of the normal modes and other coordinate systems.

Normal Modes Expressed by the Green's Function

The methodology for expressing the normal mode representations in terms of the Green's function is now presented. A mode is a spatial configuration whereby the entire field is fluctuating at the same frequency. Normal modes are a complete set of modes that span the configuration space to be able to describe any oscillatory situation by superposition. Chapter II will show the application of this formalism to infinite viscous media while Chapter III will show the formalism's ability to describe boundary value problems (media of finite extent).

There are four Fourier domains: space-time $(\vec{r};t)$, space frequency $(\vec{r};\omega)$, wavenumber-time $(\vec{k};t)$, and wavenumber-frequency $(\vec{k};\omega)$. A useful procedure is to evaluate a solution to a differential equation in the $(\vec{k};\omega)$ domain for which the evaluation is algebraic and then transform back through the other domains. These are Fourier transforms in the rectangular coordinate system. Other systems require transforms of the type: Bessel, Hankel, Sommerfeld, Kontorovich-Lebedev, Levine-Schwinger, and Legendre.

There is a simpler procedure to obtain a solution in the steady-state $(\vec{r};\omega)$ domain. In this domain the three-dimensional tensor Green's function $G_{jm}(\vec{r},\vec{r}';\omega)$ is calculated by a two-dimensional transform of the one-dimensional characteristic Green's function $g_z(z,z';h_z)$; where $\vec{r}' = (\alpha',\beta',z')$ and $\vec{r} = (\alpha,\beta,z)$ are the source and field points, respectively, and h_z is the z-direction eigenvalue. The transforms are determined by the integral representations of the Dirac delta function in the appropriate coordinate direction of a given coordinate system.

The Green's function of interest is defined by the following equation:

$$L_{ij}(\vec{r};\omega)G_{jm}(\vec{r},\vec{r}';\omega) = -\delta_{im}\delta^3(\vec{r}-\vec{r}') \quad , \qquad (1.1)$$

where L_{ij} is the appropriate partial-differential operator of the system. The solution to this equation can be evaluated

by the expression:

$$G_{jm}(\vec{r},\vec{r}';\omega) = \sum_{q} Q^{q}_{jm}\ (C.I.P.)_q (C.R.P.)_q \ , \qquad (1.2)$$

where q denotes the polarization (i.e., transverse or longitudinal), Q^{q}_{jm} is the polarization tensor defining the directionality of the energy mode q, (C.I.P.) and (C.R.P.) denote the contribution of the imaginary- and real-part of the complex-valued k-poles of the inverse of the operator L_{ij} in the $(\vec{k};\omega)$ domain, that is:

$$[L_{ij}(\vec{k};\omega)]^{-1} \ . \qquad (1.3)$$

Expression (1.3) is actually a symbolic representation of $-G_{jm}(\vec{k};\omega)$, since this solution is evaluated algebraically from the equation:

$$L_{ij}(\vec{k};\omega)G_{jm}(\vec{k};\omega) = -\delta_{im} \ . \qquad (1.4)$$

If the k-poles of expression (1.3) are given by: $k = \pm\chi$, where

$$\chi = K - i\gamma \ , \qquad (1.5a)$$

then one has:

$$C.I.P. = e^{-\gamma R} \ , \qquad R = |\vec{r}-\vec{r}'| \ , \text{ and} \qquad (1.5b)$$

$$C.R.P. = \frac{-1}{4\pi^2} \oint dh_\alpha g_\alpha(\alpha,\alpha';h_\alpha) \oint dh_\beta g_\beta(\beta,\beta';h_\beta) g_z(z,z';K,h_\alpha,h_\beta). \qquad (1.5c)$$

The polarization tensors depend on the polarization mode but are evaluated in Chapter II to be:

$$Q^T_{jm} = (\delta_{jm}+\partial_j\partial_m/\chi^2_T) \quad , \tag{1.6a}$$

for the transverse mode of viscous media and:

$$Q^L_{jm} = (\partial_j\partial_m/\chi^2_T) \quad , \tag{1.6b}$$

for the longitudinal mode of viscous media where χ^2_T is the square of the k-pole [expression (1.5a)] of the transverse term of inverse operator (1.3).

The derivation of expression (1.5c) is given in Appendix Ia. This expression is a two-dimensional transform on the characteristic Green's function g_z where the transforms are evaluated by the integral representation of the delta function shown in Appendix Ia to be:

$$\frac{\delta(\alpha-\alpha')}{w(\alpha')} = \frac{-1}{2\pi i}\oint dh_\alpha g_\alpha(\alpha,\alpha';h_\alpha) \quad , \tag{1.7a}$$

where the one-dimensional modal Green's function is shown in Appendix Ib to be evaluated according to:

$$g_\alpha(\alpha,\alpha';h_\alpha) = \frac{-A_{\pm}(\alpha)A_{\mp}(\alpha')}{p(\alpha')\ (A_+,A_-)} \quad , \tag{1.7b}$$

where in turn the A's are the homogeneous solutions to one of

the separated one-dimensional ordinary differential equations corresponding to the operator L_{ij} of equation (1.4), $p(\alpha')$ and $w(\alpha')$ are functions determined by comparing the just-mentioned operator with that of the standard form of the Sturm-Liouville equation, and Δ is the Wronskian of the two solutions (for a second-order differential equation).

One can see now that the real-part K of the k-poles of $[L_{ij}(\vec{k};\omega)]^{-1}$ contribute in the manner:

$$\text{C.R.P.} \longrightarrow \frac{\delta(\alpha-\alpha')}{w(\alpha')} \frac{\delta(\beta-\beta')}{w(\beta')} g_z(z,z';K,h_\alpha,h_\beta) \ . \qquad (1.8)$$

This is a symbolic expression where the delta functions are given by expression (1.7a). Another interpretation of the delta function is shown in Appendix Ia and this makes apparent why expression (1.2) is denoted a normal mode representation. In this form it is suitable for solving both unbounded and bounded media problems. Expression (1.8) has a propagation structure. The imaginary-part γ of the k-poles of $[L_{ij}(\vec{k};\omega)]^{-1}$ contribute as depicted in expression (1.5b) and clearly has an attenuation structure.

The integral transform representation of $G_{jm}(\vec{r},\vec{r}';\omega)$ shown in expression (1.2) has various descriptions depending on the choice of coordinate direction of the modal and characteristic one-dimensional Green's functions. The different representations are presented in the next chapter in rectangular, cylindrical, and spherical coordinate systems. The appropriate description is then selected for use in the sound

propagation model presented in Chapter III.

CHAPTER II

NORMAL MODES OF VISCOUS MEDIA

Introduction

This chapter deals with the mathematical description of the normal modes in viscous media for small disturbances (acoustical). In the rectangular coordinate system the field is derived for an infinite medium using the Fourier transforms. The field is described in the three domains $(\vec{k};\omega)$, $(\vec{k};t)$, and $(\vec{r};\omega)$. The procedure is general so that boundary conditions may easily be incorporated, as mentioned in Chapter I. Then to make apparent how the methodology may be used to derive the field in other coordinate systems, the normal modes are constructed in the steady-state $(\vec{r};\omega)$ domain in the cylindrical and spherical systems. In these coordinate systems they are no longer Fourier transforms.

Data collected by experiment in the analog form is modelled in the steady-state $(\vec{r};\omega)$ domain. Whereas digitized data would be mostly readily compared in the $(\vec{k};t)$ domain.

The procedure described in this chapter is presented for both viscous fluids and viscoelastic solids of infinite extent. The methods for the two cases is identical but the summations and/or integrations over the complex-valued eigenvalues are different due to the structure of governing field equations. For an unbounded medium (that is, infinite amount

of energy contained) the limits on the summations and/or integrations are also infinite. Hence a boundary-value problem that complicates the physical description actually reduces the computation time since fewer modes are excited (that is, the boundary confines the energy contained and limits its content to discrete frequencies).

The third section of this chapter discusses the role of the complex-valued eigenvalues that were encountered during this investigation of media that exhibit viscosity. It is seen that the real-part contributes to the propagation of energy while the imaginary-part contributes to its attenuation and modifies the natural oscillation frequency and amplitude by appearing in a damping factor. The character of the transverse and longitudinal polarizations of both the fluid and solid are then investigated by comparison with several fundamental scalar equations. The transverse mode of the fluid behaves entirely different from the longitudinal mode and both modes of the solid. A summary of the mathematical make-up of the key parameters is then presented.

Viscous Fluid

Tensor Green's Function in the Rectangular Coordinate System

To facilitate the determination of the tensor Green's function of a viscous fluid in the various domains, it is convenient to first evaluate it in the wavenumber-frequency $(\vec{k};\omega)$ domain where its solution is algebraic. This process

is accomplished below by deriving the equation of motion in the space-time $(\vec{R};T)$ domain, transforming to the $(\vec{k};\omega)$ domain, and then algebraically solving for the Green's function. From this $(\vec{k};\omega)$ domain result, the Green's function is determined in its $(\vec{k};T)$ and $(\vec{R};\omega)$ domain representations upon utilization of the appropriate inverse-Fourier temporal and spatial integral-transforms.

The linearized equation of motion of a viscous fluid in the velocity vector field v_j with external forcing per unit mass f_i can be written in the space-time $(\vec{r};t)$ domain as: $\mathcal{L}_{ij}(r;t)v_j(r;t) = \partial_t f_i$, where the partial differential operator (see Appendix IIa) is written as:

$$\mathcal{L}_{ij}(\vec{r};t) = \{\partial_t^2-(\eta/\rho)\partial^2\partial_t\}\delta_{ij} - \{C_L^2+[(3\zeta+\eta)/3\rho]\partial_t\}\partial_i\partial_j \tag{2.1}$$

and $\partial_t^2 = \partial^2/\partial t^2$, η is the shear viscosity, ρ is the density, $\partial_t = \partial/\partial t$, ∂^2 is the Laplacian operator, δ_{ij} is the Kronnecker delta, C_L is the longitudinal (L) adiabatic speed of sound, ζ is the bulk viscosity of the fluid, and ∂_i is the gradient operator $(\partial/\partial x_i)$. The partial differential equation for the tensor Green's function $G_{jm}(\vec{R};T)$ in the $(\vec{R};T)$ domain is given with reference to relation (1.1) by the expression (with a conveniently modified differential operator):

$$L_{ij}(\vec{r};t)G_{jm}(\vec{R};T) = -\delta_{im}\delta^3(\vec{R})\delta(T) \ , \tag{2.2}$$

where

$$L_{ij}(\vec{r};t) = -(\rho/\eta\partial_t)\,\mathcal{L}_{ij}(\vec{r};t)$$

$$= \{\partial^2-(\rho/\eta)\partial_t\}\delta_{ij}+\{(\rho C_L^2/\eta\partial_t)+[(3\zeta+\eta)/3\eta]\}\partial_i\partial_j \ ,$$

$\vec{R} = \vec{r} - \vec{r}'$, $T = t - t'$, $(\vec{r}';t')$ and $(\vec{r};t)$ are the location of the impulsive point source and observer point respectively, and δ^3 is the product of three spatial Dirac delta functions (one for each coordinate direction). Using the temporal and three-dimensional spatial Fourier transforms on equation (2.2), one obtains the transformed tensor Green's function in the wavenumber-frequency $(\vec{k};\omega)$ domain as (see Appendix IIb for details):

$$G_{jm}(\vec{k};\omega) = P^T_{jm}/(k^2-\chi_T^2) + P^L_{jm}\chi_L^2/\chi_T^2(k^2-\chi_L^2) \ , \qquad (2.3)$$

where the transverse (T) and longitudinal (L) components of the response are observable as distinct terms, the polarization tensors P_{jm} prescribe the directionality of each term, $P^T_{jm} = \delta_{jm} - (k_j k_m/k^2)$, $P^L_{jm} = k_j k_m/k^2$, the square of the complex-valued propagation constants (χ) are:

$$\chi_T^2 = -i\omega/D_T \quad \text{and} \quad \chi_L^2 = \omega^2/(C_L^2+i2D_L\omega) \ , \qquad (2.4)$$

and finally $D_T = \eta/\rho$ (i.e., kinematic viscosity), $D_L = (3\zeta+4\eta)/6\rho$, and $k^2 = |\vec{k}|^2$ (i.e., the square magnitude of the three-dimensional

wavenumber vector).

By applying the inverse-Fourier temporal transform to expression (2.3) one obtains the retarded tensor Green's function in the wavenumber-time $(\vec{k};T)$ domain (see Appendix IIb):

$$G_{jm}(\vec{k};T) = U(T)D_T\{P^T_{jm}e^{-\Lambda_T T} + P^L_{jm}e^{-\Lambda_L T}[\cos\omega_n(1-\xi^2)^{1/2}T - \xi(1-\xi^2)^{1/2}\sin\omega_n(1-\xi^2)^{1/2}T]\}, \quad (2.5)$$

where $U(T) = 1$ when $T > 0$ and 0 when $T < 0$, the temporal attenuation constants are $\Lambda_T = D_T k^2 = \eta k^2/\rho$ and $\Lambda_L = \xi\omega_n = D_L k^2 = (3\zeta+4\eta)k^2/6\rho$, the sound wave natural oscillation frequency is $\omega_n = C_L k$, and the damping ratio is $\xi = D_L k/C_L = \Lambda_L/\omega_n$.

The space-frequency $(\vec{R};\omega)$ domain representation of the tensor Green's function of a viscous fluid is obtained by applying the inverse-Fourier three-dimensional spatial transform to expression (2.3) (see Appendix IIb):

$$G_{jm}(R;\omega) = Q^T_{jm}e^{-\bar{\gamma}_T R}/4\pi R + Q^L_{jm}e^{-\gamma_L R}e^{-iK_L R}/4\pi R, \quad (2.6)$$

where $R = |\vec{R}|$, the polarization tensors are $Q^T_{jm} = \delta_{jm} + \partial_j\partial_m/\chi^2_T$ and $Q^L_{jm} = \partial_j\partial_m/\chi^2_T$, the propagation ($K$) and spatial attenuation (γ) constants are defined with reference to

relations (2.4) by:

$$\chi_T = K_T - i\gamma_T \quad \text{and} \quad \chi_L = K_L - i\gamma_L \ , \tag{2.7a}$$

where $K_T = \gamma_T = (\omega/2D_T)^{1/2}$, $\bar{\gamma}_T = i\chi_T = (\omega/D_T)^{1/2} e^{i\pi/4}$, and K_L and γ_L correspond to the positive (+) and negative (-) signs respectively in the expression:

$$K_L, \ \gamma_L \longrightarrow \frac{\omega}{C_L} \left\{ \frac{[1+(2\xi\omega/\omega_n)^2]^{1/2} \pm 1}{2[1+(2\xi\omega/\omega_n)^2]} \right\}^{1/2} \tag{2.7b}$$

Note that the magnitudes of the propagation and attenuation constants for the transverse mode are identical while for the longitudinal mode the propagation constant is always larger than the attenuation constant. Therefore the acoustic energy in the transverse mode follows diffusive characteristics predominantly while in the longitudinal mode it follows propagation characteristics. This corresponds to over-damped and lightly-damped harmonic vibrations respectively of a mechanical system.

The space-time $(\vec{R};T)$ domain representation of the tensor Green's function may be obtained by applying either the inverse-Fourier three-dimensional spatial transform to expression (2.5) or the inverse-Fourier temporal transform to expression (2.6). The result will not be presented at this time.

In previous studies, the temporal and spatial attenuations, if accounted for at all, are included in an ad-hoc fashion following the determination of the deterministic propagation loss result. We, therefore, present the results involving the wave properties of propagation and attenuation within the framework of the Green's function. The tensorial Green's function formalism is convenient since it systematically displays the transverse and longtitudinal polarizations of the sound waves, in addition to prescribing the acoustic response to any arbitrary excitation with the help of the three-dimensional convolution (Duhamel) integral theorem.

It is shown here that the temporal and spatial attenuation of sound waves can be observed directly from the tensor Green's function in the $(\vec{k};T)$ and $(\vec{R};\omega)$ domains as indicated in expressions (2.5) and (2.6), respectively. Temporal attenuation in the transverse part appears in the form of $e^{-\Lambda_T T}$ where $\Lambda_T = D_T k^2 = \eta k^2/\rho$ which is defined as the transverse temporal attenuation constant. The temporal attenuation in the longitudinal part appears in the exponential factor as $e^{-\Lambda_L T}$ and the effect of the attenuation modifies the natural oscillation frequency of propagation through the damping ratio ξ by the factor $(1-\xi^2)^{1/2}$ where the longitudinal temporal attenuation is $\Lambda_L = D_L k^2 = (3\zeta+4\eta)k^2/6\rho$ and the damping ratio is $\xi = \Lambda_L/C_L k$. These temporal attenuation constants of expression (2.5) compare with those obtained by Landau and Lifshitz [2] using energy relations and irreversible thermodynamics (see Appendix IIg).

The spatial attenuation constants for the transverse and longitudinal parts can be observed directly from the tensorial Green's function in the $(\vec{R};\omega)$ domain, epxression (2.6). They appear in exponential form as $e^{-\gamma_T R}$ and $e^{-\gamma_L R}$ resepctively, where $\gamma_T = (\omega/2D_T)^{1/2}$ and

$$\gamma_L = \frac{\omega}{C_L}\left\{\frac{[1+(2\xi\omega/\omega_n)^2]^{1/2}-1}{2[1+(2\xi\omega/\omega_n)^2]}\right\}^{1/2} .$$

Normal Mode Spectra (Cylindrical Coordinate System)

The preceeding section presents the tensor Green's function of sound waves in a viscous fluid of infinite extent in three domains. Once a boundary exists in any spatial direction modifications to the previous results must be made. For boundary-value problems, normal mode methods are particularly useful. Normal mode spectra will be discussed here in both rectangular $(x,y,z;\omega)$ and cylindrical $(r,\phi,z;\omega)$ coordinate systems in the steady-state case (i.e., $(\vec{R};\omega)$ domain).

Energy that is imparted to a viscous fluid shows itself to be distributed between propagation and dissipation processes. This energy partition can be predicted by examining the complex-valued k-poles of the operator $[L_{ij}(\vec{k};\omega)]^{-1}$ in the $(\vec{k};\omega)$ domain (see expression (2.8b) below). The complex-valued k-poles (denoted χ in the previous section) may be defined by $\pm(K_T - i\gamma_T)$

and $\pm(K_L - i\gamma_L)$ which correspond to the transverse (non-dilational) and longitudinal (irrotational) terms, respectively. The real-parts (i.e., K_T and K_L) are associated with the propagation of energy while the imaginary-parts (i.e, γ_T and γ_L) are associated with the attenuation of energy in the spatial domain.

The tensor Green's function in the steady-state $(\vec{R};\omega)$ domain may be related to the $(\vec{k};\omega)$ domain version by the inverse-Fourier spatial transform as:

$$G_{jm}(\vec{R};\omega) = (1/2\pi)^3 \iiint_{-\infty}^{\infty} d^3\vec{k}\, e^{-i\vec{k}\cdot\vec{R}} G_{jm}(\vec{k};\omega) \quad , \qquad (2.8a)$$

where the $(\vec{k};\omega)$ domain version is evaluated algebraically by the relation:

$$G_{jm}(\vec{k};\omega) = -[L_{jm}(\vec{k};\omega)]^{-1} \quad . \qquad (2.8b)$$

The contribution to the integral of expression (2.8) made by the real-part of a complex-valued pole (C.R.P.) can be expressed equivalently in the eigenvalue-domain in terms of two one-dimensional modal Green's functions, g_α and g_β, and one characteristic Green's function g_z. This representation can contain a Fourier, Bessel, or Hankel transform, a z-characteristic Green's function first used by Sommerfeld, and may be written in general as [see Appendix Ia, equation (vii)]:

$$C.R.P. = (-1/4\pi^2) \oint_{C_\alpha} dh_\alpha \oint_{C_\beta} dh_\beta g_\alpha(\alpha,\alpha';h_\alpha) g_\beta(\beta,\beta';h_\beta) g_z(z,z';h_z) \tag{2.9a}$$

$$= \sum_{\mu=0}^{\infty} A_\mu^*(\alpha) A_\mu(\alpha') \sum_{\nu=0}^{\infty} B_\nu^*(\beta) B_\nu(\beta') g_z(z,z';h_z) \ , \tag{2.9b}$$

where C.R.P. means the contribution by the real-part of the complex-valued pole (α,β,z) are the spatial coordinates, and (h_α,h_β,h_z) are their respective eigenvalues. The contour C_α in the complex h_α-plane encloses in the positive sense all the singularities of g_α but no others, while the contour C_β in the complex h_β-plane encloses in the positive sense all the singularities of g_β but no others (see figure 1a). Additional singularities in the h_α and/or h_β planes arise due to $g_z(z,z';h_z)$ where it is generally recognized that there exists an eigenvalue dependence $h_z = h_z(K^2,h_\alpha,h_\beta)$ where K is the real-part of the previously mentioned complex-pole, χ, i.e., K_T or K_L. The detailed dependence of h_z on h_α and h_β being dictated by the particular coordinate system representation of the α-β domain. For example, the eigenvalue relation in rectangular coordinates (x,y,z) is $h_z = K^2 - h_\alpha - h_\beta$ where $\alpha \equiv x$ and $\beta \equiv y$ while in the cylindrical coordinates (r,ϕ,z) the relation is $h_z = K^2 - h_\alpha$ where $\alpha \equiv r$ and $\beta \equiv \phi$.

Upon evaluating the contour integral in the z-characteristic Green's function representation (equation 2.9a) in terms of the discrete and/or continuous spectra arising from the pole and/or branch cut singularities, respectively, of g_α

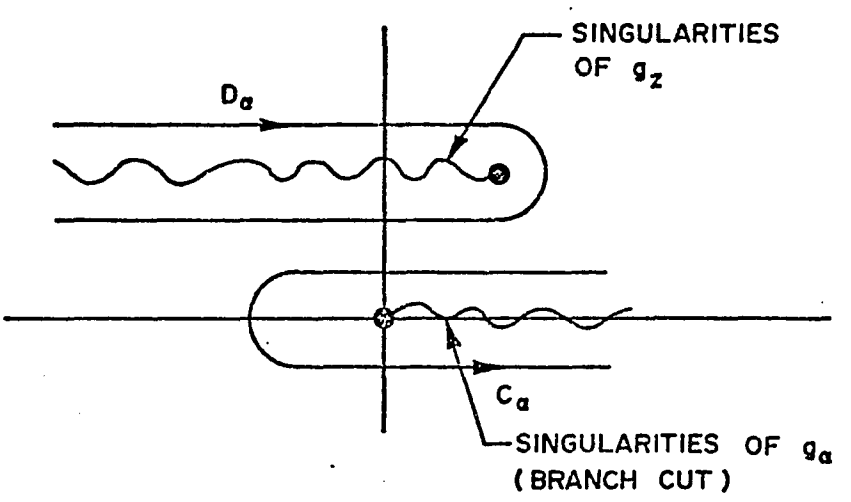

a) h_α – plane

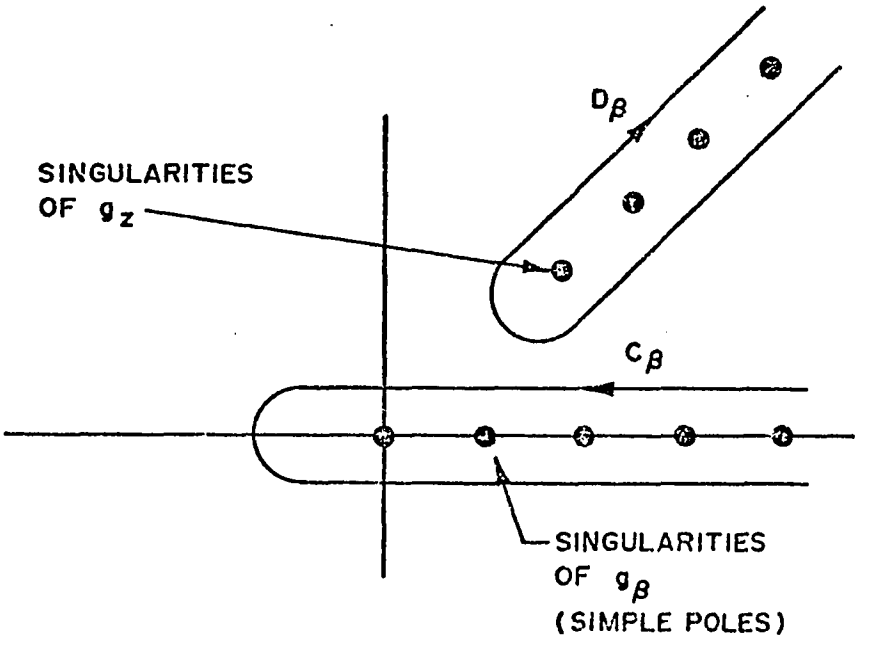

b) h_β – plane

Figure 1 Contours and singularities in the h_α and h_β planes

and g_β and noting that g_z has no singularities inside the contours C_α and C_β, one uncovers the Sommerfeld representation. A variety of integral representations are also obtainable, however, by different deformations of the contours in the h_α and h_β planes as shown in figure 1. The functions g_α, g_β, and g_z are so defined as to vanish rapidly as the various contours approach infinity in these planes.

Considering rectangular coordinates (x,y,z) (see figure 2), one has to determine the three one-dimensional Green's function and delta function representations in order to construct the C.R.P. These are evaluated from the three separated equations of the partial differential equation (2.2). For the z-characteristic direction one has the eigenvalue problem (see Appendix IIc):

$$(\frac{d^2}{dz^2} + h_z)g_z(z,z';h_z) = -\delta(z-z') \ , \qquad (2.10a)$$

where $h_z = \Omega^2 = K^2 - \mu^2 - \lambda^2$, $h_x = \mu^2$, and $h_y = \lambda^2$, with the solution:

$$g_z = e^{-i\Omega|z-z'|}/i2\Omega \ , \quad \text{(see Appendix Ib)} \quad (2.10b)$$

and corresponding delta-function (see Appendix Ia),

$$\delta(z-z') = (-1/2\pi i) \oint dh_z g_z = (1/2\pi) \int_{-\infty}^{\infty} e^{-i\Omega(z-z')} d\Omega. \quad (2.10c)$$

Then considering expression (2.9a) and realizing that similar

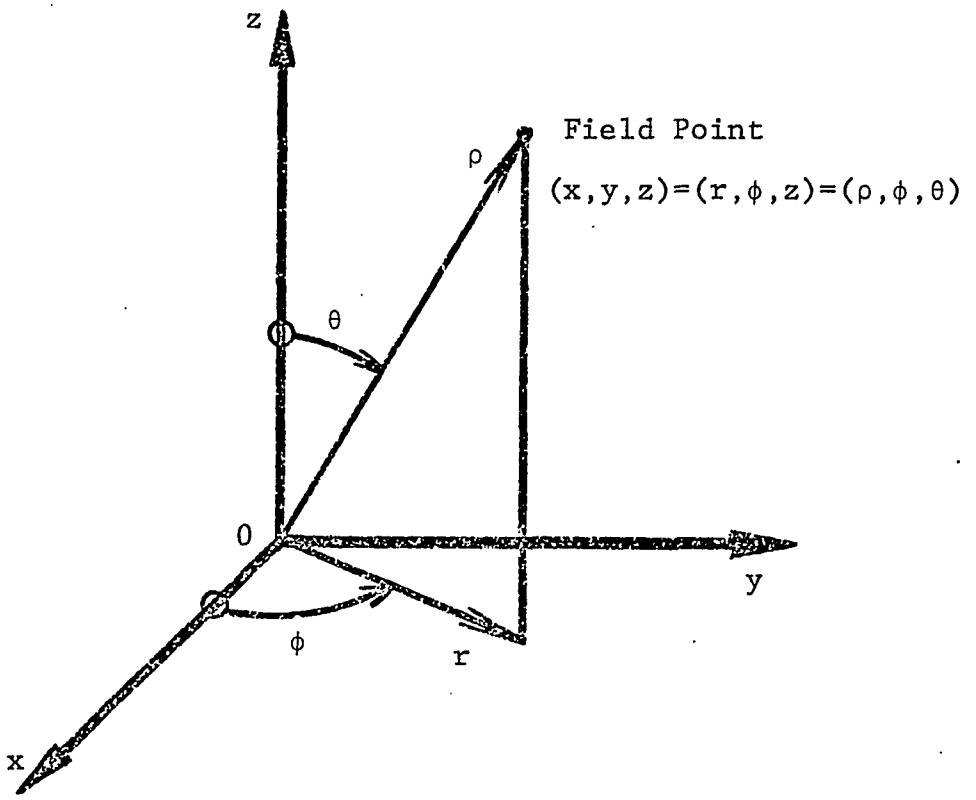

Figure 2 Definition of rectangular (x,y,z), cylindrical (r,ϕ,z), and spherical (ρ,ϕ,θ) coordinate systems

expressions hold for the x and y characteristic directions due to the linearity of this coordinate system, one may write the Fourier-Sommerfeld representation [3] as:

C.R.P.

$$= (-1/4\pi^2) \int_{-\infty}^{\infty} d\mu e^{-i\mu(x-x')} \int_{-\infty}^{\infty} d\lambda e^{-i\lambda(y-y')} \frac{e^{-i(K^2-\mu^2-\lambda^2)^{1/2}|z-z'|}}{i2(K^2-\mu^2-\lambda^2)^{1/2}} . \tag{2.11}$$

Any cyclic (or anti-cyclic) rotation of the x, y, z variables will result in a representation of identical form. In cylindrical coordinates, however, a straight rotation of the r, ϕ, z variables will not result in an equivalent result due to the geometry of the system. Different types of representations are required for the various characteristic directions and will be discussed presently.

Considering cylindrical coordinates (r,ϕ,z) (see figure 2), the path C_α in figure 1a can be deformed into the D_α path, enclosing the singularities in the h_z-plane, to yield the r-characteristic Green's function representation attributed to Levine and Schwinger [4] (see Appendix IIc, Part C):

C.R.P.

$$= (-1/4\pi^2) \oint_{D_\alpha} dh_z \oint_{C_\beta} dh_\phi g_\phi(\phi,\phi';h_\phi) g_z(z,z';h_z) g_r(r,r';K,h_\phi,h_z) \tag{2.12a}$$

$$= \sum_{\nu=0}^{\infty} \Phi_\nu^*(\phi)\Phi_\nu(\phi') \sum_{\Omega=0}^{\infty} Z_\Omega^*(z)Z_\Omega(z') g_r(r,r';K,\nu,\Omega) , \tag{2.12b}$$

where $h_z = \Omega^2$, $h_\phi = \nu^2$, $K^2 = h_r + h_z$, and the normal mode representation in equation (2.12b) has been obtained upon evaluating the integrals over the contours (figure 1b) D_α and C_β in equation (2.12a). The $Z_\Omega(z)$ denotes the eigenfunctions in the z-domain arising from the eigenvalue problem associated with g_z, with h_r being the characteristic eigenvalue.

Alternately, one may deform contour C_β into the contour D_β of the h_z-plane as shown in figure 1b to obtain the ϕ-characteristic Green's function representation attributed to Kontorovich and Lebedev [5]:

$$\text{C.R.P.} = (-1/4\pi^2) \oint_{C_\alpha} dh_r \oint_{D_\beta} dh_z g_z(z,z';h_z) g_r(r,r';h_r,h_\phi) g_\phi(\phi,\phi';h_\phi) \tag{2.13a}$$

$$= \sum_{\Omega=0}^{\infty} Z_\Omega^*(z) Z_\Omega(z') \sum_{\Gamma=0}^{\infty} R_\nu^*(\Gamma r) R_\nu(\Gamma r') g_\phi(\phi,\phi';\nu) \tag{2.13b}$$

The normal mode representation in equation (2.13b) is derived by considerations as expressed above.

Now, considering cylindrical coordinates, one has to examine the one-dimensional Green's function and delta function representations which are used to construct the various C.R.P. representations corresponding to expressions (2.9, 12, and 13). For the radial r-characteristic direction one has the eigenvalue problem:

$$\left(\frac{d}{dr} r \frac{d}{dr} - \frac{h_\phi}{r} + h_r r\right) g_r(r,r';h_r,h_\phi) = -\delta(r-r') \ , \tag{2.14a}$$

where $h_\phi = \nu^2$, $h_r = \Gamma^2 = K^2 - \Omega^2$, $K \to K_{T,L}$, and $h_z = \Omega^2$. The Green's function solution is:

$$g_r = \frac{-i\pi}{2} J_\nu(\Gamma r') H_\nu^{(2)}(\Gamma r); \qquad (2.14b)$$

and whose corresponding delta function has three different representations. The first two representations consider h_r as the eigenvalue and one has the Hankel or Bessel representations respectively as:

$$\delta(r-r')/r' = (-1/2\pi i) \oint dh_r g_r = (1/2) \int_{-\infty}^{\infty} d\Gamma\ \Gamma J_\nu(\Gamma r') H_\nu^{(2)}(\Gamma r)\ , \qquad (2.14c)$$

or

$$\delta(r-r')/r' = \int_0^{\infty} d\Gamma\ \Gamma J_\nu(\Gamma r') J_\nu(\Gamma r)\ . \qquad (2.14d)$$

The third delta-function representation considers h_ϕ as the eigenvalue and one has the Kontorovich-Lebedev representation:

$$r'\ \delta(r-r') = (-1/2\pi i) \oint dh_\phi g_r = (1/2) \int_{-i\infty}^{i\infty} d\nu\ \nu J_\nu(\Gamma r') H_\nu^{(2)}(\Gamma r)\ . \qquad (2.14e)$$

The eigenvalue problem for the angular ϕ-characteristic direction is:

$$\left(\frac{d^2}{d\phi^2} + h_\phi\right) g_\phi(\phi,\phi';h_\phi) = -\delta(\phi-\phi')\ , \quad h_\phi = \nu^2. \qquad (2.15a)$$

The Green's function solution for a periodic system is:

$$g_\phi = -\cos[\nu(\pi-|\phi-\phi'|)]/2\nu \sin \nu\pi \ , \qquad (2.15b)$$

and the corresponding delta function is:

$$\delta(\phi-\phi') = (-1/2\pi i) \oint dh_\phi g_\phi = (1/\pi) \sum_{\nu=0}^{\infty} \varepsilon_\nu \cos \nu(\phi-\phi') \ , \qquad (2.15c)$$

where $\varepsilon_\nu = 1$ for $\nu = 0$ and 2 for all other ν. Note that this integration may be performed without considering g_r since the Bessel function has no poles from parameter ν. The Green's function for a non-periodic system is:

$$g_\phi = e^{-i\nu|\phi-\phi'|}/i2\nu \ , \qquad (2.15d)$$

and the corresponding delta function is:

$$\delta(\phi-\phi') = (1/2\pi) \int_{-\infty}^{\infty} d\nu \ e^{-i\nu(\phi-\phi')} \ . \qquad (2.15e)$$

The eigenvalue problem for the z-characteristic direction is:

$$(\frac{d^2}{dz^2} + h_z) g_z(z,z';h_z) = -\delta(z-z') \ , \quad h_z = \Omega^2 \ , \qquad (2.16)$$

which is exactly equivalent to equation (2.10a). Hence the

solution and corresponding delta function have been presented already as expressions (2.10b) and (2.10c), respectively.

One may now summarize the four cylindrical two-dimensional transforms that operate on their respective one-dimensional characteristic Green's function to construct the four C.R.P. representations in the $(\vec{R};\omega)$ steady-state domain. The Levine-Schwinger, Bessel-Sommerfeld, Hankel-Sommerfeld, and Kontorovich-Lebedev representations of the C.R.P. are written respectively as:

$$(-1/4\pi^2)\left[\oint dh_\alpha g_\alpha\right]\left[\oint dh_\beta g_\beta\right] g_z$$

$$= (1/2\pi^2) \sum_{\nu=0}^{\infty} \varepsilon_\nu \cos \nu(\phi-\phi') \int_{-\infty}^{\infty} d\Omega\ e^{-i\Omega(z-z')} g_r \qquad (2.18a)$$

(from 2.15c, 10c, 14b)

$$= (1/\pi) \sum_{\nu=0}^{\infty} \varepsilon_\nu \cos \nu(\phi-\phi') \int_0^{\infty} d\Gamma\ \Gamma J_\nu(\Gamma r') J_\nu(\Gamma r) g_z \qquad (2.18b)$$

(from 2.15c, 14d, 10b)

$$= (1/2\pi) \sum_{\nu=0}^{\infty} \varepsilon_\nu \cos \nu(\phi-\phi') \int_{-\infty}^{\infty} d\Gamma\ \Gamma J_\nu(\Gamma r') H_\nu^{(2)}(\Gamma r) g_z \qquad (2.18c)$$

(from 2.15c, 14c, 10b)

$$= (1/4\pi) \int_{\infty}^{\infty} d\Omega\ e^{-i\Omega(z-z')} \int_{-i\infty}^{i\infty} d\nu\ \nu J_\nu[(K^2-\Omega^2)^{1/2} r'] H_\nu^{(2)}[K^2-\Omega^2)^{1/2} r]\, g_\phi \qquad (2.18d)$$

(from 2.10c, 14e, 15d)

where K corresponds to either K_T or K_L as: $K_T = (\rho\omega/2\eta)^{1/2}$ and

$$K_L = \frac{\omega}{C_L}\left\{\frac{(1+[\omega(3\zeta+4\eta)/3\rho C_L^2]^2)^{1/2}+1}{2(1+[\omega(3\zeta+4\eta)/3\rho C_L^2]^2)}\right\}^{1/2} .$$

The contribution to the integral of expression (2.8) made by the imaginary part (C.I.P.) of the complex-valued eigenvalue, χ, to the transverse and longitudinal parts can be presented as a tensorial expression in the form:

$$\text{C.I.P.} = Q_{jm}^T e^{-\gamma_T R} \quad \text{and} \quad \text{C.I.P.} = Q_{jm}^L e^{-\gamma_L R} \qquad (2.19)$$

where C.I.P. means the contribution by the imaginary-part of the complex-valued pole of $\iiint_{-\infty}^{\infty} d^3\vec{k}\, e^{-i\vec{k}\cdot\vec{R}} G_{jm}(k;\omega)$, i.e., expression (2.8), Q_{jm} are the appropriate polarization tensors of expression (2.6), and the spatial attenuation constants of (2.7) are: $\gamma_T = (\rho\omega/2\eta)^{1/2}$ and

$$\gamma_L = \frac{\omega}{C_L}\left\{\frac{(1+[\omega(3\zeta+4\eta)/3\rho C_L^2]^2)^{1/2}-1}{2(1+[\omega(3\zeta+4\eta)/3\rho C_L^2]^2)}\right\}^{1/2} .$$

In rectangular coordinates one has:

$$R = [(x-x')^2 + (y-y')^2 + (z-z')^2]^{1/2} .$$

In cylindrical coordinates one has:

$$R = [r^2 + r'^2 - 2rr' \cos(\phi-\phi') + (z-z')^2]^{1/2} ,$$

and expanded in normal modes expression (2.19) reads as:

$$e^{-\gamma R} = \sum_{\mu=0}^{\infty} \varepsilon_\mu (-1)^\mu I_\mu(\gamma R)\cos(2\pi\mu) ,$$

where the modified Bessel function is defined by:

$$I_\mu(x) = e^{-i\mu\pi/2} J_\mu(ix) .$$

Now the general results for the three-dimensional tensor Green's function of a viscous fluid in the steady-state domain are presented in cylindrical coordinates.

From expressions (2.18a) and (2.19) one constructs the Levine-Schwinger representation:

$$G_{jm}(R;\omega) = (Q^T_{jm}/4\pi i) \sum_{\mu=0}^{\infty} \varepsilon_\mu (-1)^\mu I_\mu(\gamma_T R)\cos(2\pi\mu)\{ \sum_{\nu=0}^{\infty} \varepsilon_\nu \cos \nu(\phi-\phi') \cdot$$

$$\cdot \int_0^{\infty} d\Omega e^{-i\Omega(z-z')} J_\nu[(K_T^2-\Omega^2)^{1/2} r'] H_\nu^{(2)}[(K_T^2-\Omega^2)^{1/2} r]\}$$

$$+ (Q^L_{jm}/4\pi i) \sum_{\mu=0}^{\infty} \varepsilon_\mu (-1)^\mu I_\mu(\gamma_L R)\cos(2\pi\mu)\{ \sum_{\nu=0}^{\infty} \varepsilon_\nu \cos \nu(\phi-\phi') \cdot$$

$$\cdot \int_0^{\infty} d\Omega e^{-i\Omega(z-z')} J_\nu[(K_L^2-\Omega^2)^{1/2} r'] H_\nu^{(2)}[(K_L^2-\Omega^2)^{1/2} r]\} ,$$

(2.20)

where $R^2 = r^2 + r'^2 - 2rr'\cos(\phi-\phi') + (z-z')^2$ for cylindrical coordinates. From expressions (2.18b) and (2.19) one constructs the Bessel-Sommerfeld representation:

$$G_{jm}(R;\omega) = (Q^T_{jm}/2\pi i)\sum_{\mu=0}^{\infty}\varepsilon_\mu(-1)^\mu I_\mu(\gamma_T R)\cos(2\pi\mu)\{\sum_{\nu=0}^{\infty}\varepsilon_\nu \cos\nu(\phi-\phi')\cdot$$

$$\cdot\int_0^{\infty} d\Gamma\ \Gamma J_\nu(\Gamma r')J_\nu(\Gamma r)[K_T^2-\Gamma^2]^{-1/2}\exp(-i[K_T^2-\Gamma^2]^{1/2}|z-z'|)\}$$

$$+ (Q^L_{jm}/2\pi i)\sum_{\mu=0}^{\infty}\varepsilon_\mu(-1)^\mu I_\mu(\gamma_L R)\cos(2\pi\mu)\{\sum_{\nu=0}^{\infty}\varepsilon_\nu \cos\nu(\phi-\phi')\cdot$$

$$\cdot\int_0^{\infty} d\Gamma\ \Gamma J_\nu(\Gamma r')J_\nu(\Gamma r)[K_L^2-\Gamma^2]^{-1/2}\exp(-i[K_L^2-\Gamma^2]^{1/2}|z-z'|)\}\ .$$

From expression (2.18c) and (2.19) one constructs the Hankel-Sommerfeld representation:

$$G_{jm}(R;\omega) = (Q^T_{jm}/4\pi i)\sum_{\mu=0}^{\infty}\varepsilon_\mu(-1)^\mu I_\mu(\gamma_T R)\cos(2\pi\mu)\{\sum_{\nu=0}^{\infty}\varepsilon_\nu \cos\nu(\phi-\phi')\cdot$$

$$\cdot\int_{-\infty}^{\infty} d\Gamma\ \Gamma J_\nu(\Gamma r')H_\nu^{(2)}(\Gamma r)[K_T^2-\Gamma^2]^{-1/2}\exp(-i[K_T^2-\Gamma^2]^{1/2}|z-z'|)\}$$

$$+ (Q^L_{jm}/4\pi i)\sum_{\mu=0}^{\infty}\varepsilon_\mu(-1)^\mu I_\mu(\gamma_L R)\cos(2\pi\mu)\{\sum_{\nu=0}^{\infty}\varepsilon_\nu \cos\nu(\phi-\phi')\cdot$$

$$\cdot\int_{-\infty}^{\infty} d\Gamma\ \Gamma J_\nu(\Gamma r')H^{(2)}(\Gamma r)[K_L^2-\Gamma^2]^{-1/2}\exp(-i[K_L^2-\Gamma^2]^{1/2}|z-z'|)\}\ .$$

(2.22)

From expressions (2.18d) and (2.19) one constructs the Kontorovich-Lebedev representation:

$$G_{jm}(R;\omega) = (Q^T_{jm}/8\pi i)\sum_{\mu=0}^{\infty}\varepsilon_\mu(-1)^\mu I_\mu(\gamma_T R)\cos(2\pi\mu)\{\int_{-\infty}^{\infty} d\Omega e^{-i\Omega(z-z')} \cdot$$

$$\cdot \int_{-i\infty}^{i\infty} d\nu\ J_\nu[(K_T^2-\Omega^2)^{1/2}r']H_\nu^{(2)}[(K_T^2-\Omega^2)^{1/2}r]\exp(-i\nu|\phi-\phi'|)\}$$

$$+ (Q^L_{jm}/8\pi i)\sum_{\mu=0}^{\infty}\varepsilon_\mu(-1)^\mu I_\mu(\gamma_L R)\cos(2\pi\mu)\{\int_{-\infty}^{\infty} d\Omega e^{-i\Omega(z-z')} \cdot$$

$$\cdot \int_{-i\infty}^{i\infty} d\nu\ J_\nu[(K_L^2-\Omega^2)^{1/2}r']H_\nu^{(2)}[(K_L^2-\Omega^2)^{1/2}r]\exp(-i\nu|\phi-\phi'|)\}\ . \qquad (2.23)$$

Note in the four preceeding representations that two of the parameters are related by: $K^2 = \Gamma^2 + \Omega^2$ and hence the appropriate parameter (Γ or Ω) is selected by the integration or summation variables.

Viscoelastic Solid

Tensor Green's Function in the Rectangular Coordinate System

To facilitate the determination of the tensor Green's function of a viscoelastic solid in the various domains, it is convenient to first evaluate it in the wavenumber-frequency $(\vec{k};\omega)$ domain where its solution is algebraic. This process is accomplished below by deriving the equation of motion in

in the space-time $(\vec{R};T)$ domain, transforming to the $(\vec{k};\omega)$ domain, and then algebraically solving for the Green's function. From this $(\vec{k};\omega)$ domain result, the Green's function is determined in its $(\vec{k};T)$ and $(\vec{R};\omega)$ domain representations upon utilization of the appropriate inverse-Fourier temporal and spatial integral-transforms.

The linearized equation of motion of a viscoelastic solid in the displacement vector field u_j with external forcing per unit mass f_i can be written in the space-time $(\vec{r};t)$ domain as: $L_{ij}(\vec{r};t)u_j(\vec{r};t) = f_i$, where the partial differential operator (see Appendix IId) is written as:

$$L_{ij}(\vec{r};t) = \{[\partial_t^2-(\mu/\rho)\partial^2]\delta_{ij}-[(\lambda+\mu)/\rho]\partial_i\partial_j\} \qquad (2.24)$$

where $\partial_t^2 = \partial^2/\partial t^2$, μ and λ are the Lame parameters which for Voigt damping may be defined by $\mu = (\mu'+\mu''\partial_t)$ and $\lambda = (\lambda'+\lambda''\partial_t)$, ∂^2 is the Laplacian, δ_{ij} is the Kronnecker delta, ρ is the density of the solid, and ∂_i is the spatial gradient operator. The partial differential equation for the tensor Green's function $G_{jm}(\vec{R};T)$ in the $(\vec{R};T)$ domain is given with reference to relation (2.24) by the expression:

$$L_{ij}(\vec{r};t)G_{jm}(\vec{R};T) = \delta_{im}\delta^3(\vec{R})\delta(T) \ , \qquad (2.25)$$

where $\vec{R} = \vec{r} - \vec{r}'$, $T = t - t'$, $(\vec{r}';t')$ and $(\vec{r};t)$ are the location of the impulsive point source and observer point respectively,

and δ^3 is the product of three spatial Dirac delta functions (one for each coordinate direction). Using the temporal and three-dimensional spatial Fourier transforms on equation (2.25) one obtains the transformed tensor Green's function in the wavenumber-frequency $(\vec{k};\omega)$ domain as (see Appendix IIe for the details):

$$G_{jm}(\vec{k};\omega) = \frac{-P^T_{jm}}{\omega^2 - i(\frac{\mu''}{\rho})k^2\omega - (\frac{\mu'}{\rho})k^2} + \frac{-P^L_{jm}}{\omega^2 - i(\frac{\lambda''+2\mu''}{\rho})k^2\omega - (\frac{\lambda'+2\mu'}{\rho})k^2}, \tag{2.26}$$

where the transverse (T) and longitudinal (L) components of the response are observable as distinct terms, the polarization tensors P_{jm} prescribe the directionality of each term, $P^T_{jm} = \delta_{jm} - (k_j k_m/k^2)$, $P^L_{jm} = k_j k_m/k^2$, and $k = |\vec{k}|$, i.e. the magnitude of the three-dimensional wavenumber vector.

By applying the inverse-Fourier temporal transform to expression (2.26) one obtains the retarded tensor Green's function in the wavenumber-time $(\vec{k};T)$ domain (see Appendix IIe):

$$G_{jm}(\vec{k};T) = U(T)\{P^T_{jm} e^{-\Lambda_T T} \omega_{nT}^{-1}(1-\xi_T^2)^{-1/2} \sin[\omega_{nT}(1-\xi_T^2)^{1/2} T]$$

$$+ P^L_{jm} e^{-\Lambda_L T} \omega_{nL}^{-1}(1-\xi_L^2)^{-1/2} \sin[\omega_{nL}(1-\xi_L^2)^{1/2} T]\} \tag{2.27}$$

where $U(T) = 1$ when $T > 0$ and 0 when $T < 0$, the temporal attenuation constants are $\Lambda_T = \mu'' k^2/2\rho$ and $\Lambda_L = (\lambda''+2\mu'')k^2/2\rho$,

the sound wave natural oscillation frequencies are ω_{nT} $= k(\mu'/\rho)^{1/2}$ and $\omega_{nL} = k[(\lambda'+2\mu')/\rho]^{1/2}$, and the damping ratios are $\xi_T^2 = \mu''^2k^2/4\mu'\rho$ and $\xi_L^2 = (\lambda''+2\mu'')^2k^2/4(\lambda'+2\mu')\rho$.

The space-frequency $(\vec{R};\omega)$ domain representation of the tensor Green's function of a viscoelastic solid is obtained by applying the inverse-Fourier three-dimensional spatial transform to expression (2.26)(see Appendix IIe):

$$G_{jm}(R;\omega) = \left[\frac{\rho(\mu'-i\omega\mu'')}{\mu'^2+\omega^2\mu''^2}\,\delta_{jm} + \frac{1}{\omega^2}\,\partial_j\partial_m\right]\frac{e^{-\gamma_T R}\,e^{-iK_T R}}{4\pi R}$$

$$- \frac{1}{\omega^2}\,\partial_j\partial_m\,\frac{e^{-\gamma_L R}\,e^{-iK_L R}}{4\pi R} \qquad (2.28a)$$

where $R = |\vec{R}|$, the propagation (K) and spatial attenuation (γ) constants correspond to the positive (+) and negative (-) signs respectively in the following expressions (where $\chi \equiv K - i\gamma$):

$$K_T,\ \gamma_T \longrightarrow \frac{\omega}{C_T}\left\{\frac{[1+(2\xi_T\omega/\omega_{nT})^2]^{1/2}\pm 1}{2[1+(2\xi_T\omega/\omega_{nT})^2]}\right\}^{1/2}, \qquad (2.28b)$$

$$K_L,\ \gamma_L \longrightarrow \frac{\omega}{C_L}\left\{\frac{[1+(2\xi_L\omega/\omega_{nL})^2]^{1/2}\pm 1}{2[1+(2\xi_L\omega/\omega_{nL})^2]}\right\}^{1/2}, \qquad (2.28c)$$

where $C_T = \mu'/\rho$ (transverse sound speed) and $C_L = (\lambda'+2\mu')/\rho$

longitudinal sound speed). Note that the magnitude of the propagation (K) constant is always greater than the attenuation (γ) constant. Therefore the acoustic energy in both the transverse and longtitudinal modes propagate in space with some attenuation due to the viscous parameters λ'' and μ''. This behavior corresponds to lightly-damped harmonic vibrations of a mechanical system.

The space-time $(\vec{R};T)$ domain representation of the tensor Green's function may be obtained by applying either the inverse-Fourier three-dimensional spatial transform to expression (2.27) or the inverse-Fourier temporal transform to expression (2.28). The result will not be presented at this time.

In previous studies, the temporal and spatial attenuations, if accounted for at all, are included in an ad-hoc fashion following the determination of the deterministic propagation loss result. We therefore present the results involving the wave properties of propagation and attenuation within the framework of the Green's function. The tensorial Green's function formalism is convenient since it systematically displays the transverse and longitudinal polarizations of the sound waves, in addition to prescribing the acoustic response to any arbitrary excitation with the help of the three-dimensional convolution (Duhamel) integral theorem in the (R;T) domain.

It is shown here that the temporal and spatial attenuation of sound waves can be observed directly from the tensor

Green's function in the $(\vec{k};T)$ and $(\vec{R};\omega)$ domains as indicated in expressions (2.27) and (2.28), respectively. The temporal attenuation constants (Λ) for both transverse and longitudinal parts appear in the exponential decay expression as $e^{-\Lambda T}$ and their effects also modify the natural oscillation frequencies by the factor $(1 - \xi^2)^{1/2}$ where ξ is the damping ratio. Since $\Lambda_T = \mu'' k^2/2\rho$ and $\Lambda_L = (\lambda''+2\mu'')k^2/2\rho$ then one can express both damping ratios in terms of these attenuation constants as $\xi_T = (\Lambda_T/\omega_{nT})$ and $\xi_L = (\Lambda_L/\omega_{nL})$. The definition of these temporal attenuation constants agree with those obtained by Landau and Lifshitz [6] using energy relations and irreversible thermodynamics.

The spatial attenuation constants for the transverse and longitudinal parts can be observed directly from the tensorial Green's function in the $(\vec{R};\omega)$ domain, expression (2.28). They appear in exponential form as $e^{-\gamma_T R}$ and $e^{-\gamma_L R}$ respectively, where:

$$\gamma_q = \frac{\omega}{C_q}\left\{\frac{[1+(2\xi_q\omega/\omega_{nq})^2]^{1/2}-1}{2[1+(2\xi_q\omega/\omega_{nq})^2]}\right\}, \quad q \to T \text{ and } L .$$

Normal Mode Spectra (Spherical Coordinate System)

The preceeding section presents the tensor Green's function for sound waves in a viscoelastic solid of infinite extent in three Fourier domains. For boundary-value problems,

normal mode methods are particularly useful. Normal mode spectra will be discussed here in the spherical (ρ,ϕ,θ) coordinate system for the steady-state case, i.e., $(\vec{R};\omega)$ domain.

The normal mode representations already presented in the rectangular and cylindrical systems (for a viscous fluid) are still valid for the viscoelastic solid. This means that equations (2.8) through (2.23) may be applied to a viscoelastic solid with only the modification of the parameters K_T, γ_T, K_L, and γ_L, which are evaluated from a different governing equation. The appropriate parameters are defined for the solid in equations (2.28b and 2.28c). The presentation following will be in the spherical system and may be analogously applied to a viscous fluid upon utilization of the appropriate K and γ parameters.

In the spherical system there are three representations of the contribution of the real-part (C.R.P.) of the complex-valued eigenvalue χ to the Green's function in the steady-state domain. These representations have been presented as expressions (2.9), (2.12), and (2.13). To obtain the necessary one-dimensional Green's functions and delta functions to construct the C.R.P., one looks at the three separated one-dimensional eigenvalue problems of the partial differential equation (2.25).

For spherical coordinates $(\alpha,\beta,\gamma) \rightarrow (\rho,\phi,\theta)$ (see Figure 2), one has the following expressions for the radial-direction (see Appendix IIc):

$$g_\rho(\rho,\rho';K_q,\ell) = iK_q j_\ell(K_q\rho')h_\ell^{(2)}(K_q\rho) \qquad (2.29a)$$

$$\frac{\delta(\rho-\rho')}{\rho^2} = \left(\frac{-1}{2\pi i}\right)\oint dh_\rho g_\rho$$

$$= (K_q/2\pi)\int_{-1/2-i\infty}^{-1/2+i\infty} d\ell(2\ell+1)j_\ell(K_q\rho')h_\ell^{(2)}(K_q\rho) \ , \qquad (2.29b)$$

where the spherical Hankel function of the first kind and Bessel function are defined by:

$$h_\ell^{(2)}(x) = (\pi/2x)^{1/2}H^{(2)}_{\ell+1/2}(x) \qquad (2.29c)$$

and

$$j_\ell(x) = (\pi/2x)^{1/2}J_{\ell+1/2}(x) \ , \qquad (2.29d)$$

respectively. The azimuthal-direction results are identical to those of the cylindrical coordinate system and have been presented as (2.15). The polar-direction results are:

$$g_\theta(\theta,\theta';\ell,\nu) = \frac{-\pi}{2}\frac{\Gamma(\ell+\nu+1)}{\Gamma(\ell-\nu+1)}\frac{P_{-\ell}^{-\nu}(\cos\theta')P_{-\ell}^{-\nu}(-\cos\theta)}{\sin\pi(\ell-\nu)} \qquad (2.30a)$$

$$\sin\theta'\delta(\theta-\theta') = \left(\frac{-1}{2\pi i}\right)\oint dh_\phi g_\theta$$

$$= \frac{i}{2}\int_{-i\infty}^{i\infty} d\nu\ \nu\frac{\Gamma(\ell+\nu+1)}{\Gamma(\ell-\nu+1)}\frac{P_\ell^{-\nu}(\cos\theta')P_\ell^{-\nu}(-\cos\theta)}{\sin\pi(\ell-\nu)}$$

(2.30b)

$$\frac{\delta(\theta-\theta')}{\sin\theta'} = \left(\frac{-1}{2\pi i}\right) \oint dh_\theta g_\theta$$

$$= \frac{1}{4\pi i} \sum_{\ell=0}^{\infty} (2\ell+1) \frac{\Gamma(\ell+\nu+1)}{\Gamma(\ell-\nu+1)} \frac{P_\ell^{-\nu}(\cos\theta')P_\ell^{-\nu}(-\cos\theta)}{\sin \pi(\ell-\nu)} \qquad (2.30c)$$

where the associated Legendre function is denoted $P_\ell^{-\nu}$ and the gamma function by Γ. The three different constructions of the C.R.P. are then presented as:

$$\text{C.R.P.} = \frac{iK_q}{2\pi} \sum_{\ell=0}^{\infty} \sum_{\nu=0}^{\ell} \varepsilon_\nu \cos\nu(\phi-\phi')(2\ell+1) \frac{\Gamma(\ell+\nu+1)}{\Gamma(\ell-\nu+1)} \cdot$$

$$\cdot \frac{P_\ell^{-\nu}(\cos\theta')P_\ell^{-\nu}(-\cos\theta)}{\sin \pi(\ell-\nu)} \; j_\ell(K_q\rho')h_\ell^{(2)}(K_q\rho) \qquad (2.31a)$$

(from 2.15c, 30c, 29a)

$$= \frac{-1}{4\pi} \int_{-1/2-i\infty}^{-1/2+i\infty} d\ell(2\ell+1) j_\ell(K_q\rho')h_\ell^{(2)}(K_q\rho) \sum_{\nu=0}^{\ell} \varepsilon_\nu \cos\nu(\phi-\phi') \cdot$$

$$\cdot \frac{\Gamma(\ell+\nu+1)}{\Gamma(\ell-\nu+1)} \frac{P_\ell^{-\nu}(\cos\theta')P_\ell^{-\nu}(-\cos\theta)}{\sin \pi(\ell-\nu)} \qquad (2.31b)$$

(from 2.29b, 15c, 30a)

$$= \frac{1}{4\pi} \int_{-1/2-i\infty}^{-1/2+i\infty} d\ell(2\ell+1) j_\ell(K_q\rho')h_\ell^{(2)}(K_q\rho) \int_{\infty}^{i\infty} d\nu \, \nu \frac{\Gamma(\ell+\nu+1)}{\Gamma(\ell-\nu+1)} \cdot$$

$$\cdot \frac{P_\ell^{-\nu}(\cos\theta')P_\ell^{-\nu}(-\cos\theta)}{\sin \pi(\ell-\nu)} \; \frac{e^{-i\nu|\phi-\phi'|}}{i2\nu} \qquad (2.31c)$$

(from 2.29b, 30b, 15c)

The contribution to the integral of expression (2.8) made by the imaginary-part (C.I.P.) of a complex-valued eigenvalue χ may be written in the form:

$$\text{C.I.P.} = Q^{T}_{jm} e^{-\gamma_T R} \quad \text{and} \quad \text{C.I.P.} = Q^{L}_{jm} e^{-\gamma_L R} , \qquad (2.32)$$

where Q_{jm} are the same polarization tensors as in (2.6) and the spatial attenuation constants γ have been given in expressions (2.28b and 2.28c). In spherical coordinates one has:

$$R = \{\rho^2+\rho'^2-2\rho\rho'[\cos\theta\cos\theta'+\sin\theta\sin\theta'\cos(\phi-\phi')]\}^{1/2}. \qquad (2.33a)$$

The expansion of (2.32) in terms of normal modes is:

$$e^{-\gamma R} = \sum_{\mu=0}^{\infty} (-1)^{\mu}(2\mu+1)P_{\mu}(\cos 2\pi\mu) i_{\mu}(\gamma R) , \qquad (2.33b)$$

where P_{μ} is the ordinary Legendre function and the modified spherical Bessel function is defined by the relation:

$$i_{\mu}(x) = (\pi/2x)^{1/2} I_{\mu}(x) = (\pi/2x)^{1/2} e^{-i\mu\pi/2} J_{\mu}(ix). \qquad (2.33c)$$

Recalling that there exist both transverse and longitudinal modes of energy transport in a viscoelastic solid, one may conbine the contributions of the real (C.R.P.) and imaginary (C.I.P.) parts of the complex-valued poles of integral (2.29) to yield the general result for the three-

dimensional tensor Green's function of a viscous fluid in the steady-state domain.

In spherical coordinates, the total tensorial Green's function has the following three representations. From expressions (2.33b and 30a) one constructs the Legendre-Levine-Schwinger representation:

$$
\begin{aligned}
&G_{jm}(R;\omega) \\
&= \frac{iQ^{T}_{jm}K_T}{2\pi}\sum_{\mu=0}^{\infty}(-1)^{\mu}(2\mu+1)P_{\mu}(\cos 2\pi\mu)i_{\mu}(\gamma_T R)\left\{\sum_{\ell=0}^{\infty}\sum_{\nu=0}^{\ell}\varepsilon_{\nu}\cos\nu(\phi-\phi')\cdot\right. \\
&\left.\cdot(2\ell+1)\frac{\Gamma(\ell+\nu+1)}{\Gamma(\ell-\nu+1)}\frac{P_{\ell}^{-\nu}(\cos\theta')P_{\ell}^{-\nu}(-\cos\theta)}{\sin\pi(\ell-\nu)}j_{\ell}(K_T\rho')h_{\ell}^{(2)}(K_T\rho)\right\} \\
&+\frac{iQ^{L}_{jm}K_L}{2\pi}\sum_{\mu=0}^{\infty}(-1)^{\mu}(2\mu+1)P_{\mu}(\cos 2\pi\mu)i_{\mu}(\gamma_L R)\left\{\sum_{\ell=0}^{\infty}\sum_{\nu=0}^{\ell}\varepsilon_{\nu}\cos\nu(\phi-\phi')\cdot\right. \\
&\left.\cdot(2\ell+1)\frac{\Gamma(\ell+\nu+1)}{\Gamma(\ell-\nu+1)}\frac{P_{\ell}^{-\nu}(\cos\theta')P_{\ell}^{-\nu}(-\cos\theta)}{\sin\pi(\ell-\nu)}j_{\ell}(K_L\rho')h_{\ell}^{(2)}(K_L\rho)\right\}.
\end{aligned}
\tag{2.34a}
$$

From expressions (2.33b and 30b) one constructs the Carslaw-spherical Hankel representation [7]:

$$G_{jm}(R;\omega)$$

$$= \frac{-Q^T_{jm}}{4\pi} \sum_{\mu=0}^{\infty} (-1)^{\mu}(2\mu+1)P_{\mu}(\cos 2\pi\mu) i_{\mu}(\gamma_T R) \left\{ \int_{-1/2-i\infty}^{-1/2+i\infty} d\ell(2\ell+1) \cdot \right.$$

$$\left. \cdot j_{\ell}(K_T\rho') h^{(2)}_{\ell}(K_T\rho) \sum_{\nu=0}^{\ell} \varepsilon_{\nu} \cos\nu(\phi-\phi') \frac{\Gamma(\ell+\nu+1)}{\Gamma(\ell-\nu+1)} \frac{P^{-\nu}_{\ell}(\cos\theta') P^{-\nu}_{\ell}(-\cos\theta)}{\sin \pi(\ell-\nu)} \right\}$$

$$- \frac{Q^L_{jm}}{4\pi} \sum_{\mu=0}^{\infty} (-1)^{\mu}(2\mu+1)P_{\mu}(\cos 2\pi\mu) i_{\mu}(\gamma_L R) \left\{ \int_{-1/2-i\infty}^{-1/2+i\infty} d\ell(2\ell+1) j_{\ell}(K_L\rho') \cdot \right.$$

$$\left. \cdot h^{(2)}(K_L\rho) \sum_{\nu=0}^{\ell} \varepsilon_{\nu} \cos\nu(\phi-\phi') \frac{\Gamma(\ell+\nu+1)}{\Gamma(\ell-\nu+1)} \frac{P^{-\nu}_{\ell}(\cos\theta') P^{-\nu}_{\ell}(-\cos\theta)}{\sin \pi(\ell-\nu)} \right\} \quad (2.34b)$$

From expressions (2.33b and 30c) one constructs the Legendre-spherical Hankel representation:

$$G_{jm}(R;\omega)$$

$$= \frac{-iQ^T_{jm}}{8\pi} \sum_{\mu=0}^{\infty} (-1)^{\mu}(2\mu+1)P_{\mu}(\cos 2\pi\mu) i_{\mu}(\gamma_T R) \left\{ \int_{-1/2-i\infty}^{-1/2+i\infty} d\ell(2\ell+1) \cdot \right.$$

$$\left. \cdot j_{\ell}(K_T\rho') h^{(2)}_{\ell}(K_T\rho) \int_{-i\infty}^{i\infty} d\nu \frac{\Gamma(\ell+\nu+1)}{\Gamma(\ell-\nu+1)} \frac{P^{-\nu}_{\ell}(\cos\theta') P^{-\nu}_{\ell}(-\cos\theta)}{\sin \pi(\ell-\nu)} e^{-i\nu|\phi-\phi'|} \right\}$$

$$- \frac{iQ^L_{jm}}{8\pi} \sum_{\mu=0}^{\infty} (-1)^{\mu}(2\mu+1)P_{\mu}(\cos 2\pi\mu) i_{\mu}(\gamma_L R) \left\{ \int_{-1/2-i\infty}^{-1/2+i\infty} d\ell(2\ell+1) j_{\ell}(K_L\rho') \cdot \right.$$

$$\left. \cdot h^{(2)}_{\ell}(K_L\rho) \int_{-i\infty}^{i\infty} d\nu \frac{\Gamma(\ell+\nu+1)}{\Gamma(\ell-\nu+1)} \frac{P^{-\nu}_{\ell}(\cos\theta') P^{-\nu}_{\ell}(-\cos\theta)}{\sin \pi(\ell-\nu)} e^{-i\nu|\phi-\phi'|} \right\} \quad (2.34c)$$

Conclusions

This chapter has laid the ground work for a general field description of two viscous media. In particular, the field of a viscous fluid and viscoelastic solid has been presented in the various Fourier domains $(\vec{k};\omega)$, $(\vec{k};T)$, and $(\vec{R};\omega)$, for the rectangular coordinate system. Then the description of the field in the space-frequency $(\vec{R};\omega)$ domain has been generalized for any orthogonal coordinate system. Here the cylindrical and spherical systems have been used as an example, but the procedure is similar for any coordinate system.

Since the field for both the fluid and solid is a vector field, the Green's function must be a second order tensor to insure a complete description. The tensor Green's function makes apparent that the acoustic energy is partitioned into two distinct polarizations, $\psi = \psi_T + \psi_L$, where ψ represents the velocity potential for the fluid, $\psi = \nabla \cdot \vec{v}$, and the displacement potential for the solid, $\vec{u} = \nabla\psi$. The two polarizations are called transverse and longitudinal. The transverse terms are rotational (non-dilational, $\nabla\cdot\vec{v}_T = 0$) motions while the longitudinal terms are dilational (irrotational, $\nabla\times\vec{v}_L = \vec{o}$) motions. When couple-stresses are considered [8], the transverse polarization itself has two distinct modes but this is not of interest here.

The transverse mode of a viscous fluid is fundamentally different from the rest. It is a purely diffusive mode, that is, energy is attenuated with no propagation, in the temporal

$(\vec{k};T)$ domain and is a highly-damped propagation mode in the spatial $(\vec{R};\omega)$ domain. On the other hand, the longitudinal mode of a viscous fluid and both modes of the viscoelastic solid exhibit identical structures, namely, lightly-damped propagation of acoustic energy in both time and space. Note that the terms "highly-damped" and "lightly-damped" propagation come from the mechanical system analogy with the damped harmonic oscillator which is applicable to the field description in the $(\vec{k};T)$ domain for temporal considerations and the $(\vec{R};\omega)$ domain for spatial considerations.

In the evaluation of the field in the $(\vec{k};T)$ domain, an integral arises for which the ω-poles are defined by the expression $\omega = \pm\omega_{nd} + i\Lambda$, where $\omega_{nd} = \omega_n\sqrt{1-\xi^2}$, $\omega_n = Ck$, $\xi = \Lambda/\omega_n$, and the Λ's are defined in the main text. As seen in expressions (2.5) and (2.27), the real-part of the complex-valued pole ω_{nd} appears in the temporal propagation factor $\sin(\omega_{nd}T)$ while the imaginary-part Λ appears in the temporal attenuation factor $e^{-\Lambda T}$. This is a general result for both fluids and solids, except for the transverse mode of the viscous fluid for which case the propagation factor does not appear.

In the evaluation of the field in the $(\vec{R};\omega)$ domain, an integral arises for which the k-poles are defined by the expression $k = \pm(K-i\gamma)$ where the K's and γ's are defined in the main text. As seen in expressions (2.6) and (2.28), the real-part of the complex-valued pole K appears in the spatial

propagation factor e^{-iKR} while the imaginary-part γ appears in the spatial attenuation factor $e^{-\gamma R}$. This is a general result for both fluids and solids and it is apparent that $K > \gamma$ in each case.

With this information one may consider the propagation and attenuation as separate processes by looking at the real-part or imaginary-part of the complex-valued poles, respectively. From figure 3 one sees that this implies that figure 3a may be simplified to figure 3b for consideration of the propagation of energy while figure 3c would be appropriate for consideration of the attenuation of energy.

The imaginary-part of the complex-valued ω-pole is the temporal attenuation constant Λ, which is directly found in the exponential decay factor $e^{-\Lambda T}$ of the $(\vec{k};T)$ domain description of the field. The Green's function methodology defines this parameter explicitly in the process of deriving the field in the $(\vec{k};T)$ domain, whereas other methodologies treat the attenuation constant as a separate problem to wrestle. The spatial attenuation constant γ is the imaginary part of the complex-valued k-poles. It is analogously found explicitly defined in the exponential decay factor $e^{-\gamma R}$ upon evaluation of the field in the $(\vec{R};\omega)$ domain using the Green's function methodology. So in using the Green's function techniques the various attenuation constants are naturally evaluated in the process of deriving the field in the various Fourier domains.

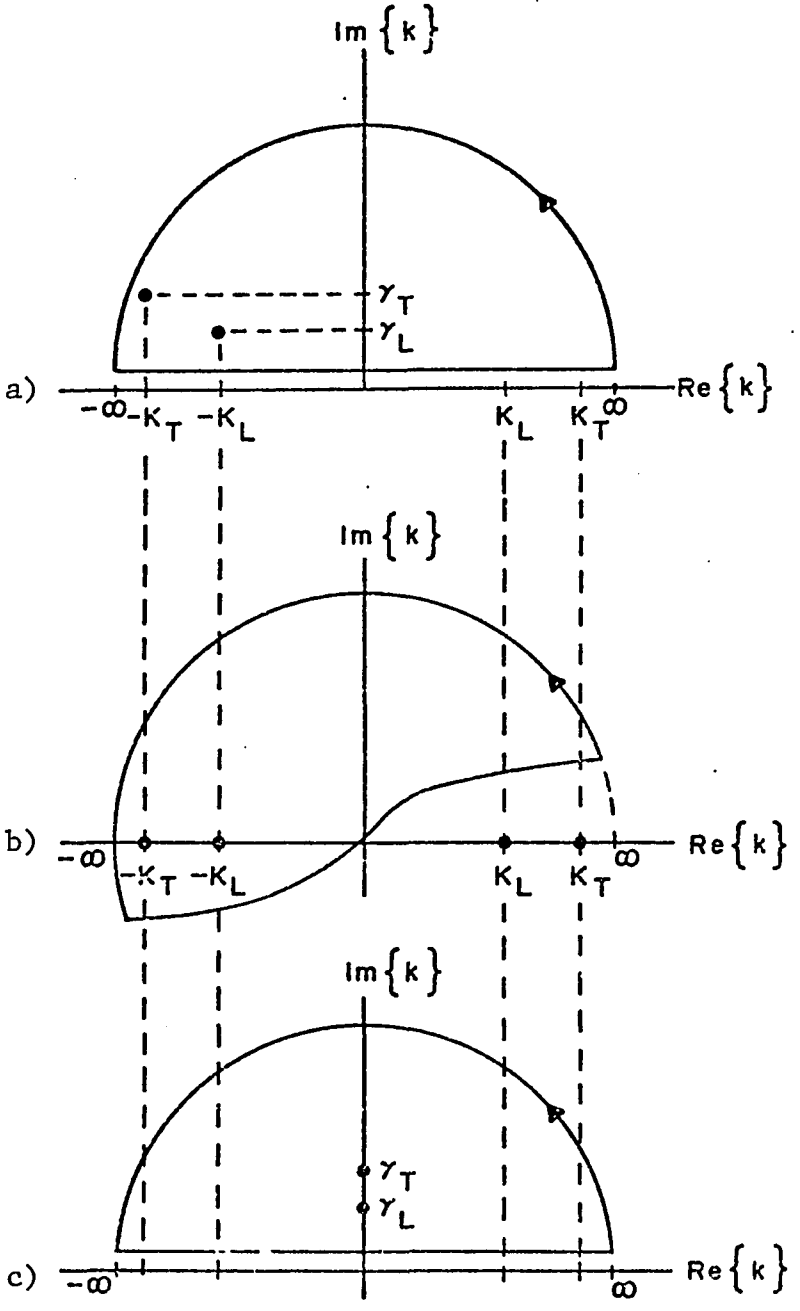

Figure 3 Separation of the real and imaginary components of the complex-valued eigenvalues χ in the $(\vec{k};\omega)$ domain

The evaluation of these attenuation constants is treated as a separate problem by Landau and Lifshitz. The authors use energy relations and irreversible thermodynamics to evaluate these parameters for both thermo-viscous fluids [2] and thermoviscoelastic solids [6]. Note that for the viscoelastic solid one has the definitions: $\zeta = (\lambda''+2\mu''/3)$ and $\eta = \mu''$. The authors appear to derive temporal attenuation constants Λ that agree with this study, but then they divide them by the sound speed to dimensionally yield a spatial attenuation constant γ, that is: $\gamma = \Lambda/C$. The temporal and spatial attenuation constants of this study are not related in this manner. Appendix IIf summarizes the Green's functions for five scalar equations in the four Fourier domains; $(\vec{k};\omega)$, $(\vec{k};T)$, $(\vec{R};\omega)$, and $(\vec{R};T)$. The equations are: the undamped wave equation, the diffusion equation, the dissipative wave equation, the dissipative wave equation with space-time coupling, and the dissipative wave equation with frequency-dependent viscosity coefficients. The purpose of this summary is for comparison with the scalar equations for the transverse and longitudinal modes of both the viscous fluid and the solid.

Since the field is described by a second-order tensor Green's function, two scalar equations may be produced from the one tensor equation. This can be accomplished due to the fact that $\nabla \cdot \vec{v}_T = 0$ and $\nabla \times \vec{v}_L = \vec{o}$ and the steps are outlined in Parts F and G for a viscous fluid and in Parts H and I for a viscoelastic solid in Appendix IIf. The conclusion

from the comparison of these scalarized equations with the various standard scalar equations is that the transverse mode of a viscous fluid is characterized by the diffusion equation while the longitudinal mode of a viscous fluid and both modes of a viscoelastic solid are characterized by the dissipative wave equation with space-time coupling.

The model of the fluid and solid used here treats the viscosity coefficients as being independent of frequency. Other models treat these coefficients as frequency-dependent. Parts D and E of Appendix IIf present the four domain representations for the frequency-independent and frequency-dependent models, respectively. Part E is found to be identical to Part D if the frequency dependence was in a linear manner, that is, $D'(\omega)=D\omega$, where D' is the D of Part E.

One may summarize the following parameters in a general way be the expressions.

i) $\omega_d = \omega_n(1-\xi^2)^{1/2}$

(temporal propagation constant)

ii) $\Lambda = Dk^2$

(temporal attenuation constant)

iii) $K = \frac{\omega}{C}\left\{\frac{[1+(2\xi\omega/\omega_n)^2]^{1/2}+1}{2[1+(2\xi\omega/\omega_n)^2]}\right\}^{1/2}$

(spatial propagation constant)

iv) $$\gamma = \frac{\omega}{C}\left\{\frac{[1+(2\xi\omega/\omega_n)^2]^{1/2}-1}{2[1+(2\xi\omega/\omega_n)^2]}\right\}^{1/2}$$

(spatial attenuation constant)

v) $$\omega_n = Ck$$

(natural frequency)

vi) $$\xi = Dk/C = \Lambda/\omega_n$$

(damping ratio)

where the parameters ω_d, ω_n, ξ, Λ, D, K, C, and γ each take on subscripts T or L corresponding to the transverse or longitudinal term, the relation $\omega = Ck$ between the frequency and wavenumber is valid only for a monochromatic sound wave propagating in a medium at rest, and

Viscous Fluid

$$D_T = \eta/\rho \qquad C_T = \text{undefined}$$

$$D_L = (3\zeta+4\eta)/6\rho \qquad C_L = [(\partial P/\partial\rho)_s]^{1/2}$$

Viscoelastic Solid

$$D_T = \mu''/\rho \qquad C_T = (\mu'/\rho)^{1/2}$$

$$D_L = (\lambda''+2\mu'')/2\rho \qquad C_L = [(\lambda'+2\mu')/\rho]^{1/2}$$

Now that the field has been evaluated for viscous fluids and viscoelastic solids of infinite extent, it now remains to show examples of how this methodology may be employed for a boundary-value problem. This is the subject of Chapter III.

CHAPTER III

APPLICATIONS--BOUNDARY VALUE PROBLEMS FOR SOUND PROPAGATION IN IDEAL FLUIDS

Introduction

The intent of this chapter is to show by several examples how to modify the theory presented in Chapter II for a medium of infinite extent to solve a problem where the medium is of finite-size, that is, a boundary-value problem.

Selected for this purpose is the study of underwater sound. The motivation for this choice of a problem came from talks with Sanders Associates of Nashua, New Hampshire. Sanders knew of a computer program that modelled sound propagation in shallow water but its results did not agree with experimental data. This computer program model utilized ray optic techniques and a solid bottom with elastic coefficients that were varied in an attempt to match the experimental data. Sanders partially funded a project for the Mechanics Research Laboratory of the University of New Hampshire to develop a computer model based on normal mode theory and utilizing a semi-infinite viscoelastic solid bottom with the parameters of the bottom taken from literature. It is this model for an ideal fluid that is described in a following section and is a simplified model of the viscous fluid of Chapter II. First,

however, some introductory remarks are made on the history of underwater sound and two preliminary problems are discussed prior to the UNH model.

Background

Considerable interest has been expressed in the literature concerning the propagation of energy from an acoustic source. Although underwater sound as a quantitative subject has its roots deep in the past, it may be said to be only about 40 years old. Its modern era began during World War II. An historical survey is found in Urick [9].

Of all the forms of radiation, sound travels through the ocean the best. In the turbid, saline water of the ocean, both light and radio waves are attenuated much more than that form of mechanical energy called sound. The velocity of propagation of small pressure disturbances is known as the speed of sound which is connected to the rate of change of pressure with respect to density by the relation $C^2 = (\partial P/\partial \rho)_s$, [10].

Fluid motion may be classified into various fields. In incompressible fluid mechanics, the fluid velocities are small compared with the speed of sound, and the fractional variation in density is insignificant; however, the fractional variation in pressure and temperature may be very large. In compressible fluid motion (also known as gas dynamics), the fluid velocities are appreciable compared with the speed of sound, and the fractional variations in pressure, temperature,

and density are all of significant magnitude. In this investigation acoustical motion is of interest and that is when the fluid velocities are extremely small compared to the speed of sound, while the fractional variations in pressure, temperature, and density are of significant magnitude. Because of these extremely small fluid velocities, acoustic theory is adequately defined with linear relationships.

The classical theory of underwater acoustics upon which most of the further investigations are based was introduced by Pekeris [11]. This work successfully predicted basic dispersion phenomena that were observed in records of sound generated by explosions. Furry [12] examined a related field by examining the propagation of electromagnetic waves near the earth's surface and was able to understand various diffraction phenomena. Marsh [13] investigated guided propagation in an ocean waveguide with absorption. This work was later reduced to numerical algorithms by Pederson and Gordon [14]. More work has been offered by Officer [15] and Tolstoy and Clay [16], while Wait [17] and Badden [18] discuss the analogous areas for electromagnetic propagation. The early investigations of Pekeris, Furry, and Marsh, as well as later ones by Tolstoy [19], Carter [20], and Eby, et al. [21] all employed normal mode theory to describe acoustic propagation in the ocean.

Underwater sound problems in the ocean are complicated by the fact that the sound speed is dependent on depth, range, and time. Some models include range-dependency but only depth-dependency is considered here. The reason for the variation

in sound speed with depth is due to a combined effect of temperature and pressure. Solar radiation heats the surface layer of the ocean and the temperature decreases below due to the decreasing intensity of the radiation penetrating the lower depths. The extreme top of the ocean may in fact be cooler than the surface layer due to convective heat transfer from the water. The magnitude of the sound speed follows this characteristic temperature pattern over this depth interval. At some point the increase in pressure with depth offsets the decreasing temperature and causes the sound speed to increase with depth. There may exist some interval of depth in the water column that the sound speed has a local minimum value where the sound may be channeled by refraction and travel long distances with very little attenuation. The classic sound channel was named the SOFAR (SOund Fixing And Ranging) channel by its discoverers, M. Ewing and J. L. Worzel [22].

In ocean acoustics most authors agree to restrict themselves to a vaguely defined band of frequencies f lying between 1 hz and 100 khz. At the high frequency end, sound absorption by sea water is very high and experiments have shown the attenuation constant to be proportional to f^2 [23]. Except for a small number of very special applications, such as acoustic image makers and side-looking sonars, which are used for very short-range studies, applications of sound transmission are limited to frequencies less than a few tens of kilohertz. At the low end, below 1 hz, such sound is generated by earthquakes and very large explosions and fall

into the field of seismology.

Absorption of acoustic energy is due in part to shear and dilational viscous losses, to chemical effects by means of a relaxation-type mechanism which exhibits a characteristic frequency and amplitude, to pressure and temperature fluctuations, to electrolytic processes, to dispersion by air bubbles and biological material, and to losses in the sediment below the water column. Attenuation by heat conduction in the water is negligible [24].

In a perfect parallel-plate waveguide one expects a $r^{-1/2}$ amplitude fall-off with distance in cylindrical coordinates where r is referenced horizontally due to the far-field approximation of the Bessel (or Hankel function):

$$J_o(\Gamma r) \cong \left(\frac{2}{\pi \Gamma r}\right)^{1/2} \cos[\Gamma r - \pi/4] \ .$$

When experimental fall-off is found to be markedly greater than $r^{-1/2}$ then one must look for attenuation. It has been found that the superposition of two mechanisms almost completely explain the guided mode attenuation. The first is the inclusion of a small imaginary component with the eigenvalue to form a complex-valued eigenvalue [25]. This eigenvalue has the geometrical interpretation of a wavenumber that is mode-dependent and now complex-valued. The second mechanism to account for attenuation is the leakage of energy into the bottom. This is due to the fact that the bottom has some

rigidity and can transmit shear waves. This bottom rigidity is neglected when one treats the bottom as another liquid layer with a higher sound speed as was the practice in the past.

There are two different methods to attack this sound propagation problem: ray optics and normal modes. The former is a geometrical procedure while the latter is a purely mathematical one. One can be obtained from the other by suitable summations. A ray optic solution is characterized by pulses (delta functions) arriving at some observation point from different image points all at the same time. This is a summation with an infinite number of terms to model a perfect waveguide since an infinite number of image points are required to construct the guide. Some of these rays may destructively interfere and hence need not be considered; but one does not know which ones they are prior to making the calculations. A normal mode solution, on the other hand, inherently sums the contribution of all rays so that the unnecessary rays are not individually and wastefully dealt with.

Since in practice one always has finite bandwidth receivers and since each mode of a waveguide has a low-frequency cut-off ($\omega_{om} = \frac{C}{H} m\pi$, for perfect waveguide, C = sound speed, H is distance between the two parallel planes, and m is the mode number), then only a finite number of terms are needed. So the mode point of view leads to a finite number of terms independent of range. On the other hand the ray optic solution for a waveguide contains at all times an infinity of

terms. At short ranges though, the higher order images can be neglected. At long ranges, the number of terms that must be considered is very large and as a result is very cumbersome and expensive. The ray solution is at its best for short ranges and broad bandwidths, while the mode solution is advantageous for long ranges and finite bandwidths. The mode method is considered here due to the obvious applications of detecting long range signals in the ocean.

The distinction between deep and shallow water is a relative one. In general one may say that the water is "shallow" if $\Gamma H \leq 10$, where Γ is the horizontal wavenumber (r-direction eigenvalue) and H is the height of the water column [16]. Hence one may consider high frequency sonar in water with physically-shallow depth to be a "deep-water" propagation problem. Similarly earthquakes in physically-deep water may be considered a "shallow-water" problem. Shallow water implies that the effect of the bottom on the propagation of sound may not be neglected.

Models that include bottom penetration of acoustic energy consist of totally and partially reflected waves from an incident wave impinging on the bottom. The total reflections are analogous to propagation in a perfect waveguide for which the eigenvalues are discrete and the energy levels are quantized due to the confinement of the energy. The partial reflections are due to energy leaving the waveguide and penetrating the bottom sediment. This corresponds to

continuous eigenvalues since the energy is not totally confined in space (an infinite number of modes are possible). Both continuous and discrete modes must be considered in evaluating the near field of a source. On the other hand for long range interest only the discrete modes need be considered because the energy transmitted into the bottom does not significantly contribute to long range propagation when compared to the energy contained in the discrete modes.

Ambient noise in the disguise of nonacoustical pressure fluctuations, flow noise, vibration, thermal noise, and surface wave noise makes for difficulty in interpreting experimentally collected data. The situation necessitates the use of signal processing to extract the signal from the noisy background.

Mathematical Considerations

So now the mathematical development of this study is presented for the modelling of compressional sound waves in an ideal water region. This methodology follows that of Chapter II but is now applied to a medium which is finite and non-viscous. Three specific boundary-value problems are now considered. The first two have been studies by Leibiger while the third is new and more physically-real. The novelty of this model is that it treats complex-valued eigenvalues, utilizes normal mode theory, and considers a viscoelastic solid boundary at the bottom of the water region.

The mathematical task at hand is to evaluate the three-dimensional Green's function for the following differential

equation that models compressional sound wave propagation properties of an ideal fluid in the steady-state $(\vec{r};\omega)$ domain (see Appendix IIIa):

$$[\nabla^2 + \frac{\omega^2}{C^2(z)}]\Psi(\vec{r};\omega) = S(\vec{r};\omega) \qquad (3.1)$$

where ∇^2 is the Laplacian operator, ω is the angular frequency of oscillation, $C(z)$ is the depth-dependent adiabatic sound-speed profile, Ψ is the displacement potential ($\vec{u}$ = displacement vector = $\nabla\Psi$) in the steady state (i.e., space-frequency $(\vec{r};\omega)$) domain, ∇ is the gradient operator, and S is an arbitrary forcing term. The Green's function G is defined in cylindrical coordinates (see figure 4):

$$[\nabla^2 + \frac{\omega^2}{C^2(z)}]G(\vec{r};\omega) = -\delta^3(\vec{r}-\vec{r}') = \frac{-1}{r'}\,\delta(r-r')\delta(\phi-\phi')\delta(z-z') \ , \qquad (3.2)$$

where δ is a spatial Dirac delta function, and the source and observation points are specified in cylindrical coordinates by $\vec{r}' = (r',\phi',z')$ and $\vec{r} = (r,\phi,z)$, respectively. One may write the differential operator explicitly in cylindrical coordinates:

$$(\nabla^2 + \frac{\omega^2}{C^2}) = (\frac{1}{r}\frac{\partial}{\partial r}\,r\,\frac{\partial}{\partial r} + \frac{1}{r^2}\frac{\partial^2}{\partial\phi^2} + \frac{\partial^2}{\partial z^2}) + \frac{\omega^2}{C^2} \qquad (3.3)$$

If one assumes $\Psi(\vec{r};\omega) = R(r)\Phi(\phi)Z(z)$ then the three separated

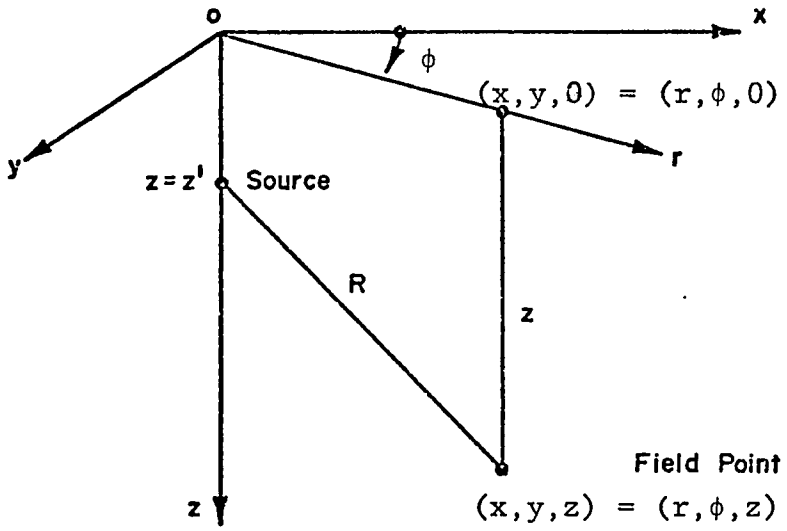

Figure 4 Diagram of the rectangular and cylindrical coordinate system showing both the source and receiver field points.

equations are:

$$[\frac{d}{dr} r\frac{d}{dr} - \frac{\nu^2}{r} + \Gamma^2 r]R(r) = 0 \ , \qquad (3.4a)$$

$$[\frac{d^2}{d\theta^2} + \nu^2]\Phi(\phi) = 0 \ , \qquad (3.4b)$$

$$[\frac{d^2}{dz^2} + \Omega^2]Z(z) = 0 \ , \qquad (3.4c)$$

where Γ^2, ν^2, and Ω^2 are the eigenvalues for the r, ϕ, and z directions, respectively, with the relationship:

$$\Gamma^2 + \Omega^2 = \frac{\omega^2}{C^2(z)} \ , \qquad (3.4d)$$

that comes directly from the separation of variables technique. For the purpose of this investigation of a depth-stratified fluid one has the following boundary conditions for the (3.4) equations above: R(r) satisfies the outgoing radiation condition, $\Phi(\phi)$ and $\partial\Phi/\partial\phi$ are periodic, and Z(z) satisfies a pressure release condition at the top of the fluid column and some bottom condition depending upon the particular problem being considered.

The three-dimensional Green's function [solution to equation (3.2)] may be symbolically represented by:

$$G(\vec{R};\omega) \longleftrightarrow \delta(\phi-\phi')\delta(z-z')g_r(r,r';\Gamma^2,\nu^2;\omega) \ , \qquad (3.5)$$

where $\vec{R} = \vec{r} - \vec{r}'$. This representation is 'symbolic' in the sense that the delta functions are in integral (or summation)

form and so the evaluation of G is not just a product of three expressions. This is one of three representations for G, called the Levine-Schwinger representation. The other two use the one-dimensional Green's function g in the ϕ and z direction, respectively. Evaluating the delta functions by integrations of the one-dimensional Green's function g over their respective eigenvalue's domain, equation (3.5) may be written explicitly as (see Appendix Ia):

$$G(\vec{R};\omega) = \frac{-1}{4\pi^2} \oint d\nu^2 g_\phi(\phi,\phi';\nu^2) \oint d\Omega^2 g_z(z,z';\Omega^2) g_r(r,r';\Gamma^2,\nu^2) \ , \tag{3.6}$$

where $\Gamma^2 = [\omega/C(z)]^2 - \Omega^2$. In this expression g_ϕ and g_z are called modal Green's functions and g_r is called the characteristic Green's function; all three are one-dimensional in the sense that each is a function of one spatial coordinate only. These functions are evaluated by the expression (see Appendix Ib):

$$g_a(a,a';h_a) = - \frac{A_{\pm}(a)A_{\mp}(a')}{p(a')\Delta(a',h_a)} \ , \tag{3.7}$$

where $A_{\pm}(a)$ is symbolic for the two linearly independent solutions to each of the equations (3.4), h_a is the appropriate eigenvalue for the given coordinate direction a, $\pm$ depends on whether $a \lesseqgtr a'$, Δ is the Wronskian of the two independent

solutions:

$$\Delta = (A_+ \frac{dA_-}{da} - A_- \frac{dA_+}{da}) \ ,$$

and p(a) is a function of the standard Sturm-Liouville equation, namely:

$$[\frac{d}{da} p(a) \frac{d}{da} - q(a) + h_a w(a)]A(a) = 0$$

whereby comparison with equation (3.4) shows that:

$$\begin{array}{llll} p(r) = r & q(r) = -\nu^2/r & h_r = \Gamma^2 & w(r) = r \\ p(\phi) = 1 & q(\phi) = 0 & h_\phi = \nu^2 & w(\phi) = 1 \\ p(z) = 1 & q(z) = 0 & h_z = \Omega^2 & w(z) = 1 \ . \end{array} \qquad (3.8)$$

For the construction of the radial characteristic Green's function g_r one may use the following two linearly independent solutions of equation (3.4a): the cylindrical Bessel function $J_\nu(\Gamma r)$ and the Hankel function of the second kind $H_\nu^{(2)}(\Gamma r)$. From (3.8) one has $p(r') = r'$ and the Wronskian for these two solutions is tabulated as: $\Delta(r') = \Delta[J_\nu(\Gamma r'), H_\nu^{(2)}(\Gamma r')] = -i2/\pi r'$. Therefore equation (3.7) for this case is:

$$g_r(r,r';\Gamma^2,\nu^2) = \frac{-J_\nu(\Gamma r')H_\nu^{(2)}(\Gamma r)}{r'(-i2/\pi r')} = \frac{-i\pi}{2} J_\nu(\Gamma r')H_\nu^{(2)}(\Gamma r) \ , \tag{3.9}$$

where J_ν is chosen to be evaluated at the source point $r = r'$ since later one considers $r' = 0$ for convenience and $H_\nu^{(2)}$ is undefined there.

The azimuthal modal Green's function g_ϕ for a periodicity is written for integral values of ν:

$$g_\phi(\phi,\phi';\nu^2) = -\cos[\nu(\pi-|\phi-\phi'|)]/2\nu\sin\nu\pi \ . \tag{3.10a}$$

The corresponding delta function is written:

$$\delta(\phi-\phi') = \frac{-1}{2\pi i}\oint d\nu^2 g_\phi = \frac{1}{\pi}\sum_{\nu=0}^{\infty}\varepsilon_\nu\cos\nu(\phi-\phi') \ , \tag{3.10b}$$

where $\varepsilon_\nu = 1$ for $\nu = 0$ and 2 for all other ν.

The depth modal Green's function g_z is constructed from the independent solutions of equation (3.4c). No analytic solutions to this equation exist for realistic functions C(z). Therefore exact solutions must be evaluated numerically or some analytic approximation may be utilized. From (3.8) one has $p(z') = 1$ and hence the general form of g_z is:

$$g_z(z,z';\Omega^2) = \frac{-Z_{\pm}(z,\Omega)Z_{\mp}(z',\Omega)}{\Delta(z',\Omega)} \tag{3.11a}$$

where the function Z_- satisfies the bottom boundary condition, Z_+ satisfies the top boundary condition, and $\pm$ depends on whether $z \lesseqgtr z'$. The corresponding delta function is evaluated by:

$$\delta(z-z') = \frac{-1}{2\pi i} \oint d\Omega^2 g_z(z,z';\Omega^2) \quad ; \text{ with } \Omega^2 = (\omega/C)^2 - \Gamma^2$$

$$= \frac{+1}{2\pi i} \oint d\Gamma^2 g_z(z,z';\Gamma^2)$$

$$= \frac{-1}{2\pi i} \oint d\Gamma^2 \frac{Z_{\pm}(z,\Gamma)Z_{\mp}(z',\Gamma)}{\Delta(z',\Gamma)} \quad ; \text{ contour encloses all the zeros of } \Delta, \text{ i.e., } \Delta(\Gamma) = 0$$

$$= -\sum_{n=1}^{\infty} \frac{(\Gamma^2-\Gamma_n^2)Z_{\pm}(z,\Gamma)_{\mp}(z',\Gamma)}{\Delta(z',\Gamma)} \Bigg|_{\Gamma^2 \to \Gamma_n^2} \quad ; \text{ for simple poles of } \Delta, \text{ i.e., } \Delta(\Gamma_n) = 0$$

$$= -\sum_{n=1}^{\infty} \frac{Z_{\pm}(z,\Gamma)Z_{\mp}(z',\Gamma)}{\frac{\partial}{\partial(\Gamma^2)}[\Delta(z',\Gamma)]} \Bigg|_{\Gamma^2 \to \Gamma_n^2} \quad ; \text{ by L'Hopital's rule}$$

$$= -2\sum_{n=1}^{\infty} \Gamma_n \frac{Z_{\pm}(z,\Gamma_n)Z_{\mp}(z';\Gamma_n)}{\frac{\partial}{\partial\Gamma}[\Delta(z',\Gamma)]\Big|_{\Gamma \to \Gamma_n}} \qquad (3.11b)$$

Combining the results of (3.10b, 11b, and 9) into (3.5) one obtains:

$$G(\vec{R};\omega) = i \sum_{\nu=0}^{\infty} \varepsilon_\nu \cos\nu(\phi-\phi') \sum_{n=1}^{\infty} \frac{Z_{\pm}(z,\Gamma_n)Z_{\mp}(z',\Gamma_n)}{\frac{\partial}{\partial\Gamma}[\Delta(z',\Gamma)]\Big|_{\Gamma \to \Gamma_n}} \Gamma_n J_\nu(\Gamma_n r') H_\nu^{(2)}(\Gamma_n r) \tag{3.12a}$$

Now if one assumes azimuthal symmetry ($\nu \to 0$) and the coordinate system is referenced so that $r' = 0$, then (3.12a) reduces to:

$$G(\vec{R};\omega) = i \sum_{n=1}^{\infty} \Gamma_n H_o^{(2)}(\Gamma_n r) \frac{Z_{\pm}(z,\Gamma_n)Z_{\mp}(z',\Gamma_n)}{\frac{\partial}{\partial\Gamma}[\Delta(z',\Gamma)]\Big|_{\Gamma \to \Gamma_n}} \tag{3.12b}$$

where the summation is over the zeros of Δ and use has been made of the fact that: $J_o(0) = 1$. For consideration of long-range propagation, one may also express the Green's function as:

$$G(\vec{R};\omega) = i\left(\frac{2}{\pi r}\right)^{1/2} \sum_{n=1}^{\infty} \Gamma_n^{1/2} e^{-i(\Gamma_n r - \pi/4)} \frac{Z_{\pm}(z,\Gamma_n)Z_{\mp}(z',\Gamma_n)}{\frac{\partial}{\partial\Gamma}[\Delta(z',\Gamma)]\Big|_{\Gamma \to \Gamma_n}} , \tag{3.12c}$$

where the far-field approximation for the zeroth-order Hankel function has been used;

$$H_o^{(2)}(\Gamma r) \sim (2/\pi\Gamma r)^{1/2} e^{-i(\Gamma r - \pi/4)} \quad ; \quad \Gamma r >> 1 \ .$$

The final step now is to evaluate the functions $Z_{\pm}$ such that they satisfy the boundary conditions for a particular problem.

Two Preliminary Problems (from the literature)

Two preliminary problems studied by Leibiger [26] will now be presented as a lead-up to the shallow ocean problem, for which an ideal fluid with a sound profile and viscoelastic subbottom are considered. The first preliminary problem addresses an ideal fluid with a constant sound speed and a rigid solid bottom. The second considers an ideal fluid with a sound profile and a bottom boundary at infinity. The first problem has an exact solution while the second will depend on an approximate solution. The approximation valid for sufficiently high frequencies that was developed in conjunction with geometrical optics is known in literature by the name of WKB or Wenzel, Kramers, Brillouin approximations to the solutions of wave equations, and will be used here.

Problem 1: Ideal Fluid--Constant Sound Speed--Rigid Solid Bottom

As an introduction to the methodology this simpler problem is considered in which asymptotic methods are not needed for its complete solution. The results obtained are also useful in clarifying discussions of the asymptotic approximations to be derived, particularly the physical interpretations to be given the normal modes.

Consider guided propagation occurring in a homogeneous medium, of constant propagation velocity C, bounded by the surface z = 0 and a rigid solid bottom at the depth z = H. The corresponding eigenvalue problem is defined by the following differential equation with suitable boundary conditions:

$$LZ \equiv \left(\frac{d^2}{dz^2} + \frac{\omega^2}{C^2}\right) Z = \Gamma^2 Z$$

$$Z(z=0) = 0 \qquad \frac{dZ}{dz}(z=H) = 0 \qquad (3.13)$$

where L is the differential operator. This problem has received considerable attention in the literature. Two linearly independent solutions to (3.13) are:

$$Z(z) = e^{\pm i\Omega z} ,$$

where $\Omega^2(\Gamma) = \frac{\omega^2}{C^2} - \Gamma^2$. Alternate solutions are obtained by appropriate linear combinations of these solutions and are the familiar sine and cosine functions that readily conform to the given boundary conditions. Using (3.7) where here p(z') = 1 and $\Delta(z') = -\Omega\cos(\Omega H)$, the Green's function for the operator $(L-\Gamma^2)$ is constructed to be:

$$g_z(z,z';\Gamma^2) = \frac{-\sin(\Omega z_<)\cos[\Omega(H-z_>)]}{\Omega\cos(\Omega H)} , \qquad (3.14a)$$

where $z_<$ or $z_>$ is the lesser or greater of z and z', and the boundary conditions are satisfied. The spectral representation of the differential operator L is obtained by integration of $g_z(z,z';\Gamma^2)$ about a suitable closed contour in the Γ^2-plane. This evaluation is accomplished by (see Appendix Ia):

$$\delta(z-z') = \frac{-1}{2\pi i}\oint d\Omega^2 g_z(z,z';\Omega^2) = \frac{+1}{2\pi i}\oint d\Gamma^2 g_z(z,z';\Gamma^2) \tag{3.14b}$$

Converting to an integration in the Γ-plane, one cuts the Γ^2-plane along some appropriate ray from the origin and define Γ by the condition that:

$$\Gamma^2 \text{ real}, \quad > 0 \qquad\qquad \Gamma = + \left|(\Gamma^2)^{1/2}\right|$$

$$\Gamma^2 \text{ real}, \quad < 0 \qquad\qquad \Gamma = -i\left|(\Gamma^2)^{1/2}\right|$$

which involves an arbitrary choice of $\pm i$ for $\Gamma^2 < 0$ but determines the contour required for convergence. Since the eigenvalues Γ^2 are known to be real-valued for this self-adjoint problem, the values of Γ appear on the positive real axis and negative imaginary axis of the Γ-plane. These values correspond to the poles of $g_z(z,z';\Gamma^2)$ or equivalently the zeros of $\cos(\Omega H)$. Realizing $d\Gamma^2 = 2\Gamma d\Gamma$ then the integral above becomes the following in the Γ-plane:

$$\delta(z-z') = \frac{1}{\pi i}\oint d\Gamma\ \Gamma g_z(z,z';\Gamma^2) \tag{3.14c}$$

where the contour encloses all the singularities of $g_z(z,z';\Gamma^2)$. In addition to the zeros of $\cos(\Omega H)$, $g_z(z,z';\Gamma^2)$ may possess a singularity at the branch point of $\Omega[= (\frac{\omega^2}{C^2} - \Gamma^2)^{1/2}]$ located on the real axis at $\Gamma = \frac{+\omega}{C}$. This spectral representation may be evaluated by integrating $g_z(z,z';\Gamma^2)$ over the contour shown in figure 5. This integral reduces to a summation of residues and a potential contribution around the branch cut. However the branch cut integral does not contribute because the integrand is an even function, and since the argument of Ω differs by π across the cut, the upward integration exactly cancels the downward integration. The residue terms arise from the contributions of the zeros of $\cos(\Omega H)$, which are evaluated in this manner:

$$\Omega H = (n - \tfrac{1}{2})\pi \qquad n = 1,2,\ldots$$

$$\text{or} \quad \Gamma_n = \left\{(\tfrac{\omega}{C})^2 - \Omega^2\right\}^{1/2} = \left\{(\tfrac{\omega}{C})^2 - [\frac{(n-\frac{1}{2})\pi}{H}]^2\right\}^{1/2} \qquad n = 1,2,\ldots$$

therefore

$$\Gamma_n = \left\{(\tfrac{\omega}{C})^2 - [\frac{(n-\frac{1}{2})\pi}{H}]^2\right\}^{1/2} \qquad n = 1,2,\ldots,n_o$$

$$n = -i\left\{[\frac{(n-\frac{1}{2})\pi}{H}]^2 - (\tfrac{\omega}{C})^2\right\}^{1/2} \qquad n = n_o+1, n_o+2,\ldots$$

where n_o is the largest integer such that $\Gamma^2 > 0$. Because

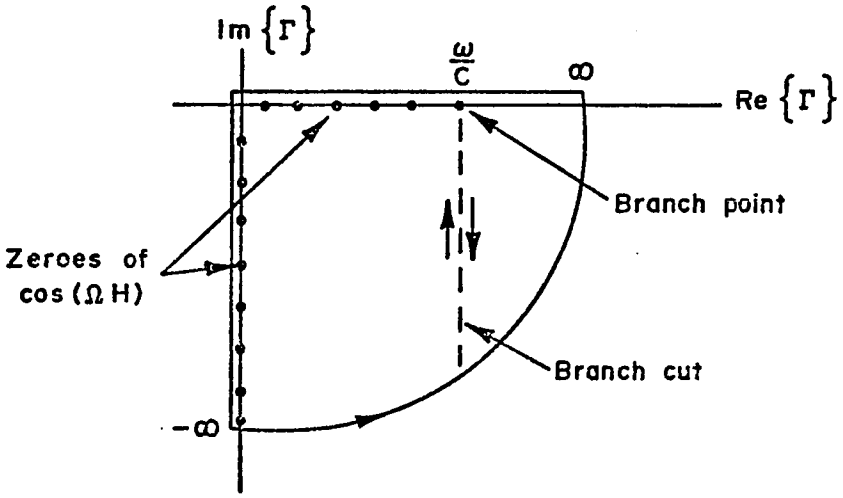

Figure 5 Definition of the Γ-contour

of the two identities:

$$\left.\begin{aligned} &\cos\{\Omega(\Gamma_n)[H-z]\} = (-1)^{n+1}\sin[\Omega(\Gamma_n)z] \\ &\frac{\partial}{\partial\Gamma}\{\Omega(\Gamma)\cos[\Omega(\Gamma)H]\}\Big|_{\Gamma\to\Gamma_n} = (-1)^{n+1}H\Gamma_n \end{aligned}\right\} \text{; for use in (3.14)}$$

then the spectral representation of the operator L is expressed:

$$\begin{aligned} \delta(z-z') &= \frac{1}{\pi i}\oint d\Gamma\ \Gamma g_z(z,z';\Gamma^2) \\ &= \frac{1}{\pi i}\left[2\pi i \sum_{n=1}^{\infty}\Gamma_n \text{Residues}\right] \\ &= \frac{-2}{H}\sum_{n=1}^{n_o}\sin[\Omega(\Gamma_n)z]\sin[\Omega(\Gamma_n)z'] \\ &\quad - \frac{2}{H}\sum_{n=n_o+1}^{\infty}\sin[\Omega(\Gamma_n)z]\sin[\Omega(\Gamma_n)z'] \end{aligned}$$

which corresponds to (3.11b). The final result, corresponding to (3.12b) is written:

$$\begin{aligned} G(\vec{R};\omega) &= \frac{2i}{H}\sum_{n=1}^{n_o}\{H_o^{(2)}(\Gamma_n r)\sin[\Omega(\Gamma_n)z]\sin[\Omega(\Gamma_n)z']\} \\ &\quad + \frac{2i}{H}\sum_{n=n_o+1}^{\infty}\{H_o^{(2)}(\Gamma_n r)\sin[\Omega(\Gamma_n)z]\sin[\Omega(\Gamma_n)z'] \end{aligned} \quad (3.15)$$

Using the far-field approximation for $H_o^{(2)}(\Gamma_n r)$ of (3.12c) it is seen that the modes with real eigenvalues represent

waves propagating outward in the radial (horizontal) direction with a phase velocity $\beta_n = \omega/\Gamma_n$. The modes with negative imaginary eigenvalues possess no propagating characteristics (exponential spatial decay, $e^{-\gamma R}$).

Problem 2: Ideal Fluid--Sound Profile--No Bottom Boundary

The preceeding problem exemplifies how the potential or Green's function $G(\vec{R};\omega)$ may be interpreted as a summation of normal modes. In this present example however three separate subsets of normal modes occur corresponding to different analytic approximations of $g_z(z,z';\Gamma^2)$ obtained which are valid over various intervals of the real axis in the Γ-plane. The physical interpretation of the normal modes leads to a particular type of standing wave function in the z-coordinate for each subset of normal modes.

If one assumes that the sound profile C(z) has no zeros, then it follows that $\Omega^2(z,\Gamma)$ is an analytic function of z and Γ for all z and Γ except the corresponding points at infinity. As a result, $g_z(z,z';\ \Gamma^2)$ is assumed to only possess simple pole singularities. Due to the lack of branch point singularities in $g_z(z,z';\Gamma^2)$ the total spectrum is discrete. From physical reasoning, since the waveguide contains the total energy inside a finite z-region, no attenuation of the outward propagation is possible, and consequently the eigenvalues Γ_n for this problem are real-valued. The poles of $g_z(z,z';\Gamma^2)$ are therefore located on the real axis of the Γ-plane.

The problem that defines the Green's function is conveniently written for this case as [where operator L has been defined in equation (3.13)]:

$$(L-\Gamma^2)Z \equiv [\frac{d^2}{dz^2} + \Omega^2(z,\Gamma)]Z(z) = 0$$

$$Z(z=0) = 0 \qquad Z(z\to\infty) \to 0 \qquad (3.16a)$$

Since the sound speed varies with depth in a non-regular way, the function $\Omega^2(z,\Gamma)$ does not allow for an exact analytical description for the solution Z. The solution Z must be solved for numerically by a digital computer or by some approximate analytical method. Here the latter choice is made and approximation technique employed is that due to Wenzel, Kramers, and Brillouin (WKB) [see Appendix IIIb]. The approximate solution is [30]:

$$Z(z) = \Omega^{-1/2}[Ae^{i\xi}+Be^{-i\xi}] \quad \text{where } \xi = \int\Omega(\bar{z},\Gamma)d\bar{z}$$

To conveniently define Ω, first define the phase velocity: $\beta(\Gamma) = \omega/\Gamma$ and then one may write equivalently:

$$\Omega^2(z,\Gamma) = \omega^2(\frac{1}{C^2} - \frac{1}{\beta^2}) = \Gamma^2[(\frac{\beta}{C})^2-1] \qquad (3.16b)$$

Since Γ is considered a complex quantity, there is a branch point of Ω in the right half of the complex Γ-plane where

$\Gamma = \omega/C$. See figure 6 for the diagram defining $\Omega(z,\Gamma)$. According to this convention, whenever Γ is real

$$\Omega(z,\Gamma) = + \Gamma[(\frac{\beta}{C})^2-1]^{1/2} \qquad \text{when} \quad \Omega^2 > 0$$

$$\Omega(z,\Gamma) = - i\Gamma[1-(\frac{\beta}{C})^2]^{1/2} = -i|\Omega| \qquad \text{when} \quad \Omega^2 < 0 \ .$$

As shown in figure 7 given value of $\beta(\Gamma)$ for real Γ intersects the sound velocity profile $C(z)$ in a number of points and thereby divides the z-ordinate into a number of intervals in which the sign of $\Omega^2(z,\Gamma)$ remains unchanged within each interval. In the WKB terminology these points of intersection are turning points for the differential equation (3.16). For the figure shown and choice of $\beta(\Gamma)$ there are three turning points, $z = \alpha_n$, $n = 1,2,3$ and as a consequence three regions have been defined. In each region, fundamental solutions to equation (3.16a) may be written as a linear combination of two WKB approximations. The arbitrary constants in each representation may be appropriately selected by the bridging conditions so that the extension of one representation across a turning point $\Omega^2 = 0$ is correct.

First one may define various expressions for real Γ over z-intervals in which $\Omega^2 > 0$:

$$\xi_1(z,\Gamma) = \int_z^{\alpha_1} \Omega(\bar{z},\Gamma)\,d\bar{z} \ , \quad \xi_2(z,\Gamma) = \int_{\alpha_2}^{z} \Omega(\bar{z},\Gamma)\,d\bar{z} \ ,$$

$$\xi_3(z,\Gamma) = \int_z^{\alpha_3} \Omega(\bar{z},\Gamma)\,d\bar{z}$$

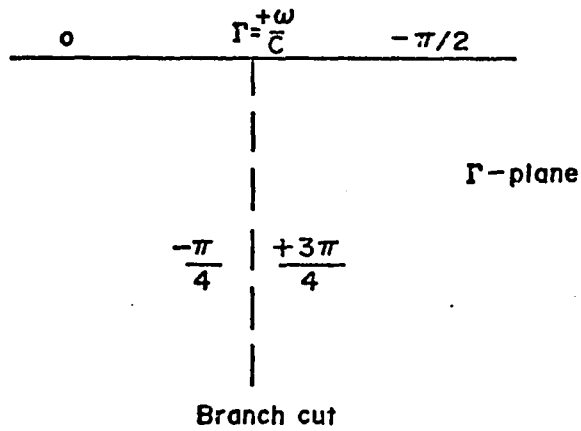

Figure 6 Definition of $[\Omega^2(z,\Gamma)]^{1/2}$, where the fractions indicate arguments of $\Omega(z,\Gamma)$ on either side of the branch cut and on the real axis. Branch cut is located at $\Omega^2 = 0$, i.e., where $\Gamma = \omega/C$.

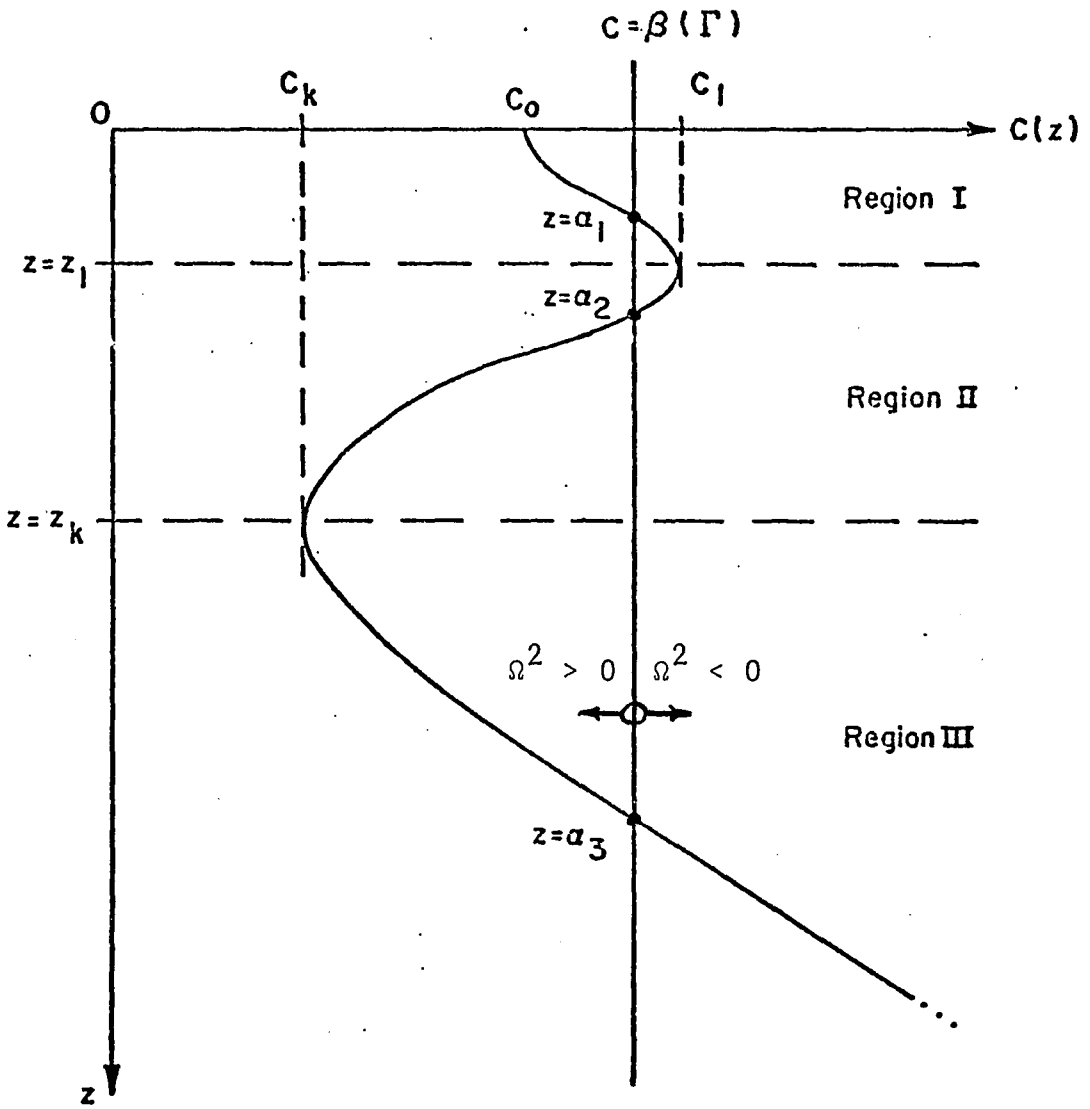

$$\Omega^2 = \frac{\omega^2}{C^2(z)} - \Gamma^2$$

$$\text{Oscillatory } \Omega^2 > 0 \begin{cases} 0 < z < \alpha_1 \\ \alpha_2 < z < \alpha_3 \end{cases} \qquad \text{Damped } \Omega^2 < 0 \begin{cases} \alpha_1 < z < \alpha_2 \\ \alpha_3 < z < \infty \end{cases}$$

Figure 7 Theoretical sound speed profile with Γ chosen to show three turning points at $z = \alpha_j$, $j = 1,2,3$

in which $\Omega^2 < 0$:

$$|\xi_1(z,\Gamma)| = \int_{\alpha_1}^{z} |\Omega(\bar{z},\Gamma)|d\bar{z} \ , \quad |\xi_2(z,\Gamma)| = \int_{z}^{\alpha_2} |\Omega(\bar{z},\Gamma)|d\bar{z} \ ,$$

$$|\xi_3(z,\Gamma)| = \int_{\alpha_3}^{z} |\Omega(\bar{z},\Gamma)|d\bar{z} \ .$$

The general form of the required linear combinations of fundamental solutions are:

Region I:

$$Z(z,\Gamma) = \begin{cases} \Omega(z,\Gamma)^{-1/2}[A_1 e^{i\xi_1(z,\Gamma)} + B_1 e^{-i\xi_1(z,\Gamma)}], & 0 \leq z < \alpha_1 \\ e^{i\pi/4}|\Omega(z,\Gamma)|^{-1/2}[C_1 e^{|\xi_1(z,\Gamma)|} + D_1 e^{-|\xi_1(z,\Gamma)|}], & \alpha_1 < z \end{cases} \tag{3.17a}$$

Region II:

$$Z(z,\Gamma) = \begin{cases} e^{i\pi/4}|\Omega(z,\Gamma)|^{-1/2}[C_2 e^{|\xi_2(z,\Gamma)|} + D_2 e^{-|\xi_2(z,\Gamma)|}], & z < \alpha_2 \\ \Omega(z,\Gamma)^{-1/2}[A_2 e^{i\xi_2(z,\Gamma)} + B_2 e^{-i\xi_2(z,\Gamma)}], & \alpha_2 < z \end{cases} \tag{3.17b}$$

Region III:

$$Z(z,\Gamma) = \begin{cases} \Omega(z,\Gamma)^{-1/2}[A_3 e^{i\xi_3(z,\Gamma)} + B_3 e^{-i\xi_3(z,\Gamma)}], & z<\alpha_3 \\ e^{i\pi/4}|\Omega(z,\Gamma)|^{-1/2}[C_3 e^{|\xi_3(z,\Gamma)|} + D_3 e^{-|\xi_3(z,\Gamma)|}], & \alpha_3<z \end{cases} \tag{3.17c}$$

in which the (A_n, B_n, C_n, D_n), $n = 1,2,3$ are constants to be related by the following bridging conditions (see Appendix IIId):

$$\begin{aligned} D_n &= A_n \\ C_n &= B_n - iA_n \end{aligned} \qquad n = 1,2,3 \tag{3.18}$$

Subject to the condition that $\Omega^2(z,\Gamma)$ behaves linearly in z near each turning point, $z = \alpha_n$.

The Green's function g_z is constructed from the fundamental solutions above. One such solution is denoted Z_- and satisfies the boundary condition at $z = 0$, while the other is denoted Z_+ and satisfies the required condition at $z = \infty$. The construction is in the form of (3.11a) with $\Omega^2 = [(\omega/C)^2 - \Gamma^2]$. To exemplify the use of expression (3.17 and 18), the following case is considered. As an arbitrary choice one considers here that the source lies in Region I ($0 \leq z' < z_\ell$) of Figure 7. The choice of $C = \beta(\Gamma)$ will be as in Figure 7 so that there are three turning points $z = \alpha_n$, $n = 1,2,3$. So one needs to evaluate $Z_+(z,\Gamma)$ and $Z_-(z',\Gamma)$ since $z > z'$.

The function $Z_+(z,\Gamma)$ is determined as follows: From (3.17c) it is clear that to satisfy the bottom boundary condition, i.e., $Z_+(\infty,\Gamma) \to 0$, one must have $C_3 = 0$. The choice of D_3 is then arbitrarily chosen to be $D_3 = e^{-i\pi/4}$. Using the bridging conditions of (3.18), one obtains $A_3 = D_3 = e^{-i\pi/4}$ and $B_3 = 0 + iA_3 = e^{i\pi/4}$, hence $Z_+(z,\Gamma)$ in Region III (3.17c) is completely specified. The coefficients for Region II are evaluated by equating the expression on either side of $z = z_k$ since the solutions only change across turning points. With the definition $\xi(\alpha_2,\alpha_3,\Gamma) = \int_{\alpha_2}^{\alpha_3} \Omega(\bar{z},\Gamma)d\bar{z}$ then it follows that:

$$\xi_3(z,\Gamma) = \xi(\alpha_2,\alpha_3,\Gamma) - \xi_2(z,\Gamma) \ .$$

Substitution of this into the appropriate solution for Region III, yields the A_2 and B_2 of Region II:

$$A_2 = B_3 e^{-i\xi(\alpha_2,\alpha_3,\Gamma)} = e^{i\pi/4} e^{-i\xi(\alpha_2,\alpha_3,\Gamma)} \ ,$$

$$B_2 = A_3 e^{i\xi(\alpha_2,\alpha_3,\Gamma)} = e^{-i\pi/4} e^{i\xi(\alpha_2,\alpha_3,\Gamma)} \ .$$

One uses the bridging conditions (3.18) to cross the turning point α_2 to evaluate C_2 and D_2:

$$C_2 = B_2 - iA_2 = 2e^{-i\pi/4}\cos\,\xi(\alpha_2,\alpha_3,\Gamma)$$

$$C_2 = A_2 = e^{i\pi/4} e^{-i\xi(\alpha_2,\alpha_3,\Gamma)}$$

Now the solution Z_+ in Region II is completely specified. Proceeding into Region II similarly, one defines $|\xi(\alpha_1,\alpha_2,\Gamma)| = \int_{\alpha_1}^{\alpha_2} |\Omega(\bar{z},\Gamma)|d\bar{z}$ and then it follows that:

$$|\xi_2(z,\Gamma)| = |\xi(\alpha_1,\alpha_2,\Gamma)| - |\xi_1(z,\Gamma)| \ .$$

Substitution of this into the appropriate solution for Region II, yields the C_1 and D_1 of Region I from comparison with the representation for $z < \alpha_2$ of Region II. It follows that:

$$C_1 = e^{i\pi/4} e^{-i\xi(\alpha_2,\alpha_3,\Gamma)} e^{-|\xi(\alpha_1,\alpha_2,\Gamma)|}$$

$$D_1 = 2e^{-i\pi/4}\cos\,\xi(\alpha_2,\alpha_3,\Gamma)e^{|\xi(\alpha_1,\alpha_2,\Gamma)} \ .$$

The bridging conditions once again are used to yield:

$$A_1 = D_1 = 2e^{-i\pi/4}\{\cos\xi(\alpha_2,\alpha_3,\Gamma)e^{|\xi(\alpha_1,\alpha_2,\Gamma)|}\}$$

$$B_1 = C_1 + iA_1 = e^{i\pi/4}\{e^{-\xi(\alpha_2,\alpha_3,\Gamma)} e^{-|\xi(\alpha_1,\alpha_2,\Gamma)|} + 2\cos\xi(\alpha_2,\alpha_3,\Gamma)e^{|\xi(\alpha_1,\alpha_2,\Gamma)|}\}$$

Consistant with the high-frequency assumption of the WKB solutions, one may use this same assumption to state [note that $\Gamma\to\infty$ as $\omega\to\infty$]:

$$\lim_{\Gamma\to\infty} |\xi(\alpha_1,\alpha_2,\Gamma)| \to \infty$$

in order for the first term in the above expression for B_1 to vanish. In the asymptotic sense, it is then safe to neglect the exponential $e^{-|\xi(\alpha_1,\alpha_2,\Gamma)|}$ in B_1 and C_1 whenever $\cos\xi(\alpha_2,\alpha_3,\Gamma) \neq 0$. For Regions I and II there are two alternatives depending on $\cos\xi(\alpha_2,\alpha_3,\Gamma)$:

1) $\cos\xi(\alpha_1,\alpha_2,\Gamma) \neq 0$

Region I:

$$Z_+(z,\Gamma) = \begin{cases} 4[\Omega(z,\Gamma)]^{-1/2}\cos\xi(\alpha_2,\alpha_3,\Gamma)e^{|\xi(\alpha_1,\alpha_2,\Gamma)|}\cos[\xi_1(z,\Gamma)-\pi/4], & z<\alpha_1 \\ 2|\Omega(z,\Gamma)|^{-1/2}\cos\xi(\alpha_2,\alpha_3,\Gamma)e^{|\xi(\alpha_1,\alpha_2,\Gamma)|}e^{-|\xi_1(z,\Gamma)|}, & z>\alpha_1 \end{cases} \tag{3.19a}$$

Region II:

$$Z_+(z,\Gamma) = \begin{cases} 2|\Omega(z,\Gamma)|^{-1/2}\cos\xi(\alpha_2,\alpha_3,\Gamma)e^{|\xi_2(z,\Gamma)|}, & z<\alpha_2 \\ 2[\Omega(z,\Gamma)]^{-1/2}\cos[\xi(\alpha_2,\alpha_3,\Gamma)-\xi_2(z,\Gamma)-\pi/4], & z>\alpha_2 \end{cases} \tag{3.19b}$$

2) $\cos\xi(\alpha_2,\alpha_3,\Gamma) = 0$

Region I:

$$Z_+(z,\Gamma) = \begin{cases} e^{-i\pi/4}[\Omega(z,\Gamma)]^{-1/2}\sin\xi(\alpha_2,\alpha_3,\Gamma)e^{-|\xi(\alpha_1,\alpha_2,\Gamma)}\, e^{-i\xi_1(z,\Gamma)}, & z<\alpha_1 \\ |\Omega(z,\Gamma)|^{-1/2}e^{-|\xi(\alpha_1,\alpha_2,\Gamma)|}\sin\xi(\alpha_2,\alpha_3,\Gamma)e^{|\xi_1(z,\Gamma)|}, & z>\alpha_1 \end{cases} \tag{3.19c}$$

Region II:

$$Z_+(z,\Gamma) = \begin{cases} |\Omega(z,\Gamma)|^{-1/2}\sin\xi(\alpha_2,\alpha_3,\Gamma)e^{-|\xi_2(z,\Gamma)|}, & z<\alpha_2 \\ 2[\Omega(z,\Gamma)]^{-1/2}\cos[\xi(\alpha_2,\alpha_3,\Gamma)-\xi_2(z,\Gamma)-\pi/4], & z>\alpha_2 \end{cases} \tag{3.19d}$$

The solutions in Region III are the same in either case:

Region III:

$$Z_+(z,\Gamma) = \begin{cases} 2[\Omega(z,\Gamma)]^{-1/2}\cos[\xi_3(z,\Gamma)-\pi/4], & z<\alpha_3 \\ |\Omega(z,\Gamma)|^{-1/2}e^{-|\xi_3(z,\Gamma)|}, & z>\alpha_3 \end{cases} \tag{3.19e}$$

For the condition $C_o < \beta(\Gamma) < C_\ell$ the function Z_+ has been fully

defined. The function Z_+ is the sum of all the values evaluated from the bottom, stepping-up to the observer position z (calculated from the above expressions for the various regions).

The next case to consider is $\beta(\Gamma) > C_\ell$. To evaluate the representations of the solutions in this case, one may directly use the results from above for Regions I and II with $\alpha_1 = \alpha_2 = z_\ell$. The functions $Z_+(z,\Gamma)$ may be determined by comparing coefficients with the solutions in Region III above, since in this case no turning points exist in Regions I and II. The results are:

Region I:

$$Z_+(z,\Gamma) = 2[\Omega(z,\Gamma)]^{-1/2}\cos[\xi(z_\ell,\alpha_3,\Gamma)+\xi_1(z,\Gamma)-\pi/4] \tag{3.20}$$

Region II:

$$Z_+(z,\Gamma) = 2[\Omega(z,\Gamma)]^{-1/2}\cos[\xi(z_\ell,\alpha_3,\Gamma)-\xi_2(z,\Gamma)-\pi/4]$$

The solutions $Z_+(z,\Gamma)$ in Region III are identical to (3.19e) and the solutions (3.20) are evaluated from it stepping up from the bottom.

For the case $C_k < \beta(\Gamma) < C_o$, one may use $\alpha_1 = 0$ in the equations (3.19) for evaluating Z_+. The representations (3.19a) and (3.19c) are superfluous when $\alpha_1 = 0$. This is a convenient form (III.7d) since the solutions are continuous in Γ across the point $\beta(\Gamma) = C_o$ between $C_k < \beta(\Gamma) < C_o$ and

$C_o < \beta(\Gamma) < C_\ell$ when $\cos \xi(\alpha_2,\alpha_3,\Gamma) = 0$.

The interval $\beta(\Gamma) < C_k$ is the last one to consider. The different modes arise from the various number and locations of zeros of Ω^2, i.e., turning points. There are no turning points on this interval $\beta(\Gamma) < C_k$ and hence the solutions are inconsequential and will not be derived here.

Now the attention can be switched to the $Z_-(z',\Gamma)$ solution. In general the solutions are formed by stepping-down from the top $z = 0$. At the very top the boundary condition $Z_-(0,\Gamma) = 0$ must be met and then the bridging conditions allow one to continue the solution down into the other regions. Here though we have taken the case that the source is in Region I, so one need only know Z_- in the Region I.

On the interval $C_k < \beta(\Gamma) < C_\ell$, the solutions $Z_+(z,\Gamma)$ themselves satisfy the boundary conditions to within a very small term whenever $\cos \xi(\alpha_2,\alpha_3,\Gamma) = 0$. If the approximation $Z_-(z,\Gamma) \sim Z_+(z,\Gamma)$ is made, the functions $Z_+(z,\Gamma)$ as previously derived are automatically approximate eigenfunctions of the operator L, and the condition $\cos \xi(\alpha_2,\alpha_3,\Gamma) = 0$ is the eigenvalue equation from which values $\Gamma = \Gamma_n = 1,2,3,\ldots$ may be determined to yield the modes. For the case $\cos \xi(\alpha_2,\alpha_3,\Gamma) \neq 0$, then the function $Z_-(z,\Gamma)$ may be evaluated from the first equation of (3.17a), valid for $z < \alpha_1$ of Region I, to be:

$$Z_-(z,\Gamma) = [\Omega(z,\Gamma)]^{-1/2} \sin[\xi_1(0,\Gamma) - \xi_1(z,\Gamma)] \ . \qquad (3.21)$$

The solution for $z > \alpha_1$ will not be required of $z' < \alpha_1$.

As a result of the approximations and various constructions made in the above, there are three resulting approximate forms for the Green's function:

$$1)\quad \cos \xi(\alpha_2,\alpha_3,\Gamma) = 0\ , \qquad C_k < \beta(\Gamma) < C_\ell \tag{3.22}$$

$$g_z(z,z';\Gamma^2) = \frac{-Z_+(z,\Gamma)Z_+(z',\Gamma)}{\Delta(z',\Gamma)}\ ;\ \text{where } Z_- \sim Z_+$$

where Z_+ is to be obtained from (3.19c,d,e) according to which region z lies. The Wronskian is evaluated conveniently at $z = z_k$ from the last equation of (3.19d) and first equation of (3.19e) to be:

$$\Delta(z_k) = 4 \sin \xi(\alpha_2,\alpha_3,\Gamma) \cos \xi(\alpha_2,\alpha_3,\Gamma)$$

$$2)\quad \cos \xi(\alpha_2,\alpha_3,\Gamma) \neq 0\ , \qquad C_o < \beta(\Gamma) < C_\ell \tag{3.23}$$

$$g_z(z,z';\Gamma^2) = \begin{cases} -Z_+(z',\Gamma)Z_-(z,\Gamma)/\Delta(z',\Gamma), & z \leq z' \\ -Z_+(z,\Gamma)Z_-(z',\Gamma)/\Delta(z',\Gamma), & z \geq z' \end{cases}$$

where Z_- is given by (3.21) and Z_+ by (3.19a,b,e). The Wronskian is evaluated conveniently at $z = 0$ to be

$$\Delta(0) = 4 \cos \xi(\alpha_2,\alpha_3,\Gamma) e^{|\xi(\alpha_1,\alpha_2,\Gamma)|} \cos[\xi_1(0,\Gamma)-\pi/4]$$

$$3)\quad \beta(\Gamma) > C_{\ell} \tag{3.24}$$

For this case g_z is constructed as is (3.23) except that Z_+ is evaluated from (3.20). The Wronskian evaluated at z = 0 then becomes:

$$\Delta(0) = 2\cos[\xi(z_{\ell},\alpha_3,\Gamma)+\xi_1(0,\Gamma)-\pi/4]$$

Now it remains to construct the delta function from the appropriate Green's functions (3.22,23, or 24) by the integration (3.14b). Suitable contours are shown in figure 8. Branch cuts have been included due to the discontinuities in $[\Omega(z,\Gamma)]^{-1/2}$ and $[\Omega(z',\Gamma)]^{-1/2}$ which occur in $Z_{\pm}(z,\Gamma)$ and $Z_{\pm}(z',\Gamma)$, respectively. The integration of (3.14b) is performed around the contours and branch cuts of figure 8. The poles arise from the zeros of the appropriate Wronskians. Corresponding to the three Green's functions constructed in (3.22,23, and 24), the Wronskian zeros are obtained from the following three conditions:

1) $\cos\,\xi(\alpha_2,\alpha_3,\Gamma) = 0$ or $\xi(\alpha_2,\alpha_3,\Gamma) = (m-\frac{1}{2})\pi$ $\quad m=1,2,\ldots,M$

2) $\cos[\xi_1(0,\Gamma)-\pi/4] = 0$ or $\xi_1(0,\Gamma) = (n-\frac{1}{4})\pi$ $\quad n=1,2,\ldots,N$

3) $\cos[\xi(z_{\ell},\alpha_3,\Gamma)+\xi_1(0,\Gamma)-\pi/4]=0$ or $\xi(z_{\ell},\alpha_3,\Gamma)+\xi_1(0,\Gamma) = (p-\frac{1}{4})\pi$

$p=p_o,\ldots,\infty$

Henceforth, the modes arising from the conditions (1), (2), and (3) will be denoted by m, n, and p-type. The m-type modes are

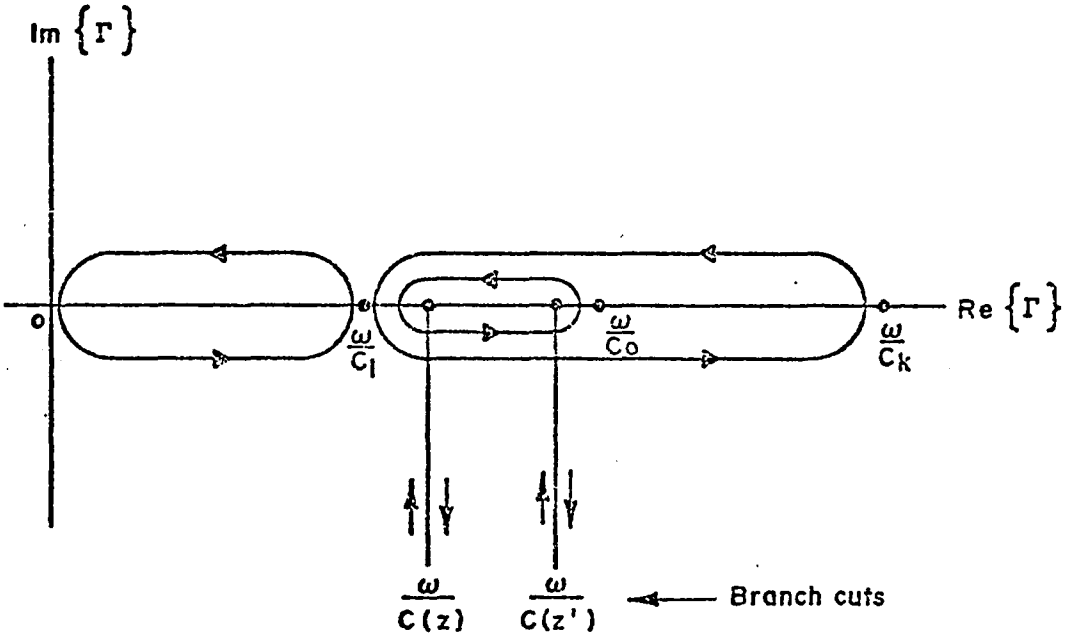

Figure 8 Contours for the determination of the modes

M in number where M is the greatest integer in the quantity $\pi^{-1}\xi(\alpha_2,\alpha_3,\Gamma)+1/2$ for the condition $\beta(\Gamma)=C_\ell$, or $\Gamma=\omega/C_\ell$. The n-type modes are N in number where N is the greatest integer in $\pi^{-1}\xi_1(0,\Gamma)+1/4$ for $\beta(\Gamma)=C_\ell$, or $\Gamma=\omega/C_\ell$. The p-type modes are infinite in number with p_o being the least integer in $\pi^{-1}[\xi(z_\ell,\alpha_3,\Gamma)+\xi_1(0,\Gamma)]+3/4$ for $\beta(\Gamma)=C_\ell$, or $\Gamma=\omega/C_\ell$.

The denominator of (3.11b) may now be evaluated. Using $\cos\xi(\alpha_2,\alpha_3,\Gamma_m)=0$, $\sin^2\xi(\alpha_2,\alpha_3,\Gamma_m)=1$, and Leibniz' rule, one has:

$$1)\quad \frac{\partial}{\partial\Gamma}[\Delta(z')]\Big|_{\Gamma=\Gamma_m} = -\{4\sin^2\xi(\alpha_2,\alpha_3,\Gamma)\frac{\partial\xi(\alpha_2,\alpha_3,\Gamma)}{\partial\Gamma}\Big|_{\Gamma=\Gamma_m}$$

$$= 4\Gamma_m\int_{\alpha_2(\Gamma_m)}^{\alpha_3(\Gamma_m)} \Omega^{-1}(\bar{z},\Gamma_m)\,d\bar{z}$$

In a similar manner

$$2)\quad \frac{\partial}{\partial\Gamma}[\Delta(z')]\Big|_{\Gamma=\Gamma_n} = (-1)^{n+1}4\Gamma_n\cos\xi(\alpha_2,\alpha_3,\Gamma_n)e^{|\xi(\alpha_1,\alpha_2,\Gamma_n)|}\cdot$$

$$\cdot\int_o^{\alpha_1(\Gamma_n)} \Omega^{-1}(\bar{z},\Gamma_n)\,d\bar{z}$$

$$3)\quad \frac{\partial}{\partial\Gamma}[\Delta(z')]\Big|_{\Gamma=\Gamma_p} = (-1)^{p+1}2\Gamma_p\int_o^{\alpha_3(\Gamma_p)} \Omega^{-1}(\bar{z},\Gamma_p)\,d\bar{z}$$

The asymptotic spectral representation (3.11b) is calculated by the three sets of residue summations, using Z_+ to approximate Z_-:

$$\delta(z-z') \sim \sum_{m=1}^{M} Z_+(z,\Gamma_m)Z_+(z',\Gamma_m)\left[\int_{\alpha_2(\Gamma_m)}^{\alpha_3(\Gamma_m)} \Omega^{-1}(\bar{z},\Gamma)d\bar{z}\right]^{-1}$$

$$+ \sum_{n=1}^{N} 2Z_+(z,\Gamma_n)Z_+(z',\Gamma_n)\left[4\cos\xi(\alpha_2,\alpha_3,\Gamma_n)e^{|\xi(\alpha_1,\alpha_2,\Gamma_n)|}\right.$$

$$\left. \cdot \int_{o}^{\alpha_1(\Gamma_n)} \Omega^{-1}(\bar{z},\Gamma_n)d\bar{z}\right]^{-1}$$

$$+ \sum_{p=p_o}^{P} Z_+(z,\Gamma_p)Z_+(z',\Gamma_p)\left[2\int_{o}^{\alpha_3(\Gamma_p)} \Omega^{-1}(\bar{z},\Gamma_p)d\bar{z}\right]^{-1} + \varepsilon(z,z',\Gamma_p) \qquad (3.25)$$

where P is some finite value and ε is the error term arising from truncation of $P < \infty$, since physically $C(z) \to \infty$ is impossible. In practice P is taken where $\alpha_3(\Gamma_p)$ exceeds the depth of the ocean bottom. For the different terms, $Z_+(z,\Gamma_m)$ comes from (3.19c,d,e) with $\sin\xi(\alpha_2,\alpha_3,\Gamma_m) = (-1)$, $Z_+(z,\Gamma_n)$ comes from (3.19a,b,e), and $Z_+(z,\Gamma_p)$ comes from (3.20).

Expression (3.25) contains no contribution from the branch cut integrations. Near the points $\Gamma = \omega/C(z)$ and $\Gamma = \omega/C(z')$, the asymptotic forms defining $Z_+(z,\Gamma)$ and $Z_-(z,\Gamma)$ in all cases are not valid and must be replaced by other forms. All real values of z with finite values of Γ are ordinary points of the differential equation (3.13). Therefore $Z_+(z,\Gamma)$ and $Z_-(z,\Gamma)$ are analytic at and near the above points on the real-Γ axis. The branch cut integrations are therefore non-contributing for the same reason as in Problem 1 of this chapter.

The WKB solutions fail near turning points, requiring alternate forms over small intervals about these points. One could always evaluate a Frobenious series near such points which were analytic and whose behavior away from the turning points coincide with any of the WKB solutions used. Other methods were developed by Langer [27]. If it is assumed that $\Omega^2(z,\Gamma)$ is linear in z near turning points, analytic solutions are available in the form of Bessel functions of order 1/3. This methodology is well-covered in literature [27], so only one example will be shown here. Consider the m-mode type with z located near α_2, the applicable solution of (3.13) with Ω^2 linear in z about $z = \alpha_2$ is:

$$Z(z,\Gamma) = 2[4\xi(z,\Gamma)/6\Omega(z,\Gamma)]^{1/2}\{J_{1/3}[\xi_2(z,\Gamma)]+J_{-1/3}[\xi_2(z,\Gamma)]\}$$

Figure 9 depicts the fundamental difference between the m, n, and p-type modes. The m-type mode functions $Z_+(z,\Gamma_m)$ for $C_o < \beta(\Gamma_m) < C_\ell$ are characterized in Figure 9a. The functions are damped exponentials below $\alpha_3(\Gamma_m)$ and between $\alpha_1(\Gamma_m)$ and $\alpha_2(\Gamma_m)$. Above $\alpha_1(\Gamma_m)$ and between $\alpha_2(\Gamma_m)$ and $\alpha_3(\Gamma_m)$ the functions are oscillatory, the latter range having a greater amplitude. For the interval $C_k < \beta(\Gamma_m) < C_\ell$ the m-type modes are different from that in Figure 9a only in that there is no oscillatory behavior at z = 0, corresponding to the lack of a turning point in Region I.

Figure 9b depicts the n-type modes. The functions $Z_+(z,\Gamma_n)$ are damped exponentials below $\alpha_3(\Gamma_n)$ and between $\alpha_1(\Gamma_n)$ and $\alpha_2(\Gamma_n)$. They are oscillatory above $\alpha_1(\Gamma_n)$ and between $\alpha_2(\Gamma_n)$ and $\alpha_3(\Gamma_n)$, the former range having a greater amplitude. These are the so-called "trapped" modes for the surface duct formed in Region I.

In figure 9c, the p-type modes are depicted. The mode function $Z_+(z,\Gamma_p)$ are oscillatory above $\alpha_3(\Gamma_p)$ and damped below this height. Again significant amplitudes are present near the surface.

The WKB method loses its validity at low frequency (below 500 Hz) or when the turning points are very close together.

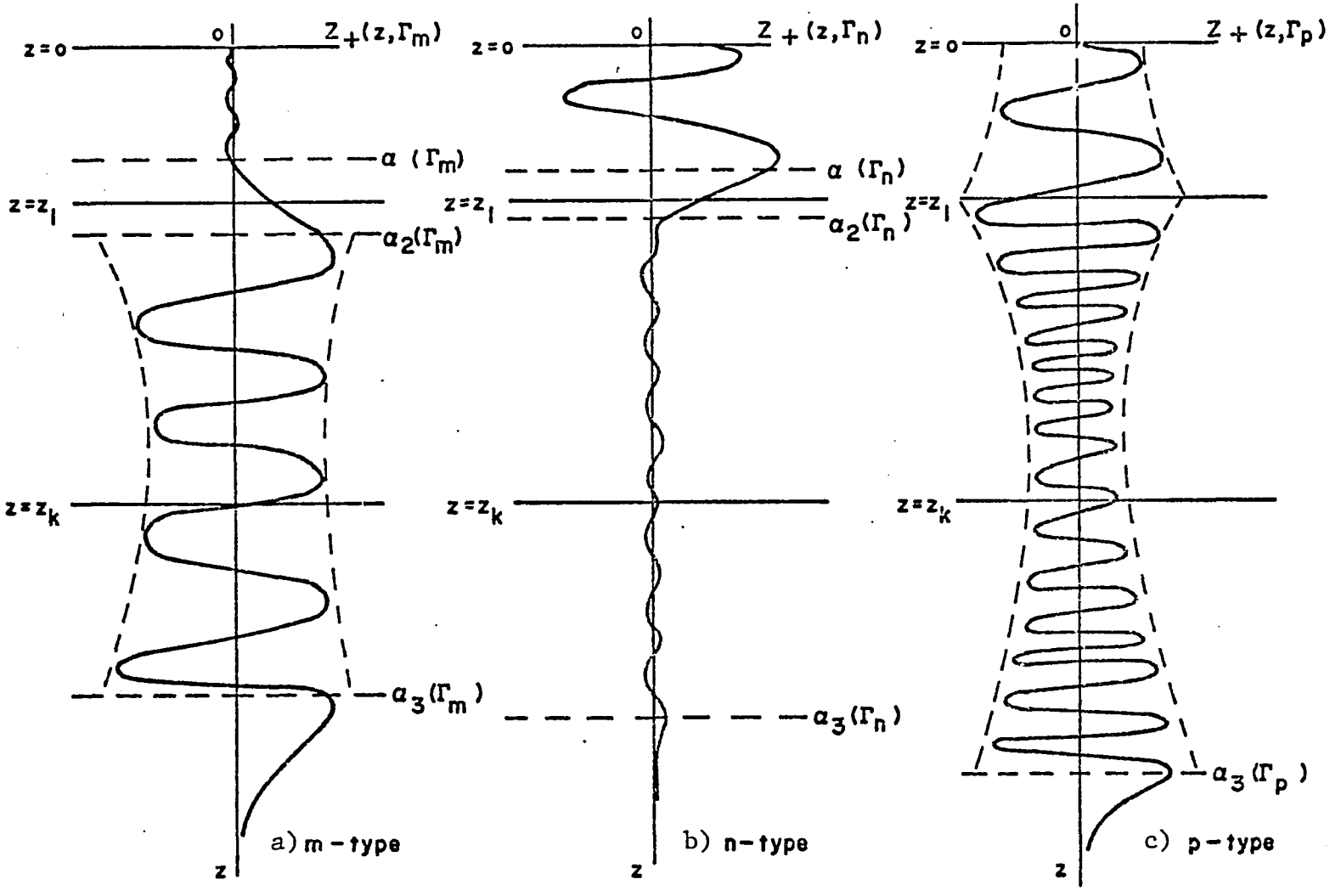

Figure 9 Mode types m, n, and p

Fluid Layer with Sound Speed Profile and Viscoelastic Solid Bottom

Introduction

Problem 1 of the previous section considers shallow water with a constant sound speed overlying a rigid solid boundary. This model neglects the potential for the sound to be trapped into a channel formed by the sound velocity profile. It also neglects the attenuation caused by partial transmission into the bottom sediment.

Problem 2 of the previous section considers deep water with a sound velocity profile with no bottom. This model accounts for the potential for channelled sound but neglects the bottom effects.

In an attempt to model the shallow water sound propagation problem more realistically this next section considers shallow water with a sound velocity profile overlying a viscoelastic solid boundary. This model accounts for both the potential for channelled sound and attenuation by the viscoelastic bottom.

In this next section plots of transmission loss are generated by a computer program with this latter model for various viscoelastic bottom types. The results are compared qualitatively with experimental data from the Baltic Sea. Again the solution involves the WKB approximation for the reasons already given in the previous section.

Boundary Conditions

The fundamental difference between this section and Problem 2 of the previous section is the boundary condition at the bottom. The former problem had the boundary at infinity; hence $Z_+(z\to\infty) \to 0$ was a convergence condition. In this present problem, a viscoelastic bottom boundary is considered. The condition is that the normal displacement and normal stress are continuous across the interface and shear stresses vanish.

The top boundary condition is the same as for the previous problem except that it is applied in a different manner. The fluid-air interface at the top is modeled as a "free" surface, that is, the gauge pressure vanishes ($P = 0$) and consequently there is total reflection here. This condition must be related to the Green's function $G(\vec{r},\vec{r}';\omega)$. One has the definition $\vec{u} = \nabla\Psi$ for the homogeneous case and therefore $\vec{u} = \nabla G$ for the impulse-forced case. The linearized Euler equation of an ideal fluid in the $(\vec{r};t)$ domain reads:

$$\rho_o \frac{\partial^2 \vec{u}}{\partial t^2} + \nabla P = \vec{o}$$

After transforming to the $(\vec{r};\omega)$ domain and substituting $\vec{u} = \nabla G$ one obtains $\nabla(P-\rho_o\omega^2 G) = \vec{o}$. Considering gauge pressures, this expression integrates to:

$$P = \rho_o \omega^2 G(\vec{r},\vec{r}';\omega) \quad . \qquad (3.26)$$

The pressure release condition (P = 0) at the top then implies: $G(\vec{r}-\vec{r}';\omega)\Big|_{z=T} = 0$. This condition is realizable when:

$$Z_{-}(z=T;\omega) = 0 \; ; \quad T = \text{depth } z \text{ at top.} \qquad (3.27a)$$

Since the exponentials equal unity for $Z_{-}(z=T;\omega)$ one sees that the prescribed boundary condition can be enforced with [see Appendix IIIc]:

$$A_T = 1 \quad \text{and} \quad B_T = -1 \; . \qquad (3.27b)$$

The solutions to (3.4c) may then be evaluated at depths below the top using the bridging conditions (3.18) for the coefficients A and B to step down over the turning point singularities.

The bottom boundary conditions require the continuity of both normal displacements and normal stresses across the interface and the vanishing of shear stresses. If one denotes the subscript "o" for the ideal fluid, "1" for the solid, uses (3.26) and notes from $\vec{u} = \nabla G$ that $u_z = \partial G/\partial z$, then the boundary condition may be stated as (all cases for depth at bottom z = B):

$$(u_z)_o = \partial G/\partial z = (u_z)_1 \qquad (3.28a)$$

$$(\sigma_{zz})_o = -p = -\rho_o \omega^2 G = (\sigma_{zz})_1 \qquad (3.28b)$$

$$(\sigma_{rz})_o = 0 = (\sigma_{rz})_1 \qquad (3.28c)$$

It is now shown that boundary conditions (3.28a and b) may be combined into a single statement by substituting them into the definition of acoustic impedance.

The acoustic impedance I is defined as: $I = P/v_z$, where P is the acoustic pressure and v_z is the normal velocity at the boundary interface and may be expressed as $v_z = i\omega u_z$ in the frequency domain. The impedance may then be defined for the solid by substituting for P using the relation: $P = -\sigma_{zz}$. Combining all of the above, one may write the impedance of the solid as:

$$I(\Gamma,\omega) = \frac{-(\sigma_{zz})_1}{i\omega(u_z)_1} = \frac{\rho_o\omega^2 G}{i\omega(\partial G/\partial z)} \quad , @z=B. \qquad (3.29a)$$

This expression (3.29a) may be rearranged to read:

$$\left[G - \frac{i}{\rho_o\omega} I \frac{\partial G}{\partial z}\right]\Big|_{z=B} = 0 \ , \qquad (3.29b)$$

where B is the depth of the bottom. This condition on $G(\vec{r},\vec{r}';\omega)$ reduces to a condition on Z_+ since the other factors of (3.12c) are not functions of the depth-variable z except for Z_- which has been accounted for by the top boundary condition. This condition on Z_+ of (3.17c) is insured by the following selection of the coefficients [see Appendix IIIc]:

$$A_B = \rho_o\omega I\Omega(z=B) - 1 \quad \text{and} \quad B_B = \rho_o\omega I\Omega(z=B) + 1 \ . \qquad (3.30a)$$

The bottom impedance $I(\Gamma,\omega)$ has been shown by Stewart [28] to be evaluated according to:

$$I_1(\Gamma,\omega) = \frac{-i\rho_1\omega}{a_{L1}K_{T1}^4}\left[(2\Gamma^2-K_{T1}^2)^2-4a_{L1}a_{T1}\Gamma^2\right] , \quad (3.30b)$$

where the subscript 1 denotes the parameters of the bottom (not fluid), $a_T^2 = \Gamma^2-K_T^2$, $a_L^2 = \Gamma^2-K_L^2$, $K_T^2 = \rho\omega^2/\bar{\mu}$, $K_L^2 = \rho\omega^2/(\bar{\lambda}+2\bar{\mu})$, $\bar{\mu} = \mu'+i\omega\mu''$, $\lambda = \lambda'+i\omega\lambda''$, the single primes refer to the ordinary Lame parameters, and the double primes refer to Voigt damping parameters. Using this impedance concept, any type bottom may be specified once the μ', μ'', λ', and λ'' are determined. The other coefficients, for regions above the bottom, are evaluated from the bridging conditions (3.18) that allow one to step over turning points into the next region above.

Computer Generated Plots of Transmission Loss Versus Range

Employing the same procedure depicted in Problem 2 of the previous section one may evaluate numerical results using a digital computer. Used here was the VAX system (Digital Corporation) of the High Energy Physics Laboratory of Harvard University, Massachusetts. The parameters for the viscoelastic bottom are published by Hamilton [29]. The specific source depth and frequency, receiver depth and range, and ocean depth and sound velocity profile were chosen so as to compare these theoretical results with experimental results from a report

[30] provided by Sanders Associates of Nashua, New Hampshire.

The numerical results, being transmission loss as a function of horizontal source-receiver separation distance, were evaluated in three steps. For the first step, the user interactively selected the bottom, source, and receiver specifics and the type of plot desired. The second step generated the eigenvalues and coefficients, while the third step combined the data from the first and second steps to construct the Green's function of (3.12c) and plot the transmission loss, TL:

$$TL = 10 \log_{10}|G(\vec{R};\omega)| \ . \qquad (3.31)$$

The computer programs are presented in the final Appendix of this dissertation.

The input data for the computer simulation is taken to model the physical description of the experimental site in the Baltic Sea (1974). The same source frequency (1.7khz) and depth (7 meters), receiver depth (10.5 meters), horizontal range (1 to 9 nautical miles) are used. The difference between the computer and experimental input data are as follows. The model has a constant ocean depth while the real data was collected over an ocean bottom that varied from 17 to 26 meters in depth. The model treats the static case where both source and receiver are stationary while the real data was collected with the source being towed at 4 knots causing the frequency of the sound received by the moving observer to

be: $f = f_o[1-(v/c)\cos\theta]$, where θ is the angle between the velocity of the source and that of the wave number vector $\vec{k}$, and

$$\frac{v}{c} = \frac{4 \text{ knots}}{1466(\text{m/sec})} = \frac{2.05(\text{m/sec})}{1466(\text{m/sec})} = 0.00141 \ .$$

This doppler shift is negligible. The model considers a constant bottom composition while the real test site varied from being primarily silt and changed to mud and fine sand at the shallower depths [see figure 10]. The model's sound velocity profile was a seven-part piecewise linear approximation [figure 11b] to the real profile [figure 11a] of October 30, 1974.

The model was run for nine different viscoelastic bottom types ranging from coarse sand to silty-clay. The viscoelastic parameters are published by Hamilton [29] and presented in Tables 1 and 2. The bottom depth was varied from 17 to 27 meters in 2 meter intervals. So between the variation of these two parameters there are fourteen models run as diagrammed in Table 3, which also serves the purpose of defining the notation for labelling the plots.

Transmission loss TL (normalized at 1000 meters) is plotted on a scale of 0 to 30 decibels versus the horizontal range of the source/receiver separation in both meters and nautical miles. The transmission loss is calculated from the Green's function (3.12c) by the relation (3.31). Note that

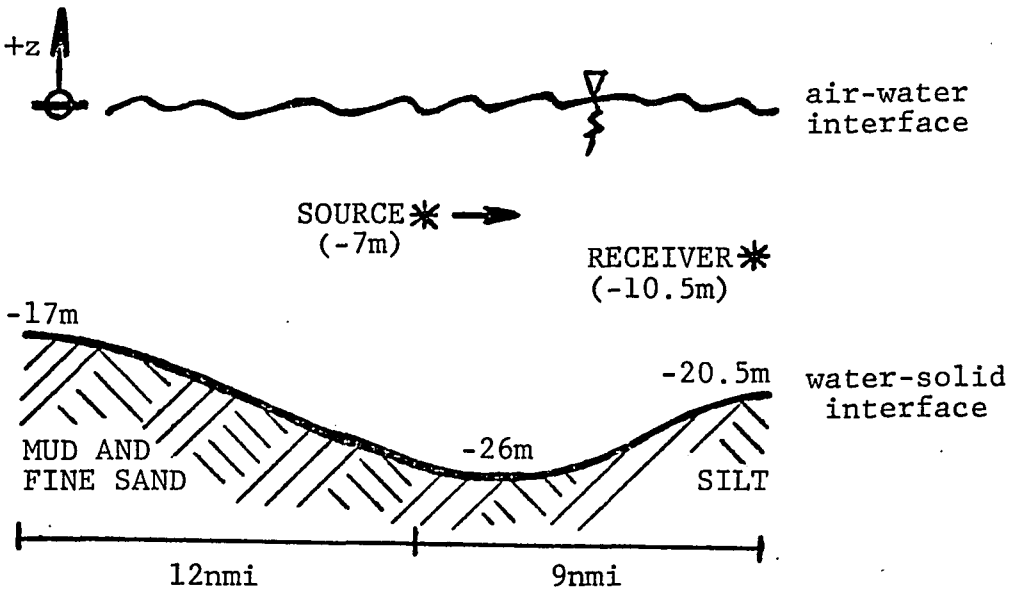

Figure 10 Input data

"...The water depth in this shallow water basin (off the eastern point of the island Fehmarn) along the track varies from 20.5m at the receiving array to a maximum of 26m at 8nmi and then slowly decreases to approximately 17m at 21nmi and beyond. The bottom type was primarily silt, changing to mud and fine sand at the shallower depths. The receiving array of hydrophones was located 10.5m underwater during each experiment. One C-W (continuous wave) source, a calibrated ITC 1022 transducer, was utilized on two occasions, 30 October and 4 November 1974.

On 30 October the source frequency was set at 1.7khz. The transducer was towed at a depth of 7m with a speed of advance (SOA) of about 4knots. Measurements made shortly before the exercise indicated winds near 17knots and a significant sea wave height ($\overline{H}_{1/3}$) of 64cm. Because the wind and sea direction were from 020°T, the wavecrests were nearly parallel to the sound propagation direction. The velocity profile obtained prior to the measurement (figure 11) indicated that the source was situated slightly above and the receiving hydrophones well below the positive sound speed gradient." [see reference 30]

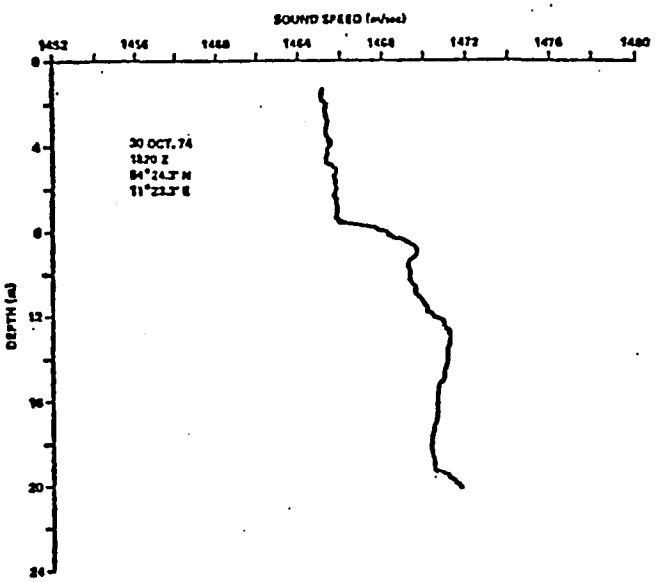

a) Experimentally measured profile

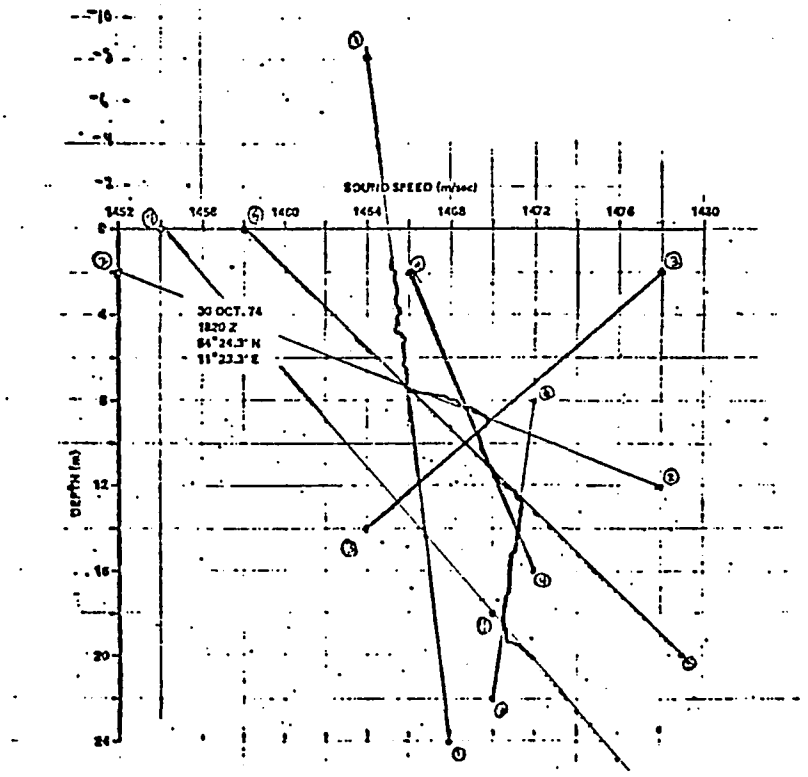

b) Piece-wise linear approximation

Figure 11 Sound speed profile in the Baltic Sea(1974) [see reference 30]

Table 1 IN-SITU ELASTIC PROPERTIES OF MARINE SEDIMENTS*

Sediment Type	η %	ρ g/cm^3	c_L m/sec	κ dynes/cm^2 $\times 10^{10}$	λ' dynes/cm^2 $\times 10^{10}$	μ' dynes/cm^2 $\times 10^{10}$	c_T m/sec $\times 10^{1}$
Continental terrace (shelf and slope)							
1. Coarse sand	38.6	2.06	1808	6.69	6.70	0.030	12
2. Fine sand	44.8	1.95	1727	5.51	5.35	0.23	35
3. Very fine sand	49.8	1.86	1672	5.02	4.95	0.14	27
4. Silty sand	53.8	1.80	1642	4.50	4.3	0.26	37
5. Sandy silt	52.5	1.81	1638	4.45	4.2	0.31	41
6. Silt	54.2	1.77	1599	4.33	4.2	0.15	29
7. Sand-silt-clay	67.2	1.58	1555	3.59	3.5	0.17	33
8. Clayey silt	72.6	1.47	1522	3.32	3.28	0.060	20
9. Silty clay	75.9	1.43	1496	3.15	3.12	0.038	16

η, porosity; ρ, bulk saturated density; c_L, compressional-wave velocity; κ, bulk modulus; λ' μ', Lamé's constants; c_T, shear-wave velocity.

*Elastic properties were taken from laboratory values reported by Hamilton (1974a), and corrected to in-situ values by the techniques outlined by Hamilton (1971b). Elastic properties are given for a water depth of 31 meters in the San Diego Trough where the water density $\rho_0 = 1.025$ g/cm^3 and compressional-wave velocity $c_0 = 1505.37$ m/sec.

Table 2 IN-SITU VISCOELASTIC PROPERTIES OF MARINE SEDIMENTS*

Sediment Type	b_L sec $\times 10^{-4}$	b_T sec $\times 10^{-4}$	λ' dynes/cm^2 $\times 10^{10}$	λ'' dyne-sec/cm^2 $\times 10^{6}$	μ' dynes/cm^2 $\times 10^{10}$	μ'' dyne-sec/cm^2 $\times 10^{6}$
Continental terrace (shelf and slope)						
1. Coarse sand	0.010	1.7	6.70	-0.035	0.030	0.051
2. Fine sand	0.010	0.19	5.35	-0.030	0.23	0.045
3. Very fine sand	0.013	0.35	4.95	-0.035	0.14	0.051
4. Silty sand	0.013	0.17	4.3	-0.030	0.26	0.045
5. Sandy silt	0.014	0.17	4.2	-0.035	0.31	0.051
6. Silt	0.013	0.30	4.2	-0.030	0.15	0.045
7. Sand-silt-clay	0.0020	0.035	3.5	-0.0038	0.17	0.0057
8. Clayey silt	0.0016	0.070	3.28	-0.0028	0.060	0.0041
9. Silty clay	0.0014	0.083	3.12	-0.0021	0.038	0.0032

b_L and b_T, damping coefficients; λ' and μ', elastic contribution of complex Lamé constants; λ'' and μ'', viscous contribution of complex Lamé constants.

*In-situ viscous properties were predicted by the method developed by Hamilton (1972), and adjusted to describe the Voigt viscoelastic model for the frequency $f = 5$kHz .

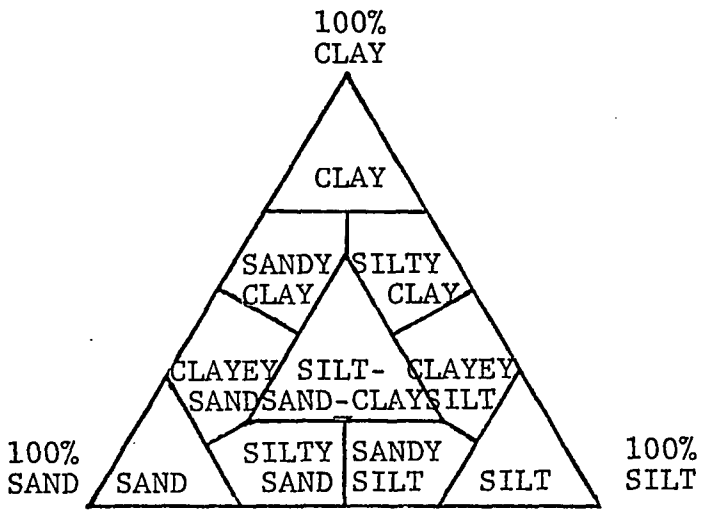

Bottom Type (composition)		Bottom Depth (meters) 17	19	21	23	25	27
COARSE SAND,	#1				123		
FINE SAND,	#2				223		
VERY FINE SAND,	#3				323		
SILTY SAND,	#4				423		
SANDY SILT,	#5	517	519	521	523	525	527
SILT,	#6				623		
SAND-SILT-CLAY,	#7				723		
CLAYEY SILT,	#8				823		
SILTY CLAY,	#9				923		

Table 3 Sample runs -- Variable bottom type and depth

when the transmission loss TL is greater than 30 dB the data point is off-the-scale of the plot but is printed at 30 dB misleadingly. Above this transmission loss plot is a plot of the phase versus range where the phase is plotted between $-\pi$ and $+\pi$ and hence it can only be determined up to arbitrary additions of 2π. The phase is obtained simply by evaluating the argument of the complex-valued Green's function (3.12c).

The first nine plots are each with a 23 meter ocean depth and the parameter being tested is the bottom type (figures 12a through 12i). The model runs are denoted #123 to #923, consistent with the notation of Table 3. The next six plots are each with the "sandy-silt" bottom type #5 and the parameter being tested is the ocean depth (figures 13a through 13f). The model runs are denoted #517 to #527. Note that #523 is repeated, that is, it appears in figure 12e and 13d to keep consistent and complete sequences.

The plots are now presented followed by a discussion and a comparison with a single set of experimental data.

Discussion

The major statement that may be made on viewing figures 12 is the very significant effect that the bottom type has on the transmission loss over several nautical miles, a fact observed by MacKenzie [31] in 1959. This indicates qualitatively that a lossy bottom may be included in a model of

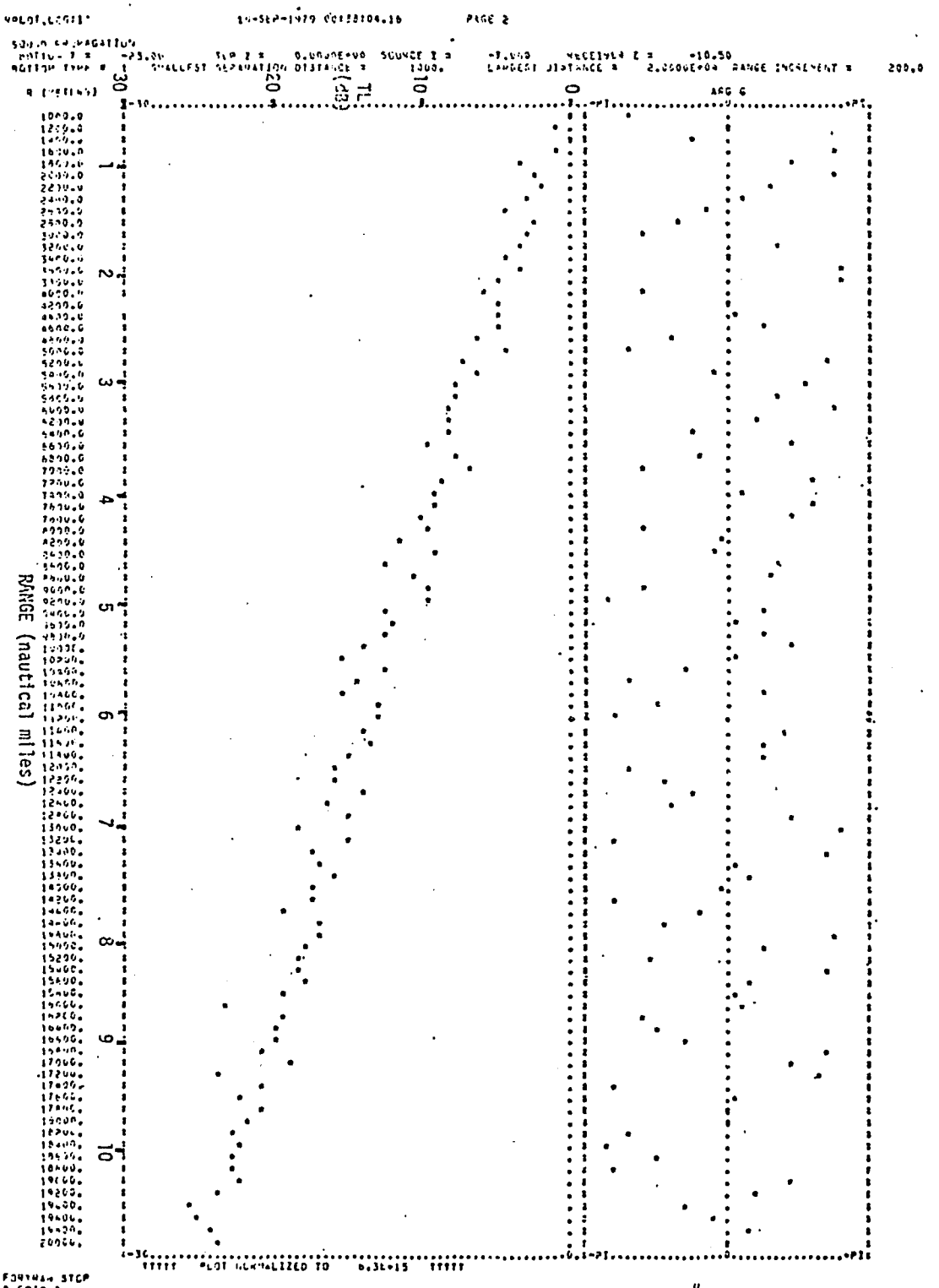

#123

COARSE SAND

23 meter depth

Figure 12a

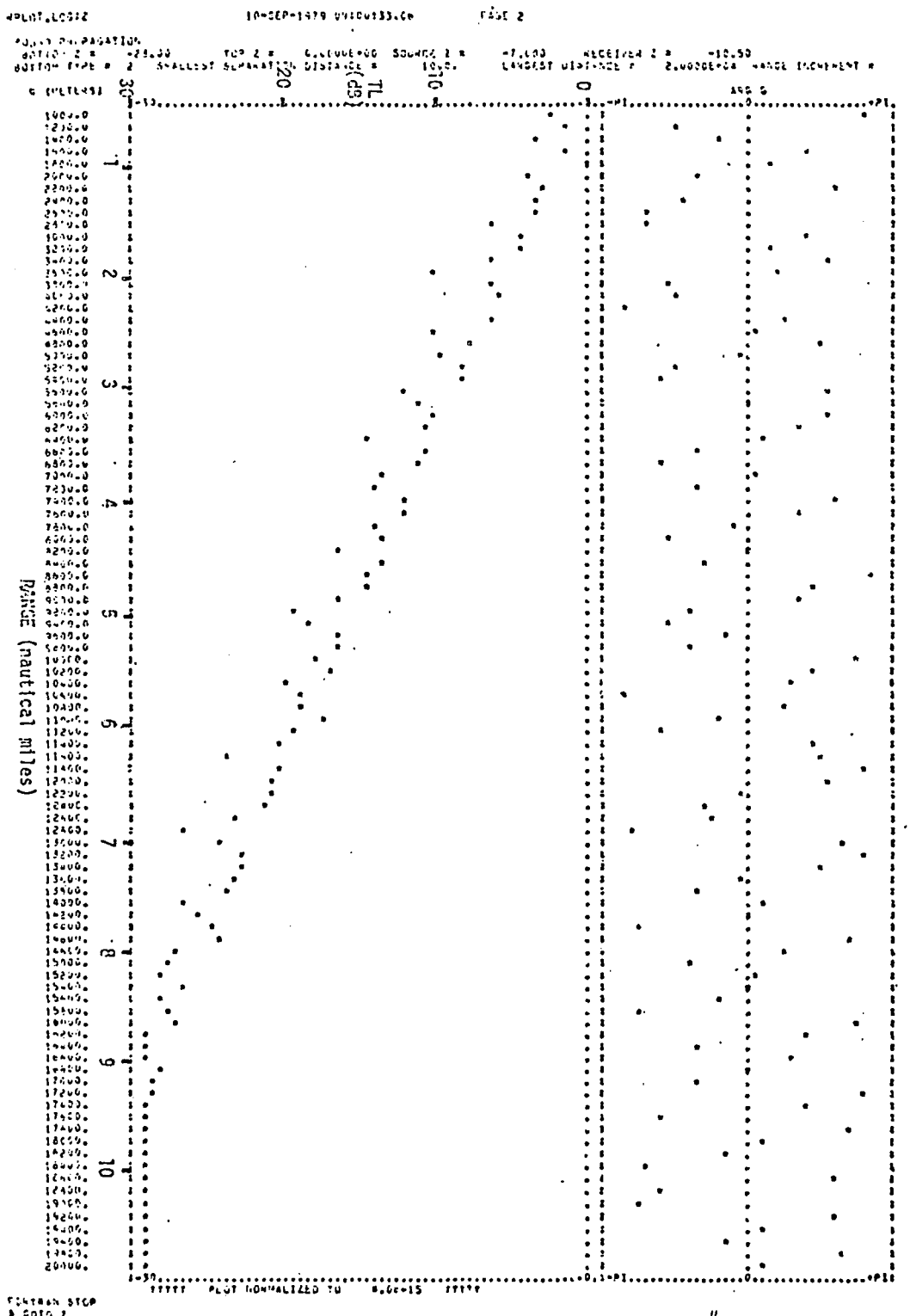

#223

FINE SAND

Figure 12b 23 meter depth

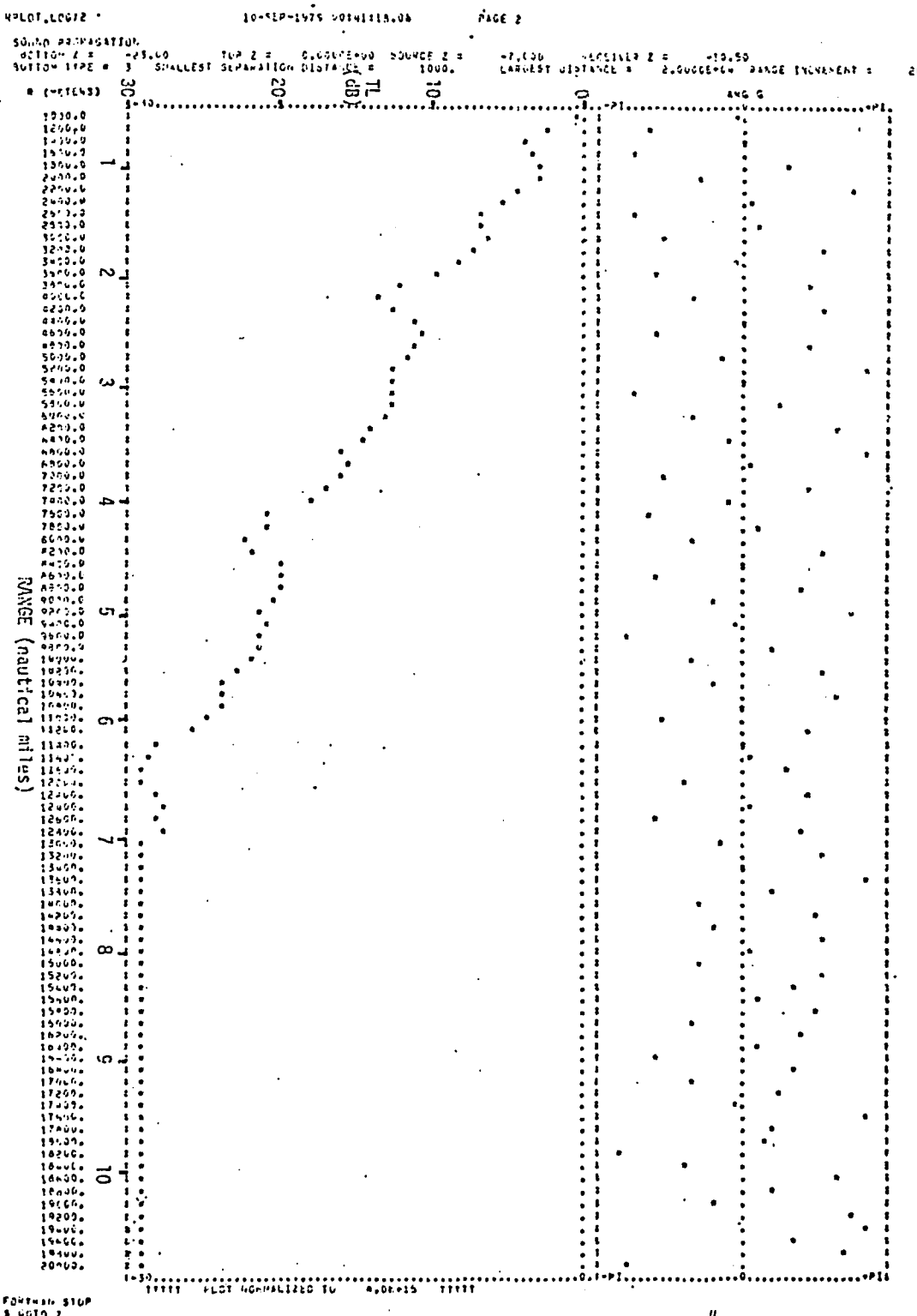

#323

VERY FINE SAND

23 meter depth

Figure 12c

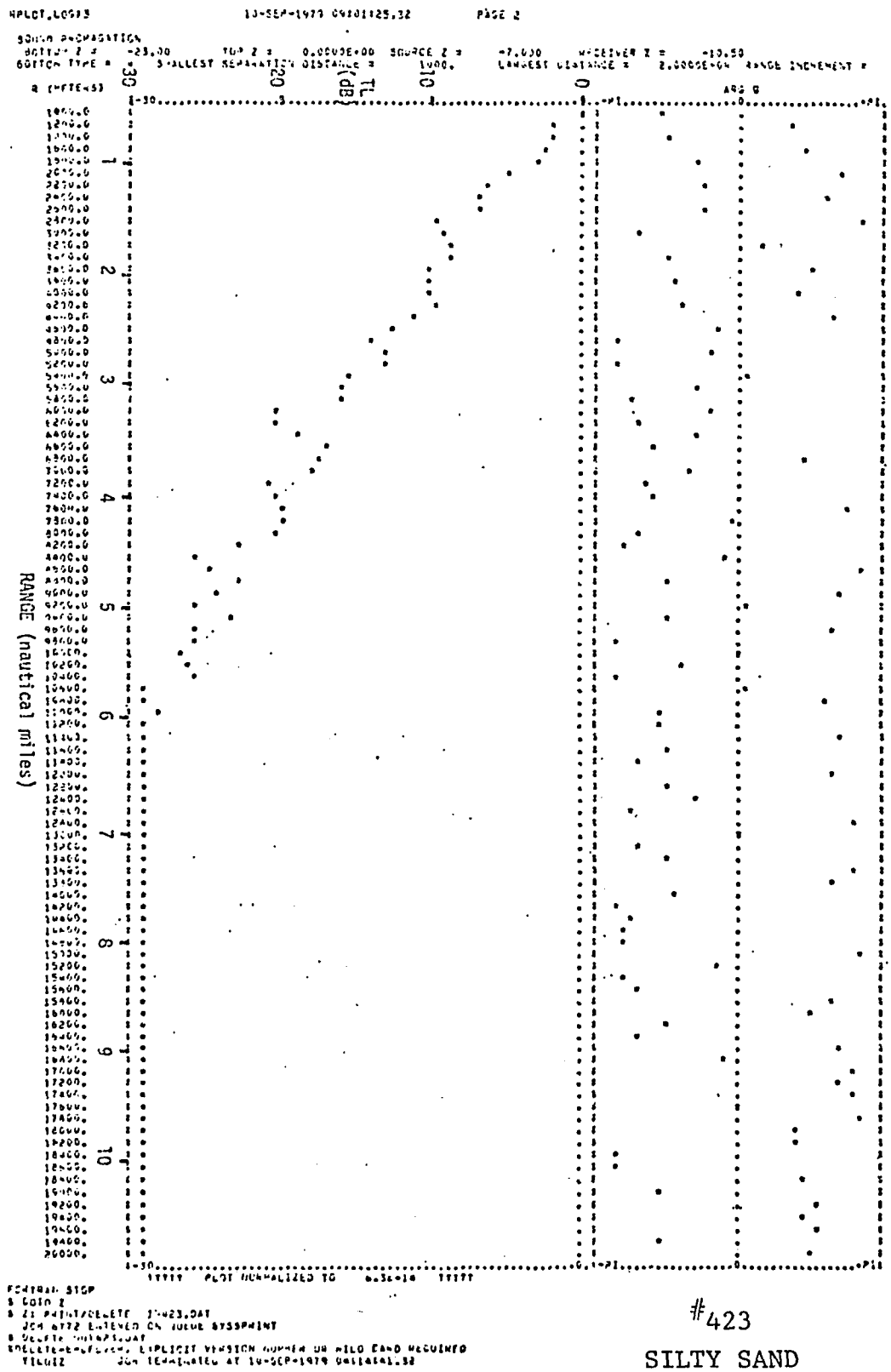

#423

SILTY SAND

23 meter depth

Figure 12d

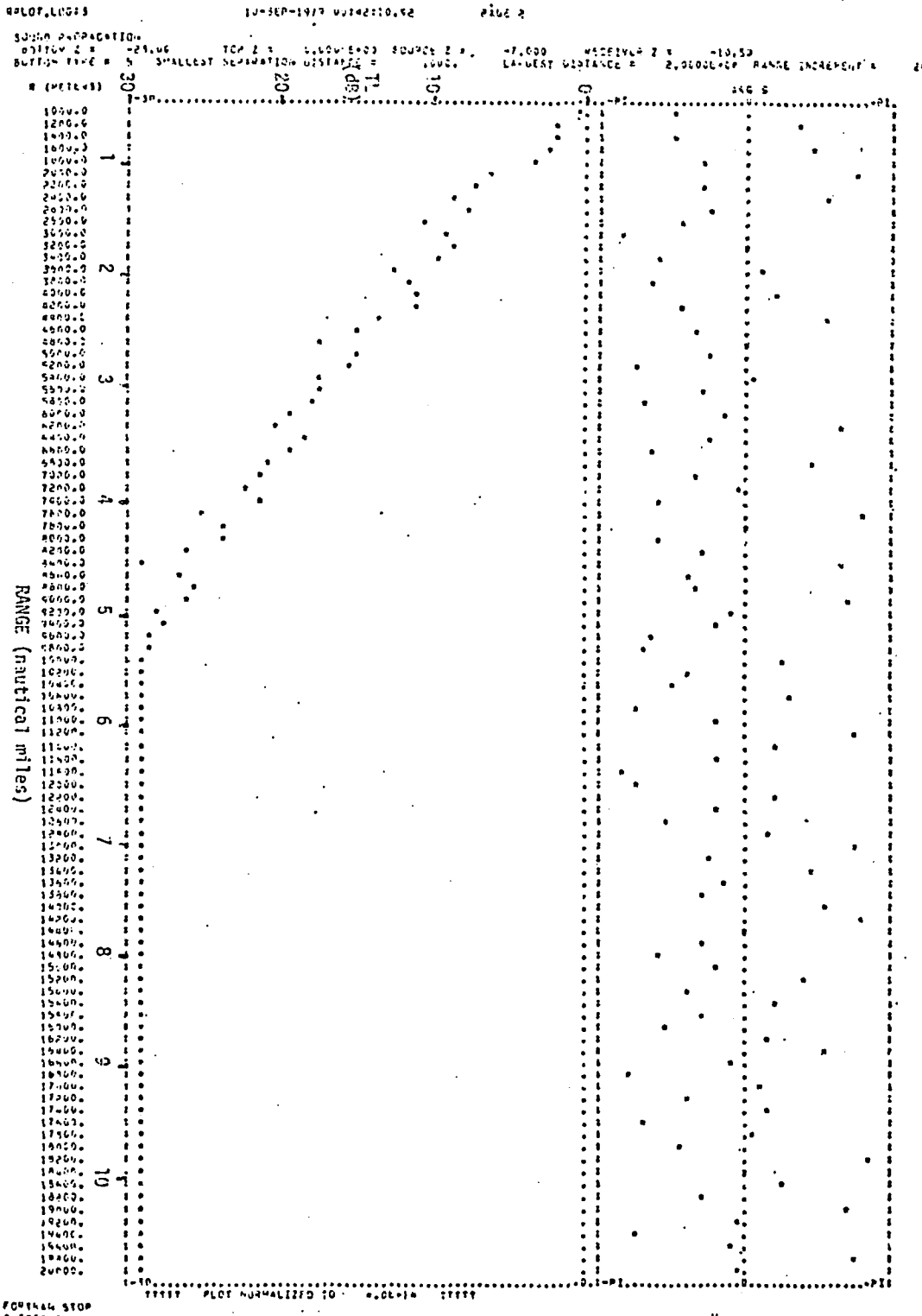

#523

SANDY SILT

Figure 12e 23 meter depth

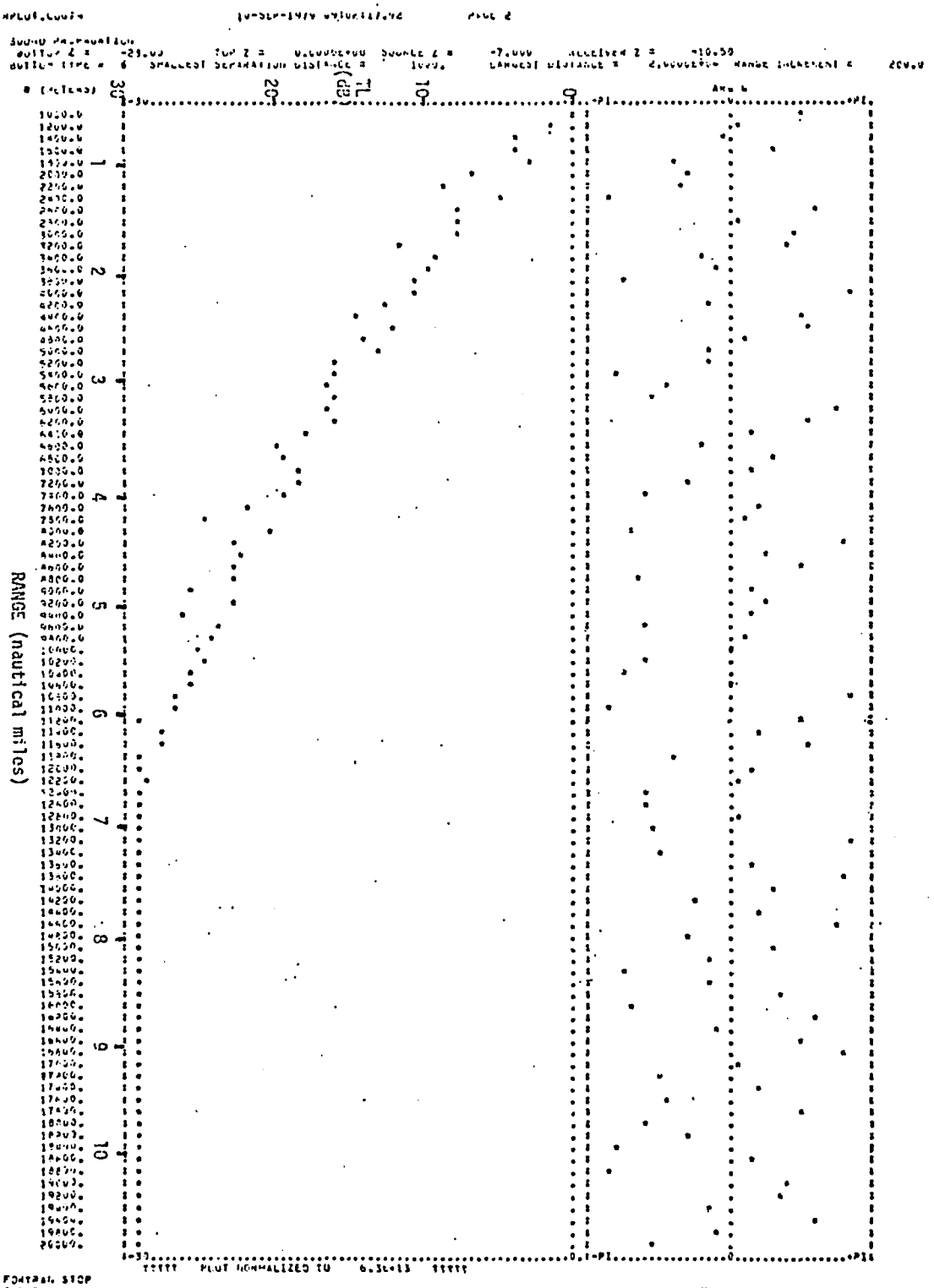

#623

SILT

Figure 12f 23 meter depth

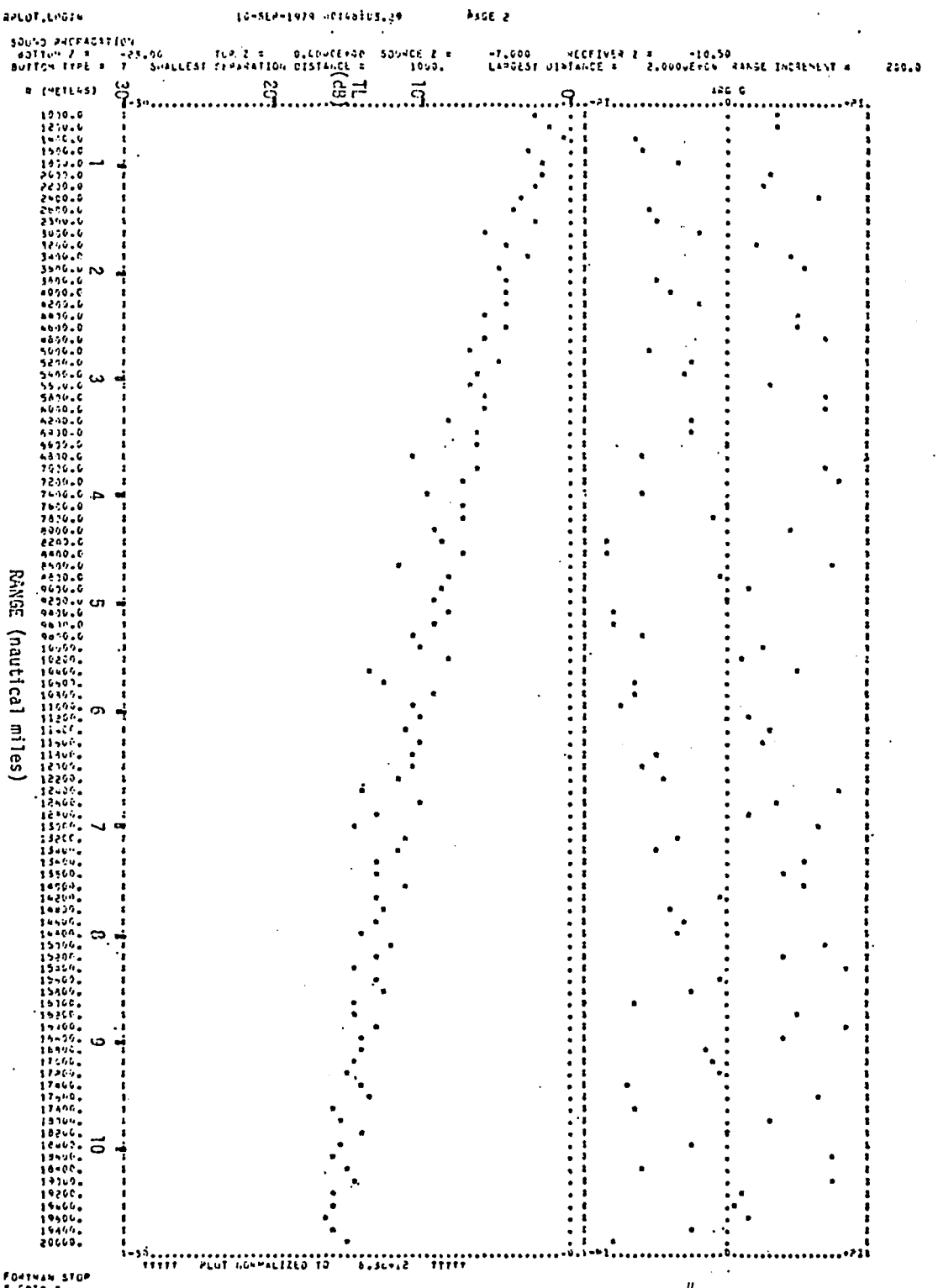

#723

SAND-SILT-CLAY

23 meter depth

Figure 12g

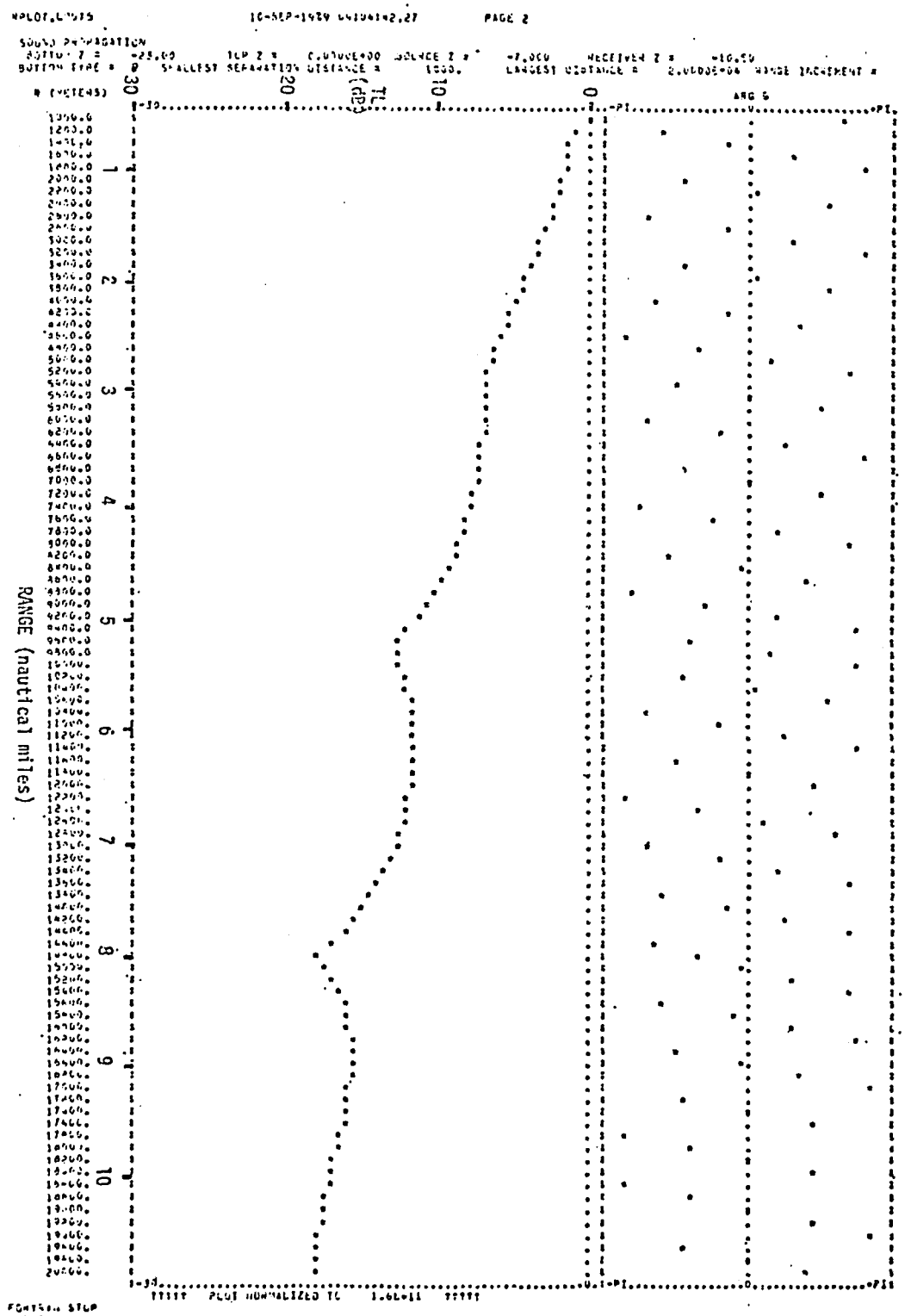

#823

CLAYEY SILT

23 meter depth

Figure 12h

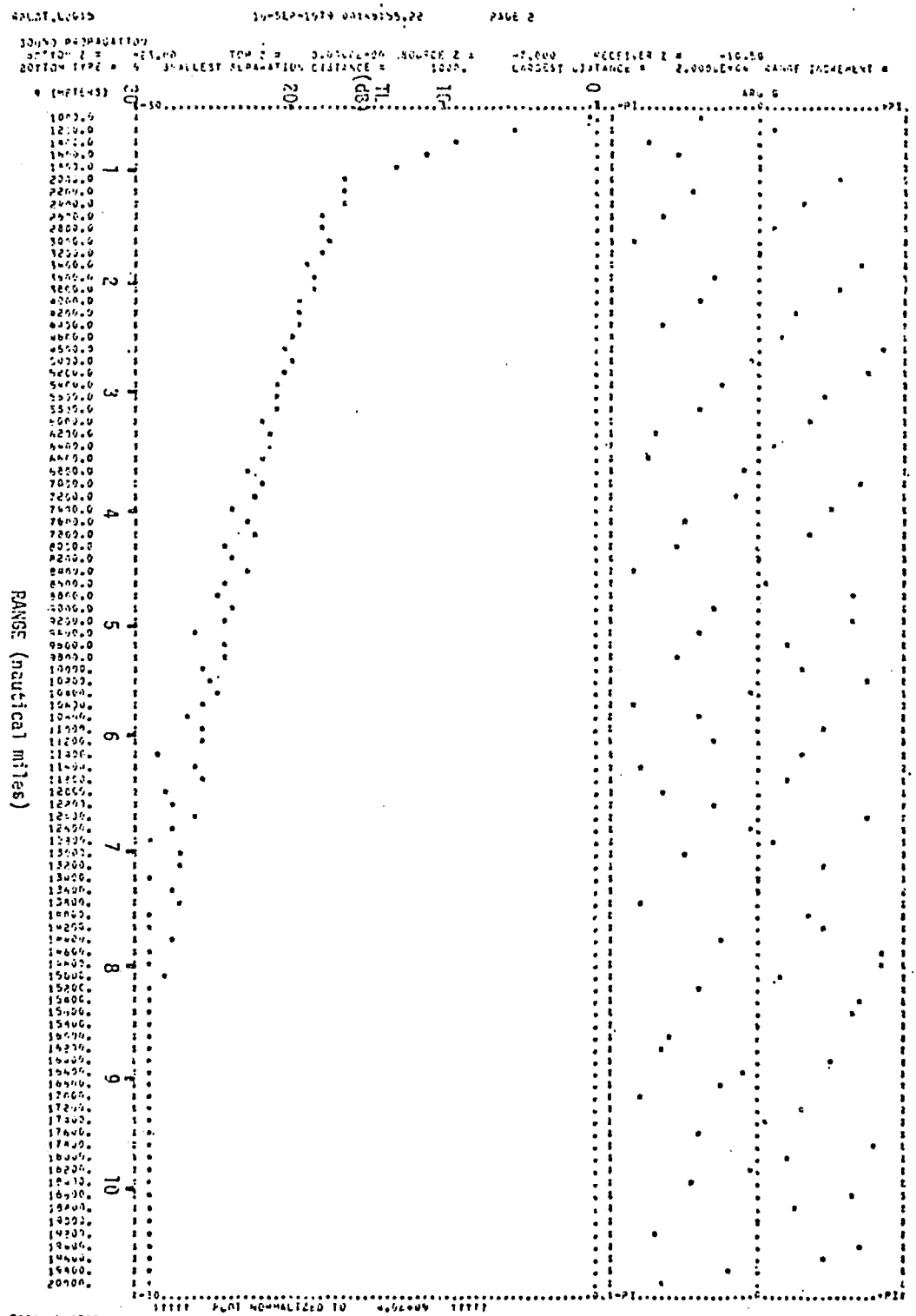

#923

SILTY CLAY

Figure 12i 23 meter depth

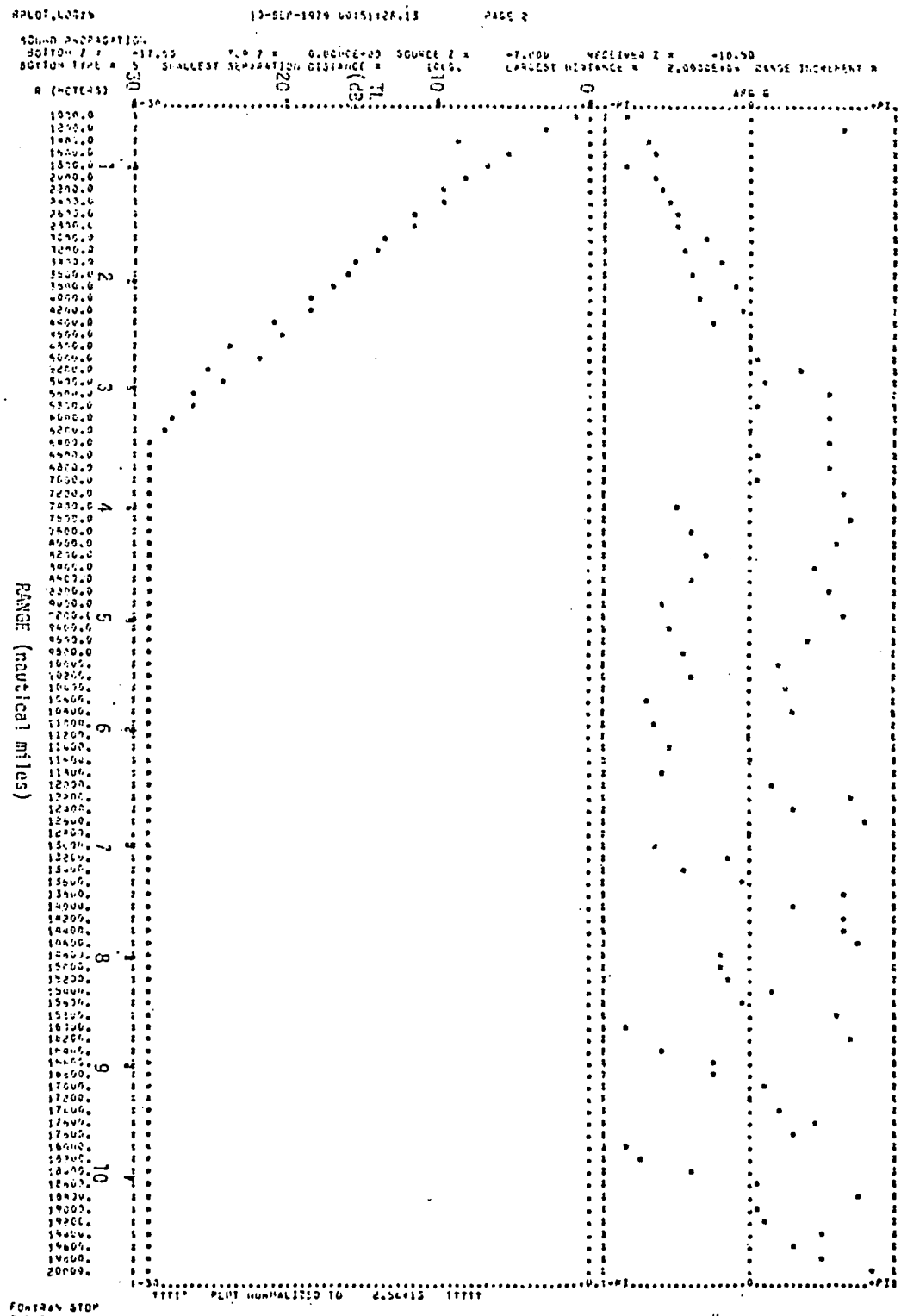

#517

Sandy Silt

17 METER DEPTH

Figure 13a

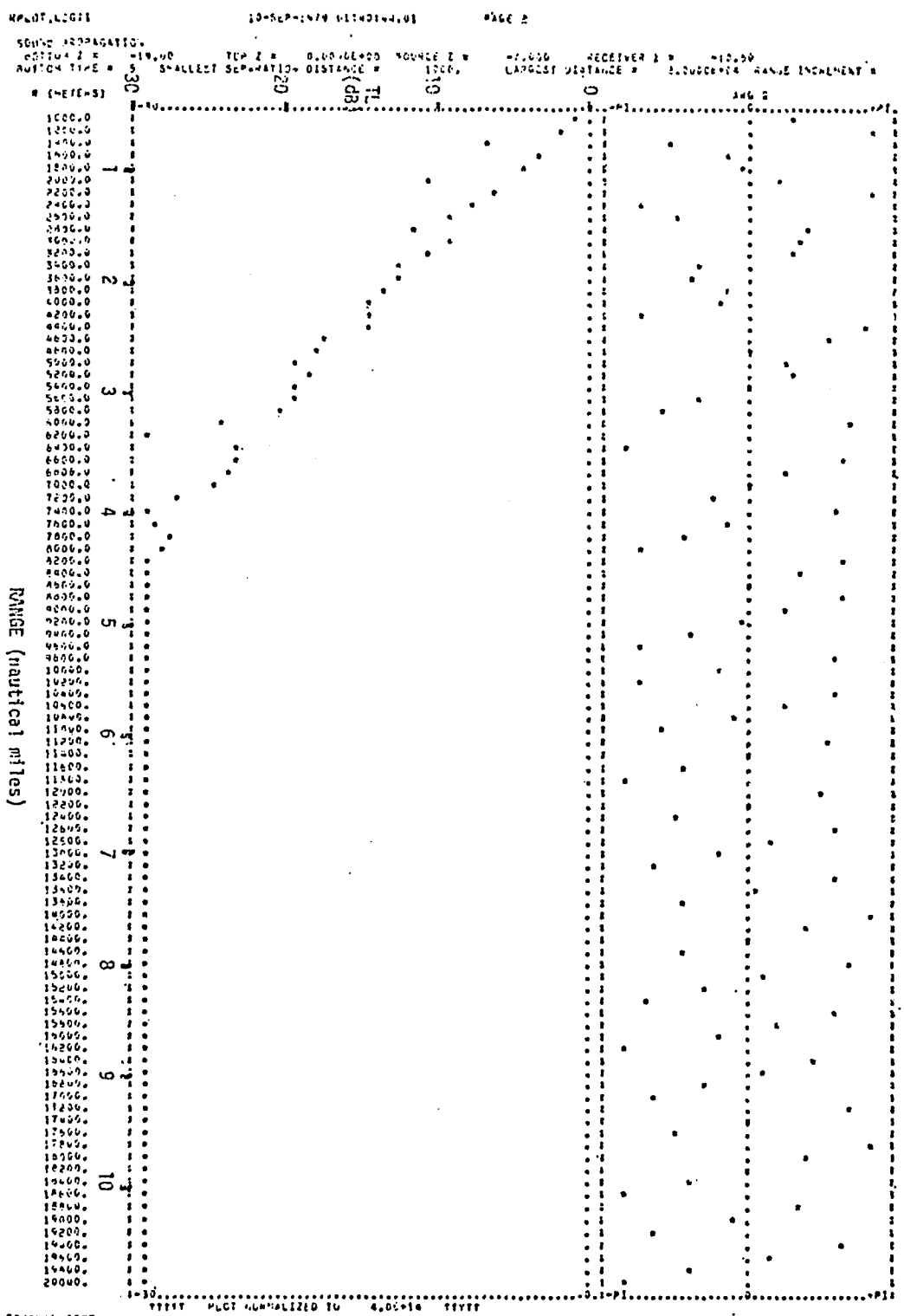

#519

Sandy Silt

19 METER DEPTH

Figure 13b

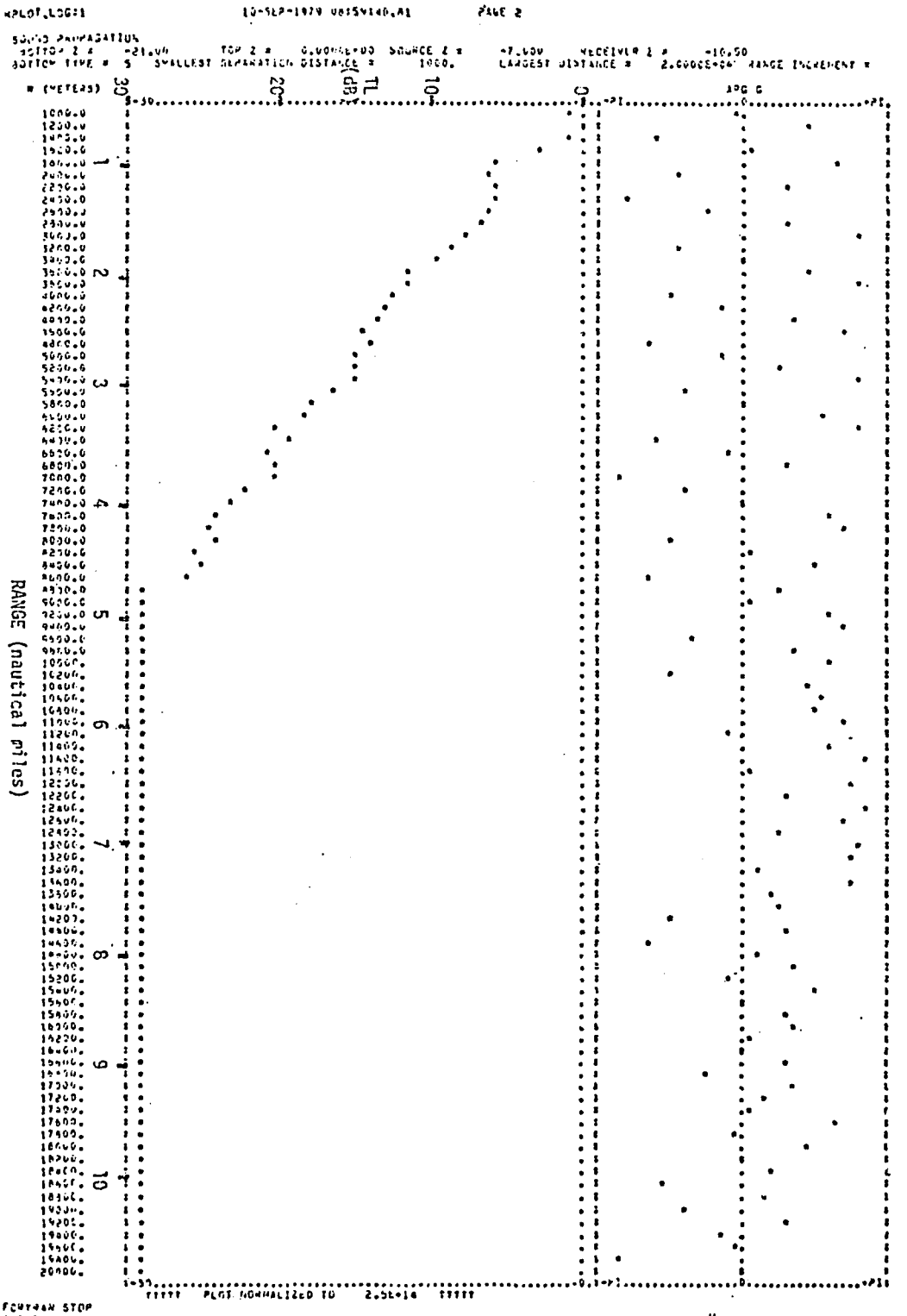

#521

Sandy Silt

21 METER DEPTH

Figure 13c

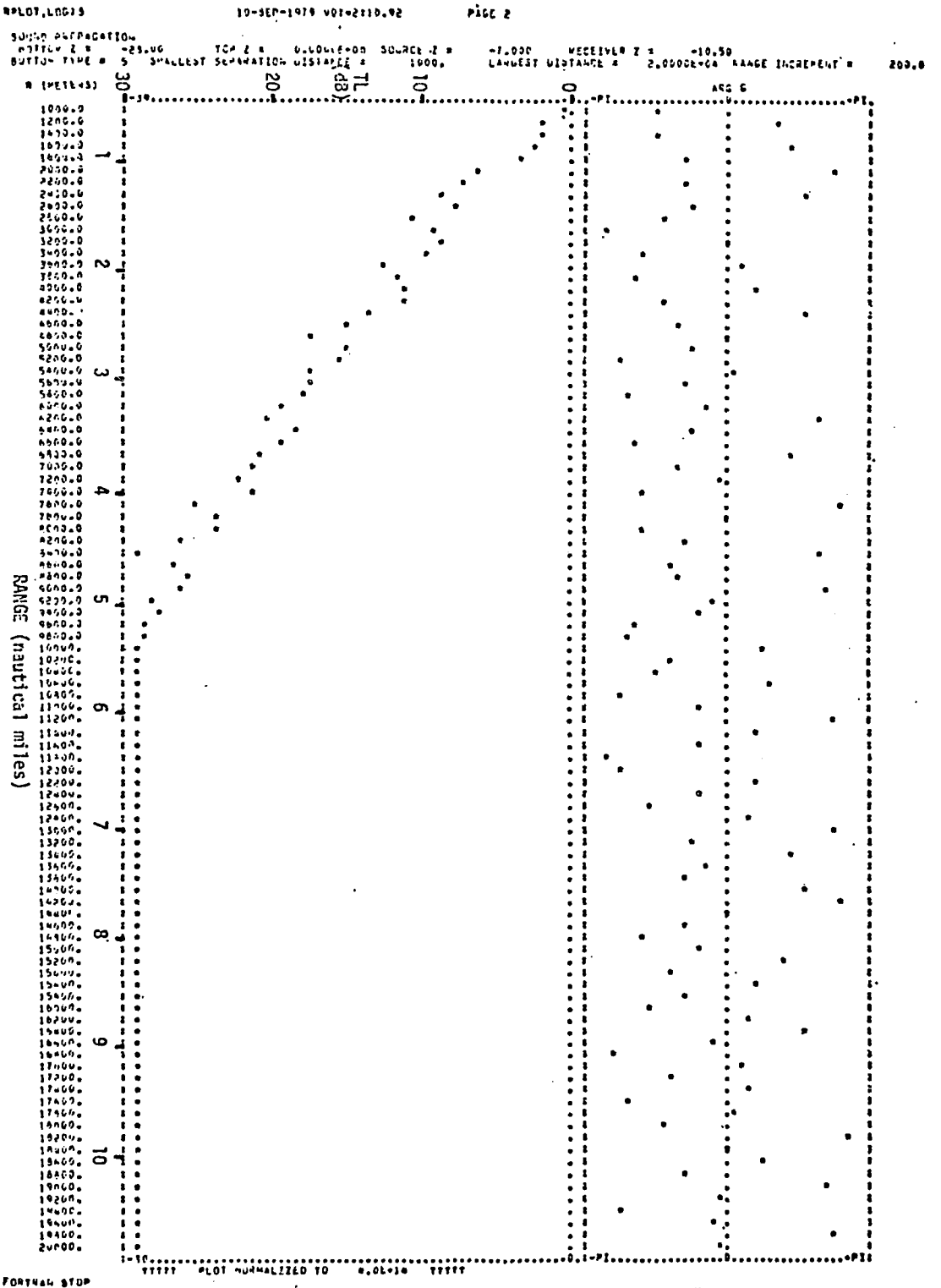

#523

Sandy Silt

23 METER DEPTH

Figure 13d

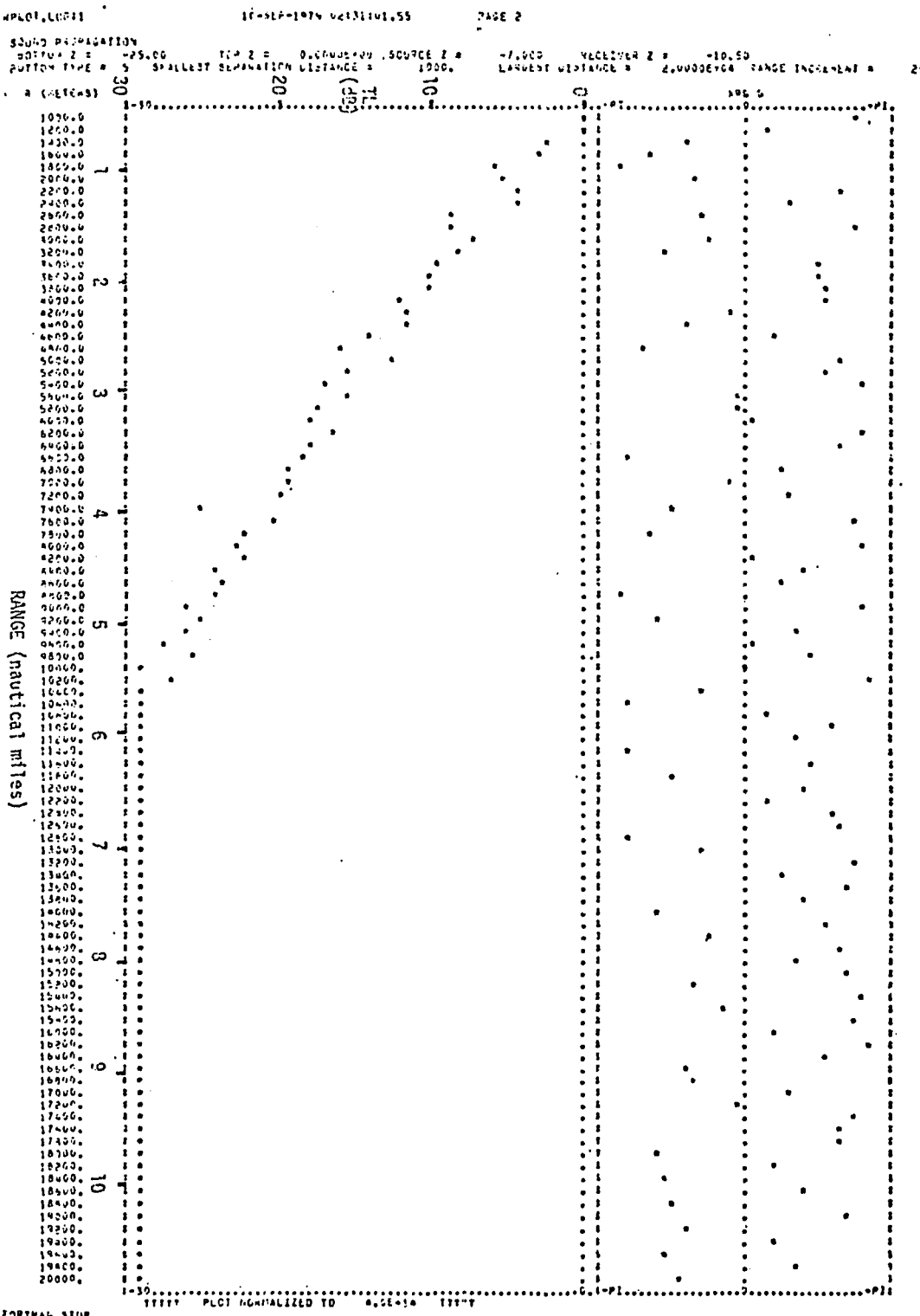

#525

Sandy Silt

25 METER DEPTH

Figure 13e

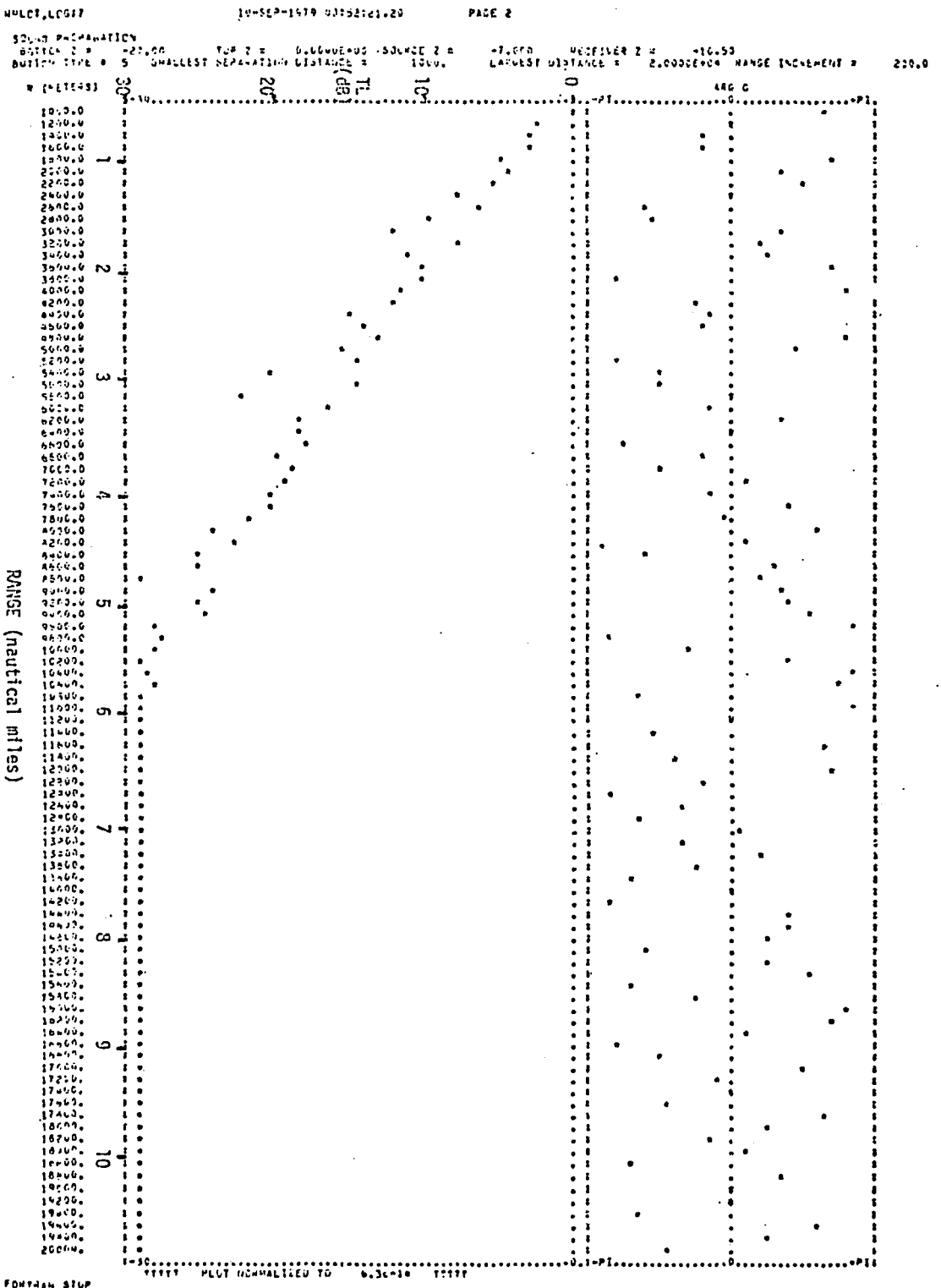

#527

Sandy Silt

27 METER DEPTH

Figure 13f

underwater sound propagation and that the determination of the viscoelastic bottom parameters is indeed critical.

The major statement to be said from figures 13 is that the effect of increasing the depth is to allow more modes to be excited and hence the transmission loss decreases. The number of eigenvalues evaluated for a bottom depth of 17 meters was 37 and increased to 60 for a depth of 27 meters. As the bottom gets deeper it has less of an effect on the attenuation of energy since the compressional wavefronts "see the bottom" less frequently. As the bottom depth was increased further, the situation would asymptotically approach the limiting case of propagation in a semi-infinite fluid, that is, unbounded below.

The following summary pages (Tables 4 and 5) give an overview of the sequences of different bottom type and increasing bottom depth (from figures 12 and 13, respectively). A majority of the plots show the transmission loss to drop-off linearly with range. This implies an exponential decay of the sound pressure field with range.

The ordering of the bottom type by Hamilton seems to follow a consistent decrease in the longitudinal sound speed C_L. The plots (figures 12) suggest a different ordering if one tried to determine a logical progression in their shape. None of the other viscoelastic parameters follow this ordering either. This indicates that the response is some combined effect of the propagation and damping parameters.

Table 4 Summary of plot shapes -- Progression in bottom type

Constant: Bottom Depth = 23 meters

COARSE SAND (#123)

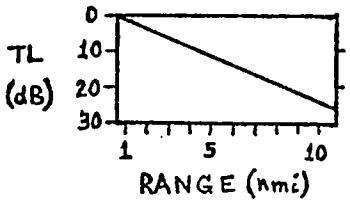

FINE SAND (#223)

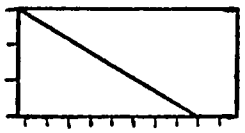

VERY FINE SAND (#323)

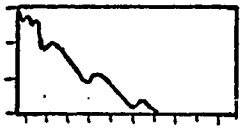

SILTY SAND (#423)

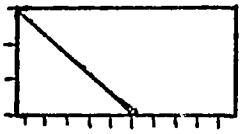

SANDY SILT (#523)

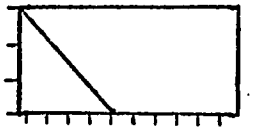

SILT (#623)

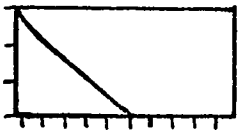

SAND-SILT-CLAY (#723)

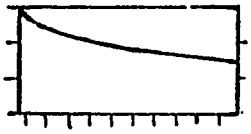

CLAYEY SILT (#823)

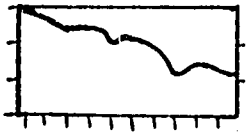

SILTY CLAY (#923)

Table 5 Summary of plot shapes -- Progression in bottom depth

Constant: Bottom Type = Sandy Silt

17 METERS (#517)

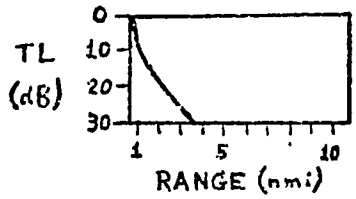

19 METERS (#519)

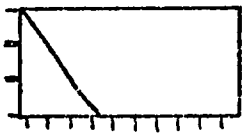

21 METERS (#521)

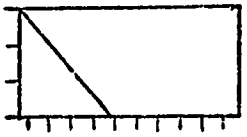

23 METERS (#523)

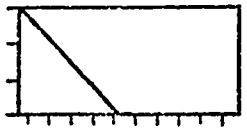

25 METERS (#525)

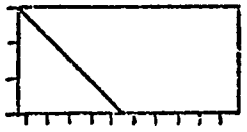

27 METERS (#527)

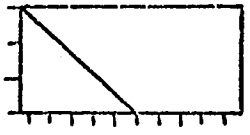

The shape of bottom type #923 indicates that there is a majority of energy transmitted into the bottom at large grazing angles (reference from horizontal) but little energy transmitted for smaller angles. Bottom types #323, 823, and 521 indicate some resonance conditions in the bottom and/or convergence (or shadow) zones in the water layer.

Comparison with Published Experimental Data

The experimentally generated transmission loss plot is presented as figure 14. There are three data lines in this figure corresponding to three different sound velocity profiles appropriate to the conditions on three data collection dates in the fall of 1974 at Mecklenburger Bay of the Baltic Sea. The sound profile used for the computer simulation (figure 11) was gathered on October 30, 1974.

The general trend of figure 14 is for a 30 dB drop in sound intensity over a horizontal distance of 9 nautical miles. This trend is qualitatively predicted by the model. The closest agreement with figure 14 from the computer plots #123 to #923 comes from #223 whose bottom parameters came from a sediment that Hamilton denoted "fine sand".

A direct quantitative comparison of the model with the real data is not completely justified. The differences between the two are considerable. Figure 10 depicts the bottom composition and depths for the real site while the model had a constant composition and depth. The direction in which the

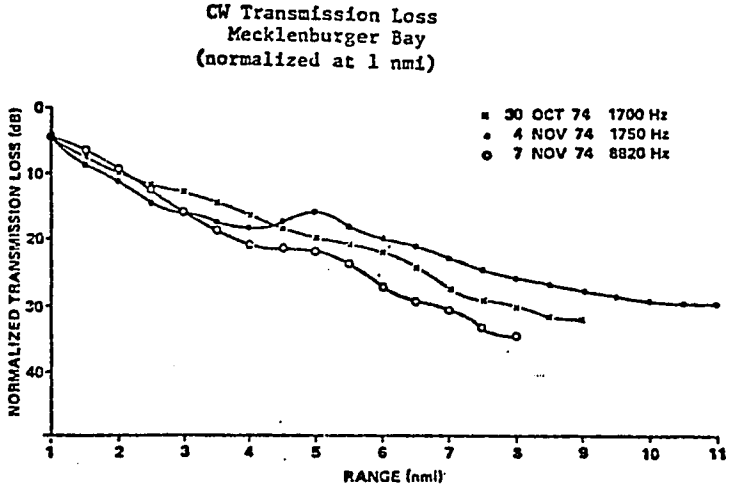

Figure 14 Transmission loss by measurement[30]

source was towed at the data collection site (i.e., toward or away from the receiver) may have made a slight difference in the results of the real data when this effect is coupled with ocean currents, surface waves (which were mentioned in the report as being significant, figure 10), and direction of the slope of the bottom surface. Another factor that makes a qualitative comparison less meaningful is the arbitrariness of the definition of the bottom type. The "silt" according to the model [Hamilton] may not be the same "silt" denoted by the experimentalists [Koenigs and Scholz].

In conclusion, the model simulation results for underwater sound propagation do not discount the validity of this model. Further study would be warranted to investigate the effect of the shape of the sound speed profile on the model's performance given another set of experimental data.

Improvements could be made by including sloped and/or random bottom surfaces, range-dependent sound speed profiles, and having less-arbitrarily defined bottom types.

Ray Optics and its Relation to Normal Modes

The governing equation (3.32a, below) can often be solved exactly when the variables are separable in some suitably chosen coordinate system [32]. For stratified media, in which C is a function of one coordinate (z), the rectangular and cylindrical coordinates have considerable utility.

Assuming harmonic plane waves, the two-dimensional problem in rectangular coordinates has the form

$$[\frac{\partial^2}{\partial x^2} + \frac{\partial^2}{\partial z^2} + \frac{\omega^2}{C^2(z)}]\Psi = 0 \qquad (3.32a)$$

with the solution

$$\Psi(x,z;t) = \phi(z)e^{-i(\pm\alpha x-\omega t)} \qquad (3.32b)$$

This solution assumes waves propagating in the direction of increasing x (+ sign) and decreasing x (- sign) with the phase velocity β:

$$\beta = \omega/\alpha \qquad (3.32c)$$

Substituting the given solution into the differential equation yields:

$$[\frac{d^2}{dz^2} + \Omega^2]\phi(z) = 0, \quad \Omega^2 = \frac{\omega^2}{C^2(z)} - \alpha^2 = \alpha^2[\frac{\beta^2}{C^2(z)} - 1] \qquad (3.33)$$

This equation is the separated space-form of the wave equation and is common to many fields in physics (optics, acoustics, and quantum theory).

In the special case of a homogeneous medium, both C and Ω are constant, the solution is: $\phi(z) = Ae^{i\Omega z} + Be^{-i\Omega z}$.

If the solution ϕ is substituted into Ψ then one sees that the first term corresponds to waves traveling in the direction of increasing z, that is propagating downwards as in figure 15, and that the second term corresponds to up-going waves.

The relation of (3.33) may be rewritten as:

$$\frac{\omega^2}{C^2(z)} = k^2 = \alpha^2 + \Omega^2 \ , \qquad (3.34)$$

where k, the wavenumber in the direction of propagation, is the magnitude of the vector $\vec{k}$ normal to the surfaces of constant phase or wave fronts $k = |\vec{k}|$. So $\vec{k}$ defines the ray direction, and α and Ω are its x and z components (see figure 15). The wavelength in the ray direction, i.e., that of $\vec{k}$, is $\lambda = 2\pi/k$. If the angle θ is between k and the vertical then one has:

$$\alpha = k \sin \theta \quad \text{and} \quad \Omega = k \cos \theta \qquad (3.35)$$

In a homogeneous medium $\vec{k}$ is a constant. In stratified media, however, k, λ, and Ω are functions of z, and α remains constant by equation (3.35) and Snell's law (see Appendix IIIe):

$$\frac{\sin \theta}{C(z)} = \text{constant.} \qquad (3.36)$$

When the rays are horizontal, $\alpha = k$ and by (3.33), $\Omega^2 = 0$ which also implies $\beta = C(z)$ and $\theta = \pi/2$. The condition

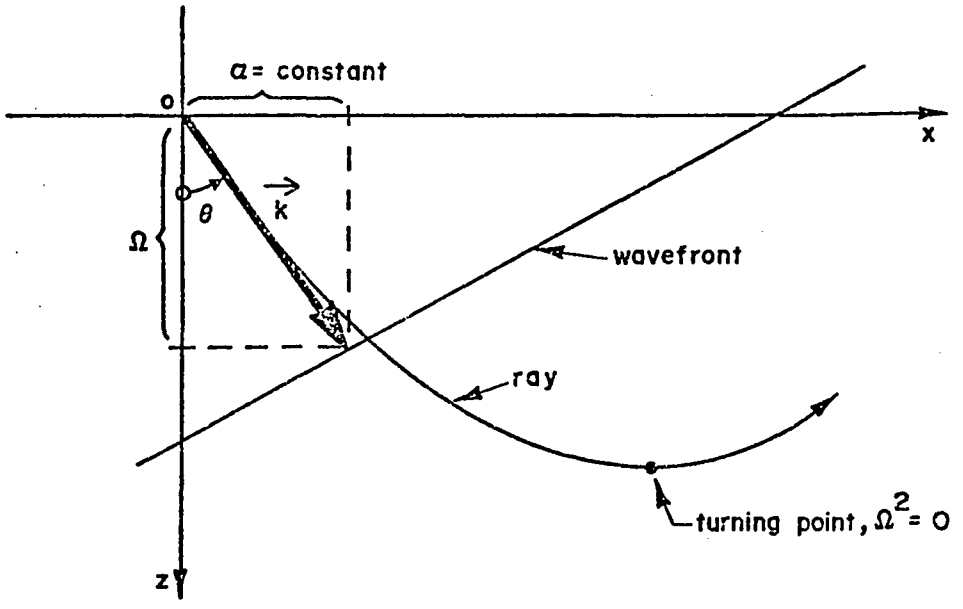

Figure 15 The turning point from a ray point of view.

(Note: α = constant, by Snell's law)

$\Omega^2 = 0$ defines a turning point of the differential equation (3.33) corresponding to a point at which the rays become horizontal.

The superposition of waves traveling in opposite directions with equal amplitudes result in standing waves. So for a homogeneous medium, $\phi = \frac{A}{2}[e^{i\Omega z} + e^{-i\Omega z}] = A \cos \Omega z$ is a standing-wave system obtained by superposing up- and down-traveling waves. Substituting this relation for ϕ into (3.32b), one finds that Ψ represents a wave pattern which is standing in the z-direction yet traveling in the x-direction with the phase velocity β [equation (3.32c)]. Standing wave solutions are often called modes, since they represent motions for which the whole medium is oscillating at the single frequency ω. Conversely, one may obtain traveling waves by superposing modes: $A \cos\alpha x \cos\omega t + A \sin\alpha x \sin\omega t = A \cos(\alpha x - \omega t)$.

For the case of axial symmetry of the medium about the z-axis, it is often useful to work with the cylindrical coordinate system. In this system equation (3.32a) becomes:

$$[\frac{\partial^2}{\partial r^2} + \frac{1}{r}\frac{\partial}{\partial r} + \frac{\partial^2}{\partial z^2} + \frac{\omega^2}{C^2(z)}]\Psi = 0, \quad r = (x^2+y^2)^{1/2}, \qquad (3.37a)$$

with harmonic wave solutions:

$$\Psi = \phi(z) H_o^{(1,2)}(\Gamma r) e^{i\omega t}, \qquad (3.37b)$$

where Γ is the horizontal component of the wave number and

$H_o^{(1,2)}$ are the 0th order (azimuthal symmetry) Hankel functions of the first and second kind. These are progressive cylindrical waves. It is important to notice that the $\phi(z)$ used in this solution is identical to that of equation (3.33) for the plane-wave case. Also, note that all expressions (3.32c) to (3.37a) are again valid upon replacement of α by Γ.

With consideration of the asymptotic approximation:

$$H_o^{(1,2)}(\Gamma r) \sim (2/\pi\Gamma r)^{1/2} e^{\pm i(\Gamma r - \pi/4)}, \quad \Gamma r >> 1$$

one sees from (3.32b) that $H_o^{(1)}$ corresponds to waves converging to the $r = 0$ axis while $H_o^{(2)}$ is an outward traveling wave. Standing waves or radial modes are obtained upon superposing the two:

$$\Psi = \phi(z)e^{-i\omega t}[H_o^{(1)}(\Gamma r)+H_o^{(2)}(\Gamma r)]$$

$$= 2\ \phi(z)J_o(\Gamma r)e^{-i\omega t}$$

In infinite homogeneous media, situations involving spherical symmetry occur for point sources. Equation (3.32a) is then

$$[\frac{\partial^2}{\partial\rho^2} + \frac{2}{\rho}\frac{\partial}{\partial\rho} + \frac{\omega^2}{C^2(z)}]\Psi = 0, \quad \rho = (x^2+y^2+z^2)^{1/2} \qquad (3.38a)$$

The general solution for this equation for the source at $\rho = 0$ is:

$$\Psi = \frac{1}{\rho} f(\rho \pm Ct) \ , \qquad (3.38b)$$

corresponding to converging and diverging spherical wave fronts.

REFERENCES

REFERENCES

1. Ahluwalia, D.S. and Keller, J.B., Wave Propagation and Underwater Acoustics, Keller, J.B. and Papadakis, J.S. (editors), Lecture Notes in Physics #70, Springer-Verlag, New York, 1977, Chapter II.

2. Landau, L.D. and Lifshitz, E.M., Fluid Mechanics, Pergamon Press, New York, 1959, pp. 47-49, 298-301.

3. Sommerfeld, A., Partial Differential Equations in Physics, Academic Press, New York, 1967, p. 210ff.

4. Levine, H. and Schwinger, J., "On the Radiation of Sound from an Unflanged Circular Pipe," Physical Review, Vol. 73, No. 4, February 15, 1948, p. 392.

5. Kontorovich, P. and Lebedev, N.N., Journal of Physics (Moscow), Vol. 1, 1939, p. 229.

6. Landau, L.D. and Lifshitz, E.M., Theory of Elasticity, 2nd ed., Pergamon Press, New York, 1970, pp. 17-20, 101-104, 155-159.

7. Carslaw, H.S. and Jaeger, J.C., Conduction of Heat in Solids, 2nd ed., Oxford University Press, 1959.

8. Yildiz, A., "Wave Propagation in an Elastic Field with Couple Stresses", Journal of Applied Mechanics, December 1972, pp. 1146-1147.

9. Urick, R.J., Principles of Underwater Sound for Engineers, McGraw-Hill Book Company, New York, 1967, pp. 2-11.

10. Shapiro, A.H., The Dynamics and Thermodynamics of Compressible Fluid Flow, Vol. I, The Ronald Press Company, New York, 1953, pp. 45-49.

11. Pekeris, C.L., "Theory of Propagation of Explosive Sound in Shallow Water," Geological Society of America, Memoir 27, Propagation of Sound in the Ocean, 1948.

    Ibid, "Theory of Propagation of Sound in a Halfspace of Variable Sound Velocity," Journal of the Acoustical Society of America, Vol. 18, 1946, p. 295.

12. Furry, W.H., The Bilinear Modified-Index Profile, Propagation of Short Radio Waves, Kerr, D.E. (ed), MIT Radiation Laboratory Series, Vol. 13, McGraw-Hill, New York, 1951, pp. 140-180.

13. Marsh, H.W., Theory of Anomalous Propagation of Acoustic Waves in the Ocean, Ph.D. dissertation, Brown University, 1950.

14. Pedersen, M.A. and Gordon, D.F., "Normal Mode Theory Applied to Short-Range Propagation in an Underwater Acoustic Surface Duct," Journal of the Acoustical Society of America, Vol. 37, 1965, p. 105.

15. Officer, C.B., Introduction to the Theory of Sound Transmission, McGraw-Hill, New York, 1958.

16. Tolstoy, I., and Clay, C.S., Ocean Acoustics, McGraw-Hill, New York, 1966.

17. Wait, J.R., Electromagnetic Waves in Stratified Media, The MacMillan Company, New York, 1962.

18. Budden, K.G., The Wave Guide Mode Theory of Wave Propagation, Prentice-Hall, Englewood Cliffs, NJ, 1962.

19. Tolstoy, I., "Note on the Propagation of Normal Modes in Inhomogeneous Media," Journal of the Acoustical Society of America, Vol. 27, 1955, p. 274.

Ibid, "Guided Waves in a Fluid with Continuously Variable Velocity Overlying an Elastic Solid: Theory and Experiment," Journal of the Acoustical Society of America, Vol. 32, 1960, p. 81.

20. Carter, A.H., Multi-Mode Acoustic Propagation in an Inhomogeneous Bounded Medium, Ph.D. disseration, Brown University, 1963.

21. Eby, R.K., et al., "Study of Acoustic Propagation in a Two-Layered Model," Journal of the Acoustical Society of America, Vol. 32, 1960, p. 88.

22. Ewing, W.M. and Worzel, J.L., Geological Society of America, Memoir 27, 1948.

23. "Physics of Sound in the Sea," part I, Transmission, National Research Council, Research Analysis Group, 1946, pp. 27-28, 105.

24. Herzfeld, K.F. and Litovitz, T.A., Absorption and Dispersion of Ultrasonic Waves, Academic Press Inc., New York, 1959.

25. Kornhauser, E.T. and Raney, W.P., Journal of the Acoustical Society of America, Vol. 27, 1955.

26. Leibiger, G.A., Wave Propagation in an Inhomogeneous Medium with Slow Spatial Variation, Ph.D. dissertation, Stevens Institute of Technology, 1968, pp. 25-46, 153-159.

27. Langer, R.E., "On the Connection Formulas and Solutions of the Wave Equation," Physical Review, Vol. 51, 1937, p. 669.

Ibid, "On the Asymptotic Solutions of Ordinary Differential Equations with an Application to the Bessel Functions of Large Order," Transactions of the American Mathematical Society, Vol. 33, 1931, p. 23.

Ibid, "On the Asymptotic Solutions of Ordinary Differential Equations with an Application to the Bessel Functions of Large Complex Order," Transactions of the American Mathematical Society, Vol. 34, 1932, p. 447.

Ibid, "The Asymptotic Solutions of Certain Linear Ordinary Differential Equations of the Second Order," Transactions of the American Mathematical Society, Vol. 36, 1934, p. 90.

28. Stewart, G.K., Wave Propagation in Viscoelastic Media, Ph.D. dissertation, Theoretical and Applied Mechanics Program, University of New Hampshire, 1976, pp. 162-173, 195-196.

29. Hamilton, E.L., et al., Journal of the Acoustical Society of America, Vol. 28, No. 1, 1956.

Hamilton, E.L., "Elastic Properties of Marine Sediments," Journal of Geophysical Research, Vol. 76, No. 2, January 10, 1971, pp. 579-604.

Ibid, "Compressional-Wave Attenuation in Marine Sediments," Geophysics, Vol. 37, No. 4, August 1972, pp. 620-646.

30. Koenigs, P.D. and Scholz, B., "Horizontal Coherence, Transmission Loss, and Ambient Noise Measurements in the Baltic Sea," Naval Underwater Systems Center, New London Laboratory, Technical Memorandum Mo. 312-68-76, August 31, 1976, pp. 12-13, 49, 56.

31. MacKenzie, K.V., "Reflections of Sound from Coastal Bottoms," Journal of the Acoustical Society of America, Vol. 32, No. 2, February 1960, pp. 221-231.

32. Morse, P.M. and Feshbach, H., Methods of Theoretical Physics, Part I, McGraw-Hill Book Company, New York, 1953, Chapter 7.

33. Cushing, J.T., Applied Analytical Mathematics for Physical Scientists, John Wiley and Sons, New York, 1975, pp. 430, 529, 537.

34. Brekhovshikh, L.M., Waves in Layered Media, Academic Press Inc., New York, 1960, p. 290.

35. Collatz, L., Eigenwertaufgaben, mit Technischen Anwendungen Akademische, Verlag, Leipzig, 1949.

36. Clay, C.S., Journal of the Acoustical Society of America, Vol. 31, 1959, p. 1973.

37. DiNapoli, F.R. and Deavenport, R.L., Ocean Acoustics, DeSanto, J.A. (ed.), Topics in Current Physics Series, Springer-Verlag Berlin Heidenberg, 1979, Chapter 3.

38. Ewing, W.M., Jardetzky, W.S. and Press, F., Elastic Waves in Layered Media, McGraw-Hill Book Company Inc., New York, 1957.

39. Ide, J.M., Post, R.F. and Fry, W.J., U.S. Naval Research Laboratory, Report S-2113, 1943.

40. Jackson, J.D., Classical Electrodynamics, 2nd ed., John Wiley and Sons, Inc., New York, 1975, pp. 62, 84-89, 119-120.

41. Magnuson, A.H., Sound Propagation in a Liquid Overlying a Viscoelastic Halfspace, Ph.D. dissertation, Theoretical and Applied Mechanics Program, University of New Hampshire, 1972.

42. Morse, P.M. and Ingard, L.V., Theoretical Acoustics, McGraw-Hill Book Company, New York, 1968, pp. 319-322, 352-353, 364-366.

43. Mosberg, W. and Yildiz, M., "Mean-Square Response of a Thermoviscoelastic Medium to Nonstationary Random Excitation," Journal of Applied Mechanics, Vol. 98, Trans. ASME, Vol. 43, Series E, March 1976, pp. 150-158.

44. Sundkvist, K., Fluctuations and Dissipations in a Thermally Conducting Viscous Hydrodynamic Medium, Ph.D. dissertation, Theoretical and Applied Mechanics Program, University of New Hampshire, 1979.

45. Titchmarsh, E.C., Eigenfunction Expansions Associated with Second-Order Differential Equations, Oxford, Clarendon, 1946.

46. Tolstoy, I., Journal of the Acoustical Society of America, Vol. 30, 1958, p. 348.

47. Voigt, W., Theoretische Studien uber die Elasticit atsuer haltnisse der Krystalle, Abh. Ges. Wiss., Gottingen, Vol. 34, 1887.

48. Wallace, P.R., Mathematical Analysis of Physical Problems, Holt, Rinehart, and Winston, Inc., New York, 1972, pp. 395-399.

49. Yildiz, A., "On the Science and Technology of Utilizing the Bottom Resources of the Continental Shelf," Technical Report to the National Sea Grant Office, 1970.

50. Yildiz, A., Mechanical Engineering 822 Lecture Notes: Continuum Mechanics, Fall Semester, 1977.

Ibid, Mechanical Engineering 826 Lecture Notes: Theory of Elasticity, Spring Semester, 1979.

Ibid, Mechanical Engineering 838 Lecture Notes: Theoretical Acoustics, Fall Semester, 1978.

51. Yildiz, M., "Spectral Representation of Wave Propagation in Thermoviscoelastic Medium," Journal of Applied Mechanics, Vol. 98, Trans. ASME, Vol. 43, Series E, March 1976, pp. 177-178.

52. Yildiz, M., Mechanical Engineering 781 Lecture Notes: Mathematical Methods in Engineering Science I, Fall Semester, 1977 and 1978.

Ibid, Mechanical Engineering 882 Lecture Notes: Mathematical Methods in Engineering Science II, Spring Semester, 1978 and 1979.

Ibid, Mechanical Engineering 727 Lecture Notes: Advanced Mechanics of Solids, Fall Semester, 1978.

APPENDICES
(FOR CHAPTER I)

APPENDIX Ia

Derivation of two representations of the one-dimensional delta function and corresponding three-dimensional Green's function

A. First representation of the delta function

Use the completeness condition to expand the one-dimensional Green's function g as an infinite series of orthonormal functions X_m with coefficients $a_m(x';h)$ where x is a coordinate and h is the corresponding eigenvalue:

$$g_x(x,x';h_x) = \sum_m^\infty a_m(x';h_x)X_m(x) \qquad \text{(i)}$$

To evaluate the a_m's, multiply both sides of (i) by $dxw(x)X_n^*(x)$ and integrate over x (where w is the weight function of equation (iii) below and superscript * denotes complex-conjugate):

$$\int dxw(x)\phi_n^*(x)g_x(x,x';h_x)$$

$$= \sum_m^\infty a_m(x';h_x)\int dxw(x)X_n^*(x)X_m(x) = \sum_m^\infty a_m(x';h_x)\delta_{mn} = a_n(x;h_x)$$

where the limits of integration depend on the orthonormal set of functions, δ_{mn} is the Kronnecker delta and the orthonormality condition has been invoked:

$$\delta_{mn} = \int dxw(x)X_n^*(x)X_m(x).$$

The coefficeints then can be written:

$$a_m(x';h_x) = \int d\bar{x} w(\bar{x}) X_m(\bar{x}) g_x(\bar{x},x';h_x) \ ,$$

and when substituted into equation (i) with some rearranging yields:

$$g_x(x,x';h_x) = \int d\bar{x} g_x(\bar{x},x';h_x) \sum_m^\infty w(\bar{x}) X_m(x) X_m^*(\bar{x}) \ .$$

Comparison of this with the integration property of the delta function:

$$f(x) = \int d\bar{x} f(\bar{x}) \delta(\bar{x}-x)$$

then one has:

$$\delta(\bar{x}-x) = w(\bar{x}) \sum_m^\infty X_m(x) X_m^*(\bar{x})$$

and in the final form (using the even-function property of δ)

$$\delta(x-x')/w(x') = \sum_m^\infty X_m(x) X_m^*(x') \qquad \text{(ii)}$$

B. Second representation of the delta function

The Sturm-Liouville equations are of the standard

form:

$$\left[\frac{d}{dx}\, p(x)\frac{d}{dx} - q(x) + h_m w(x)\right]X_m(x) = 0 \qquad \text{(iii)}$$

$$\left[\frac{d}{dx}\, p(x)\frac{d}{dx} - q(x) + h_x w(x)\right]g_x(x,x';h_x) = -\delta(x-x') \qquad \text{(iv)}$$

Substituting (i) and (ii) into (iv) yields:

$$\left[\frac{d}{dx}p(x)\frac{d}{dx}-q(x)+h_x w(x)\right]\sum_m^{\infty} a_m(x';h_x)X_m(x) = -w(x')\sum_m^{\infty} X_m(x)X_m^*(x')$$

Adding zero in the form $[h_m w(x)-h_m w(x)]$ in the brackets on the left side, using equation (iii), and equating terms of the m-summation:

$$a_m(x';h_x) = \frac{-X_m^*(x')}{h_x - h_m}$$

Substituting this into (i), one obtains:

$$g_x(x,x';h_x) = -\sum_m^{\infty} \frac{X_m(x)X_m^*(x')}{h_x - h_m}$$

Multiplying both sides by $\left(\frac{-dh_x}{2\pi i}\right)$ and integrating around a closed contour about the single simple-pole singularity at $h_x = h_m$ and realizing from the residue theorem that:

$$\oint \frac{dh_x}{h_x - h_m} = 2\pi i$$

then one has the result:

$$\frac{-1}{2\pi i}\oint dh_x g_x(x,x';h_x) = \sum_m^{\infty} X_m(x)X_m^*(x') \ .$$

Combining (ii) and this last relation one has the final result:

$$\frac{\delta(x-x')}{w(x')} = \sum_m^{\infty} X_m(x)X_m^*(x') = \frac{-1}{2\pi i}\oint dh_x g_x(x,x';h_x) \qquad (v)$$

C. The three-dimensional Green's function, G

Another expression similar to (v) may be written for the y-coordinate direction:

$$\frac{\delta(y-y')}{w(y')} = \sum_n^{\infty} Y_n(y)Y_n^*(y') = \frac{-1}{2\pi i}\oint dh_y g_y(y,y';h_y) \ . \qquad (vi)$$

Multiplying (v) and (vi) one obtains the relations:

$$\frac{\delta(x-x')}{w(x')}\ \frac{\delta(y-y')}{w(y')} = \sum_m^{\infty} X_m(x)X_m^*(x')\sum_n^{\infty} Y_n(y)Y_n^*(y')$$

$$= \frac{-1}{4\pi^2}\oint dh_x g_x(x,x';h_x)\oint dh_y g_y(y,y';h_y). \qquad (vii)$$

A three-dimensional delta function does not exist in the sense of (vii) since the third eigenvalue is not independent of the others, i.e., $h_z = h_z(h_x,h_y)$. One can post-multiply both

sides of (vii) by g_z, however, which results in a two-dimensional integral transform defined by integral representations of the delta functions:

$$\frac{\delta(x-x')}{w(x')} \frac{\delta(y-y')}{w(y')} g_z(z,z';h_x,h_y)$$

$$= \frac{-1}{4\pi^2} \oint dh_x g_x(x,x';h_x) \oint dh_y g_y(y,y';h_y) g_z(z,z';h_x h_y) \ . \qquad \text{(viii)}$$

One can now prove that this transform (viii) yields the three-dimensional Green's function in the steady-state domain $G(\vec{R},\omega)$.

To do this let us consider the rectangular coordinate system for which the transforms will be readily recognizable as Fourier transforms. Let us look at the scalar undamped wave equation in the steady-state domain (i.e., K^2 is real-valued):

$$(\nabla^2+K^2)G(\vec{R};\omega) = -\delta^3(\vec{r}-\vec{r}') = -\delta(x-x')\delta(y-y')\delta(z-z') \ . \qquad \text{(ix)}$$

The separated equations for this partial differential equation (ix) are presented in Part B of Appendix IIc. These three equations are of the same form and from Appendix Ib the corresponding one-dimensional Green's functions are written:

$$g_x(x,x';\mu^2) = \frac{e^{-i\mu|x-x'|}}{2i\mu} \ . \qquad \text{(x)}$$

The corresponding delta function is evaluated from (v) to be:

$$\delta(x-x') = \frac{1}{2\pi}\int d\mu\ e^{-i\mu(x-x')} \qquad \text{(xi)}$$

Assembling expression (viii) from (x) and (xi) one obtains:

$$G(\vec{R};\omega) = \frac{1}{4\pi^2}\int_{-\infty}^{\infty} d\mu e^{-i\mu(x-x')}\int_{-\infty}^{\infty} d\lambda e^{-i\lambda(y-y')} g_z(z,z';K^2,\mu^2,\lambda^2)\ , \qquad \text{(xii)}$$

where $h_z = K^2 - \mu^2 - \lambda^2$. This is apparently a two-dimensional Fourier transform of a one-dimensional Green's function. To prove that this is a consistent result, let us substitute this (xii) into (ix):

$$\frac{1}{4\pi^2}\left(\frac{\partial^2}{\partial x^2} + \frac{\partial^2}{\partial y^2} + \frac{\partial^2}{\partial z^2} + K^2\right)\int_{-\infty}^{\infty} d\mu e^{-i\mu(x-x')}\int_{-\infty}^{\infty} d\lambda e^{-i\lambda(y-y')}$$

$$\cdot\ g_z(z,z';K^2,\mu^2,\lambda^2) = -\frac{1}{4\pi^2}\int_{-\infty}^{\infty} d\mu e^{-i\mu(x-x')}\int_{-\infty}^{\infty} d\lambda e^{-i\lambda(y-y')}\delta(z-z'),$$

which reduces to:

$$\left(\frac{d^2}{dz^2} + \Omega^2\right) g_z(z,z';\Omega^2) = -\delta(z-z')\ , \qquad \text{(xiii)}$$

where $\Omega^2 = h_z = K^2 - \mu^2 - \lambda^2$. This is a consistent definition

for g_z and so this completes the proof.

In conclusion it has been proven that in the steady-state domain the undamped Green's function may be evaluated by:

$$G(\vec{R};\omega) = \frac{-1}{4\pi^2} \oint dh\ g_\alpha(\alpha,\alpha';h_\alpha) \oint dh_\beta g_\beta(\beta,\beta';h_\beta) g_\gamma(\gamma,\gamma';K^2,h_\alpha,h_\beta) \qquad \text{(xiv)}$$

where $\vec{r} = (\alpha,\beta,\gamma)$ is written for an arbitrary coordinate system. In rectangular coordinates this expression (xiv) is a two-dimensional Fourier transform, and two other representations may be obtained by cyclic rotation of the α, β, γ and h_α, h_β, h_γ variables. In cylindrical and spherical coordinates the transforms are no longer Fourier ones. These two coordinate systems are investigated in the sections on viscous fluids and solids, respectively, of the main text.

Expression (xii) is identical to (2.11) of the main text when treating the undamped case. In general one may have a complex-valued eigenvalue [K of expression (ix)], call it χ where $\chi = K - i\gamma$. Therefore (xiv) is valid for the undamped (real-valued eigenvalue) case $\gamma = 0$, but for the general case of a complex-valued eigenvalue $\gamma \neq 0$ then (xiv) is only the contribution to $G(\vec{R};\omega)$ made by the real-part K as depicted in (2.11) by the notation C.R.P.

APPENDIX Ib

Derivation of expression that constructs the one-dimensional Green's function

A. General Sturm-Liouville equation, with operator denoted by L:

$$L\phi(x) = [\frac{d}{dx}p(x)\frac{d}{dx}-q(x)+h_x w(x)]\phi(x) = F(x)$$

the functions u(x) and v(x) are two linearly independent solutions of the related homogeneous equation: $Lu(x) = 0$, $Lv(x) = 0$.

B. One-dimensional Green's function g satisfies the equation:

$$Lg(x,x') = -\delta(x-x')$$

Let: g_- be valid on the interval $a \leq x \leq x'$

g_+ be valid on the interval $x' \leq x \leq b$

That is:

$$Lg_- = 0 \qquad a \leq x \leq x'$$

$$Lg = -\delta(x-x') \qquad x = x'$$

$$Lg_+ = 0 \qquad x' \leq x \leq b$$

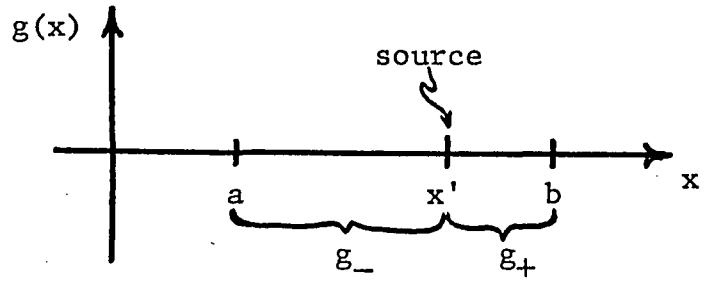

C. Function g satisfies the homogeneous conditions prescribed at the endpoints.

g_- satisfies condition at $x = a$

g_+ satisfies condition at $x = b$

D. Function g is continuous at $x = x'$.

$$g_-(x') = g_+(x')$$

E. The derivative of g has a discontinuity of magnitude $\frac{-1}{p(x')}$ at $x = x'$ due to delta function at this location:

$$g_+'(x') - g_-'(x') = \frac{-1}{p(x')}$$

where prime on a function indicates differentiation w.r.t. x.

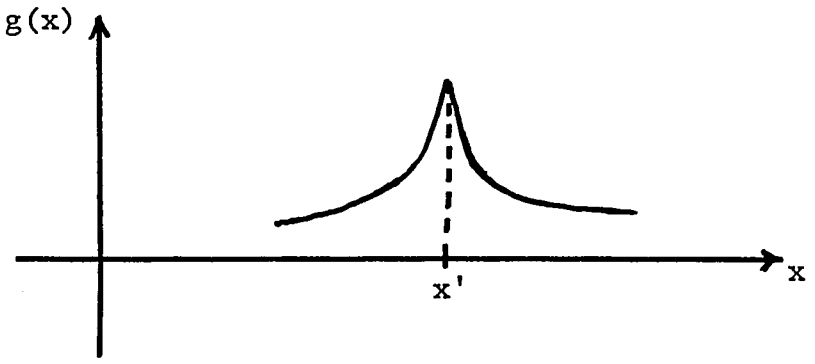

Proof: $[\frac{d}{dx}p(x)\frac{d}{dx}-q(x)+h_x w(x)]g(x) = -\delta(x-x')$

Integrating over just the "jump" at $x = x'$, with limit $\varepsilon \to 0$

$$\lim_{\varepsilon\to o}\int_{x'-\varepsilon}^{x'+\varepsilon} dx\frac{d}{dx}p(x)\frac{d}{dx}g(x) - \lim_{\varepsilon\to o}\int_{x'-\varepsilon}^{x'+\varepsilon} dx[q(x)-h_x w(x)]g(x)$$

$$= -\lim_{\varepsilon\to o}\int_{x'-\varepsilon}^{x'+\varepsilon} dx\ \delta(x-x')$$

since second term is continuous at $x = x'$:

$$\lim_{\varepsilon\to o}[p(x)\frac{d}{dx}g(x)]_{x'-\varepsilon}^{x'+\varepsilon} - 0 = -1$$

$$g_+'(x') - g_-'(x') = \frac{-1}{p(x')} \quad \text{Q.E.D.}$$

Now let $u(x)$ [or $v(x)$] be a solution of $Lu(x) = 0$ [or $Lu(x) = 0$] which satisfies the homogeneous condition at $x = a$ [or $x = b$]. An arbitrary constant times these functions still solves the same equations hence:

$$L[c_1 u(x)] = 0, \quad L[c_2 v(x)] = 0$$

Conditions B. and C. are satisfied if:

$$g_-(x) = c_1 u(x), \quad a \le x \le x' \qquad \text{(i)}$$

$$g_+(x) = c_2 v(x), \quad x' \le x \le b \qquad \text{(ii)}$$

Conditions D. and E. will now determine the c_1 and c_2 constants

in terms of x':

$$\text{D. } g_-(x') = g_+(x') \qquad \text{or } c_1u(x') - c_2v(x') = 0 \qquad \text{(iii)}$$

$$\text{E. } g_+'(x') - g_+'(x') = \frac{-1}{p(x')} \text{ or } -c_1u'(x') + c_2v'(x') = \frac{-1}{p(x')} \qquad \text{(iv)}$$

A unique solution to (iii) and (iv) exists if the determinant of the coefficients of c_1 and c_2 does not vanish

$$\begin{vmatrix} u(x') & -v(x') \\ -u'(x') & v'(x') \end{vmatrix} = u(x')v'(x') - v(x')u'(x') \equiv \Delta(x') \neq 0$$

This determinant Δ is called the Wronskian and it will not vanish as long as u and v are linearly independent.

Abel's formula is now proven that allows evaluation of the Wronskian Δ. The statements: $Lu(x) = 0$ and $Lv(x) = 0$ imply that:

$$[\frac{d}{dx}p(x)\frac{du}{dx} - qu + h_x wu] = [(pu')' - (q-h_x w)u] = 0 \qquad \text{(v)}$$

$$[\frac{d}{dx}p(x)\frac{dv}{dx} - qv + h_x wv] = [(pv')' - (q-h_x w)v] = 0 \qquad \text{(vi)}$$

Upon multiplying (v) by -v, (vi) by u, and adding the two one has:

$$u(pv')' - v(pu')' = 0 \qquad \text{(vii)}$$

Noting that: $[p(uv'-vu')]' = u(pv')' - v(pu')'$ then

integrating (vii) one obtains:

$$p(uv'-vu') = A = \text{constant} = p\Delta \qquad \text{Q.E.D.}$$

Then for $x = x'$ one has:

$$A = p(x')\Delta(x') = [p(uv'-vu')]_{x=x'} \qquad \text{(viii)}$$

Solving system (iii) and (iv): $c_1 = \frac{-v(x')}{p(x')\Delta(x')}$, $c_2 = \frac{-u(x')}{p(x')\Delta(x')}$
Now substitute into equations for g_- and g_+; that is: (i) and (ii)

$$g(x,x') = \begin{cases} g_-(x,x') = \dfrac{-u(x)v(x')}{p(x')\Delta(x')}, & a \leq x \leq x' \\ g_+(x,x') = \dfrac{-u(x')v(x)}{p(x')\Delta(x')}, & x' \leq x \leq b \end{cases}$$

or symbolically:

$$g(x,x') = \frac{-u(x_<)v(x_>)}{p(x')\Delta(x')}$$

where < and > refer to the argument being the lesser and greater, respectively, of x and x' on the interval under consideration that is: $x_< = \min(x,x')$ and $x_> = \max(x,x')$. The minus sign is consistent with the minus sign in front of the delta function in step B. of this appendix.

APPENDICES
(FOR CHAPTER II)

APPENDIX IIa

Derivation of the Equation of Motion of a Viscous Fluid

The general equation of motion is written as:

$$\partial_t(\rho v_i) = \rho f_i - \partial_j \pi_{ij} \ , \qquad \text{(i)}$$

and the momentum flux density tensor π_{ij} for a viscous fluid is given as:

$$\pi_{ij} = P\delta_{ij} + \rho v_i v_j - [\zeta - (2\eta/3)]\partial_t \varepsilon_{\ell\ell}\delta_{ij} - 2\eta\ \partial_t \varepsilon_{ij} \ , \qquad \text{(ii)}$$

where P is pressure and $\partial_t \varepsilon_{ij}$ is the rate of strain tensor, $(\partial_j v_i + \partial_i v_j)/2$. The second term of (ii) is neglected since it is of the second order in velocity [2]. After substituting for $\partial_t \varepsilon_{ij}$ and taking the divergence ∂_j, expression (ii) becomes:

$$\begin{aligned} \partial_j \pi_{ij} &= \partial_i P - [\zeta - (2\eta/3)]\partial_i \partial_j v_j - \eta(\partial^2 v_i + \partial_i \partial_j v_j) \\ &= \partial_i P - [\zeta + (\eta/3)]\partial_i \partial_j v_j - \eta \partial^2 v_i \ . \end{aligned} \qquad \text{(iii)}$$

Linearizing, using (ii) and (iii), and noting $\partial_i P = (\partial P/\partial \rho)_s \partial_i \rho$, expression (i) becomes:

$$\rho \partial_t v_i = \rho f_i - (C_L^2 \partial_i \rho - [\zeta + (\eta/3)]\partial_i \partial_j v_j - \eta \partial^2 v_i) \ , \qquad \text{(iv)}$$

where $C_L^2 = (\partial P/\partial \rho)_s$ [10] for isentropic acoustic considerations.

Rearranging the terms in (iv) and differentiating with respect to time, one obtains:

$$\rho\partial_t^2 v_i - \eta\partial_t\partial^2 v_i + C_L^2\partial_i\partial_t\rho - [\zeta+(\eta/3)]\partial_t\partial_i\partial_j v_j = \eta\partial_t f_i \ . \quad (v)$$

Using the continuity equation, i.e., $\partial_t\rho + \rho\partial_j v_j = 0$, replacement of $\partial_t\rho$ in (v) yields:

$$\rho\partial_t^2 v_i - \eta\partial_t\partial^2 v_i - \rho C_L^2\partial_i\partial_j v_j - [\zeta+(\eta/3)]\partial_t\partial_i\partial_j v_j = \rho\partial_t f_i \ .$$

Dividing by ρ and regrouping terms then yields the form for extracting the operator as presented by expression (2.1) of the main text.

APPENDIX IIb

Evaluation of the Tensor Green's function of a Viscous Fluid in Three Domains

A. The $(\vec{k};\omega)$ Domain

Transforming equation (2.2) of the main text with the operator defined in expression (2.1) from the $(\vec{r};t)$ domain into the $(\vec{k};\omega)$ domain using the Fourier transforms, one has:

$$L_{ij}(\vec{k};\omega)G_{jm}(\vec{k};\omega) = -\delta_{im} \ , \qquad \text{(i)}$$

where

$$L_{ij}(\vec{k};\omega) = (\chi_T^2-k^2)\delta_{ij} + [(\chi_L^2-\chi_T^2)/\chi_L^2]k_ik_j \ . \qquad \text{(ii)}$$

Since (i) is purely algebraic it is clear that:

$$G_{jm}(\vec{k};\omega) = -L_{ij}^{-1}(\vec{k};\omega)\delta_{im} = -L_{mj}^{-1}(\vec{k};\omega) \ , \qquad \text{(iii)}$$

where L^{-1} is the inverse operator of (ii) and is evaluated by considering the identity:

$$[L_{mj}^{-1}(\vec{k};\omega)][L_{ij}(\vec{k};\omega)] = \delta_{im} \ . \qquad \text{(iv)}$$

To solve this, one may assume $L_{mj}^{-1}(\vec{k};\omega)$ is of the same structure as $L_{ij}(\vec{k};\omega)$, i.e., $L_{mj}^{-1}(\vec{k};\omega) = A\delta_{mj} + Bk_mk_j$, where the coefficients A and B are evaluated in terms of k, χ_T, and χ_L using relation (iv). The result is the Green's function of relation (iii) and is presented in the main text as

expression (2.3).

B. The $(\vec{k};T)$ Domain

Using expression (2.3) of the main text and the following definition of the inverse temporal Fourier transform:

$$G_{jm}(\vec{k};T) = (1/2\pi) \int_{-\infty}^{\infty} d\omega \; e^{i\omega t} G_{jm}(\vec{k};\omega) \;,$$

the tensor Green's function in the $(\vec{k};T)$ domain is easily evaluated by two contour integrations. The transverse term result is determined by the integral: $I_1 = (D_T/2\pi i) \int_{-\infty}^{\infty} d\omega \; e^{i\omega t}/(\omega - i\Lambda_T)$, for which an appropriate contour is shown in figure A1. For the case of $T > 0$ one may use the residue theorem to write:

$$\oint \frac{e^{izT}}{z - i\Lambda_T} \, dz = \int_{-\infty}^{\infty} \frac{e^{i\omega T}}{\omega - i\Lambda_T} \, d\omega + \lim_{|z|\to\infty} \curvearrowleft \frac{e^{izT}}{z - i\Lambda_T} \, dz = 2\pi i \; \mathrm{Res}\{i\Lambda_T\}$$

which yields the result: $I_1 = U(T) D_T \, e^{-\Lambda_T T}$. The longitudinal term result is determined by the integral:

$$I_2 = (D_T/2\pi i) \int_{-\infty}^{\infty} d\omega \; \omega e^{i\omega T}/(\omega^2 - i2\Lambda_L \omega - \omega_n^2) \;,$$

for which an appropriate contour is shown in figure A2. For the case of $T > 0$ one may use the residue theorem to write:

$$\oint \frac{z e^{izT}}{z^2 - i2\Lambda_L z - \omega_n^2} \, dz = \int_{-\infty}^{\infty} \frac{\omega e^{i\omega T}}{\omega^2 - i2\Lambda_L \omega - \omega_n^2} \, d\omega + \lim_{|z|\to\infty} \curvearrowleft \frac{z e^{izT}}{z^2 - i2\Lambda_L z - \omega_n^2} \, dz$$

$$= 2\pi i [\mathrm{Res}\{1\} + \mathrm{Res}\{2\}],$$

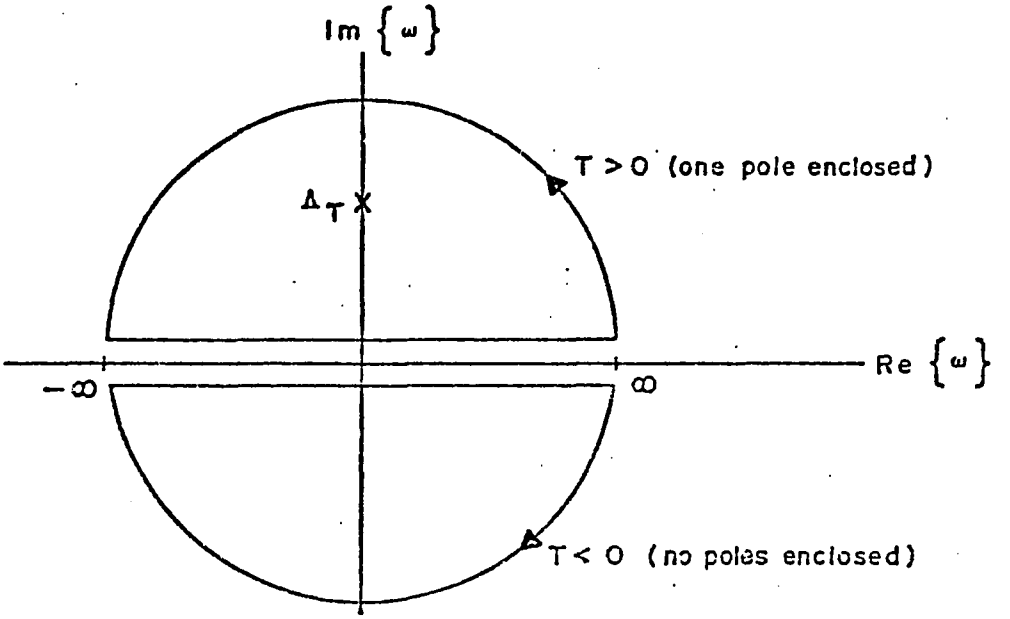

Figure A1 Contours appropriate for evaluating the transverse term of $G_{jm}(\vec{k};T)$

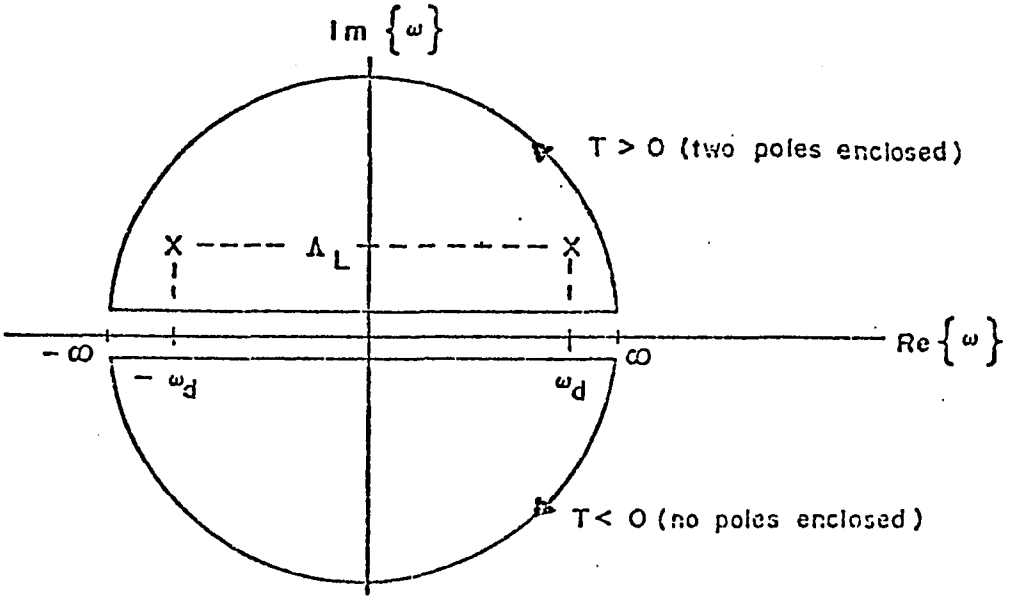

Figure A2 Contours appropriate for evaluating the longitudinal term of $G_{jm}(\vec{k};T)$ where $\omega_d \equiv \omega_n(1-\xi^2)^{1/2}$.

where the residues Res{1} and Res{2} are the contributions of the two poles shown in figure A2. The result of this integration is:

$$I_2 = U(T)D_T e^{-\Lambda_L T}\{\cos[\omega_n(1-\xi^2)^{1/2}T] - \xi(1-\xi^2)^{-1/2}\sin[\omega_n(1-\xi^2)^{1/2}T]\}.$$

The combined result is the tensor Green's function in the $(\vec{k};T)$ domain and is presented as expression (2.5) of the main text.

C. The $(\vec{R};\omega)$ Domain

Using expression (2.3) of the main text and the following definition of the inverse Fourier three-dimensional spatial transform:

$$G_{jm}(\vec{R};\omega) = (1/2\pi)^3 \iiint_{-\infty}^{\infty} d^3\vec{k}\ e^{-i\vec{k}\cdot\vec{R}} G_{jm}(\vec{k};\omega)\ ,$$

the tensor Green's function $G_{jm}(\vec{R};\omega)$ is easily evaluated by two types of contour integrations. The first term of the transverse part converts to spherical coordinates readily and reduces to the single integral:

$$I_3 = (1/2\pi)^3 \iiint_{-\infty}^{\infty} d^3\vec{k}\ e^{-i\vec{k}\cdot\vec{R}}/(k^2-\chi_T^2)$$

$$= (1/i4\pi^2 R) \int_{-\infty}^{\infty} dk\ k e^{ikR}/(k^2-\chi_T^2)\ ,$$

for which an appropriate contour is shown in figure A3 where the following definition has been established: $\chi_T = K_T - i\gamma_T$.

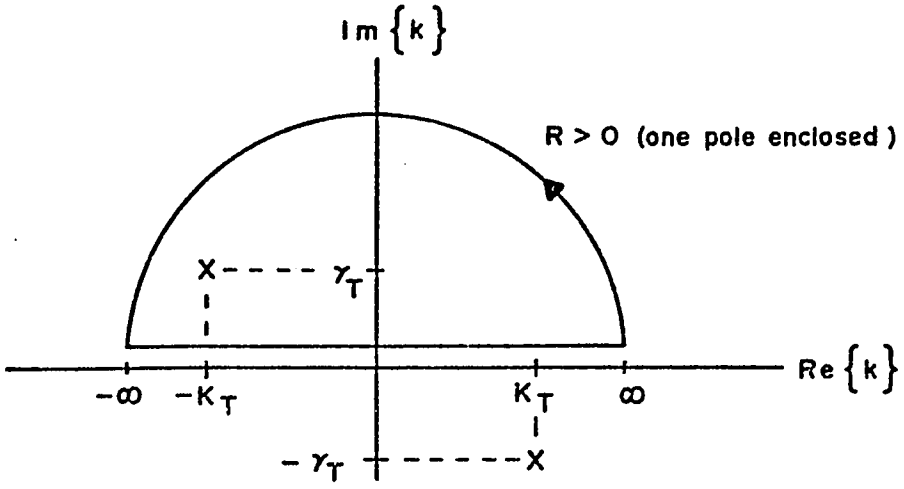

Figure A3 Contour appropriate for evaluating the first term of the transverse part of $G_{jm}(\vec{R};\omega)$; note: $K_T = \gamma_T$.

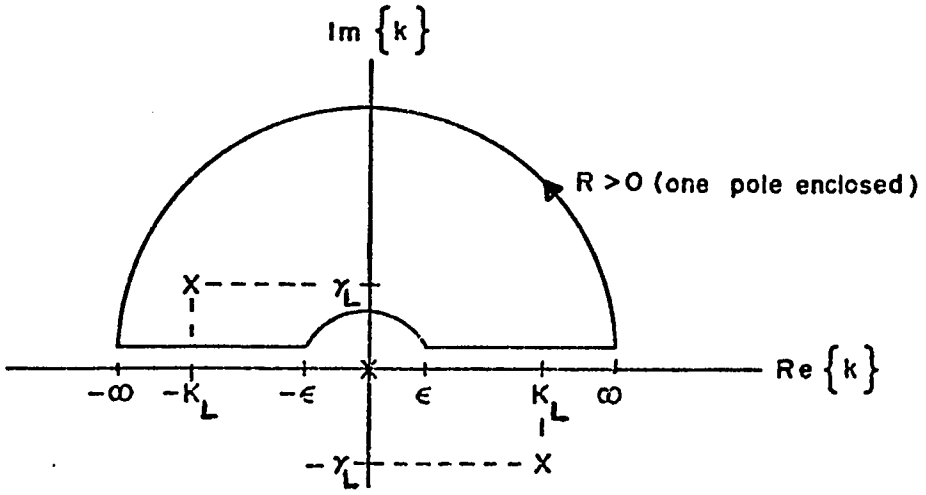

Figure A4 Contour appropriate for evaluating the second term of the transverse part and the longitudinal part of $G_{jm}(\vec{R};\omega)$; note: $K_L > \gamma_L$ while $K_T = \gamma_T$.

One may use the residue theorem to write:

$$\oint \frac{ze^{-izR}}{(z-\chi_T)(z+\chi_T)}dz = \int_{-\infty}^{\infty} \frac{ke^{-ikR}}{(k-\chi_T)(k+\chi_T)}dk + \lim_{|z|\to\infty} \uparrow \frac{ze^{-izR}}{(z-\chi_T)(z+\chi_T)}dz$$

$$= 2\pi i \text{ Res}\{-\chi_T\}$$

which yields the result: $I_3 = e^{-\gamma_T R} e^{-iK_T R}/4\pi R$. The longitudinal term and second term of the transverse part are both of the same form and convert to spherical coordinates as:

$$I_4 = (1/2\pi)^3 \iiint_{-\infty}^{\infty} d^3\vec{k}\, e^{-i\vec{k}\cdot\vec{R}}/k^2(k^2-\chi^2)$$

$$= (1/i4\pi^2 R) \int_{-\infty}^{\infty} dk\, e^{-ikR}/k(k^2-\chi^2) \ ,$$

for which an appropriate contour is given in figure A4. One may use the residue theorem to write:

$$\oint \frac{e^{-izR}}{z(z-\chi)(z+\chi)}dz = \int_{-\infty}^{\infty} \frac{e^{-ikR}}{k(k-\chi)(k+\chi)}dk + \lim_{|z|\to\infty} \uparrow \frac{e^{-izR}}{z(z-\chi)(z+\chi)}dz$$

$$= 2\pi i \text{ Res}\{-\chi\}$$

where the residue contribution of the pole at the origin has been neglected due to hindsight because it results in a constant term that vanishes when operated on by the spatial operators of Q_{jm}. The result of this integration is: $I_4 = e^{-\gamma R} e^{-iKR}/4\pi R\chi^2$, where $\chi = K - i\gamma$. The combined result

is the tensor Green's function in the $(\vec{R};\omega)$ domain and is presented as expression (2.6) of the main text.

APPENDIX IIc

The separated wave equation (in three coordinate systems) appropriate to the construction of the various C.R.P. representations.

A. In general coordinates: $(\nabla^2+K_q^2)\Psi = 0$, where K_q is defined in part E below.

B. In rectangular coordinates: $\Psi(x,y,z) = X(x)Y(y)Z(z)$

$$(\frac{d^2}{dx^2} + h_x)X(x) = 0 , \quad h_x = \mu^2;$$

$$(\frac{d^2}{dy^2} + h_y)Y(y) = 0 , \quad h_y = \lambda^2;$$

$$(\frac{d^2}{dz^2} + h_z)Z(z) = 0 , \quad h_z = \Omega^2;$$

and

$$K_q^2 = \mu^2 + \lambda^2 + \Omega^2 .$$

Note: The h's are the different eigenvalues.

C. In cylindrical coordinates: $\Psi(r,\phi,z) = R(r)\Phi(\phi)Z(z)$

$$(\frac{d}{dr} r \frac{d}{dr} - \frac{h_\phi}{r} + hr)R(r) = 0 , \quad h_r = \Gamma^2;$$

$$(\frac{d^2}{d\phi^2} + h_\phi)\Phi(\phi) = 0 , \quad h_\phi = \nu^2;$$

$$(\frac{d^2}{dz^2} + h_z)Z(z) = 0 , \quad h_z = \Omega^2;$$

and

$$K_q^2 = \Gamma^2 + \Omega^2 \ .$$

D. In spherical coordinates: $\Psi(\rho,\phi,\theta) = R(\rho)\Phi(\phi)\Theta(\theta)$

$$(\frac{d}{d\rho}\rho^2\frac{d}{d\rho} + h_\rho\rho^2 - h_\theta)R(\rho) = 0 \ , \quad h_\rho = K_q^2;$$

$$(\frac{d^2}{d\phi^2} + h_\phi)\Phi(\phi) = 0 \ , \quad h_\phi = \nu^2;$$

$$(\frac{d}{d\theta}\sin\frac{d}{d\theta} - \frac{h_\phi}{\sin\theta} + h_\theta\sin\theta)\Theta(\theta) = 0 \ , \quad h_\theta = n^2;$$

and $n^2 = \ell(\ell+1)$ for convergence of the solution.

E. The K_q may be various expressions depending on the problem.

i) for the undamped wave equation:

$$K_q \to K_o = \omega/C, \quad C = \text{sound speed, for example;}$$

ii) for the transverse mode of a viscous fluid [see equation (2.7a)]:

$$K_q \to K_T = (\rho\omega/2\eta)^{1/2}, \quad \rho = \text{fluid density,}$$

η = shear viscosity;

iii) for the longitudinal mode of a viscous fluid [see equation (2.7b)]:

$$K_q \to K_L = \frac{\omega}{C_L}\left\{\frac{(1+[\omega(3\zeta+4\eta)/3\rho C_L^2]^2)^{1/2}+1}{2(1+[\omega(3\zeta+4\eta)/3\rho C_L^2]^2)}\right\}^{1/2} \ ,$$

C_L = compressional sound speed, ζ = bulk viscosity;

iv) for the transverse mode of a viscoelastic solid [see equation (2.28b)]

$$K_q \to K_T = \frac{\omega}{C_T}\left\{\frac{[1+(\frac{\mu''}{\mu'})^2\omega^2]^{1/2}+1}{2[1+(\frac{\mu''}{\mu'})^2\omega^2]}\right\}^{1/2},$$

$C_T = (\mu'/\rho)^{1/2}$ (transverse sound speed), μ' = Lame parameter, μ'' = the corresponding Voigt damping parameter;

v) for the longitudinal mode of a viscoelastic solid [see equation (2.28c)]:

$$K_q \to K_L = \frac{\omega}{C_L}\left\{\frac{[1+(\frac{\lambda''+2\mu''}{\lambda'+2\mu'})^2\omega^2]^{1/2}+1}{2[1+(\frac{\lambda''+2\mu''}{\lambda'+2\mu'})^2\omega^2]}\right\}^{1/2},$$

$C_L = [(\lambda'+2\mu')/\rho]^{1/2}$ (longitudinal sound speed), λ' = Lame parameter, λ'' = the corresponding Voigt damping parameter.

APPENDIX IId

The general equation of motion of a solid is written:

$$\partial_t^2(\rho u_\ell) = \rho f_\ell + \partial_k \sigma_{k\ell} \ , \qquad \text{(i)}$$

and the isotropic equation of state is given as:

$$\sigma_{k\ell} = E_{k\ell mn}\varepsilon_{mn} = E_{k\ell mn}\partial_m u_n \ , \qquad \text{(ii)}$$

where $\sigma_{k\ell}$ is the stress tensor, $E_{k\ell mn}$ is the generalized Young's modulus, ε_{mn} is the strain tensor that is defined by: $\varepsilon_{mn} = [\partial_m u_n + \partial_n u_m + (\partial_m u_\ell)(\partial_n u_\ell)]/2$, but is used here in its linear isotropic form as: $\varepsilon_{mn} = \partial_m u_n$ with u_n denoting the displacement vector. The isotropic expansion of $E_{k\ell mn}$ that utilizes the symmetries of the field may be written [6]:

$$E_{k\ell mn} = \lambda\delta_{k\ell}\delta_{mn} + \mu(\delta_{kn}\delta_{\ell m} + \delta_{km}\delta_{\ell n}) \ , \qquad \text{(iii)}$$

where λ and μ are the well known Lame parameters. Substituting (iii) into (ii), leave one with:

$$\sigma_{k\ell} = \lambda\delta_{k\ell}\partial_n u_n + \mu(\partial_\ell u_k + \partial_k u_\ell) \ ,$$

whereupon taking the divergence one has:

$$\partial_k \sigma_{k\ell} = \lambda\partial_\ell\partial_n u_n + \mu(\partial_\ell\partial_k u_k + \partial^2 u_\ell) \ . \qquad \text{(iv)}$$

$$= (\lambda+\mu)\partial_\ell\partial_n u_n + \mu\partial^2 u_\ell$$

Substituting (iv) into (i) and assuming constant density ρ, one has:

$$[(\rho\partial_t^2-\mu\partial^2)\delta_{\ell n} - (\lambda+\mu)\partial_\ell\partial_n]u_n = \rho f_\ell \ ,$$

which after dividing by ρ is in an appropriate form for extracting the operator as presented by expression (2.24) of the main text.

APPENDIX IIe

Evaluation of the Tensor Green's function of a Viscoelastic Solid in Three Domains

A. The $(\vec{k};\omega)$ Domain

Transforming equation (2.25) of the main text with the operator defined in expression (2.24) from the $(\vec{r};t)$ domain into the $(\vec{k};\omega)$ domain using the Fourier transforms, one has:

$$L_{ij}(\vec{k};\omega)G_{jm}(\vec{k};\omega) = \delta_{im} \ , \qquad \text{(i)}$$

where $L_{ij}(\vec{k};\omega) = \{[(\frac{\mu'+i\omega\mu''}{\rho})k^2-\omega^2]\delta_{ij} + [\frac{(\lambda'+\mu')+i\omega(\lambda''+\mu'')}{\rho}]k_ik_j\}$ (ii)

Since (i) is purely algebraic it is clear that:

$$G_{jm}(\vec{k};\omega) = L_{ij}^{-1}(\vec{k};\omega)\delta_{im} = L_{mj}^{-1}(\vec{k};\omega) \ , \qquad \text{(iii)}$$

where L^{-1} is the inverse operator of (ii) and is evaluated by considering the identity:

$$[L_{mj}^{-1}(\vec{k};\omega)][L_{ij}(\vec{k};\omega)] = \delta_{im} \ . \qquad \text{(iv)}$$

To solve this, one may assume $L_{mj}^{-1}(\vec{k};\omega)$ is of the same structure as $L_{ij}(\vec{k};\omega)$, i.e., $L_{mj}^{-1}(\vec{k};\omega) = A\delta_{mj} + Bk_mk_j$, where the coefficients A and B are evaluated in terms of K, χ_T, and χ_L

using relation (iv). The result is the Green's function of relation (iii) and is presented in the main text as expression (2.26).

B. The $(\vec{k};T)$ Domain

Using expression (2.26) of the main text and the following definition of the inverse temporal Fourier transform:

$$G_{jm}(\vec{k};T) = (1/2\pi) \int_{-\infty}^{\infty} d\omega \; e^{i\omega t} G_{jm}(\vec{k};\omega) \;,$$

the tensor Green's function in the $(\vec{k};T)$ domain is easily evaluated by two contour integrations. In each of the following parts (B. and C.), where the integrations for the transverse (T) and longitudinal (L) parts are of identical form, both will be represented using a subscript q to signify either T or L. Both terms then reduce to evaluating an integral of the form:

$$I_1 = (1/2\pi) \int_{-\infty}^{\infty} d\omega \; e^{i\omega T}/(\omega^2 - i2\Lambda_q\omega - \omega_{nq}^2) \;,$$

for which an appropriate contour is shown in figure A5. For the case of $T > 0$ one may use the residue theorem to write:

$$\oint \frac{e^{izT}}{z^2 - i2\Lambda_q z - \omega_{nq}^2} \, dz = \int_{-\infty}^{\infty} \frac{e^{i\omega T}}{\omega^2 - i2\Lambda_q\omega - \omega_{nq}^2} \, d\omega + \lim_{|z|\to\infty} \int \frac{e^{izT}}{z^2 - i2\Lambda_q z - \omega_{nq}^2} \, dz$$

$$= 2\pi i[\text{Res}\{1\} + \text{Res}\{2\}],$$

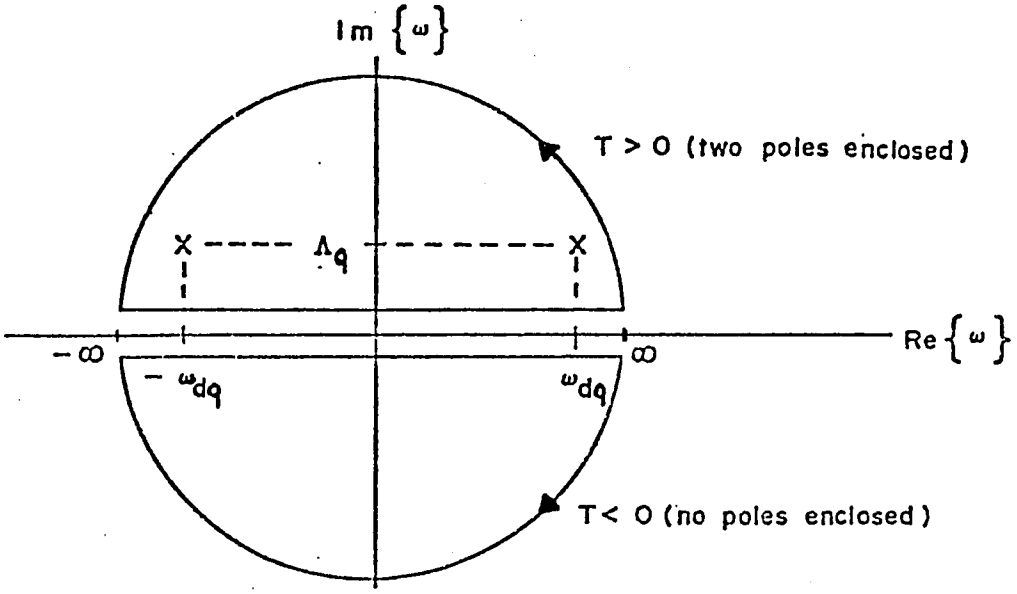

Figure A5 Contours appropriate for evaluating both terms of $G_{jm}(\vec{k};T)$ where $\omega_{dq} \equiv \omega_{nq}(1-\xi_q^2)^{1/2}$.

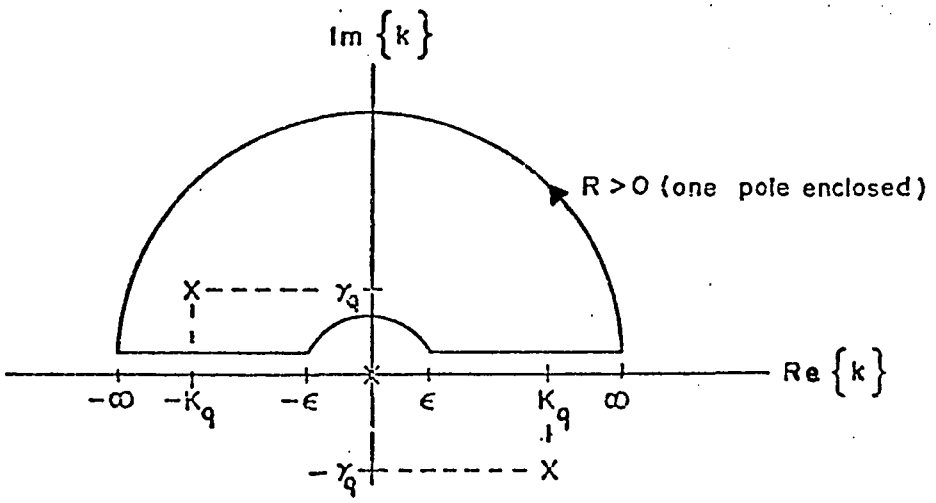

Figure A6 Contour appropriate for evaluating both terms of $G_{jm}(\vec{R};\omega)$; note: $K_q > \gamma_q$.

where the residues Res{1} and Res{2} are the contributions of the two poles shown in figure A5. The result of this integration is:

$$I_1 = U(T)e^{-\Lambda_q T}(\omega_{nq})^{-1}(1-\xi_q^2)^{-1/2}\sin[\omega_{nq}(1-\xi_q^2)^{1/2}T] \ .$$

The combined result is the tensor Green's function in the $(\vec{k};T)$ domain and is presented as expression (2.27) of the main text.

C. The $(\vec{R};\omega)$ Domain

Using expression (2.26) of the main text and the following definition of the inverse Fourier three-dimensional spatial transform:

$$G_{jm}(\vec{R};\omega) = (1/2\pi)^3 \iiint_{-\infty}^{\infty} d^3\vec{k}\ e^{-i\vec{k}\cdot\vec{R}} G_{jm}(\vec{k};\omega) \ ,$$

the tensor Green's function $G_{jm}(\vec{R};\omega)$ is easily evaluated by two types of contour integrations. The first term of the transverse part converts to spherical coordinates readily and reduces to the single integral:

$$I_2 = -(1/2\pi)^3 \iiint_{-\infty}^{\infty} d^3\vec{k}\ \frac{e^{-i\vec{k}\cdot\vec{R}}}{(\frac{\mu'+i\omega\mu''}{\rho})k^2-\omega^2}$$

$$= \frac{-\rho}{i4\pi^2 R(\mu'+i\omega\mu'')} \int_{-\infty}^{\infty} dk\ \frac{ke^{-ikR}}{k^2-(\frac{\rho\omega^2}{\mu'+i\omega\mu''})}$$

for which an appropriate contour is shown in figure A6, except that there is no pole at the origin. One may use the residue theorem to write:

$$\oint \frac{ze^{-izR}}{(z-\chi_T)(z+\chi_T)}dz = \int_{-\infty}^{\infty} \frac{ke^{-ikR}}{(k-\chi_T)(k+\chi_T)}dk + \lim_{|z|\to\infty} \oint \frac{ze^{-izR}}{(z-\chi_T)(z+\chi_T)}dz$$

$$= 2\pi i \text{ Res}\{-\chi_T\} ,$$

where $\chi_T^2 = \rho\omega^2/(\mu'+i\omega\mu'')$ which yields the result: $I_2 = (-\chi_T^2/\omega^2)e^{-\gamma_T R}e^{-iK_T R}/4\pi R$ where $\chi_T = K_T - i\gamma_T$. The longitudinal term and second term of the transverse part are both of the same form and convert to spherical coordinates as:

$$I_3 = \frac{-\chi_q^2}{\omega^2(2\pi)^3} \iiint_{-\infty}^{\infty} d^3\vec{k}\, e^{-i\vec{k}\cdot\vec{R}}/k^2(k^2-\chi_q^2) = \frac{-\chi_q^2}{i4\pi^2 R\omega^2} \int_{-\infty}^{\infty} dk\, e^{-ikR}/k(k^2-\chi_q^2),$$

where χ_T^2 is defined above and $\chi_L^2 = \rho\omega^2/[\lambda'+2\mu'+i\omega(\lambda''+2\mu'')]$. An appropriate contour is given in figure A6. One may use the residue theorem to write:

$$\oint \frac{e^{-izR}}{z(z-\chi_q)(z+\chi_q)}dz = \int_{-\infty}^{\infty} \frac{e^{-ikR}}{k(k-\chi_q)(k+\chi_q)}dk + \lim_{|z|\to\infty} \oint \frac{e^{-izR}}{z(z-\chi_q)(z+\chi_q)}dz$$

$$= 2\pi i \text{ Res}\{-\chi_q\}$$

where the residue contribution of the pole at the origin has been neglected due to hindsight because it results in a constant

term that vanishes when operated on by the spatial operators. The result of this integration is: $I_3 = e^{-\gamma R} e^{-iKR}/4\pi R\omega^2$, where $\gamma = K - i\gamma$. The combined result is the tensor Green's function in the $(\vec{R};\omega)$ domain and is presented as expression (2.28) of the main text.

APPENDIX IIf

Summary of Green's functions for five scalar equations (Parts A,B,C,D and E) and comparison to the transverse and longitudinal parts of the tensor Green's function of a viscous fluid (Parts F and G) and viscoelastic solid (Parts H and I).

A. Undamped Wave Equation: $[\partial^2-(1/C^2)\partial_t^2]f_1 = 0$

$$G(\vec{k};\omega) = 1/(k^2-\chi^2) \quad , \quad \chi = \omega/C \quad ;$$
$$G(\vec{k};T) = U(T)(C/k)\sin(CkT) \quad ;$$
$$G(\vec{R};\omega) = e^{-iKR}/4\pi R \quad , \quad R = |\vec{R}| \quad ;$$
$$G(\vec{R};T) = \delta(T-R/C)/4\pi R \quad .$$

B. Diffusion Equation: $[\partial^2-(1/D)\partial_t]f_2 = 0$

$$G(\vec{k};\omega) = 1/(k^2-\chi^2) \quad , \quad \chi^2 = -i\omega/D \quad ;$$
$$G(\vec{k};T) = U(T)D\, e^{-\Lambda T} \quad , \quad \Lambda = Dk^2 \quad ;$$
$$G(\vec{R};\omega) = e^{-\bar{\gamma}R}/4\pi R \quad , \quad \bar{\gamma} = i\Gamma = (\omega/D)^{1/2}e^{i\pi/4} \quad ;$$
$$G(\vec{R};T) = U(T)^{-1/2}(4\pi T)^{-3/2}e^{-R^2/4DT} .$$

C. Dissipative Wave Equation: $[\partial^2-(2/D)\partial_t-(1/C^2)\partial_t^2]f_3 = 0$

$$G(\vec{k};\omega) = 1/(k^2-\chi^2) \quad , \quad \chi^2 = 1/[DC^2(D\omega^2+i2C^2\omega)] \quad ;$$
$$G(\vec{k};T) = U(T)D[\xi(1-\xi^2)^{1/2}]^{-1}e^{-\Lambda T}\sin[\omega_n(1-\xi^2)^{1/2}T] \quad ,$$
$$\Lambda = \xi\omega_n \quad , \quad \xi = C/Dk \quad , \quad \text{and} \quad \omega_n = Ck \quad ;$$
$$G(\vec{R};\omega) = e^{-\gamma R}e^{-iKR}/4\pi R \quad , \quad \chi = K - i\gamma \quad \text{and}$$

K is the positive (+) sign and γ is the negative sign of the expression:

$$K,\ \gamma \longrightarrow \frac{\omega}{C}\left\{\frac{[1+(2\xi\omega_n/\omega)^2]^{1/2}\pm 1}{2}\right\}^{1/2} ;$$

$$G(\vec{R};T) = U(T)[Ce^{-\Lambda T}/4\pi R]\{\delta(CT-R) + U(CT-R)CRD^{-1}[R^2-(CT)^2]^{-1/2}J_1(CD^{-1}[R^2-(CT)^2]^{1/2})\}$$

(see [33]) .

D. Dissipative Wave Equation with Space-Time Coupling:

$$[\partial^2+(2D/C^2)\partial_t\partial^2-(1/C^2)\partial_t^2]f_4 = 0$$

$G(\vec{k};\omega) = \chi^2/\chi_0^2(k^2-\chi^2)$, $\chi_0 = \omega/C$ and $\chi^2 = \omega^2/(C^2+i2D_L\omega)$;

$G(\vec{k};T) = U(T)D[\xi(1-\xi^2)^{1/2}]^{-1}e^{-\Lambda T}\sin[\omega_n(1-\xi^2)^{1/2}T]$,

$\Lambda = \xi\omega_n$, $\xi = Dk/C$, and $\omega_n = Ck$;

$G(\vec{R};\omega) = \chi^2 e^{-\gamma R}e^{-iKR}/4\pi RK_0^2$, $\chi = K - i\gamma$ and

K is the positive (+) sign and γ is the negative (-) sign of the expression:

$$K,\ \gamma \longrightarrow \frac{\omega}{C}\left\{\frac{[1+(2\xi\omega/\omega_n)^2]^{1/2}\pm 1}{2[1+(2\xi\omega/\omega_n)^2]}\right\}^{1/2} ;$$

$$G(\vec{R};T) = U(T)(C/i4\pi^2R)\int_{-\infty}^{\infty} dk\frac{e^{-DTk^2+ikR}\sin\{CT[1-(Dk/C)^2]^{1/2}k\}}{[1-(Dk/C)^2]^{1/2}} .$$

E. Dissipative Wave Equation with Frequency-Dependent Viscosity Coefficients:

$[\partial^2+i(2D/C^2)\partial^2-(1/C^2)\partial_t^2]f_5 = 0$, where $D = D(\omega)$

$G(\vec{k};\omega) = \chi^2/\chi_0^2(k^2-\chi^2)$, $\chi_0 = \omega/C$ and $\chi^2 = \omega^2/(C^2+i2D)$;
$G(\vec{k};T) = (\chi^2/2)e^{-\Lambda|T|}e^{i\omega_d|T|}$, where ω_d is the positive (+) sign and γ is the negative (-) sign of the expression:

$$\omega_d,\ \Lambda \longrightarrow \left(\frac{k^2C^2}{2}\right)^{1/2}\left\{\left[1+\left(\frac{2D}{C^2}\right)^2\right]^{1/2}\pm 1\right\}^{1/2} ;$$

$G(\vec{R};\omega) = [1+i(\frac{2D}{C^2})\omega]^{-1}\ \frac{e^{-\gamma R}e^{-iKR}}{4\pi R}$, $\chi = K - i\gamma$, where K is the positive (+) sign and γ is the negative (-) sign of the expression:

$$K,\ \gamma \longrightarrow \frac{\omega}{C}\left\{\frac{[1+(2\xi/\omega_n)^2]^{1/2}\pm 1}{2[1+(2\xi/\omega_n)^2]}\right\}^{1/2} ,$$

and $\xi = \frac{Dk}{C}$, $\omega_n = Ck$;
$G(\vec{R};T) = (1/i8\pi^2R)\int_{-\infty}^{\infty}dk\ k\chi^2e^{-\Lambda|T|}e^{-i(kR-\omega_d|T|)}$, where $\omega_d = \omega_d(k)$ and $\Lambda = \Lambda(k)$.

F. The curl of the tensor operator of a viscous fluid (expression (2.1) of the main text) directly relates the transverse mode to diffusion equation:

In vector notation, the curl of the homogeneous form

of expression (2.1) is:

$$\nabla\times\{[\frac{\partial^2}{\partial t^2}-(\eta/\rho)\frac{\partial}{\partial t}\nabla^2]\vec{v}-(C_L^2+[(3\zeta+\eta)/3\rho]\frac{\partial}{\partial t})\nabla(\nabla\cdot\vec{v})\} = \vec{0}$$

Consider the following:

$\vec{v} = \vec{v}_T + \vec{v}_L$ (velocity vector separated into transverse and longitudinal components, respectively)

$\nabla \times \vec{v}_L = \vec{0}$ (the longitudinal mode is irrotational)

$\nabla \times \nabla\Psi = \vec{0}$ (an identity for any scalar Ψ)

then the above expression reduces to:

$$(\frac{\partial^2}{\partial t^2} - D_T \frac{\partial}{\partial t}\nabla^2)(\nabla\times\vec{v}_T) = \vec{0}\ , \quad D_T = \eta/\rho$$

which rearranges after an integration with respect to time to:

$$[\nabla^2-(1/D_T)\frac{\partial}{\partial t}](\nabla\times\vec{v}_T) = \vec{0}$$

A comparison of this equation to the diffusion equation of Part B of this appendix clearly displays the diffusive characteristic of the transverse mode. Further agreement is shown on comparing the results of Part B with the transverse terms of equations (2.3, 4, 5, 6, and 7) of the main text.

G. <u>The divergence of the tensor operator of a viscous fluid directly relates the longitudinal mode to a dissipative wave equation with space-time coupling</u>:

In vector notation, the divergence of the homogeneous form of expression (2.1) of the main text is:

$$\nabla\cdot\{[\frac{\partial^2}{\partial t^2} - (\eta/\rho)\frac{\partial}{\partial t}\nabla^2]\vec{v} - (C_L^2+[(3\zeta+\eta)/3\rho]\frac{\partial}{\partial t})\nabla(\nabla\cdot\vec{v})\} = 0$$

Consider the following:

$\vec{v} = \vec{v}_T + \vec{v}_L$ (transverse and longitudinal components, respectively)

$\nabla \cdot \vec{v}_T = 0$ (the transverse mode is non-dilational)

then the above expression reduces to:

$$[\frac{\partial^2}{\partial t^2} - (\eta/\rho)\frac{\partial}{\partial t}\nabla^2](\nabla\cdot\vec{v}_L) - (C_L^2+[(3\zeta+\eta)/3\rho]\frac{\partial}{\partial t})\nabla^2(\nabla\cdot\vec{v}_L) = 0$$

$$\{\frac{\partial^2}{\partial t^2} - [\eta+(\zeta+\eta/3)]\rho^{-1}\frac{\partial}{\partial t}\nabla^2 - C_L^2\nabla^2\}(\nabla\cdot\vec{v}_L) = 0$$

with $D_L \equiv (3\zeta+4\eta)/6\rho$, this rearranges to:

$$[\nabla^2+(2D_L/C_L^2)\nabla^2\frac{\partial}{\partial t} - (1/C_L^2)\frac{\partial^2}{\partial t^2}](\nabla\cdot\vec{v}_L) = 0$$

A comparison of this equation to the dissipative wave equation with space-time coupling of Part D of this appendix clearly displays the lightly-damped characteristic of the longitudinal mode. Further agreement is shown on comparing the results of Part D with the longitudinal terms of equations (2.3, 4, 5, 6, and 7) of the main text.

H. The curl of the tensor operator of a viscoelastic solid (expression (2.24) of the main text) directly relates the transverse mode to dissipative wave-equation with space-time coupling:

In vector notation, the curl of the homogeneous form

of expression (2.24) is:

$$\nabla\times\{[\frac{\partial^2}{\partial t^2} - (\frac{\mu}{\rho})\nabla^2]\vec{u} - (\frac{\lambda+\mu}{\rho})\nabla(\nabla\cdot\vec{u})\} = \vec{0}$$

Consider the following:

$\vec{u} = \vec{u}_T + \vec{u}_L$	(displacement vector separated into transverse and longitudinal components, respectively)
$\nabla \times \vec{u}_L = \vec{0}$	(the longitudinal mode is irrotational)
$\nabla \times \nabla\Psi = \vec{0}$	(an identity for any scalar Ψ)
$\mu \rightarrow \mu' + \mu'' \frac{\partial}{\partial t}$	(expand Lame parameter to include Voigt damping)

then the above expression reduces to:

$$[\frac{\partial^2}{\partial t^2} - (\frac{\mu'+\mu''\frac{\partial}{\partial t}}{\rho})\nabla^2](\nabla\times\vec{u}_T) = \vec{0} \ ,$$

which after multiplying by $(-\rho/\mu')$ rearranges to:

$$[\nabla^2+(2D_T/C_T^2)\nabla^2 \frac{\partial}{\partial t} - (1/C_T^2)\frac{\partial^2}{\partial t^2}](\nabla\times\vec{u}_T) = \vec{0} \ ;$$

where $D_T = \mu''/2\rho$ and $C_T = (\mu'/\rho)^{1/2}$. A comparison of this equation with that of the dissipative wave equation with space-time coupling (Part D of this appendix) clearly displays the lightly-damped characteristic of the transverse mode of a viscoelastic solid (equations 2.26, 27, and 28).

I. <u>The divergence of the tensor operator of a viscoelastic solid directly relates the longitudinal mode to a dissipative wave equation with space-time coupling</u>:

In vector notation, the divergence of the homogeneous form of expression (2.24) of the main text is:

$$\nabla\cdot\{[\frac{\partial^2}{\partial t^2} - (\frac{\mu}{\rho})\nabla^2]\vec{u} - (\frac{\lambda+\mu}{\rho})\nabla(\nabla\cdot\vec{u}) = 0 \ .$$

Consider the following:

$\vec{u} = \vec{u}_T + \vec{u}_L$	(transverse and longitudinal components, respectively)
$\nabla \cdot \vec{u}_T = 0$	(the transverse mode is non-dilational)
$\lambda \rightarrow \lambda' + \lambda'' \frac{\partial}{\partial t}$	(expand Lame parameter to include Voigt damping)

then the above expression reduces to:

$$[\frac{\partial^2}{\partial t^2} - (\frac{\mu'+\mu''\frac{\partial}{\partial t}}{\rho})\nabla^2](\nabla\cdot\vec{u}_L) - [\frac{(\lambda'+\mu'')+(\lambda''+\mu'')\frac{\partial}{\partial t}}{\rho}]\nabla^2(\nabla\cdot\vec{u}_L) = 0$$

$$[\frac{\partial^2}{\partial t^2} - (\frac{\mu''}{\rho}+\frac{\lambda''+\mu''}{\rho})\nabla^2\ \frac{\partial}{\partial t} - (\frac{\mu'}{\rho}+\frac{\lambda'+\mu''}{\rho})\nabla^2](\nabla\cdot\vec{u}_L) = 0$$

$$[\frac{\partial^2}{\partial t^2} - (\frac{\lambda''+2\mu''}{\rho})\nabla^2\ \frac{\partial}{\partial t} - (\frac{\lambda'+2\mu'}{\rho})\nabla^2](\nabla\cdot\vec{u}_L) = 0$$

which after multiplying by $-(\lambda'+2\mu')/\rho$ rearranges to:

$$[\nabla^2+(2D_L/C_L^2)\nabla^2\ \frac{\partial}{\partial t} - (1/C_L^2)\frac{\partial^2}{\partial t^2}](\nabla\cdot\vec{u}_L) = 0 \ ,$$

where $D_L = (\lambda''+2\mu'')/2\rho$ and $C_L = [(\lambda'+2\mu')/\rho]^{1/2}$. A comparison of this equation with that of the dissipative wave

equation with space-time coupling (Part D of this appendix) clearly displays the lightly-damped characteristic of the longitudinal mode of a viscoelastic solid (equations 2.26, 27, and 28).

APPENDIX IIg

Landau and Lifshitz [2,6] calculate the rate of dissipation of mechanical energy, i.e., $\partial E_{mech}/\partial t$, by using the following argument. In passing from a given non-equilibrium state to one of thermodynamic equilibrium the maximum amount of work that can be done is just the mechanical energy, E_{mech}. Hence $\partial E_{mech}/\partial t$ is equal to $-(\partial E/\partial s)(\partial s/\partial t)$ where $E_{mech} = E_0 - E(s)$. The attenuation constant is then evaluated to be:

$$\Lambda = |\langle \partial E_{mech}/\partial t \rangle|/(2\langle E \rangle) \ ,$$

where $\langle\ \rangle$ denotes temporal averaging and $|\ |$ denotes the "magnitude of" the argument.

Landau and Lifshitz evaluate the temporal attenuation constant for sound waves in a viscous fluid [2, p. 300] which agrees with the longitudinal (compressional) attenuation constant determined in this investigation ($\Lambda_L = D_L k^2$) obtained directly from the exponential decay factor of the longitudinal part of the $(\vec{k};T)$ domain tensor Green's function, expression (2.5). Similarly Landau and Lifshitz calculate the transverse Λ_T and longitudinal Λ_L temporal attenuation constant for an elastic solid [6, p. 157] which expression (2.27) reduces to [note: definitions $\xi = (\lambda''+2\mu''/3)$ and $\eta = \mu''$].

The only discrepancy between this study and Landau and Lifshitz is that the latter calls this attenuation term a

spatial one by dividing Λ by the sound speed for dimensional reasons, that is: $e^{-\Lambda T}$ vs. $e^{-\Lambda R/C} = e^{-\gamma R}$. This study finds no such simple relation between the temporal Λ and spatial γ attenuation constants.

APPENDICES
(FOR CHAPTER III)

APPENDIX IIIa

Derivation of the equation of motion for an ideal fluid

Euler equation: $$\partial_t(\rho\vec{v}) + \nabla P = \rho\vec{f} \qquad \text{(i)}$$

Equation of state: $dP = (\partial P/\partial\rho)_s d\rho$, $(\ )_s$ = isentropic partial derivative

For acoustic purposes: $$\nabla P = C^2\nabla\rho \qquad \text{(ii)}$$

where $C^2 = (\partial P/\partial\rho)_s$ = adiabatic compressional sound speed [10]

Continuity equation: $$\partial_t\rho + \rho_o(\nabla\cdot\vec{v}) = 0 \qquad \text{(iii)}$$

Substitute (ii) into (i), linearize, and differentiate w.r.t. time:

$$\rho_o\partial_t^2\vec{v} + C^2\nabla\partial_t\rho = \rho_o\partial_t\vec{f} \qquad \text{(iv)}$$

Substitute (iii) into (iv), divide by ρ_o, and let $\vec{v} = \partial_t\vec{u}$:

$$\partial_t^2(\partial_t\vec{u}) - C^2\nabla[\nabla\cdot(\partial_t\vec{u})] = \partial_t\vec{f} \qquad \text{(v)}$$

Integrate (v) w.r.t. time: $\partial_t^2\vec{u} - C^2\nabla(\nabla\cdot\vec{u}) = \vec{f}$

Let $\vec{u} = \nabla\Psi$ and $\vec{f} = -\nabla(C^2S)$; Ψ and S are potentials:

$$\nabla(\partial_t^2\Psi - C^2\nabla^2\Psi) = -\nabla(C^2S)$$

Integrate (3-D) spatially: $(\partial_t^2 - C^2\nabla^2)\Psi = -C^2S$

Divide by $(-C^2)$ and take temporal Fourier transform:

$$[\nabla^2 + (\omega/C)^2]\Psi(\vec{r};\omega) = S(\vec{r};\omega) \qquad \text{(vi)}$$

APPENDIX IIIb

Derivation of the WKB solution and validity criterion [16]

A. The WKB solution:

The basic equation:

$$\left[\frac{d^2}{dz^2} + \Omega^2\right] Z = 0 \qquad \text{(i)}$$

where

$$\Omega^2 = (\omega/C)^2 - \Gamma^2 \qquad \text{(ii)}$$

If

$$Z = \rho e^{is} , \qquad \text{(iii)}$$

with ρ and s functions to be evaluated. Then

$$Z_z = (\rho_z + i\rho s_z)e^{is} ;$$

where subscript z denotes partial differentiation in this Appendix only

$$Z_{zz} = [(\rho_{zz} - \rho s_z^2) + i(2\rho_z s_z + \rho s_{zz})]e^{is}$$

Substitution of these into (i), division by e^{is}, and separation into real and imaginary parts yields:

$$\text{Real:} \qquad \rho_{zz} - \rho(s_z^2 - \Omega^2) = 0 \qquad \text{(iv)}$$

$$\text{Imaginary:} \qquad \rho s_{zz} + 2\rho_z s_z = 0 \qquad \text{(v)}$$

Solving (v), with $t = s_z$:

$$\frac{s_{zz}}{s_z} = \frac{-2\rho_z}{\rho} = \frac{t_z}{t}$$

where $-2 \ln\rho = \ln t + \ln(A^{-2})$, the last term is an integration constant

$$\rho = At^{-1/2} = As_z^{-1/2} \qquad \text{(vi)}$$

Divide (iv) by ρ and introduce the standard approximation that:

$$\left|\frac{1}{\Omega^2}\frac{\rho_{zz}}{\rho}\right| << 1 \qquad \text{(vii)}$$

From (iv) then:

$$s_z = \pm\Omega \quad \text{and} \quad s = \pm\int_{z_o}^{z} \Omega(\bar{z})\,d\bar{z} + s_o \qquad \text{(viii)}$$

Note that in (iii): $s = s(\Gamma r+\Omega z-\omega t)$ hence Z is a progressive plane wave solution, then from (iii), (vi), and (viii) one has the two <u>WKB solutions</u>:

$$Z_{\pm} = e^{is} \sim A\Omega^{-1/2} e^{\pm i\int_{z_o}^{z} \Omega(\bar{z})\,d\bar{z}}, \qquad \text{(ix)}$$

A being complex valued.

B. The validity criterion of WKB solution:

From (vi) and (viii): $\rho = A\Omega^{-1/2}$, $\rho_z = \frac{-A}{2}\Omega^{-1/2}\frac{d}{dz}(\ln\Omega)$

$$\rho_{zz} = \frac{A}{4}\Omega^{-1/2}(\frac{d}{dz}\ln\Omega)^2 - \frac{A}{2}\Omega^{-1/2}\frac{d^2}{dz^2}(\ln\Omega)$$

Then (vii) becomes:

$$\frac{1}{2}\left|\frac{1}{\Omega^2}\frac{d^2}{dz^2}(\ln\Omega) - \frac{1}{2}\frac{1}{\Omega^2}(\frac{d}{dz}\ln\Omega)^2\right| << 1 \qquad \text{(x)}$$

In a medium of slowly varying Ω, one may make the second approximation that Ω varies linearly with depth ($\Omega \sim \alpha z$).

This assumption is equivalent to taking the first term of a Taylor expansion. Note that: $\frac{d}{dz}(\ln \alpha z) = \frac{1}{z}$. Then (x) becomes:

$$\frac{3}{4}\left|\frac{1}{\Omega^2}(\frac{d}{dz}\ln \alpha z)^2\right| << 1$$

which simplifies to:

$$\frac{1}{\Omega}\left|\frac{d}{dz}\ln \Omega\right| << 1 \qquad \text{(xi)}$$

This condition (xi) means that the rate of variation per wavelength (of the z-component of wavelength, Ω) is small, implying that ρ in (iii) is slowly varying.

For steep rays and high frequencies $\omega/C >> \Gamma$, which implies that $\Omega \sim \omega/C$, and then $\frac{d}{dz}(\ln \Omega) \sim \frac{-1}{C}\frac{dC}{dz}$. Using

$\omega = 2\pi C/\lambda$ where λ is the wavelength along the ray, then (xi) becomes:

$$\frac{1}{2\pi} \frac{\lambda}{C} \frac{dC}{dz} << 1 \ . \qquad \text{(xii)}$$

This statement of the WKB validity criterion illustrates the high-frequency and/or low-gradient nature of the approximation.

APPENDIX IIIc

Selection of WKB-solution coefficients from boundary conditions

A. Top boundary condition: $Z_+(z=T) = 0, \quad T = z@top$ (i)

Since: $Z_+(z) = \Omega^{-1/2}[A_+e^{i\xi(T,z)}+B_+e^{-i\xi(T,z)}]$;

$$\xi(T,z) = \int_T^z \Omega(\bar{z})\,d\bar{z}$$

Then: $\xi(T,T) = 0$, $[A_+e^{o}+B_+e^{o}] = 0$

If we select:

$$A_+ = 1 \ , \quad \text{then:} \quad B_+ = -1 \qquad \text{(ii)}$$

B. Bottom boundary condition: $[1-i\frac{I}{\rho_o\omega}\frac{d}{dz}]Z_-(z=B) = 0$, (iii)

$B = z@bottom$, ρ_o = fluid density

Since: $Z_-(z) = \Omega^{-1/2}[A_-e^{i\xi(B,z)}+B_-e^{-i\xi(B,z)}]$;

$$\xi(B,z) = \int_B^z \Omega(\bar{z})\,d\bar{z}$$

Then:

$$\frac{dZ_-}{dz} = \frac{-1}{2}\,\Omega^{-3/2}\,\frac{d\Omega}{dz}[A_-e^{i\xi(B,z)}+B_-e^{-i\xi(B,z)}]$$

$$+ \Omega^{-1/2}[A_-(i\Omega(z=B)-0)+B_-(-i\Omega(z=B)-0)] \qquad \text{(iv)}$$

where Leibniz rules have been utilized on the second term:

$$\frac{d}{d\alpha}\int_{u_o(\alpha)}^{u_1(\alpha)} f(x)\,dx = f(u_1)\,\frac{du_1}{d\alpha} - f(u_o)\,\frac{du_o}{d\alpha}$$

Neglecting the first term of (iv) because $(d\Omega/dz)$ is small, one has:

$$\frac{dZ_{-}}{dz} = \Omega^{-1/2}[iA_{-}\Omega(z=B)-iB_{-}\Omega(z=B)]$$

Substituting this into condition (iii), one has:

$$A_{-}[\frac{I}{\rho_o\omega}\Omega(z=B)+1] - B_{-}[\frac{I}{\rho_o\omega}\Omega(z=B)-1] = 0$$

If select:

$$A_{-} = [\frac{I}{\rho_o\omega}\Omega(z=B)-1] \quad , \quad \text{then:} \quad B_{-} = [\frac{I}{\rho_o\omega}\Omega(z=B)+1] \qquad (v)$$

APPENDIX IIId

The Bridging Conditions [26]

It is known that the WKB approximate solutions are not valid near the turning points [zeros of $\Omega^2(z,\Gamma)$]. The zeros of $\Omega^2(z,\Gamma)$ are singularities of the approximate solutions but are not singular points for the exact differential equations. Hence the coefficients A and B necessary for a specific WKB solution must change abruptly as z takes on different values in complex plane about the singular point. This characteristic behavior of asymptotic approximations, known as Stokes phenomenon, requires a set of bridging conditions to be derived which specify exactly how a solution is to be continued in the separate regions of the complex plane.

To be specific, let $z = \alpha_j$ by any turning point. Furthermore, let $\delta > 0$ be a constant such that the WKB solutions may be considred valid outside the interval $-\delta < \mathrm{Re}\{z-\alpha_j\} < \delta$. For sufficiently large frequencies (large k), δ is a small number. In this interval and in a region about $z = \alpha_j$, the function $\Omega^2(z,\Gamma)$ is expandable as a power series of which the first term dominates:

$$\Omega^2(z,\Gamma) = M_j^2(z-\alpha_j) + 0\{(z-\alpha_j)^2\}$$

where M_j is a constant. Note that this assumes that Ω^2 is approximately linear in z near a singular point. Letting

$\beta_j = z - \alpha_j$ then to within first order

$$\Omega(z,\Gamma) = M_j \beta_j^{1/2} \qquad \beta_j \geq 0, \quad \Omega^2 \geq 0$$

$$\Omega(z,\Gamma) = -iM_j |\beta_j|^{1/2} \qquad \beta_j < 0, \quad \Omega^2 < 0$$

and

$$\xi \equiv \int \Omega(\bar{z})\, d\bar{z}$$

so

$$\xi_j(z,\Gamma) = \tfrac{2}{3} M_j \beta_j^{3/2}$$

$$\xi_j(z,\Gamma) = i\tfrac{2}{3} M_j |\beta_j|^{3/2}$$

The bridging condition may now be derived. Consider the z-plane around the point $z = \alpha_j$ (see figure A7). As z traverses around this point in a counter-clockwise path the arguments of ξ_j are as shown in the figure below.

Introducing a branch cut as shown, ξ is found to be purely imaginary on the dashed lines, known as Stoke's lines. On the solid lines however ξ_j is real with the signs as indicated, hence the WKB solutions are oscillatory on these lines. Along the Stoke's lines the solutions are real exponentials with one exponent being positive and the other negative. The solution with the positive exponent is named the dominant solution, the other the subdominant solution. The basic premise for deriving the bridging conditions is that only coefficients of the subdominant terms may be altered on

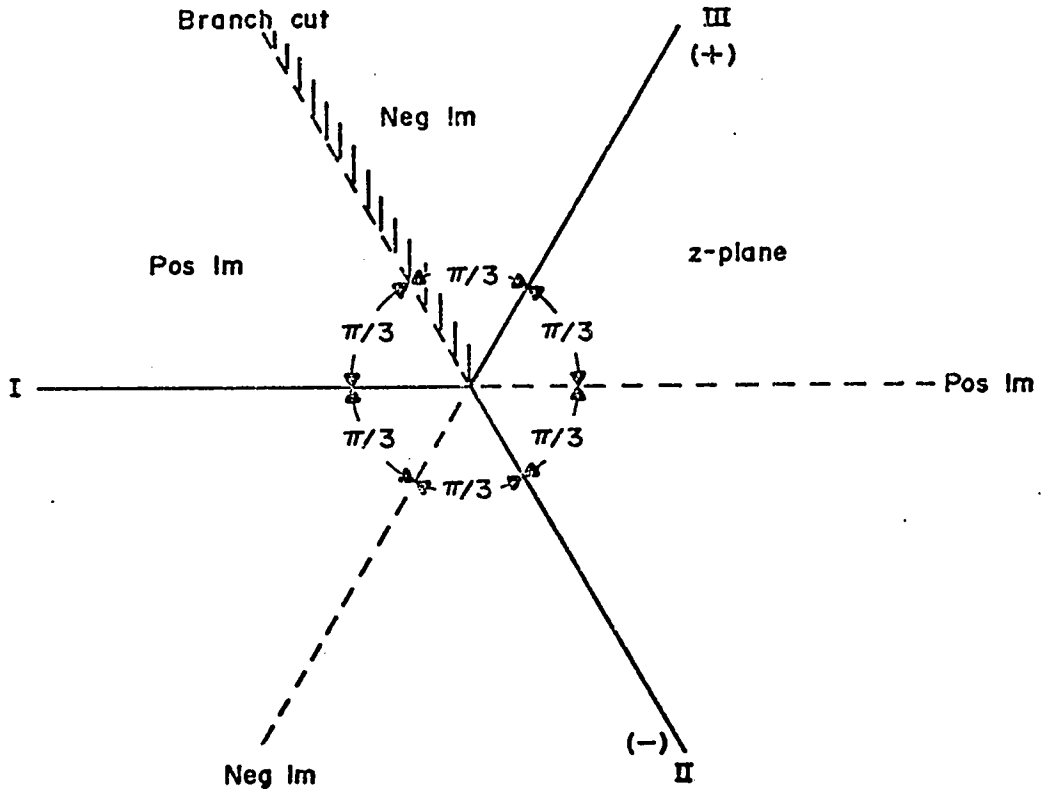

Figure A7 Complex z-plane to define the argument of ξ.

crossing the Stoke's lines provided that the coefficient of the dominant term is not zero.

Let us suppose in Region I the coefficients A_I and B_I are known, hence

$$Z(z) = A_I\Omega^{-1/2}e^{i\xi_1} + B_I\Omega^{-1/2}e^{-i\xi_1}$$

with the Stoke's lines between Region I and II, the function multiplying A_I is dominant, hence if we write the solutions in Region II as:

$$Z(z) = A_{II}\Omega^{-1/2}e^{i\xi_2} + B_{II}\Omega^{-1/2}e^{-i\xi_2}$$

it follows that:

$$A_{II} = A_I \quad \text{and} \quad B_{II} = B_I + aA_I$$

where a is a constant to be determined shortly. This combination of coefficients insures that the coefficient of the subdominant term can only change value when A_I, the coefficient of the dominant term is not zero. By the same reasoning it follows that a set of coefficients for Region III is given by

$$B_{III} = B_{II} \quad \text{and} \quad A_{III} = A_{II} + bB_{II}$$

where b is another constant to be determined. To connect the coefficients of Region II back to those of Region I, let $\Omega^{1/2}$ be defined as a single-valued function by the same branch cut as shown in figure A7. On the shaded side of the cut, the argument of $\Omega^{1/2}$ is therefore equal to the argument of the unshaded side minus $\pi/2$. Let $\Omega^{1/2}$ and ξ, refer to values of

these functions on the unshaded site, i.e., to Region I. Then the solutions on each side may be written:

$$Z(z) = A_I \Omega^{-1/2} e^{i\xi_1} + B_I \Omega^{-1/2} e^{-i\xi_1}$$

$$Z(z) = A_{III} e^{i\pi/2} \Omega^{-1/2} e^{-i\xi_2} + B_{III} e^{i\pi/2} \Omega^{-1/2} e^{i\xi_2} ,$$

i.e., the coefficients of the dominant terms must be equal, hence

$$B_I = iA_{III} .$$

By using these results one can obtain an expression relating A_I and B_I in the following form:

$$(i+b)B_i = (1+ab)A_I = 0$$

If this expression is to be valid for all A_I and B_I, the quantities within the parenthesis must be zero, hence

$$b = -i \quad \text{and} \quad a = -i$$

The bridging conditions are therefore:

$$A_{II} = A_I \qquad B_{II} = B_I - iA_I$$

and

$$A_{III} = A_{II} - iB_{II} \qquad B_{III} = B_{II}$$

It may be shown that the same formulae apply also to the remaining turning points. This completes the derivation of the bridging conditions.

APPENDIX IIIe

Transition from wave theory to ray optics (includes derivation of Snell's Law)

In general, the transition from wave theory to ray optics is effected as follows [16]: In the harmonic case

$$(\nabla^2+k^2)\Psi = 0 \; ; \quad k^2 = \omega^2/C^2 \tag{i}$$

one defines:

$$\Psi = Ae^{iS} \tag{ii}$$

where S is the eikonal. Substituting (ii) into (i), and collecting real and imaginary terms,

$$\nabla^2 A - (S_x^2+S_y^2+S_z^2)A + k^2 A = 0 \tag{iii}$$

$$2\nabla A \cdot \nabla S + A\nabla^2 S = 0 \tag{iv}$$

These equations are exact and are generalizations of equations (iv) and (v) of Appendix IIIb to three dimensions.

The first assumption usually made in ray otpics is:

$$\frac{\nabla^2 A}{A} << k^2 \tag{v}$$

which is simply the generalization of (viii) of Appendix IIIb. This condition is valid far away from turning points and at high frequency. Equation (iii) then becomes:

$$S_x^2 + S_y^2 + S_z^2 = k^2 \tag{vi}$$

which is called the eikonal equation.

The surfaces of constant phase, S = constant, are the wave fronts and the normals to these, of direction cosines S_x, S_y, and S_z, are the rays. It is only after using the approximation of equation (v) that the rays acquire an approximate character.

If one takes a new coordinate system (ξ,η,ζ)

$$d\xi = kdx \ , \quad d\eta = kdy \ , \quad d\zeta = kdz \tag{vii}$$

then the eikonal equation becomes:

$$S_\xi^2 + S_\eta^2 + S_\zeta^2 = 1 \ , \tag{viii}$$

i.e., in the (ξ,η,ζ) space the rays are straight lines; these are geodesics in the (ξ,η,ζ) space. Thus if

$$d\sigma^2 = d\xi^2 + d\eta^2 + d\zeta^2 \tag{ix}$$

it follows that:

$$\delta\int d\sigma = 0 \tag{x}$$

where the variation δ is performed with fixed end points.

By (vii) and (ix) one may write

$$d\sigma^2 = k^2 dl^2 \ ; \quad dl^2 = dx^2 + dy^2 + dz^2$$

and then (x) becomes:

$$\delta\int kdl = \omega\delta\int\frac{dl}{C} = 0$$

where the integral measures the time of travel along a ray. The rays are therefore paths of stationary time, this is

Fermat's principle. It allows one to construct the rays for any C(x,y,z)-law, a process known as ray tracing. Ray tracing is difficult when C varies in all three directions but fortunately oceans are mostly stratified in the vertical direction. For the two-dimensional case (x and z) with C a function of z only, Fermat's principle reads:

$$\delta\int\frac{dl}{C} = \delta\int\frac{1}{C}[1+(\frac{\partial x}{\partial z})^2]^{1/2}dz = 0$$

where

$$dl = (dx^2+dy^2+dz^2)^{1/2} = [[(\frac{\partial x}{\partial z})^2+(\frac{\partial y}{\partial z})^2+(\frac{\partial z}{\partial z})^2]dz^2]^{1/2} ,$$

and $\frac{\partial y}{\partial z} = 0$. Applying the Euler-Lagrange equations:

$$\frac{\partial f}{\partial y_i} - \frac{d}{dz}\frac{\partial f}{\partial(\frac{\partial y_i}{\partial z})} = 0$$

where f is the integrand $f = f[z,C(z),\frac{\partial x}{\partial z}] = \frac{1}{C}[1+(\frac{\partial x}{\partial z})^2]^{1/2}$ for the equation with $y_i \rightarrow x$ one obtains:

$$0 - \frac{d}{dz}\frac{(\partial x/\partial z)}{C[1+(\partial x/\partial z)^2]^{1/2}} = 0$$

or

$$\frac{1}{C}\frac{(\partial x/\partial z)}{[1+(\partial x/\partial z)^2]^{1/2}} = \text{constant} . \qquad \text{(xi)}$$

Considering figure 15 one sees that $\frac{\partial x}{\partial z} = \tan\theta$ and then (xi) becomes Snell's Law:

$$\frac{\sin\theta}{C} = \text{constant} \qquad \text{(xii)}$$

Integrating (xi) gives the equation for the rays:

$$x = \pm a \int_o^z \frac{C dz}{(1-a^2C^2)^{1/2}} = \pm \int_o^z \tan \theta \, dz$$

where a is a constant.

Note that from Snell's Law (xii) the horizontal wavenumber (α) is a constant for any depth z, since $\alpha = k \sin \theta$. Also note that a caustic is generated by the reflection of spherical waves from a half space with increasing sound velocity (see figure A8). The caustic is a line that is the envelope of the family of rays. The field has a maximum on the caustic and decreases in an oscillatory manner as one goes away from the caustic in the direction that leads us into the region where at every point, two rays intersect (in this figure, to the right of the caustic). The oscillation is due precisely to the interference between these rays. On the other side of the caustic, the field decreases monotonically.

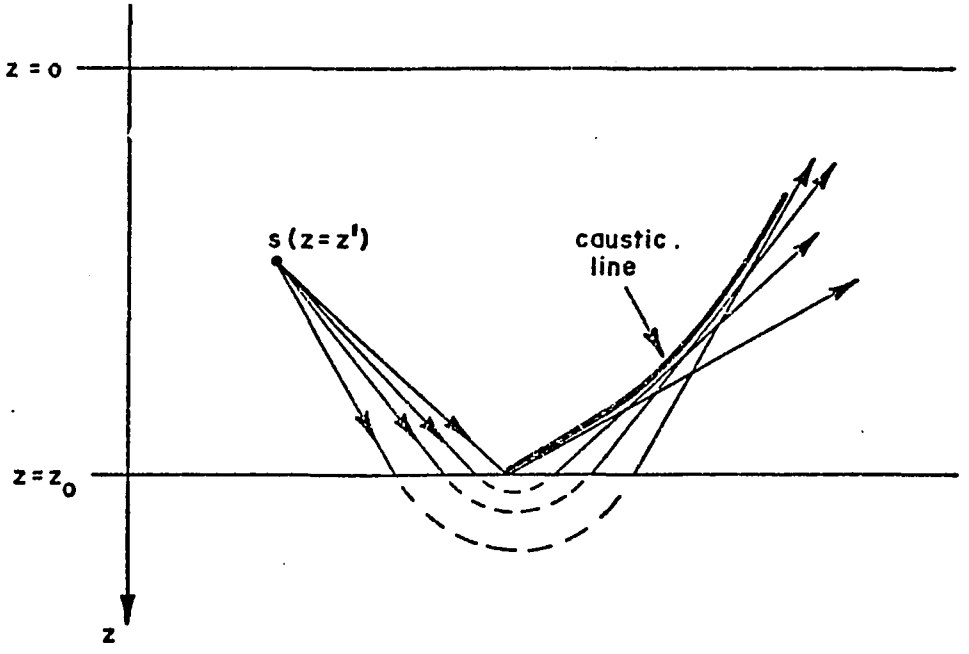

Figure A8 Caustic produced by relflection os spherical waves from a halfspace with increasing sound speed [34].
(s is the source point)

APPENDIX IIIf

INPUT.FOR

The next five pages constitute the interactive program that enables the user to select the source frequency, the various depths (bottom, source, and receiver), the viscoelastic bottom parameters, and the type of plot for the results desired. The information is stored in a data file.

```
INPUT.FOR;1                    8-SEP-1979 16:33:50.20          PAGE 1

  100   C THIS IS THE INTERACTIVE PROGRAM
  200   C
  300   C
  400         IMPLICIT DOUBLE PRECISION (A - H, K, O - Z)
  500         CHARACTER*1 PLOTTYP
  600         COMMON W, W2, B, T
  700         PI = 4.D0 * ATAN(1.D0)
  800         TYPE *,'       UNITS ASSUMED COMPATIBLE WITH ',
  900        2   'C(Z) AND Z(K) PROGRAMS.'
 1000   C
 1100   C  SELECT WATER DEPTH AND SOURCE FREQUENCY
 1200   C
 1300         TYPE *,' PLEASE ENTER DEPTH OF WATER:',
 1400         READ *, B
 1500         B = -DABS(B)
 1600         T = 0.D0
 1700         TYPE *,' PLEASE ENTER FREQUENCY OF SOURCE (HZ):',
 1800         READ *,W
 1900         W = 2.D0 * PI * W
 2000         W2 = W**2
 2100   C
 2200   C  SELECT BOTTOM TYPE AND ITS PARAMETERS
 2300   C
 2400         TYPE *,' ENTER BOTTOM TYPE:  1 = COARSE SAND; 2 = FINE SAND;',
 2500        C' 3 = VERY FINE SAND; 4 = SILTY SAND; 5 = SANDY SILT;',
 2600        C' 6 = SILT; 7 = SAND-SILT-CLAY; 8 = CLAYEY SILT; 9 = SILTY CLAY;',
 2700        C' 0 = OTHER (PREPARE TO PROVIDE PARAMETERS).'
 2800         READ *,IBOT
 2900         GO TO (1,2,3,4,5,6,7,8,9) IBOT
 3000   C
 3100   C  INPUT YOUR OWN SUBBOTTOM PARAMETERS (IF DESIRED, BOTTOM TYPE # 0)
 3200   C
 3300         TYPE *,' PRESENTLY 8/2/79 UNITS ARE:',
 3400        C ' METERS AND SECONDS'
 3500         TYPE *,' DENSITY (G/CC):',
 3600         READ *,RHO
 3700         TYPE *,' CL = LONGITUDINAL SOUND SPEED:',
 3800         READ *,CL
 3900         TYPE *,' CT = TRANSVERSE SOUND SPEED:',
 4000         READ *,CT
 4100         TYPE *,' BL = LONGITUDINAL DAMPING COEFFICIENT:',
 4200         READ *,BL
 4300         TYPE *,' BT = TRANSVERSE DAMPING COEFFICIENT:',
 4400         READ *,BT
 4500         GO TO 10
 4600   C
 4700   C  BOTTOM PARAMETERS FOR TYPE # 1
 4800   C
 4900       1 RHO = 2.0600
 5000         CL = 1808.00
 5100         CT = 120.00
 5200         BL = 1.00-6
 5300         BT = 1.70-4
 5400         GO TO 10
 5500   C
 5600   C  BOTTOM PARAMETERS FOR TYPE # 2
 5700   C
 5800       2 RHO = 1.9500
 5900         CL = 1727.00
```

```
 6000          CT = 350.D0
 6100          BL = 1.0D-6
 6200          BT = 0.19D-4
 6300          GO TO 10
 6400    C
 6500    C  BOTTOM PARAMETERS FOR TYPE # 3
 6600    C
 6700       3 RHO = 1.8600
 6800         CL = 1672.D0
 6900         CT = 270.D0
 7000         BL = 1.3D-6
 7100         BT = 0.35D-4
 7200         GO TO 10
 7300    C
 7400    C  BOTTOM PARAMETERS FOR TYPE # 4
 7500    C
 7600       4 RHO = 1.8000
 7700         CL = 1642.D0
 7800         CT = 370.D0
 7900         BL = 1.3D-6
 8000         BT = 0.17D-4
 8100         GO TO 10
 8200    C
 8300    C  BOTTOM PARAMETERS FOR TYPE # 5
 8400    C
 8500       5 RHO = 1.8100
 8600         CL = 1638.D0
 8700         CT = 410.D0
 8800         BL = 1.4D-6
 8900         BT = 0.17D-4
 9000         GO TO 10
 9100    C
 9200    C  BOTTOM PARAMETERS FOR TYPE # 6
 9300    C
 9400       6 RHO = 1.7700
 9500         CL = 1599.D0
 9600         CT = 290.D0
 9700         BL = 1.3D-6
 9800         BT = 0.30D-4
 9900         GO TO 10
10000    C
10100    C  BOTTOM PARAMETERS FOR TYPE # 7
10200    C
10300       7 RHO = 1.5800
10400         CL = 1555.D0
10500         CT = 330.D0
10600         BL = 0.2D-6
10700         BT = 0.035D-4
10800         GO TO 10
10900    C
11000    C  BOTTOM PARAMETERS FOR TYPE # 8
11100    C
11200       8 RHO = 1.4700
11300         CL = 1522.D0
11400         CT = 200.D0
11500         BL = 0.16D-6
11600         BT = 0.070D-4
11700         GO TO 10
11800    C
```

```
11900    C  BOTTOM PARAMETERS FOR TYPE # 9
12000    C
12100         9 RHO = 1.43D0
12200           CL = 1496.D0
12300           CT = 160.D0
12400           AL = 0.14D-6
12500           BT = 0.063D-4
12600           GO TO 10
12700    C
12800    C  PROCEED
12900    C
13000       10 RATRH = RHO/1.025D0
13100    C
13200    C  WRITE SOURCE FREQ., BOTTOM PARAMETERS, AND OCEAN DEPTH INTO FILE
13300    C
13400           WRITE (20, 100) W, W2, IBOT, RATRH, CL, CT, AL, BT
13500           WRITE (20, 101) B, T
13600           TYPE *, ' PLEASE ENTER PLOT TYPE (SINGLE LETTER IN APOSTROPHES):'
13700           READ *, PLOTTYP
13800    C
13900    C  WRITE PLOT TYPE INTO FILE
14000    C
14100           WRITE (20, 105) PLOTTYP
14200     105 FORMAT (X, A1, ' PLOT TYPE')
14300    C
14400    C  SELECT RECEIVER-ARRAY TYPE AND APPROPRIATE RANGE DATA
14500    C  AND WRITE INTO FILE WITH APPROPRIATE FORMAT
14600    C
14700       30 TYPE *, ' PLEASE ENTER RECEIVER ARRAY TYPE:'
14800          TYPE *, '       1 = SINGLE HORIZONTAL RANGE WITH'
14900          TYPE *, '             UNIFORM STEP'
15000          TYPE *, '       2 = ANY NUMBER OF HORIZONTAL RANGES WITH'
15100          TYPE *, '             UNIFORM SPACING AND STEPS'
15200          TYPE *, '       3 = UP TO TEN HORIZONTAL RANGES WITH'
15300          TYPE *, '             ARBITRARY SPACING AND STEPS'
15400          TYPE *, ' RECEIVER ARRAY TYPE #',
15500          READ *, IRTYP
15600    C
15700    C  WRITE RECEIVER-ARRAY TYPE INTO FILE
15800    C
15900          WRITE (20, 106) IRTYP
16000     106 FORMAT (4X, 'IRTYP=', I6)
16100          IF (IRTYP .NE. 1) GO TO 40
16200    C
16300    C  RANGE TYPE #1
16400    C
16500          TYPE *,' PLEASE ENTER RANGE OF SOURCE TO RECEIVER',
16600         C ' DISTANCES.'
16700          TYPE *,' SMALLEST SEPARATION DISTANCE:',
16800          READ *,RMIN
16900          TYPE *,' IF ONLY A SINGLE SEPARATION DISTANCE IS',
17000         C ' DESIRED, THEN ENTER ZERO FOR THE FOLLOWING.'
17100          TYPE *,' LARGEST SEPARATION DISTANCE:',
17200          READ *,RMAX
17300          IF (RMAX .GT. RMIN) THEN
17400           TYPE *,' ENTER INCREMENT:',
17500           READ *,RDEL
17600          ELSE
17700           RMAX = RMIN
```

```
17800           RDEL = 1.00
17900           END IF
18000     C
18100     C  WRITE RANGE DATA INTO FILE
18200     C
18300           WRITE (20, 103) RMIN, RMAX, RDEL
18400       103 FORMAT (4X, 'RMIN=', 1PG30.15, 'RMAX=', G30.15, 'RDEL=', G30.15)
18500           GO TO 90
18600        40 IF (IRTYP .NE. 2) GO TO 50
18700     C
18800     C  RANGE TYPE #2
18900     C
19000           TYPE *, ' ENTER OVERALL SOURCE-RECEIVER HORIZONTAL RANGE DATA'
19100           TYPE *, '   MINIMUM OVERALL SEPARATION DISTANCE:'
19200           READ *, RMN
19300           TYPE *, '   MAXIMUM OVERALL SEPARATION DISTANCE:'
19400           READ *, RMX
19500           TYPE *, '   SAMPLING SPACING:'
19600           READ *, RSP
19700           TYPE *, ' ENTER SAMPLE RANGE DATA'
19800           TYPE *, '   WIDTH OF SAMPLE:'
19900           READ *, RWID
20000           TYPE *, '   STEP INCREMENT:'
20100           READ *, RDEL
20200     C
20300     C  WRITE RANGE DATA INTO FILE
20400     C
20500           WRITE (20, 104) RMN, RMX, RSP, RWID, RDEL
20600       104 FORMAT (4X, 'RMN=', 1PG30.15, 'RMX=', G30.15,/
20700          2   4X, 'RSP=', G30.15, 'RWIDTH=', G30.15, 'RDEL=', G30.15)
20800           GO TO 90
20900        50 IF (IRTYP .NE. 3) GO TO 30
21000     C
21100     C  RANGE TYPE #3
21200     C
21300           TYPE *, ' SOURCE-RECEIVER HORIZONTAL SEPARATION DISTANCE DATA'
21400           TYPE *, ' ENTER NUMBER OF SAMPLED RANGES DESIRED  (UP TO 10):'
21500           READ *, NUMRG
21600           IF (NUMRG .LE. 0) GO TO 30
21700     C
21800     C  WRITE NUMBER OF RANGES INTO FILE
21900     C
22000           WRITE (20, 112) NUMRG
22100       112 FORMAT (4X, 'NUMBER OF RANGES =', I6)
22200           DO 60 NCASE = 1, NUMRG
22300           WRITE (6, 119) NCASE
22400       119 FORMAT (X, ' CASE #', I2)
22500           TYPE *, '   MINIMUM HORIZONTAL SEPARATION DISTANCE:'
22600           READ *, RNOW
22700           TYPE *, '   WIDTH OF SAMPLE (FROM MINIMUM VALUE JUST ENTERED):'
22800           READ *, RWID
22900           TYPE *, '   STEP INCREMENT:'
23000           READ *, RDEL
23100     C
23200     C  WRITE RANGE DATA INTO FILE
23300     C
23400           WRITE (20, 111) NCASE, RNOW, RWID, RDEL
23500       111 FORMAT (4X, 'CASE #', I6, 20X, 'RNOW=', 1PG30.15, /
23600          2    4X, 'RWIDTH=', G30.15, 'RDEL=', G30.15)
```

```
23700       60 CONTINUE
23800          GO TO 90
23900    C
24000    C  SELECT NUMBER OF SOURCE-RECEIVER DEPTH COMBINATIONS AND THEIR VALUES
24100    C
24200      90  TYPE *,' ENTER TOTAL NUMBER OF SOURCE AND RECEIVER DEPTH',
24300         C' COMBINATIONS TO BE EXECUTED FOR THIS SET OF PARAMETERS:'
24400          READ *, ITZ
24500    C
24600    C  WRITE TOTAL NUMBER OF SOURCE AND RECEIVER DEPTH COMBINATIONS DESIRED
24700    C  INTO FILE
24800    C
24900          WRITE (20, 106) ITZ
25000      106 FORMAT (4X, 'ITZ=', I6)
25100          DO 13 IT = 1, ITZ
25200          TYPE *,' CASE ',IT,':  ENTER SOURCE DEPTH:',
25300          READ *, ZS
25400          ZS = -DABS(ZS)
25500          TYPE *,' CASE ',IT,':  ENTER RECEIVER DEPTH:',
25600          READ *, ZR
25700          ZR = -DABS(ZR)
25800    C
25900    C  WRITE SOURCE-RECEIVER DEPTHS INTO FILE
26000    C
26100          WRITE (20, 102) IT, ZS, ZR
26200       13 CONTINUE
26300      100 FORMAT(X, 'W=', 1PG30.15, 6X, 'W2=', G30.15/X,'BOT. TYPE #',I3,
26400         2   19X,'RATRH=',G30.15/X,'CL=',G30.15,5X,'CT=',G30.15
26500         3   /X, 'BL=', G30.15, 5X, 'BT=', G30.15)
26600      101 FORMAT (X, 'B=', 1PG30.15, 6X, 'T=', G30.15)
26700      102 FORMAT (4X, 'IT:', I3, 5X, 'ZS=', 1PG30.15, 'ZR=', G30.15)
26800    C
26900    C  END OF INTERACTIVE PROGRAM
27000    C
27100          TYPE*,' END OF INTERACTIVE PROGRAM; NAME FILE FOR THIS DATA THEN'
27200          TYPE *, '     RUN EITHER GENERATING OR PLOTTING PROGRAMS'
27300          END
```

APPENDIX IIIg

GENER.FOR

The next eleven pages constitute the program to generate the eigenvalues (Γ; called KI here), compute the coefficients A and B of the Z-direction solutions ($Z_{\pm}$; called UPLUS and UMIN here) at the different depth ranges, and stores the information in a data file. This program reads the data file written by INPUT.FOR.

The following eleven pages contain support subroutines for the main part of GENER.FOR.

```
  100   C  THIS FILE ALSO CONTAINS PLUS, TURN
  200   C  AFTER CHANGES, RECOMPILE AND LINK SPECIFYING
  300   C  @FORLINK GENER 'C'      WHERE FILE 'C'.OBJ HAS C(Z)
  400   C
  500   C
  600   C  THIS IS THE GENERATING PROGRAM
  700   C
  800         IMPLICIT DOUBLE PRECISION (A-H, K, O-Z)
  900         DIMENSION TEM1(2), TEM2(2), D(2)
 1000         EXTERNAL C
 1100         COMMON W, W2, B, TOP /TEST/ EPS, NODD, NS, NP
 1200         DIMENSION A(0:10), ZCR(11)
 1300         COMMON /FILE/ N9, NK, EPSLIM, NREJ, RCR(0:12), NCR, NE
 1400         COMMON /ZK/ RATRH, KL2(2), KT2(2)
 1500         PI = 4.D0*ATAN(1.D0)
 1600         READ *, N9
 1700         OPEN (UNIT = 20, READONLY, TYPE = 'OLD', SHARED)
 1800   C
 1900   C  READ INPUT DATA FROM DATA FILE
 2000   C  THAT IS: SOURCE FREQ. , BOTTOM PARAMETERS, AND OCEAN DEPTH
 2100   C
 2200         READ (20, 200) W, W2, IBOT, RATRH, CL, CT, BL, BT
 2300     200 FORMAT (3X, G30.15, 9X, G30.15, / 12X, I3, 25X, G30.15,/
 2400        2  4X, G30.15, 6X, G30.15, /4X, G30.15, 8X, G30.15)
 2500         READ (20, 201) B, TOP
 2600     201 FORMAT (3X, G30.15, 8X, G30.15)
 2700   C
 2800   C  CALCULATE COMPLEX KL**2 (KL2(1), KL2(2))
 2900   C
 3000         TEM1(1) = W2/CL**2
 3100         TEM1(2) = 0.D0
 3200         TEM2(1) = 1.D0
 3300         TEM2(2) = W*BL
 3400         CALL CDIV(TEM1, TEM2, KL2)
 3500   C
 3600   C  CALCULATE COMPLEX KT**2 (KT2(1), KT2(2))
 3700   C
 3800         TEM1(1) = W2/CT**2
 3900         TEM2(2) = W*BT
 4000         CALL CDIV(TEM1, TEM2, KT2)
 4100         TYPE *, '  KL2=', KL2, '  KT2=', KT2
 4200   C
 4300   C  INITIALIZE Z STEP SIZE AND COUNTERS
 4400   C
 4500         EPS = 0.1D0
 4600         NODD = 0
 4700         NCUM = 0
 4800         NREJ = 0
 4900   C
 5000   C  LOCATE DEPTHS AT WHICH SPEED OF SOUND HAS RELATIVE EXTREMA
 5100   C  STORE THESE DEPTHS IN ARRAY 'A'
 5200   C
 5300         CALL TURN(C, B, TOP, A, SGB, NT, 10)
 5400         A(0) = B
 5500         A(NT + 1) = TOP
 5600   C
 5700   C  ON INTERVAL (B, T) FIND KCR = W/C(Z) AT TURNING POINTS
 5800   C  REORDER THE DEPTHS AND KCRIT VALUES BY INCREASING K
 5900   C  AND STORE IN 'ZCR' AND 'RCR' ARRAYS RESPECTIVELY
```

```
 6000    C
 6100    C  INITIALIZE
 6200    C
 6300          RCR(0) = 0.D0
 6400          RCR(1) = W/C(B)
 6500          ZCR(1) = B
 6600    C
 6700    C
 6800          DO 1 I = 1, NT + 1
 6900          Z = A(I)
 7000          RN = W/C(Z)
 7100          IF (RN .GT. RCR(I)) THEN
 7200           RCR(I + 1) = RN
 7300           ZCR(I + 1) = Z
 7400          ELSE
 7500           DO 3 J = I, 1, -1
 7600           IF (RN .LT. RCR(J)) THEN
 7700            RCR(J + 1) = RCR(J)
 7800            ZCR(J + 1) = ZCR(J)
 7900            RCR(J) = RN
 8000            ZCR(J) = Z
 8100           END IF
 8200         3  CONTINUE
 8300          END IF
 8400         1 CONTINUE
 8500          RX = RCR(NT + 2)
 8600          RCR(NT + 3) = 2.D0 * RX
 8700    C
 8800    C  PRINT DATA ON LOCATION OF EXTREMA IN SOUND PROFILE
 8900    C
 9000          WRITE (6, 100) 'A=', (A(I), I = 0, NT + 1)
 9100          WRITE (6, 100) 'Z=', 0., (ZCR(I), I = 1, NT + 2)
 9200          WRITE (6, 100) 'K=', (RCR(I), I = 0, NT + 3)
 9300      100 FORMAT (5X, A, 4(2X, 1PG20.10))
 9400    C
 9500    C  ESTIMATE SEARCH FINENESS NEEDED
 9600    C  ... IN CRITICAL K-REGION
 9700    C
 9800          DO 4 I = 1, NT + 1
 9900          EPK = RCR(I + 1) - RCR(I)
10000          IF (EPK .LT. 0.D0) THEN
10100           TYPE *, ' RCR OUT OF ORDER'
10200           STOP
10300          ELSE IF (EPK .EQ. 0.D0) THEN
10400           TYPE *, ' RCR DUPLICATES'
10500          ELSE IF ( EPK .LT. EPS) THEN
10600           EPS = EPK
10700          END IF
10800         4 CONTINUE
10900          EPS = EPS/5.D0
11000    C
11100    C  ... IN EARLY K-REGION  (ANALYTIC ESTIMATE GIVES 'NEST' AS OVERCOUNT
11200    C   (BY FACTOR PI) OF EIGENMODE NUMBER)
11300    C
11400          NEST = PHI(B, TOP, 0.D0)
11500          EPSK = RX/(NEST + 1)
11600          EPSK = EPSK/3.D0
11700          IF (EPSK .LT. EPS) EPS = EPSK
11800          TYPE *, ' NEST=', NEST, ' EPS=', EPS
```

```
11900    C
12000    C  INITIALIZE VARIABLES FOR SEARCH FOR EIGENVALUES
12100    C  'NKTRY' COUNTS NUMBER OF K'S LOOKED AT
12200    C  'NE' COUNTS NUMBER OF EXTREMA DETECTED
12300    C
12400          NCR = 0
12500          PK = 0.D0
12600          NKTRY = 0
12700          NK = 0
12800          ABDPR = 0.D0
12900          SGN = 1.D0
13000          NE = 0
13100          EPSLIM = 1.D-4
13200          K = 0.1D0 * EPS
13300          PKPR = 0.D0
13400    C
13500    C  EVALUATE 'DELTA' (LOOKING FOR K'S SUCH THAT 'DELTA' IS NEAR ZERO
13600    C    IN THE COMPLEX PLANE; ABS(DELTA) WILL BE NEAR ZERO AMONG
13700    C    POSITIVE REALS, THUS NEAR A LOCAL MINIMUM
13800    C
13900       2  CALL DELTA(K, D)
14000          ABD = CAB(D)
14100          IF (K .GT. RCR(NCR)) NCR = NCR + 1
14200    C
14300    C  IF ABS(DELTA) HAS NOT CHANGED FROM PREVIOUS K (REAL-VALUED) THEN ...
14400    C
14500          IF (ABD .EQ. ABDPR) THEN
14600           TYPE *, '   ABD FLAT      K=', K
14700           EPS = EPS/2.D0
14800           NKTRY = NKTRY + 1
14900    C
15000    C  TRY 'DELTA' WITH K BETWEEN PRESENT AND PREVIOUS VALUES
15100    C
15200           CALL DELTA(PK + EPS, TEM1)
15300           ABDP2 = CAB(TEM1)
15400           IF (ABDP2 .EQ. ABD) THEN
15500    C
15600    C  PROBLEM: 'DELTA' NOT CHANGING; RETURN TO PREVIOUS STEP SIZE;
15700    C           THIS MAY HAVE TO BE DEALT WITH ON 'AD HOC' BASIS
15800    C
15900            TYPE *, '  ABD VERY FLAT    K & EPS =', K, EPS
16000           EPS = 2.D0 * EPS
16100          ELSE IF ( (ABDP2 - ABDPR)*SGN .LT. 0.D0) THEN
16200    C
16300    C  ABS(DELTA) HAS /\/ OR \/\ SHAPE; NOTE TWO EXTREMA
16400    C  DETERMINE WHICH IS MINIMUM AND GO TO 'REFINE'
16500    C
16600           NE = NE + 2
16700           PKPR = PK + EPS
16800           IF (SGN .GT. 0.D0) THEN
16900            CALL REFINE(PKPR, ABDPR, ABDP2, ABD)
17000           ELSE
17100            NKTRY = NKTRY + 1
17200            CALL DELTA(PK-EPS, TEM2)
17300            CALL REFINE(PK, CAB(TEM2), ABDPR, ABDP2)
17400           END IF
17500          ELSE
17600           PKPR = PK + EPS
17700    C
```

```
17800   C                \
17900   C  ABS(DELTA) HAS \/ OR /\ SHAPE; NOTE ONE EXTREMUM
18000   C                 /
18100   C  DETERMINE MINIMUM OR MAXIMUM; IF MINIMUM THEN 'REFINE'
18200   C
18300         IF (SGN .LT. 0.D0) CALL REFINE(PKPR, APDPR, ABDP2, ABD)
18400   C
18500   C  CHANGE 'SIGN' (I.E. IF JUST FOUND MAX. , ONE NOW SEEKS MIN.)
18600   C
18700          SGN = -SGN
18800          NE = NE + 1
18900         END IF
19000   C
19100   C  UPDATE 'DELTA' PARAMETERS
19200   C
19300         ABDPR = ABDP2
19400         GO TO 23
19500        ELSE IF ((ABD - ABDPR)*SGN .LT. 0.D0) THEN
19600   C
19700   C  THIS STEP REACHED IF ...
19800   C  'DELTA' HAS /\ OR \/ SHAPE; NOTE ONE EXTREMUM
19900   C  DETERMINE MAXIMUM OR MINIMUM; IF MINIMUM THEN 'REFINE'
20000   C
20100         IF (SGN .LT. 0.D0) CALL REFINE(PK, ABDP2, ABDPR, ABD)
20200   C
20300   C  DECREASE STEP SIZE IF TURNING POINTS ARE CLOSE,
20400   C  UNLESS ALREADY TOO SMALL
20500   C
20600         IF (PK - PKPR .LT. 4.D0*EPS .AND. EPS .GT. EPSLIM)
20700        2      EPS = EPS/2.D0
20800          PKPR = PK
20900          NE = NE + 1
21000          SGN = -SGN
21100         END IF
21200   C
21300   C  UPDATE PARAMETERS
21400   C
21500     23  PK = K
21600         ABDP2 = ABDPR
21700         ABDPR = ABD
21800         K = K + EPS
21900         NKTRY = NKTRY + 1
22000   C
22100   C  LOOK FOR MORE EIGENVALUES PROVIDED UPPER LIMIT NOT ALREADY REACHED
22200   C
22300         IF (K .LT. 1.1D0 * RX) GO TO 2
22400   C
22500   C  END EIGENVALUE (K) SEARCH; REPORT FINAL PARAMETERS
22600   C
22700         TYPE *, '  NKTRY=', NKTRY, '  EPSFIN=', EPS, '  NE=', NE
22800         TYPE*,'NK=', NK, 'NODD=', NCUM, 'NODD2=', NCUM2, 'NODDTOT=', NODD
22900         TYPE *, 'NTURN=', NS, 'NPHI=', NP, 'NREJ=', NREJ
23000         END
23100   C
23200   C
23300   C
23400   C
23500         SUBROUTINE REFINE (KN, ABDPR, ABD, ABDNX)
23600   C
```

```
23700    C  THIS SUBROUTINE REFINES THE SELECTION OF THE EIGENVALUES THAT
23800    C  MINIMIZE THE FUNCTION 'DELTA'
23900    C
24000          IMPLICIT DOUBLE PRECISION (A-H, K, O-Z)
24100          DIMENSION TEM1(2), TEM2(2), TEM3(2), TEM4(2), D(2)
24200          COMMON W, W2, B, TOP /TEST/ EPS, NODD, NS, NP
24300          COMMON/FILE/N9, NK, EPSLIM, NREJ, RCR(0:12), NCR, NE, NCUM, NCUM2
24400          COMMON /A/ AD(0:6), AM(0:5,2), BM(0:5,2), NDEL, SGD
24500          COMMON /PLUS/ AP(0:5,2), BP(0:5,2)
24600    C
24700    C  INITIALIZE
24800    C
24900          PI = 4.D0 * ATAN(1.D0)
25000          K = KN
25100          EN = EPS
25200          NI = 0
25300          IFL = 0
25400          NLNR = 0
25500    C
25600    C  ERECT FLAG IF NEAR TURNING POINT
25700    C
25800          IF (ABS(KN - RCR(NCR)) .LT. 2.D0 * EPS .OR.
25900         2    ABS(KN - RCR(NCR - 1)) .LT. 2.D0 * EPS) IFL = 3
26000    C
26100    C  FIT A PARABOLA TO 3 CURVE POINTS AS ESTIMATOR OF MINIMUM
26200    C
26300          AB2D = ABDNX + ABDPR - 2.D0 * ABD
26400          ABDER = ABDNX - ABDPR
26500    C
26600    C  TEST FOR WRONG CURVATURE
26700    C
26800          IF (AB2D .LE. 0.D0) THEN
26900           WRITE (6, 150) NE, NI, EPS/EN, 'WRONG CURV', KN
27000           WRITE (6, 200) K - EN, TEM1, ABDPR, NC1, NDEL, K, D, ABD
27100           WRITE (6, 250) K + EN, TEM2, ABDNX
27200           GO TO 3
27300    C
27400    C  TEST FOR LINEARITY (SO DENOMINATOR IN MINIMUM ESTIMATE IS FINITE)
27500    C
27600          ELSE IF (AB2D .LT. EN**2) THEN
27700           NLNR = NLNR + 1
27800           WRITE (6, 150) NE, NI, EPS/EN, '  LINEAR  ', KN
27900           WRITE (6, 200) K - EN, TEM1, ABDPR, NC1, NDEL, K, D, ABD
28000           WRITE (6, 250) K + EN, TEM2, ABDNX
28100           IF (NLNR .GE. 2) GO TO 4
28200           EN = 2.D0 * EN
28300           GO TO 2
26400    C
28500    C  CALCULATE NEW MINIMUM (T) FROM TRIPLET
28600    C
28700          ELSE
28800           NLNR = 0
28900           T = K - (EN/2.D0) * ABDER/AB2D
29000    C
29100    C  CHECK MOVEMENT OF T FROM KN
29200    C
29300           IF (ABS(T - KN) .GT. EPS) THEN
29400    C
29500    C  CORRECTION ON LOCATION OF MINIMUM IS TOO LARGE
```

```
29600    C
29700             GO TO 5
29800           ELSE IF (T - K .GT. EN) THEN
29900    C
30000    C  MOVE AN EPSILON TO THE RIGHT AND CONTINUE
30100    C
30200             T = K + EN
30300           ELSE IF (T - K .LT. -EN) THEN
30400    C
30500    C  MOVE AN EPSILON TO THE LEFT AND CONTINUE
30600    C
30700             T = K - EN
30800           ELSE IF (ABS(T - K) .GT. EN/3.D0) THEN
30900    C
31000    C  ADJUST SIZE OF EPSILON
31100    C
31200             EN = EN/2.D0
31300           ELSE IF (ABS(T - K) .LT. EPSLIM * 1.D-1) THEN
31400    C
31500    C  CORRECTION WAS SMALL;  SKIP AN ITERATION STEP
31600    C
31700             NI = NI + 1
31800    C
31900    C  SUCCESSFUL;  EXIT WITH 'T' FOR LOCATION OF MINIMUM
32000    C
32100             IF (NI .GT. 2) GO TO 7
32200    C
32300             EN = EN/10.D0
32400             IF (EN .LT. EPSLIM*5.D-2) GO TO 8
32500           ELSE
32600             EN = EN/3.D0
32700             IF (EN .LT. EPSLIM*1.D-1) GO TO 8
32800           END IF
32900           NI = NI + 1
33000         END IF
33100    C
33200    C  IF 5 REFINEMENTS HAVE NOT PRODUCED A GOOD EXIT,
33300    C  PRINT WARNING AND EXIT ANYWAY
33400    C
33500         IF (NI .GE. 5) THEN
33600           WRITE (6, 150) NE, NI, EPS/EN, 'NI=5; EXIT', KN, T
33700           WRITE (6, 200) K - EN, TEM1, ABDPR, NC1, NDEL, K, D, ABD
33800           WRITE (6, 250) K + EN, TEM2, ABDNX
33900    C
34000    C  RELUCTANT;  EXIT WITH 'T'
34100    C
34200             GO TO 6
34300    C
34400         END IF
34500    C
34600    C  REACH HERE IF 'LINEAR' BUT 'NLNR' < 2  OR IF STILL REFINING (UP TO
34700    C  5 ITERATIONS) WITHOUT ANY COMPLICATIONS
34800    C
34900        2 K = T
35000          NOP = NODD
35100          CALL DELTA(T + EN, TEM2)
35200          CALL DELTA(T - EN, TEM1)
35300          CALL DELTA(T , D)
35400          NC1 = NODD - NOP
```

```
35500          ABDNX = CAB(TEM2)
35600          ABDPR = CAB(TEM1)
35700          ABD = CAB(D)
35800          GO TO 1
35900    C
36000    C  REACH HERE IF CURVATURE LOOKS WRONG (I.E.  A MAXIMUM INSTEAD OF
36100    C  A MINIMUM OF 'DELTA').  PROBLEM SHOULD BE DUE TO ROUND-OFF ERROR,
36200    C  SO LOOK AT THIS REGION MORE CLOSELY
36300    C
36400    C  CHECK WARNING COUNTER (IFL), IF HAS REACHED 3 THEN EXIT
36500    C
36600         3 IF (IFL .GE. 3) THEN
36700            WRITE (6, 150) NE, NI, EPS/EN, 'CURV IFL=3', KN, T
36800            GO TO 30
36900           END IF
37000    C
37100    C  LOOK TWO-INTERVALS EITHER SIDE OF POTENTIAL EXTREMUM (T)
37200    C
37300           CALL DELTA(T - 2.D0*EN, TEM3)
37400           CALL DELTA(T + 2.D0*EN, TEM4)
37500    C
37600    C  THIS CURVATURE PROBLEM WEIGHTS A SINGLE UNIT OF TROUBLE
37700    C
37800           IFL = IFL + 1
37900           ABD2PR = CAB(TEM3)
38000           ABD2NX = CAB(TEM4)
38100           D2PR = ABD2PR + ABD - 2.D0*ABDPR
38200           D2NX = ABD2NX + ABD - 2.D0*ABDNX
38300           DDB = ABD2PR + ABD2NX - 2.D0*ABD
38400    C
38500    C  TEST FOR WRONG CURVATURE OVER THIS (TWO-EPSILON) INTERVAL
38600    C
38700           IF (DDB .LE. 0.D0) THEN
38800    C
38900    C  TEST FOR WRONG CURVATURE OVER TWO SIDE (ONE-EPSILON) INTERVALS
39000    C
39100            IF (D2PR .LE. 0.D0 .OR. D2NX .LE. 0.D0) THEN
39200    C
39300    C  THIS CASE: REJECT ANY HOPE FOR EIGENVALUE SELECTION ON THIS INTERVAL
39400    C
39500             WRITE (6, 150) NE, NI, EPS/EN, 'CURV  3OF4', KN
39600             WRITE (6, 200) T - 2.D0*EN, TEM3, ABD2PR, NC1, NDEL
39700             WRITE (6, 250) T - EN, TEM1, ABDPR, T, D, ABD, T + EN, TEM2,
39800           2      ABDNX, T + 2.D0*EN, TEM4, ABD2NX
39900             GO TO 30
40000    C
40100    C  REPOSITION 'T' TO ITERATE AGAIN
40200    C
40300           ELSE IF (D2PR .GT. D2NX) THEN
40400    C
40500    C  MINIMUM IS TO LEFT OF PRESENT 'T'
40600    C
40700             T = T - EN
40800             K = T
40900             ABDNX = ABD
41000             ABD = ABDPR
41100             ABDPR = ABD2PR
41200             GO TO 1
41300           ELSE
```

```
41400    C
41500    C  MINIMUM IS TO RIGHT OF PRESENT 'T'
41600    C
41700           T = T + EN
41800           K = T
41900           ABDPR = ABD
42000           ABD = ABDNX
42100           ABDNX = ABD2NX
42200           GO TO 1
42300          END IF
42400    C
42500    C  REACH HERE IF NO CURVATURE PROBLEM OVER (TWO-EPSILON) INTERVAL
42600    C
42700          ELSE IF (D2PR .GT. MAX(0.D0, D2NX)) THEN
42800    C
42900    C  MINIMUM IS TO LEFT OF PRESENT 'T';  REPOSITION AND ITERATE
43000    C
43100           T = T - EN
43200           K = T
43300           ABDNX = ABD
43400           ABD = ABDPR
43500           ABDPR = ABD2PR
43600           GO TO 1
43700          ELSE IF (D2NX .GT. 0.D0) THEN
43800    C
43900    C  MINIMUM IS TO RIGHT OF PRESENT 'T';  REPOSITION AND ITERATE
44000    C
44100           T = T + EN
44200           K = T
44300           ABDPR = ABD
44400           ABD = ABDNX
44500           ABDNX = ABD2NX
44600           GO TO 1
44700          ELSE
44800    C
44900    C  CURVATURE PROBLEM IN BOTH SIDE-WING (ONE-EPSILON) INTERVALS BUT
45000    C  NOT IN THE EXTENDED (TWO-EPSILON) INTERVAL
45100    C
45200           WRITE (6, 150) NE, NI, EPS/EN, 'CURV N LAR', KN
45300            WRITE (6, 200) T - 2.D0*EN, TEM3, ABD2PR, NC1, NDEL
45400            WRITE (6, 250) T - EN, TEM1, ABDPR, T, D, ABD, T + EN, TEM2,
45500         2       ABDNX, T + 2.D0*EN, TEM4, ABD2NX
45600           GO TO 30
45700          END IF
45800    C
45900    C  REACH HERE IF ENCOUNTERED LINEARITY PROBLEM
46000    C
46100    C  CHECK WARNING COUNTER (IFL), IF REACHED 3  THEN EXIT
46200    C
46300        4 IF (IFL .GE. 3) THEN
46400           WRITE (6, 150) NE, NI, EPS/EN, 'LINE IFL=3', KN
46500           GO TO 30
46600          END IF
46700    C
46800    C  THIS LINEARITY PROBLEM WIGHTS A DOUBLE UNIT OF TROUBLE
46900    C
47000          IFL = IFL + 2
47100    C
47200    C  ENLARGE EPSILON, SELECT NEW TRY (T), AND ITERATE AGAIN
```

```
47300    C
47400          EN = 2.D0 * EN
47500          GO TO 2
47600    C
47700    C  REACH HERE IF CORRECTION ON LOCATION OF MINIMUM TAKES ESTIMATE
47800    C  BEYOND INTERVAL IT WAS SEARCHING
47900    C
48000        5 WRITE (6, 150) NE, NI, EPS/EN, ' K MOVES  ', KN, T
48100          WRITE (6, 200) K - EN, TEM1, ABDPR, NC1, NDEL, K, D, ABD
48200          WRITE (6, 250) K + EN, TEM2, ABDNX
48300          IF (IFL .GE. 3) THEN
48400           WRITE (6, 150) NE, NI, EPS/EN, 'MOVE IFL=3', KN
48500           GO TO 30
48600          END IF
48700    C
48800    C  THIS MOVEMENT PROBLEM WEIGHTS A DOUBLE UNIT OF TROUBLE
48900    C
49000          IFL = IFL + 2
49100          T = KN + (T - KN)/ABS(T - KN) * EPS/2.D0
49200          GO TO 2
49300    C
49400    C  REACH HERE IF THERE WAS NOT A SUCCESSFUL EXIT AFTER 5 ITERATIONS,
49500    C  YET NO MAJOR COMPLICATIONS EITHER (OR SUM OF SMALL ONES)
49600    C
49700        6 T = K + (T - K) * 0.9D0
49800          WRITE (6, 150) NE, NI, EPS/EN, 'AT LABEL 6', KN, T
49900          GO TO 7
50000        8 WRITE (6, 150) NE, NI, EPS/EN, 'EN .LT.LIM', KN, T
50100          EN = EPSLIM*1.D-1
50200    C
50300    C  REACH HERE IF INTENDING TO SAVE THIS EIGENVALUE
50400    C
50500        7 K = T
50600          NOP = NODD
50700    C
50800    C  EVALUATE SIDE-VALUES FOR DERIVATIVE CALCULATION COMING UP
50900    C
51000          CALL DELTA(K - EN, TEM3)
51100          ABDPR = CAB(TEM3)
51200          CALL DELTA(K + EN, TEM4)
51300          ABDNX = CAB(TEM4)
51400          NC1 = NODD - NOP
51500          NOP = NODD
51600    C
51700    C  FINAL CALL FOR SUBROUTINE 'DELTA' TO UPDATE AND STORE THE AM & BM
51800    C  COEFFICIENTS ASSOCIATED WITH THIS EIGENVALUE FOR UMINUS OF THE
51900    C  GREEN'S FUNCTION
52000    C
52100          CALL DELTA(K, D)
52200          ABD = CAB(D)
52300          NC2 = NODD - NOP
52400          WRITE (6, 300) NK, NI, EPS, EPS/EN, K, D, ABD, NC2, NDEL
52500    C
52600    C  CALCULATE DERIVATIVE OF 'DELTA'  (TEM1(1), TEM1(2))
52700    C
52800          TEM1(1) = (TEM4(1) - TEM3(1))/(2.D0*EN)
52900          TEM1(2) = (TEM4(2) - TEM3(2))/(2.D0*EN)
53000          IF (CAB(TEM1) .LT. 1.D0) THEN
53100           TYPE *, '  SMALL ABS(DER)=', CAB(TEM1), '  K=', K, '  KN=', KN
```

```
53200           GO TO 30
53300          END IF
53400    C
53500    C  CALCULATE COMPLEX POSITION OF EXACT ROOT: NEWTON'S METHOD
53600    C
53700          CALL CDIV(D, TEM1, TEM2)
53800          TEM2(1) = K - TEM2(1)
53900          TEM2(2) = -TEM2(2)
54000    C
54100    C  IF REAL PART OF KI IS FAR FROM REAL-AXIS MINIMUM: PRINT WARNING
54200    C
54300          IF (ABS(TEM2(1) - K) .GT. EPS/10.D0) THEN
54400           TYPE *, '  KI FAR=', TEM2, '  K=', K, '  KN=', KN
54500          END IF
54600    C
54700    C  CHECK TO INSURE A NEGATIVE IMAGINARY PART FOR EIGENVALUE,
54800    C  SO DAMPING AND NOT GROWTH IS SEEN
54900    C
55000          IF (TEM2(2) .GT. 0.D0) THEN
55100           WRITE (6, 150) NE, NI, EPS/EN, 'K IMAG POS', KN, T
55200           WRITE (6, 200) K - EN, TEM3, ABDPR, NC1, NDEL, K, D, ABD
55300           WRITE (6, 250) K + EN, TEM4, ABDNX
55400    C
55500    C  IF WARNING COUNTER HAS REACHED 3 UNITS THEN REJECT THIS EIGENVALUE
55600    C
55700           IF (IFL .GE. 3) GO TO 30
55800    C
55900    C  THIS POSITIVE-IMAGINARY PART PROBLEM WEIGHTS A UNIT OF TROUBLE
56000    C
56100           IFL = IFL + 1
56200    C
56300    C  OBTAIN NEW ESTIMATE BASED ON AVERAGE OF THE SIDE VALUES
56400    C
56500          TEM2(1) = (TEM3(1) + TEM4(1))/2.D0
56600          TEM2(2) = (TEM3(2) + TEM4(2))/2.D0
56700          CALL CDIV(TEM2, TEM1, TEM2)
56800          TEM2(1) = K - TEM2(1)
56900          TEM2(2) = -TEM2(2)
57000    C
57100    C  CHECK TO INSURE A NEGATIVE IMAGINARY PART FOR NEW ESTIMATE
57200    C
57300          IF (TEM2(2) .GT. 0.D0) THEN
57400           WRITE (6, 150) NE, NI, EPS/EN, 'K IMAG POS', KN, T
57500           IF (IFL .GE. 3) GO TO 30
57600           IFL = IFL + 1
57700           EN = 2.D0 * EN
57800           GO TO 7
57900          END IF
58000         END IF
58100    C
58200    C  GENERATE AP & BP COEFFICIENTS FOR UPLUS OF GREEN'S FUNCTION
58300    C
58400         CALL PLUS(K)
58500    C
58600    C  STORE NEW COEFFICIENTS IN PERMANENT EIGENVALUE FILE
58700    C
58800          NK = NK + 1
58900          WRITE (N9) NK, K, TEM2, NDEL, D, TEM1, (AD(ID), ID = 0,
59000        2    NDEL + 1), ((AM(ID, JD), JD = 1, 2), (BM(ID, JD), JD = 1, 2),
```

```
59100          3    (AP(ID, JD), JD = 1, 2), (BP(ID, JD), JD = 1, 2),
59200          4    ID = 0, NDEL)
59300    C
59400    C  INCREMENT VARIOUS COUNTERS AND RETURN
59500    C
59600           NCUM = NCUM + NC2
59700           NCUM2 = NCUM2 + NC1
59800           RETURN
59900    C
60000    C  REJECT THE SELECTION OF ANY EIGENVALUE ON THIS INTERVAL BEING
60100    C  SEARCHED FOR ANY OF THE ABOVE COMPLICATIONS
60200    C
60300       30 NREJ = NREJ + 1
60400          RETURN
60500    C
60600    C  FORMAT STATEMENTS
60700    C
60800      150 FORMAT (2X, '  NE=', I5, '  NI=', I3, '  ERAT=', 1PG12.3, A,
60900         2    '  KN=', G20.10, :, '  T=', G20.10)
61000      200 FORMAT (X, '  K=', 1PG20.10, 5X, ' D=', 2G20.10,
61100         2    5X, ' ABS=', G20.10, :, ' NODD=', I4, ' NT=', I3)
61200      250 FORMAT (X, '  K=', 1PG20.10, 5X, ' D=', 2G20.10,
61300         2    5X, ' ABS=', G20.10)
61400      300 FORMAT ('   NK =', I6, ' NI=', I4, ' EPS=', 1PG15.6,
61500         2     ' ERAT=', G12.3 / 9X, '  K=', G20.10, 5X, ' D=',
61600         3     2G20.10, 5X, ' ABS=', G20.10, ' NODD=', I4, ' NT=', I3)
61700          END
```

```
  100          SUBROUTINE PLUS(K)
  200    C
  300    C  GENERATE AP & BP COEFFICIENTS FOR UPLUS OF GREEN'S FUNCTION
  400    C
  500          IMPLICIT DOUBLE PRECISION (A-H, K, O-Z)
  600          COMMON W, W2, B, T /TEST/ EP, NERR
  700          COMMON /A/ A(0:5), AM(0:5, 2), BM(0:5, 2), NT, SGB
  800          COMMON /PLUS/ AP(0:5, 2), BP(0:5, 2)
  900    C
 1000    C  FIND SIGN AT TOP (SGN)
 1100    C
 1200          SGN = SGB*(-1)**NT
 1300    C
 1400    C  INITIALIZE
 1500    C
 1600          J = NT
 1700          ZP = T
 1800    C
 1900    C  ASSIGN COEFFICIENT VALUES AT TOP (FROM BOUNDARY CONDITION)
 2000    C
 2100          AP(J, 1) = 1.D0
 2200          AP(J, 2) = 0.D0
 2300          BP(J, 1) = -1.D0
 2400          BP(J, 2) = 0.D0
 2500    C
 2600    C  EXIT WHEN ALREADY SEEN THE LAST OF THE TURNING POINTS
 2700    C
 2800       50 IF (J .LE. 0) RETURN
 2900    C
 3000    C  OBTAIN NEXT TURNING PT. DEPTH (STEPPING DOWN FROM TOP)
 3100    C
 3200          ZI = A(J)
 3300          J = J - 1
 3400    C
 3500    C  PHI INTEGRATES ABS(Q) FROM NEWEST TURNING POINT UP TO PREVIOUS ONE
 3600    C
 3700          PH = PHI(ZI,ZP,K)
 3800    C
 3900    C  CHECK 'SIGN' OF Q2 AT J+1 LEVEL
 4000    C
 4100          IF (SGN) 60,20,80
 4200    C
 4300    C  Q2 IS NEGATIVE; SO ON OTHER (LOWER, J) SIDE OF TURNING POINT
 4400    C  EXPONENT WILL BE REAL-VALUED
 4500    C  LIMIT SIZE OF ARGUMENT OF REAL EXPONENT IF NECESSARY
 4600    C
 4700       60 IF (PH .GT. LOG(1.D10)) THEN
 4800           TEM = 1.D10
 4900           NERR = NERR + 1
 5000          ELSE
 5100           TEM = EXP(PH)
 5200          END IF
 5300    C
 5400    C  CALCULATE COEFFICIENTS ON OTHER (LOWER) SIDE OF TURNING POINT
 5500    C  USING BRIDGING CONDITIONS (CASE: EXPONENT REAL-VALUED)
 5600    C
 5700          BP(J, 1) = BP(J + 1, 1)*TEM
 5800          BP(J, 2) = BP(J + 1, 2)*TEM
 5900          AP(J, 1) = AP(J + 1, 1)/TEM - BP(J, 2)
```

```
 6000          AP(J, 2) = AP(J + 1, 2)/TEM + BP(J, 1)
 6100          GO TO 90
 6200    C
 6300    C  Q2 IS POSITIVE; SO ON OTHER (LOWER) SIDE OF TURNING POINT
 6400    C  EXPONENT WILL BE COMPLEX-VALUED
 6500    C
 6600       80  CS = COS(PH)
 6700           SN = SIN(PH)
 6800    C
 6900    C  CALCULATE COEFFICIENTS ON OTHER (LOWER) SIDE OF TURNING POINT
 7000    C  USING BRIDGING CONDITIONS (CASE: EXPONENT COMPLEX-VALUED)
 7100    C
 7200          AP(J, 1) = AP(J + 1, 1)*CS + AP(J + 1, 2)*SN
 7300          AP(J, 2) = AP(J + 1, 2)*CS - AP(J + 1, 1)*SN
 7400          BP(J, 1) = BP(J+1, 1)*CS - BP(J+1, 2)*SN + AP(J, 2)
 7500          BP(J, 2) = BP(J+1, 1)*SN + BP(J+1, 2)*CS - AP(J, 1)
 7600    C
 7700    C  UPDATE PARAMETERS FOR LOOKING BEYOND NEXT TURNING POINT
 7800    C
 7900       90 SGN = -SGN
 8000          ZP = ZI
 8100          GO TO 50
 8200    C
 8300    C  Q2 IS ZERO (INCREMENT 'NERR' COUNTER) PRINT WARNING
 8400    C
 8500       20 NERR = NERR + 1
 8600          TYPE *,'ERROR PLUS    J=', J
 8700          RETURN
 8800    C
 8900    C  TO CONSTRUCT FUNCTION 'UPLUS' FROM THE AP & BP COEFFICIENTS ...
 9000    C  UPLUS(Z) =  (AP(I + 1)*EXP(-PH) + BP(I + 1)*EXP(PH))/SQRT(Q)
 9100    C  PROVIDED A(I) < Z < A(I+1) , WHERE PH = SG * PHI(Z, A(I+1), K)
 9200    C  AND COMPLEX SG = (0,1) IF SGB*(-1)**I = -1 ELSE COMPLEX SG = (1,0)
 9300    C
 9400          END
 9500    C
 9600    C
 9700    C
 9800    C
 9900          SUBROUTINE TURN(F, B, T, A, SGB, NT, NL)
10000    C
10100    C  LOCATES EXTREMA OF F IN (B,T).  IF F INCR/DECR AT B, RETURNS
10200    C  SGB = +/-1.  RETURNS NOS. OF EXTREMA IN NT,LIST OF DEPTHS IN ARRAY A
10300    C  'EXTERNAL F' STATEMENT REQUIRED IN CALLING PROGRAM; F CAN'T BE A
10400    C  STATEMENT FUNCTION.
10500    C
10600          IMPLICIT DOUBLE PRECISION (A-H, K, O-Z)
10700          DIMENSION A(0:NL)
10800          COMMON /TEST/ EPS, NODD, NERR, NP
10900    C
11000    C  INITIALIZE
11100    C
11200          NT = 0
11300          FB = F(B)
11400          SGB = 1.D0
11500    C
11600    C  POSITION DEPTH POINTER AT MIDPOINT OF FIRST 'EPS' INTERVAL
11700    C
11800          ZI = B + EPS/2.D0
```

```
11900    C
12000    C  CALCULATE SLOPE(DER) OF FUNCTION(F) AT MIDPT. OF 1ST 'EPS' INTERVAL
12100    C
12200         5 FI = F(ZI + EPS/2.D0)
12300           DER = (FI - FB)/EPS
12400           FB = FI
12500    C
12600    C  ASSIGN A 'SIGN' TO SLOPE ON 1ST 'EPS' INTERVAL
12700    C
12800           IF (DER) 1,2,3
12900         1 SGB = -SGB
13000         3 SGN = SGB
13100    C
13200    C  INCREMENT DEPTH POINTER TO MIDPOINT OF NEXT 'EPS' INTERVAL
13300    C  (STEPPING UP FROM THE BOTTOM)
13400    C
13500         4 ZI = ZI + EPS
13600    C
13700    C  EXIT IF NEW DEPTH IS > OR = TO THE OCEAN DEPTH
13800    C
13900           IF (ZI .GE. T) RETURN
14000    C
14100    C  CALCULATE NEW SLOPE(DI) OF FUNCTION(F) AT MIDPOINT OF 'EPS' INTERVAL
14200    C
14300           FI = F(ZI + EPS/2.D0)
14400           DI = (FI - FB)/EPS
14500           IF (DI .NE. 0.D0) THEN
14600            IF (DI*SGN .LT. 0.D0) THEN
14700             IF (DER .EQ. 0.D0) THEN
14800    C
14900    C  PREVIOUS CHOICE WAS A FLAT INFLECTION POINT, DISCARD IT
15000    C
15100               NT = NT - 1
15200               SGN = -SGN
15300               NERR = NERR + 1
15400              ELSE
15500    C
15600    C  EXTREMA; USE 1ST ORDER TAYLOR EXPANSION TO REFINE Z-LOCATION
15700    C
15800               NT = NT + 1
15900               A(NT) = ZI - DI*EPS/(DI - DER)
16000               SGN = -SGN
16100              END IF
16200             END IF
16300            ELSE
16400             IF (DER .NE. 0.D0) THEN
16500    C
16600    C  EXTREMA; NO REFINING REQUIRED FOR Z-LOCATION
16700    C
16800               NT = NT + 1
16900               A(NT) = ZI
17000               SGN = -SGN
17100               ELSE
17200    C
17300    C  MOVE Z-LOCATION UP IF EXTENDED ZERO-SLOPE SECTION IN 'F'
17400    C
17500                A(NT) = A(NT) + EPS/2.D0
17600             END IF
17700            END IF
```

```
17800    C
17900    C  UPDATE SLOPE AND 'F' VALUES TO RECEIVE NEW ONES
18000    C
18100          DER = DI
18200          F8 = FI
18300          GO TO 4
18400    C
18500    C  INITIAL SLOPE IS ZERO (INCREMENT 'NERR' COUNTER) CONTINUE
18600    C
18700        2 ZI = ZI + EPS
18800          NERR = NERR + 1
18900          IF (ZI .GE. T) RETURN
19000          GO TO 5
19100          END
```

CRUSCH.FOR;2 8-SEP-1979 16:36:35.20 PAGE 1

```
      FUNCTION C(Z)
C
C  EVALUATES SPEED OF SOUND (C) IN OCEAN AT A SPECIFIED DEPTH (Z)
C  DATA FROM W. RUSCH OF SANDERS 7/30/79
C
      DOUBLE PRECISION C, CC, Z, ZZ
C
C  DEPTH (Z) IN MAIN PROGRAM IS NEGATIVE DOWN FROM WATER-AIR SURFACE
C  THIS PROGRAM REFERENCES Z POSITIVE DOWN FROM OCEAN-AIR SURFACE
C
      ZZ = -Z
C
C  BEGIN SELECTION OF SPEED OF SOUND (PIECE-WISE LINEAR)
C       THERE ARE 7 LINE SEGMENTS FOR THIS PROFILE
C
      IF (ZZ .LE. 6.D0) THEN
       C = 0.12500 * ZZ + 1465.D0
       CC = 2.6D0 * ZZ + 1446.8D0
       IF (CC .GT. C) C = CC
      ELSE IF (ZZ .LE. 10.D0) THEN
       C = 2.6D0 * ZZ + 1446.8D0
       CC = (8862.D0 - 7.D0 * ZZ) / 6.D0
       IF (CC .LT. C) C = CC
       CC = (3.D0 * ZZ + 10256.D0) / 7.D0
       IF (CC .GT. C) C = CC
      ELSE IF (ZZ .LE. 12.D0) THEN
       C = (3.D0 * ZZ + 10256.D0) / 7.D0
       CC = (21.D0 * ZZ + 29160.D0) / 20.D0
       IF (CC .GT. C) C = CC
      ELSE IF (ZZ .LE. 16.D0) THEN
       C = (21.D0 * ZZ + 29160.D0) / 20.D0
       CC = (10312.D0 - ZZ) / 7.D0
       IF (CC .LT. C) C = CC
      ELSE
       C = (10312.D0 - ZZ) / 7.D0
       CC = (8.D0 * ZZ + 13086.D0) / 9.D0
       IF (CC .GT. C) C = CC
      END IF
      RETURN
      END
```

BIMP.FOR;1 8-SEP-1979 16:36:25.97 PAGE 1

```
      SUBROUTINE Z(K, ZK)
C
C  CALCULATES BOTTOM IMPEDANCE (ZK) FROM K-VALUE AND BOTTOM PARAMETERS
C
      IMPLICIT DOUBLE PRECISION (A-H, K, O-Z)
      DIMENSION KLRT(2), KTRT(2), T(2), T1(2), ZK(2)
      COMMON /ZK/ RATRH, KL2(2), KT2(2)
C
C  PERFORM SOME INTERMEDIATE CALCULATIONS
C
      T(1) = K**2 - KL2(1)
      T(2) = -KL2(2)
      CALL CSQR(T, KLRT)
      T(1) = K**2 - KT2(1)
      T(2) = -KT2(2)
      CALL CSQR(T, KTRT)
      IF (CAB(KLRT) .LT. 1.D-6) THEN
       KLRT(1) = 1.D-6
       TYPE *, '  TOO SMALL KLRT ', K
      END IF
      T(1) = T(1) + K**2
      CALL CMUL(T, T, T1)
      CALL CMUL(KLRT, KTRT, T)
      T(1) = T1(1) - 4.D0*K**2 *T(1)
      T(2) = T1(2) - 4.D0*K**2 *T(2)
      CALL CMUL(KT2, KT2, T1)
      CALL CMUL(KLRT, T1, T1)
      CALL CDIV(T, T1, T)
C
C  CALCULATE COMPLEX IMPEDANCE (ZK(1), ZK(2))
C
      ZK(1) = RATRH * T(2)
      ZK(2) = -RATRH * T(1)
      RETURN
      END
```

```
  100   C  THIS FILE CONTAINS DELTA, ZEROS, PHI
  200   C
  300   C
  400          SUBROUTINE DELTA(K, DEL)
  500   C
  600   C  'DELTA' IS THE WRONSKIAN OF THE Z-SOLUTION FUNCTIONS
  700   C
  800          IMPLICIT DOUBLE PRECISION (A-H, K, O-Z)
  900          COMMON W, W2, B, T
 1000          COMMON /A/ A(0:6), AM(0:5, 2), BM(0:5, 2), NT, SGB
 1100          DIMENSION ZK(2),  DEL(2)
 1200          COMMON /TEST/ EP, NODD
 1300   C
 1400   C  FUNCTION STATEMENT
 1500   C
 1600          Q2(Z) = W2/C(Z)**2 - K**2
 1700   C
 1800   C  LOCATE DEPTHS OF TURNING POINTS IN ARRAY A, NUMBER OF TURNING POINTS
 1900   C  IN NT, SIGN OF Q2 AT BOTTOM IN SGB
 2000   C  [ TURNING PT. WHERE Q2(Z) = 0 = Q(Z,K)**2 = (W/C(Z))**2 - K**2 ]
 2100   C
 2200          CALL ZEROS (A,SGB,NT,K)
 2300          J = 0
 2400          ZP = B
 2500   C
 2600   C  OBTAIN BOTTOM IMPEDANCE (ZK) AT GIVEN K-VALUE
 2700   C
 2800          CALL Z(K, ZK)
 2900   C
 3000   C  ASSIGN COEFFICIENT VALUES AT THE SUBBOTTOM FROM BOUNDARY CONDITION
 3100   C  IF 'SIGN' OF Q2 AT BOTTOM (SGB) IS POSITIVE (NEGATIVE) THEN
 3200   C  QB IS REAL- (IMAGINARY-) VALUED HENCE, THE TWO FOLLOWING CASES
 3300   C
 3400          IF (SGB .LT. 0.D0) THEN
 3500           QB = SQRT(-Q2(B))
 3600           TER = QB*ZK(2)
 3700           TEI = -QB*ZK(1)
 3800           AM(0, 1) = TER - 1.D0
 3900           AM(0, 2) = TEI
 4000           BM(0, 1) = TER + 1.D0
 4100           BM(0, 2) = TEI
 4200   C
 4300   C  GO TO 3 SINCE QB IS IMAGINARY-VALUED
 4400   C
 4500           GO TO 3
 4600          ELSE
 4700           QB = SQRT(Q2(B))
 4800           TER = QB*ZK(1)
 4900           TEI = QB*ZK(2)
 5000           AM(0, 1) = TER - 1.D0
 5100           AM(0, 2) = TEI
 5200           BM(0, 1) = TER + 1.D0
 5300           BM(0, 2) = TEI
 5400   C
 5500   C  GO TO 4 SINCE QB IS REAL-VALUED
 5600   C
 5700          END IF
 5800   C
 5900   C  CHECK IF STEPPED PAST ALL TURNING POINTS
```

```
 6000    C
 6100        4  IF (J .GE. NT) THEN
 6200    C
 6300    C  PHI INTEGRATES ABS(Q) FROM LAST TURNING PT. TO TOP AT GIVEN K-VALUE
 6400    C
 6500            PH = PHI(ZP,T,K)
 6600    C
 6700    C  INTERMEDIATE CALCULATIONS PRIOR TO EXITING SUBROUTINE
 6800    C
 6900            CS = COS(PH)
 7000            SN = SIN(PH)
 7100            DEL(1) = AM(J, 1)*CS - AM(J, 2)*SN + BM(J, 1)*CS + BM(J, 2)*SN
 7200            DEL(2) = (AM(J, 2) + BM(J, 2))*CS + (AM(J, 1) - BM(J, 1))*SN
 7300            GO TO 5
 7400           ELSE
 7500    C
 7600    C  OBTAIN NEW TURNING POINT DEPTH (STEPPING UP FROM BOTTOM)
 7700    C
 7800            J = J + 1
 7900            ZI = A(J)
 8000    C
 8100    C  PHI INTEGRATES ABS(Q) FROM PREVIOUS TO CURRENT TURNING PT. DEPTH
 8200    C
 8300            PH = PHI(ZP,ZI,K)
 8400    C
 8500    C  CALCULATE COEFFICIENTS AM & BM (CASE: Q IS IMAGINARY-VALUED)
 8600    C
 8700            CS = COS(PH)
 8800            SN = SIN(PH)
 8900            BM(J, 1) = BM(J-1, 1)*CS + BM(J-1, 2)*SN
 9000            BM(J, 2) = BM(J-1, 2)*CS - BM(J-1, 1)*SN
 9100            AM(J, 1) = AM(J-1, 1)*CS - AM(J-1, 2)*SN + BM(J, 2)
 9200            AM(J, 2) = AM(J-1, 2)*CS + AM(J-1, 1)*SN - BM(J, 1)
 9300            ZP = ZI
 9400           END IF
 9500    C
 9600    C  CHECK IF STEPPED PASSED ALL TURNING POINTS
 9700    C
 9800        3 IF (J .GE. NT) THEN
 9900    C
10000    C  PHI INTEGRATES ABS(Q) FROM LAST TURNING POINT TO THE TOP
10100    C
10200            PH = PHI(ZP,T,K)
10300    C
10400    C  LIMIT SIZE OF ARGUMENT FOR REAL EXPONENT
10500    C
10600            IF (PH .GE. LOG(1.010)) THEN
10700             TEM = 1.010
10800             NODD = NODD + 1
10900            ELSE
11000             TEM = EXP(PH)
11100            END IF
11200    C
11300    C  INTERMEDIATE CALCULATIONS PRIOR TO EXITING SUBROUTINE
11400    C
11500            DEL(1) = AM(J, 1)*TEM + BM(J, 1)/TEM
11600            DEL(2) = AM(J, 2)*TEM + BM(J, 2)/TEM
11700            GO TO 5
11800           ELSE
```

```
11900    C
12000    C  OBTAIN NEW TURNING POINT DEPTH (STEPPING UP FROM BOTTOM)
12100    C
12200          J = J + 1
12300          ZI = A(J)
12400    C
12500    C  PHI INTEGRATES ABS(Q) FROM PREVIOUS TO CURRENT TURNING PT. DEPTH
12600    C
12700          PH = PHI(ZP,ZI,K)
12800    C
12900    C  LIMIT SIZE OF ARGUMENT FOR REAL EXPONENT
13000    C
13100          IF (PH .GE. LOG(1.D10)) THEN
13200           TEM = 1.D10
13300           NODD = NODD + 1
13400          ELSE
13500           TEM = EXP(PH)
13600          END IF
13700    C
13800    C  CALCULATE COEFFICIENTS AM & BM (CASE: Q IS REAL-VALUED)
13900    C
14000          AM(J, 1) = AM(J-1, 1)*TEM
14100          AM(J, 2) = AM(J-1, 2)*TEM
14200          BM(J, 1) = BM(J-1, 1)/TEM - AM(J, 2)
14300          BM(J, 2) = BM(J-1, 2)/TEM + AM(J, 1)
14400          ZP = ZI
14500         END IF
14600         GO TO 4
14700    C
14800    C  CALCULATE COMPLEX 'DELTA' (DEL(1), DEL(2)) AND RETURN
14900    C
15000       5 TEM = DEL(1)
15100         DEL(1) = 2.D0*DEL(2)
15200         DEL(2) = -2.D0*TEM
15300         RETURN
15400    C
15500    C  TO CONSTRUCT FUNCTION 'DELTA' FROM THE AM & BM COEFFICIENTS ...
15600    C  UMINUS = (AM(I)*EXP(SG*PH)+ BM(I)*EXP(-SG*PH))/SQRT(Q) IF A(I) < Z < A(I + 1
15700    C  WHERE PH = PHI(A(I),Z,K), SG = (0, 1) IF Q2(Z)<0. ELSE SG = (1, 0)
15800    C  1/SQRT(Q) = SQRT(SG)/SQRT(SQRT(ABS(Q2))).  WHERE Q2 = Q**2
15900    C  IF Q2(Z) = 0 (UMINUS IS SINGULAR), THEN SET UMINUS = 0.
16000    C
16100         END
16200    C
16300    C
16400    C
16500    C
16600         SUBROUTINE ZEROS (A,SGB,NT,K)
16700    C
16800    C  LOCATES ZEROS OF Q2 IN (B,T).  BOTTOM ZEROS AND EXTENDED ZEROS
16900    C  IGNORED.   RETURNS SGB = +1 IF Q2(B) STARTS NONNEGATIVE. RETURNS
17000    C  NUMBER OF ZEROS IN NT, LIST OF DEPTH OF ZEROS IN ARRAY A.
17100    C  (ZERO OF Q2 AT GIVEN K-VALUE IS A 'TURNING POINT')  Q2 = Q**2
17200    C  NEED DIMENSION STATEMENT IN MAIN FOR 1ST ARGUMENT.
17300    C
17400         IMPLICIT DOUBLE PRECISION (A-H, K, O-Z)
17500         DIMENSION A(0:6)
17600         COMMON W,W2,B,T /TEST/ EP,NER,NODD,NP
17700         PARAMETER EPS = 0.1D0
```

```
17800    C
17900    C  STATEMENT FUNCTION
18000    C
18100          Q2(Z) = W2/C(Z)**2 - K**2
18200    C
18300    C  INITIALIZE
18400    C
18500          NT = 0
18600          ZI = B
18700          A(0) = B
18800          SGB = 1.D0
18900    C
19000    C  OBTAIN 'SIGN' OF Q2 AT BOTTOM (SGB)
19100    C
19200       4  QB = Q2(ZI)
19300          IF (QB) 1,2,3
19400       1  SGB = -SGB
19500       3  SGN = SGB
19600    C
19700    C  INCREMENT DEPTH POINTER (STEPPING UP FROM BOTTOM)
19800    C
19900       8  ZI = ZI + EPS
20000    C
20100    C  EXIT IF NEW DEPTH IS > OR = TO OCEAN DEPTH
20200    C
20300          IF (ZI .GE. T) THEN
20400           A(NT + 1) = T
20500           RETURN
20600          END IF
20700    C
20800    C  Q2 AT NEW DEPTH
20900    C
21000          QI = Q2(ZI)
21100    C
21200    C  IF Q2 CHANGES SIGN THEN HAVE FOUND A TURNING POINT
21300    C  USE LINEAR INTERPOLATION TO REFINE DEPTH VALUE
21400    C  STORE IN ARRAY A
21500    C
21600          IF (QI*SGN .LT. 0.D0) THEN
21700           NT = NT + 1
21800           A(NT) = ZI - QI*EPS/(QI - QB)
21900           SGN = -SGN
22000          END IF
22100          QB = QI
22200          GO TO 8
22300    C
22400    C  INITIAL Q2 IS ZERO (INCREMENT 'NODD' COUNTER)
22500    C
22600       2  ZI = ZI + EPS
22700          NODD = NODD + 1
22800          IF (ZI .GE. T) THEN
22900           A(NT + 1) = T
23000           RETURN
23100          END IF
23200          GO TO 4
23300          END
23400    C
23500    C
23600    C
```

```
23700    C
23800          FUNCTION PHI(Z1,Z2,K)
23900    C
24000    C  INTEGRATES ABS(Q(Z,K)) FROM Z1 TO Z2.  IGNORES REGIONS BEYOND SIGN CHANGES.
24100    C
24200          IMPLICIT DOUBLE PRECISION (A-H, K, O-Z)
24300          COMMON W,W2,B,T /TEST/ EP,NER,NO,NODD
24400          PARAMETER EPS = 0.100
24500    C
24600    C  STATEMENT FUNCTION
24700    C
24800          Q2(Z) = W2/C(Z)**2 - K**2
24900    C
25000    C  INITIALIZE
25100    C
25200          PHI = 0.D0
25300          SGN = 1.D0
25400          NI = Z1/EPS
25500          NF = Z2/EPS
25600    C
25700    C  'SIGN' OF Q2BAR INDICATES 'SIGN' OF Q2 ON INTERVAL (Z1, Z2)
25800    C
25900          Q2BAR = Q2((Z1 + Z2)/2.D0)
26000        4 ZI = (NI + 0.5D0) * EPS
26100          IF (Q2BAR) 1, 2, 3
26200        1 SGN = -SGN
26300        3 CONTINUE
26400    C
26500    C  LOOP TO SUM HEIGHTS AT MIDPOINTS OF PARTITIONS
26600    C
26700          DO 9 I = NI, NF
26800    C
26900    C  PLACE DEPTH POINTER AT MIDPOINT OF PARTITION
27000    C
27100          ZI = (I + 0.5D0) * EPS
27200    C
27300    C  EXIT IF REACHED END OF INTERVAL
27400    C
27500          IF (ZI .GT. Z2) GO TO 10
27600          QT = Q2(ZI)*SGN
27700          IF (QT .GT. 0.D0) THEN
27800           PHI = PHI + SQRT(QT)
27900          ELSE
28000           NODD = NODD + 1
28100          END IF
28200        9 CONTINUE
28300    C
28400    C  AREA CALCULATION
28500    C
28600       10  PHI = PHI*EPS
28700          RETURN
28800    C
28900    C  Q2BAR = 0, SELECT NEW Q2BAR (INCREMENT 'NODD' COUNTER)
29000    C
29100        2 Q2BAR = Q2(ZI)
29200          NODD = NODD + 1
29300          IF (ZI .GT. Z2) RETURN
29400          NI = NI + 1
29500          GO TO 4
29600          END
```

APPENDIX IIIh

PLOT.FOR

The next four pages constitute the program that reads the data file written by GENER.FOR, calculates the Green's function, calculates the transmission loss and phase from this value, and prints a plot of the results in the format specified in the data file written by INPUT.FOR.

The following eight pages contain support subroutines for the main part of PLOT.FOR.

```
PLOT.FOR;2                          8-SEP-1979 16:35:19.57          PAGE 1

  100   C  THIS FILE ALSO CONTAINS GREEN, YOU, PHI
  200   C  AFTER CHANGES, RECOMPILE AND LINK SPECIFYING
  300   C  LINK PLOT+CARITH+'C'  WHERE FILE 'C'.OBJ IS FUNCTION C(Z)
  400   C
  500   C  THIS IS THE PLOTTING PROGRAM
  600   C
  700         IMPLICIT DOUBLE PRECISION (A - H, K, O - Z)
  800         CHARACTER*1 PLOTTYP, PLOTDAT
  900         COMMON W, W2, B, T /FLAG/ IFLAG /PARAM/ N9, N17
 1000         DIMENSION RNUM(10), RWIDTH(10), RD(10), GRN(2)
 1100         READ *, N9, N16, N17
 1200         OPEN (UNIT=N9,READONLY,TYPE='OLD',FORM='UNFORMATTED',SHARED)
 1300         OPEN (UNIT = N16, TYPE = 'SCRATCH', FORM = 'UNFORMATTED')
 1400         OPEN (UNIT = N17, TYPE = 'SCRATCH', FORM = 'UNFORMATTED')
 1500         OPEN (UNIT = 20, READ ONLY, TYPE = 'OLD', SHARED)
 1600   C
 1700   C  INITIALIZE
 1800   C
 1900         NCASE = 0
 2000         PI = 4.D0 * ATAN(1.D0)
 2100   C
 2200   C  READ INPUT DATA FROM UNFORMATTTED FILE; SOURCE FREQUENCY,
 2300   C  BOTTTOM PARAMETERS, AND OCEAN DEPTH
 2400   C
 2500         READ (20, 200) W, W2, IBOT, RATRH, CL, CT, BL, BT
 2600     200 FORMAT (3X, G30.15, 9X, G30.15, / 12X, I3, 25X, G30.15,/
 2700        2  4X, G30.15, 8X, G30.15, /4X, G30.15, 8X, G30.15)
 2800         READ (20, 201) B, T
 2900     201 FORMAT (3X, G30.15, 8X, G30.15)
 3000   C
 3100   C  KREF IS REFERENCE K-VALUE TO RID PHASE OF FUNDAMENTAL PERIODICITY
 3200   C  ASSOCIATED WITH SOURCE FREQUENCY; ARBITRARILY CHOOSE C(AT TOP)
 3300   C  TO DETERMINE THIS KREF-VALUE
 3400   C
 3500         KREF = W/C(T)
 3600         TYPE *, '  KREF', KREF
 3700   C
 3800   C  SEARCH FILE FOR THE APPROPRIATE TYPE OF DATA DESIRED FOR PLOT
 3900   C
 4000         READ *, PLOTTYP
 4100         TYPE *, '  PLOT TYPE ', PLOTTYP
 4200      14 READ (20, 215, END = 13) PLOTDAT
 4300     215 FORMAT (X, A1)
 4400         IF (PLOTDAT .EQ. PLOTTYP) GO TO 11
 4500         GO TO 14
 4600      13 TYPE *, '  PLOTTYP NOT IN DATA FILE'
 4700         STOP
 4800      11 CONTINUE
 4900   C
 5000   C  READ RECEIVER-ARRAY TYPE FROM FILE
 5100   C
 5200         READ (20, 205) IRTYP
 5300     205 FORMAT (10X, I6)
 5400         IF (IRTYP .NE. 1) GO TO 40
 5500   C
 5600   C  READ RANGE DATA FOR RECEIVER-ARRAY TYPE #1
 5700   C
 5800         READ (20, 203) RMIN, RMAX, RDEL
 5900     203 FORMAT (9X, G30.15, 5X, G30.15, 5X,  G30.15)
```

```
 6000          GO TO 30
 6100       40 IF (IRTYP .NE. 2) GO TO 50
 6200    C
 6300    C  READ RANGE DATA FOR RECEIVER-ARRAY TYPE #2
 6400    C
 6500          READ (20, 204) RMN, RMX, RSP, RWID, RDEL
 6600      204 FORMAT(8X, G30.15,4X, G30.15/8X, G30.15, 7X, G30.15, 5X, G30.15)
 6700          RMNS = RMN
 6800          RMIN = RMN
 6900          RMAX = RMIN + RWID
 7000          GO TO 30
 7100       50 IF (IRTYP .NE. 3) STOP
 7200    C
 7300    C  READ RANGE DATA FOR RECEIVER-ARRAY TYPE #3
 7400    C
 7500          READ (20, 212) NUMRG
 7600      212 FORMAT (22X, I6)
 7700          DO 5 NCASE = 1, NUMRG
 7800          READ (20, 211) N1, R2, R3, R4
 7900      211 FORMAT (10X, I6, 25X, G30.15/ 11X, G30.15, 5X, G30.15)
 8000          IF (N1 .NE. NCASE) STOP
 8100          RNOW(NCASE) = R2
 8200          RWIDTH(NCASE) = R3
 8300          RD(NCASE) = R4
 8400        5 CONTINUE
 8500          NCASE = 1
 8600          RMIN = RNOW(NCASE)
 8700          RMAX = RMIN + RWIDTH(NCASE)
 8800          RDEL = RD(NCASE)
 8900          GO TO 30
 9000    C
 9100    C ALTERNATE ARRAY TYPE DATA TO BE READ IN HERE
 9200    C
 9300    C  READ NUMBER OF SOURCE AND RECEIVER DEPTH COMBINATIONS DESIRED
 9400    C
 9500       30 READ (20, 208) ITZ
 9600      208 FORMAT (8X, I6)
 9700    C
 9800    C  READ NEXT SOURCE AND RECEIVER DEPTH CASE
 9900    C
10000        2 READ (20, 202) IT, ZS, ZR
10100      202 FORMAT (7X, I3, 8X, G30.15, 3X, G30.15)
10200    C
10300    C  PRINT HEADING FOR PLOT
10400    C
10500          WRITE (6,101) B,T,ZS,ZR,IBOT,RMIN,RMAX,RDEL
10600      101 FORMAT (1H1/' SOUND PROPAGATION'/'  BOTTOM Z =', 1PG14.4,
10700         2   2X, ' TOP Z =', G14.4, 2X, 'SOURCE Z = ', G14.4,
10800         3   ' RECEIVER Z = ', G14.4/ '  BOTTOM TYPE # ', I2, 2X,
10900         4   ' SMALLEST SEPARATION DISTANCE = '
11000         5   G14.4, 2X, 'LARGEST DISTANCE =', G14.4, 2X,
11100         6   'RANGE INCREMENT =', G14.4// 4X, 10HR (METERS), 29X,
11200         7   11HAMPL G (DB), 45X, 5HARG G / 17X, 4H.-30, 58(1H.), 6H0..-PI,
11300         8   16(1H.), 1H0, 16(1H.), 4H+PI.)
11400    C
11500    C  INITIALIZE
11600    C
11700       90 REWIND N16
11800          XNOR = 0.00
```

```
11900          IFLAG = 0
12000    C
12100    C  LOOP THROUGH THE SOURCE-RECEIVER HORIZONTAL SEPARATION RANGE
12200    C
12300          DO 1 R = RMIN, RMAX, RDEL
12400          REWIND N9
12500    C
12600    C  EVALUATE COMPLEX GREEN'S FUNCTION (GRN(1), GRN(2))
12700    C
12800          CALL GREEN(ZS, ZR, R, GRN)
12900          IFLAG = 1
13000    C
13100    C  CALCULATE ABSOLUTE VALUE OF AMPLITUDE (XG)
13200    C
13300          XG = CAB(GRN)
13400    C
13500    C  CALCULATE PHASE (PH) ON INTERVAL (-180, +180) IN DEGREES
13600    C
13700          IF (ABS(GRN(1)) .LT. 1.D-10) THEN
13800           PH = 90.D0
13900          ELSE
14000           PH = ATAN(GRN(2)/GRN(1))*180.D0/PI
14100          END IF
14200          IF (GRN(1) .LT. 0.D0) THEN
14300           IF (GRN(2) .GE. 0.D0) THEN
14400            PH = PH + 180.D0
14500           ELSE
14600            PH = PH - 180.D0
14700           END IF
14800          END IF
14900    C
15000    C  RID THE PHASE POINT OF ITS FUNDAMENTAL FREQUENCY COMPONENT ...
15100    C  THAT IS; THE FREQ. OF THE SOURCE
15200    C
15300          PH = PH + KREF*R*180.D0/PI
15400          NPI = PH/360.D0 + 0.5D0
15500          PH = PH - NPI*360.D0
15600    C
15700    C  WRITE AMPLITUDE AND PHASE DATA POINTS INTO TEMPORARY FILE;
15800    C  KEEP LARGEST VALUE OF AMPLITUDE (XG) IN VARIABLE 'XNOR'
15900    C
16000          WRITE (N16) XG, PH
16100          IF (XG .GT. XNOR) XNOR = XG
16200        1 CONTINUE
16300    C
16400    C  SET SCALE FACTOR (XNOR) FOR DECIBEL AMPLITUDE
16500    C
16600          NOR = 5.D0 * LOG10(XNOR) + 0.6D0
16700          XNOR = NOR
16800          XNOR = 10.D0**(XNOR/5.D0)
16900          REWIND N16
17000    C
17100    C  LOOP TO PLOT POINTS FOR EACH SEPARATION DISTANCE ON RANGE
17200    C
17300          DO 4 R = RMIN,RMAX,RDEL
17400          READ (N16) XG, PH
17500    C
17600    C  SCALE AMPLITUDE DATA POINT (IN DECIBEL SCALE)
17700    C
```

```
17800          NX = 10.D0 * LOG10(XG)
17900          NX = NX + 60 - 2*NOR
18000          IF (NX .LT. 0) NX = 0
18100          NX = NX + 1
18200    C
18300    C  SCALE PHASE DATA POINT (IN LINEAR SCALE)
18400    C
18500          NY = PH/10.D0
18600          NY = NY + 19
18700    C
18800    C  PRINT A LINE OF PLOT; R VALUE, AMPLITUDE, PHASE, AND PLOT EDGES
18900    C
19000          WRITE (6,100) R
19100          WRITE (6, 103)
19200        4 CONTINUE
19300      100 FORMAT (1X, 1PG15.5, X, 1H:, <NX>X, 1H*, <62 - NX>X, 1H:,
19400         2     <NY>X, 1H*, <38 - NY>X, 1H:)
19500      103  FORMAT (1H+, 78X, 1H., 21X, 1H.)
19600    C
19700    C  WRITE THE NORMALIZATION FOR THE PLOT
19800    C
19900          WRITE (6,102) XNOR
20000      102  FORMAT (17X, 4H:-30, 58(1H.), 6H0.:-PI, 16(1H.), 1H0, 16(1H.),
20100         2     4H+PI:/ 20X, 5(1H1), '   PLOT NORMALIZED TO ',
20200         3     1PG10.1, 3X, 5(1H1))
20300    C
20400    C  OBTAIN NEXT SOURCE-RECEIVER HORIZONTAL SEPARATION RANGE ACCORDING
20500    C  TO THE RECEIVER ARRAY TYPE
20600    C
20700          IF (IRTYP .EQ. 1) GO TO 70
20800          IF (IRTYP .NE. 2) GO TO 85
20900          RMN = RMN + RSP
21000          IF (RMN .LE. RMX) GO TO 80
21100          RMN = RMNS
21200          RMIN = RMN
21300          RMAX = RMIN + RWID
21400          GO TO 70
21500       85 IF (IRTYP .NE. 3) STOP
21600          IF (NCASE .GE. NUMRG) NCASE = 0
21700          NCASE = NCASE + 1
21800          RMN = RNOW(NCASE)
21900          RWID = RWIDTH(NCASE)
22000          RDEL = RD(NCASE)
22100       80 RMIN = RMN
22200          RMAX = RMIN + RWID
22300          IF (NCASE .EQ. 1) GO TO 70
22400          WRITE (6, 110) IBOT, RMIN, RMAX, RDEL
22500      110 FORMAT (1H1/ '  BOTTOM TYPE # ', I2, 2X,
22600         4    ' SMALLEST SEPARATION DISTANCE = '
22700         5    G14.4, 2X, 'LARGEST DISTANCE =', G14.4, 2X,
22800         6    'RANGE INCREMENT =', G14.4// 4X, 10HR (METERS), 29X,
22900         7    11HAMPL G (DB), 45X, 5HARG G / 17X, 4H.-30, 58(1H.), 6H0..-PI,
23000         8    16(1H.), 1H0, 16(1H.), 4H+PI.)
23100          GO TO 90
23200    C
23300    C  OBTAIN NEXT SOURCE AND RECEIVER DEPTHS
23400    C
23500       70 ITZ = ITZ - 1
23600    C
```

```
23700    C  NEXT LINE IS CONDITION TO STOP RUNNING OF PLOTTING PROGRAM
23800    C
23900           IF (ITZ .LE. 0) STOP
24000    C
24100    C  CONTINUE
24200    C
24300           GO TO 2
24400           END
24500    C
24600    C
24700    C
24800    C
24900           SUBROUTINE GREEN (ZS, ZR, R, GRN)
25000    C
25100    C  THIS SUBROUTINE EVALUATES THE GREEN'S FUNCTION FOR GIVEN SEPARATION
25200    C  DISTANCE (R)
25300    C
25400           IMPLICIT DOUBLE PRECISION (A - H, K, O - Z)
25500           DIMENSION COEF(2), DER(2), GRN(2), HANK2(2), KI(2)
25600           DIMENSION UU(2), XPON(2)
25700           COMMON /FLAG/ IFLAG /PARAM/ N9, N17
25800    C
25900    C  INITIALIZE
26000    C
26100           PI = 4.D0 * ATAN(1.D0)
26200           GRN(1) = 0.D0
26300           GRN(2) = 0.D0
26400    C
26500    C  AFTER CALLING 'YOU' FOR A GIVEN SOURCE AND RECEIVER DEPTH THEN
26600    C  NO NEED TO CALL IT AGAIN UNTIL A NEW S AND R DEPTH COMBINATION
26700    C
26800           IF (IFLAG .EQ. 1) GO TO 2
26900           CALL YOU(ZS, ZR, NK)
27000         2 REWIND N17
27100    C
27200    C  SUM THE CONTRIBUTION OF EACH EIGENMODE TO THE GREEN'S FUNCTION
27300    C
27400           DO 1 IK = 1, NK
27500           READ (N17) KI, DER, UU
27600           COEF(1) = 2.D0/(PI * R)
27700           COEF(2) = 0.D0
27800           CALL CDIV(COEF, KI, COEF)
27900           CALL CSQR(COEF, COEF)
28000           XPON(1) = EXP(KI(2)*R) * COS(KI(1)*R + PI/4.D0)
28100           XPON(2) = EXP(KI(2)*R) * (-SIN(KI(1)*R + PI/4.D0))
28200           CALL CMUL(COEF, XPON, HANK2)
28300           HANKT = HANK2(1)
28400    C
28500    C  EVALUATE COMPLEX HANKEL(2) FUNCTION (HANK2(1), HANK2(2))
28600    C
28700           HANK2(1) = -HANK2(2)
28800           HANK2(2) = HANKT
28900    C
29000           CALL CMUL(HANK2, UU, UU)
29100           CALL CMUL(UU, KI, KI)
29200           CALL CDIV(KI, DER, DER)
29300           DER(1) = DER(1)/2.D0
29400           DER(2) = DER(2)/2.D0
29500    C
```

```
29600    C  GREEN'S FUNCTION PRESENTLY IS: (GRN(1), GRN(2))
29700    C
29800          GRN(1) = GRN(1) - DER(1)
29900          GRN(2) = GRN(2) - DER(2)
30000    C
30100    C  PROCEED TO OBTAIN GREEN'S FUNCTION WITH ONE MORE EIGENMODE
30200    C  CONTRIBUTION; PROVIDED ANOTHER EIGENVALUE EXISTS
30300    C
30400         1 CONTINUE
30500           RETURN
30600           END
30700    C
30800    C
30900    C
31000    C
31100          SUBROUTINE YOU(ZS, ZR, J)
31200    C
31300    C  THIS SUBROUTINE EVALUATES 'UMINUS' FROM AM & BM COEFFICIENTS
31400    C  GENERATED IN SUBROUTINE DELTA, EVALUATES 'UPLUS' FROM AP & BP
31500    C  COEFFICIENTS GENERATED IN SUBROUTINE PLUS, AND ASSEMBLES
31600    C  THEIR PRODUCT IN ARRAY 'UU'
31700    C
31800          IMPLICIT DOUBLE PRECISION (A - H, K, O - Z)
31900          DIMENSION D(2), DER(2), KI(2), TE(2), UMIN(2), UPL(2), UU(2)
32000          COMMON W, W2, B, T /A/ P(0:6), AM(0:5,2), BM(0:5,2), NT, SGB
32100          COMMON /PLUS/ AP(0:5,2), BP(0:5,2) /PARAM/ N9, N17
32200    C
32300    C  STATEMENT FUNCTION
32400    C
32500          G2(Z) = W2/C(Z)**2 - K**2
32600    C
32700    C  INITIALIZE
32800    C
32900          REWIND N17
33000          IK = 0
33100    C
33200    C  LOOP UNTIL 'IK' EQUALS THE NUMBER OF EIGENVALUES
33300    C
33400         3 IK = IK + 1
33500    C
33600    C  READ NEXT EIGENMODE DATA LIST
33700    C  EXIT FROM SUBROUTINE 'YOU' IF AT END OF FILE 'N9'; GO TO LABEL '5'
33800    C
33900          READ (N9, END = 5) J, K, KI, NDEL, D, DER, (P(ID), ID = 0,
34000         2     NDEL + 1), ((AM(ID, JD), JD = 1, 2), (BM(ID, JD), JD = 1, 2),
34100         3     (AP(ID, JD), JD = 1, 2), (BP(ID, JD), JD = 1, 2),
34200         4     ID = 0, NDEL)
34300    C
34400    C  IF 'J' IS NOT EQUAL 'IK' THEN SOMETHING IS WRONG; ABORT JOB
34500    C
34600          IF (J .NE. IK) GO TO 4
34700    C
34800    C  BEGIN 'K' WITH THE REAL PART OF THE COMPLEX EIGENVALUE (KI)
34900    C
35000          K = KI(1)
35100    C
35200    C  IF EITHER G2(ZS) OR G2(ZR) IS ZERO (SINGULARITY) THEN SET 'UU' TO 0
35300    C
35400          IF (G2(ZS)*G2(ZR) .NE. 0.D0) GO TO 20
```

```
35500          UU(1) = 0.D0
35600          UU(2) = 0.D0
35700          GO TO 30
35800    C
35900    C  FIX SO 'ZS' IS ALWAYS 'LOWER' THAN 'ZR'
36000    C  (RECIPROCITY THEOREM; HORIZONTAL BOTTOM INTERFACE)
36100    C
36200      20  IF (ZR .LT. ZS) THEN
36300           ZD = ZR
36400           ZR = ZS
36500           ZS = ZD
36600          END IF
36700    C
36800    C  FIND REGION OF ZS (LOWER)
36900    C
37000          I = 1
37100        1 IF (P(I) .LE. ZS) THEN
37200           I = I + 1
37300           GO TO 1
37400          END IF
37500    C
37600    C  EVALUATE COMPLEX 'UMINUS' FUNCTION  (UMIN(1), UMIN(2))
37700    C
37800          IS = I - 1
37900          PH = PHI(P(IS),ZS,K)
38000          TQ = Q2(ZS)
39100          IF (TQ .LT. 0.D0) THEN
38200    C
38300    C  IF EXPONENT IS COMPLEX-VALUED THEN ...
38400    C
38500           CS = COS(PH)
38600           SN = SIN(PH)
38700           UMIN(1) = AM(IS, 1)*CS - AM(IS, 2)*SN
38800          2          + BM(IS, 1)*CS + BM(IS, 2)*SN
39900           UMIN(2) = AM(IS, 2)*CS + AM(IS, 1)*SN
39000          2          + BM(IS, 2)*CS - BM(IS, 1)*SN
39100           TE(1) = 0.D0
39200           TE(2) = 1.D0/SQRT(-TQ)
39300           CALL CSQR(TE, TE)
39400    C
39500    C  CALCULATE 'UMINUS'  (IN 'UMIN' ARRAY)
39600    C
39700           CALL CMUL(UMIN, TE, UMIN)
39800          ELSE
39900    C
40000    C  IF EXPONENT IS REAL-VALUED THEN ...
40100    C  (AND LIMIT SIZE OF ARGUMENT OF REAL EXPONENT IF NECESSARY)
40200    C
40300           IF (PH .GT. LOG(1.D10)) THEN
40400            TEM = 1.D10
40500            NODD = NODD + 1
40600           ELSE
40700            TEM = EXP(PH)
40800           END IF
40900    C
41000    C  CALCULATE 'UMINUS'  (IN 'UMIN' ARRAY)
41100    C
41200           UMIN(1) = (AM(IS, 1)*TEM + BM(IS, 1)/TEM)/ SQRT(SQRT(TQ))
41300           UMIN(2) = (AM(IS, 2)*TEM + BM(IS, 2)/TEM)/ SQRT(SQRT(TQ))
```

```
41400          END IF
41500    C
41600    C  FIND REGION OF ZR (HIGHER)
41700    C
41800          I = IS
41900       2  IF (P(I) .LE. ZR) THEN
42000           I = I + 1
42100           GO TO 2
42200          END IF
42300    C
42400    C  EVALUATE COMPLEX 'UPLUS' FUNCTION  (UPL(1), UPL(2))
42500    C
42600          PH = PHI(ZR,P(I),K)
42700          I = I - 1
42800          TQ = G2(ZR)
42900          IF (TQ .LT. 0.D0) THEN
43000    C
43100    C  IF EXPONENT IS COMPLEX-VALUED THEN ...
43200    C
43300           CS = COS(PH)
43400           SN = SIN(PH)
43500           UPL(1) = AP(I, 1)*CS - AP(I, 2)*SN
43600         2        + BP(I, 1)*CS + BP(I, 2)*SN
43700           UPL(2) = AP(I, 2)*CS + AP(I, 1)*SN
43800         2        + BP(I, 2)*CS - BP(I, 1)*SN
43900           TE(1) = 0.D0
44000           TE(2) = 1.D0/SQRT(-TQ)
44100           CALL CSQR(TE, TE)
44200    C
44300    C  CALCULATE 'UPLUS'  (IN 'UPL' ARRAY)
44400    C
44500           CALL CMUL(UPL, TE, UPL)
44600          ELSE
44700    C
44800    C  IF EXPONENT IS REAL-VALUED THEN ...
44900    C  (AND LIMIT SIZE OF ARGUMENT OF REAL EXPONENT IF NECESSARY)
45000    C
45100           IF (PH .GT. LOG(1.D10)) THEN
45200            TEM = 1.D10
45300            NODD = NODD + 1
45400           ELSE
45500            TEM = EXP(PH)
45600           END IF
45700    C
45800    C  CALCULATE 'UPLUS'  (IN 'UPL' ARRAY)
45900    C
46000           UPL(1) = (AP(I, 1)/TEM + BP(I, 1)*TEM)/ SQRT(SQRT(TQ))
46100           UPL(2) = (AP(I, 2)/TEM + BP(I, 2)*TEM)/ SQRT(SQRT(TQ))
46200          END IF
46300    C
46400    C  MULTIPLY 'UMINUS' WITH 'UPLUS' , WRITE INTO TEMPORARY FILE,
46500    C  AND GO BACK FOR ANOTHER CALCULATION IF ANOTHER EIGENVALUE EXISTS
46600    C
46700          CALL CMUL(UMIN, UPL, UU)
46800       30 WRITE (N17) KI, DER, UU
46900          GO TO 3
47000    C
47100    C  SOMETHING IS INCONSISTANT; ABORT THE JOB
47200    C
```

```
47300        4 TYPE *, 'FILE NK .NE. IK'
47400          STOP
47500        5 RETURN
47600          END
47700    C
47800    C
47900    C
48000    C
48100          FUNCTION PHI(Z1,Z2,K)
48200    C
48300    C  INTEGRATES ABS(Q(Z,K)) FROM Z1 TO Z2.  IGNORES REGIONS BEYOND SIGN CHANGES.
48400    C
48500          IMPLICIT DOUBLE PRECISION (A-H, K, O-Z)
48600          COMMON W, W2, B, T /TEST/ EP, NER, NO, NODD
48700          PARAMETER EPS = 0.1D0
48800    C
48900    C  STATEMENT FUNCTION
49000    C
49100          Q2(Z) = W2/C(Z)**2 - K**2
49200    C
49300    C  INITIALIZE
49400    C
49500          PHI = 0.D0
49600          SGN = 1.D0
49700          NI = Z1/EPS
49800          NF = Z2/EPS
49900    C
50000    C  'SIGN' OF Q2BAR INDICATES 'SIGN' OF Q2 ON INTERVAL (Z1, Z2)
50100    C
50200          Q2BAR = Q2((Z1 + Z2)/2.D0)
50300        4 ZI = (NI + 0.5D0) * EPS
50400          IF (Q2BAR) 1, 2, 3
50500        1 SGN = -SGN
50600        3 CONTINUE
50700    C
50800    C  LOOP TO SUM HEIGHTS AT MIDPOINTS OF PARTITIONS
50900    C
51000          DO 9 I = NI, NF
51100    C
51200    C  PLACE DEPTH POINTER AT MIDPOINT OF PARTITION
51300    C
51400          ZI = (I + 0.5D0) * EPS
51500    C
51600    C  EXIT IF REACHED END OF INTERVAL
51700    C
51800          IF (ZI .GT. Z2) GO TO 10
51900          QT = Q2(ZI)*SGN
52000          IF (QT .GT. 0.D0) THEN
52100           PHI = PHI + SQRT(QT)
52200          ELSE
52300           NODD = NODD + 1
52400          END IF
52500        9 CONTINUE
52600    C
52700    C  AREA CALCULATION
52800    C
52900       10  PHI = PHI*EPS
53000          RETURN
53100    C
```

```
53200    C  Q2BAR = 0, SELECT NEW Q2BAR (INCREMENT 'NODD' COUNTER)
53300    C
53400         2 Q2BAR = Q2(ZI)
53500           NODD = NODD + 1
53600           IF (ZI .GT. Z2) RETURN
53700           NI = NI + 1
53800           GO TO 4
53900           END
```

CARITH.FOR;1 8-SEP-1979 16:36:29.08 PAGE 1

```
  100          FUNCTION CAB(A)
  200    C
  300    C  DOUBLE PRECISION COMPLEX-VALUED ABSOLUTE VALUE ROUTINE
  400    C
  500          IMPLICIT DOUBLE PRECISION (A-C)
  600          DIMENSION A(2)
  700          CAB = SQRT(A(1)**2 + A(2)**2)
  800          RETURN
  900          END
 1000    C
 1100    C
 1200    C
 1300    C
 1400          SUBROUTINE CMUL(A, B, C)
 1500    C
 1600    C  DOUBLE PRECISION COMPLEX-VALUED MULTIPLICATION ROUTINE
 1700    C
 1800          IMPLICIT DOUBLE PRECISION (A-C)
 1900          DIMENSION A(2), B(2), C(2)
 2000          CR = A(1)*B(1) - A(2)*B(2)
 2100          C(2) = A(1)*B(2) + A(2)*B(1)
 2200          C(1) = CR
 2300          RETURN
 2400          END
 2500    C
 2600    C
 2700    C
 2800    C
 2900          SUBROUTINE CDIV(A, B, C)
 3000    C
 3100    C  DOUBLE PRECISION COMPLEX-VALUED DIVISION ROUTINE
 3200    C
 3300          IMPLICIT DOUBLE PRECISION (A-C)
 3400          DIMENSION A(2), B(2), C(2)
 3500          BR = B(1)
 3600          BI = B(2)
 3700          BD = BR**2 + BI**2
 3800          CR = (A(1)*BR + A(2)*BI)/BD
 3900          C(2) = (A(2)*BR - A(1)*BI)/BD
 4000          C(1) = CR
 4100          RETURN
 4200          END
 4300    C
 4400    C
 4500    C
 4600    C
 4700          SUBROUTINE CSQR(A, B)
 4800    C
 4900    C  DOUBLE PRECISION COMPLEX-VALUED SQUARE ROOT ROUTINE
 5000    C
 5100          IMPLICIT DOUBLE PRECISION (A-C)
 5200          DIMENSION A(2), B(2)
 5300          API = 4.D0*ATAN(1.D0)
 5400          AR = A(1)
 5500          AI = A(2)
 5600          AM = SQRT(AR**2 + AI**2)
 5700          AM = SQRT(AM)
 5800          IF (ABS(AR) .LT. 1.D-20) THEN
 5900           ARG = API/2.D0
```

```
 6000          IF (AI .LT. 0.D0) ARG = -ARG
 6100         ELSE
 6200          ARG = ATAN(AI/AR)
 6300         END IF
 6400         IF (AR .LT. 0.D0) THEN
 6500          IF (AI .GT. 0.D0) THEN
 6600           ARG = ARG + API
 6700          ELSE
 6800           ARG = ARG - API
 6900          END IF
 7000         END IF
 7100         ARG = ARG/2.D0
 7200         B(1) = AM*COS(ARG)
 7300         B(2) = AM*SIN(ARG)
 7400         RETURN
 7500         END
```